

## **M.Sc. thesis 2011**

**for**

**Stud.tech. Ziguang Zhao**

# **Calculation of fatigue damage for tensioned risers from vortex induced vibrations**

Vortex induced vibrations (VIV) are known to contribute significantly to fatigue damage of marine risers. However, important uncertainties are still present when it comes to methods for calculation of damage for risers in sheared current. The uncertainties are associated to fundamental understanding of vortex induced vibrations in situations where a large number of frequencies may become active. At least four different approaches are today used:

- One frequency is assumed to dominate, and the response is assumed to be harmonic with a fixed amplitude
- The response is assumed to take place at one frequency, but the amplitude is controlled by a low-frequency envelope process
- A number of response frequencies act simultaneously. Each of these frequencies are harmonic, and the phase between the components are random. This approach might be characterized as "concurrent frequencies", or "space sharing" with reference to the definition of excitation zones on the structure without overlaps.
- A number of response frequencies compete in time and dominates consecutively. The response is always assumed to be harmonic, but the frequency will vary from one period of time to the next. This approach is often referred to as "consecutive frequencies" or "time sharing". Excitation zones on the structure may overlap according to this approach.

Marintek and NTNU have access to measurements from several high quality VIV experiments. The experiments cover a large range of parameters like response frequency order, number of possibly active frequencies, relative influence on lateral stiffness from tension and bending and length to diameter ratio. The aim of the present MSc project is to analyse data from selected experiments and classify the response according to the categories listed above, and thereby identify conditions that will lead to the various response types and even be able to find models to describe the competition between frequencies in a quantitative way.

The work should be carried out in the following steps:

1. Literature study that should include models for fatigue accumulation from VIV in general, and alternative methods for processing data from measurements
2. Identify interesting cases from available experimental data for further analysis
3. Analyse selected cases and classify the observed response according to the mentioned categories
4. Quantify how alternative frequencies appear in time or in intensity when competing with other active frequencies.
5. Establish general models that can describe the frequency competition in a convenient way for fatigue analysis of slender structures subjected to VIV.

The work may show to be more extensive and complex than anticipated. Some topics may therefore be left out after discussion with the supervisor without any negative influence on the grading.

The candidate should in her/his report give a personal contribution to the solution of the problem formulated in this text. All assumptions and conclusions must be supported by mathematical models and/or references to physical effects in a logical manner.

The candidate should apply all available sources to find relevant literature and information on the actual problem.

The report should be well organised and give a clear presentation of the work and all conclusions. It is important that the text is well written and that tables and figures are used to support the verbal presentation. The report should be complete, but still as short as possible.

The final report must contain this text, an acknowledgement, summary, main body, conclusions and suggestions for further work, symbol list, references and appendices. All figures, tables and equations must be identified by numbers. References should be given by author name and year in the text, and presented alphabetically by name in

the reference list. The report must be submitted in two copies unless otherwise has been agreed with the supervisor.

The supervisor may require that the candidate should give a written plan that describes the progress of the work after having received this text. The plan may contain a table of content for the report and also assumed use of computer resources.

From the report it should be possible to identify the work carried out by the candidate and what has been found in the available literature. It is important to give references to the original source for theories and experimental results.

The report must be signed by the candidate, include this text, appear as a paperback, and - if needed - have a separate enclosure (binder, DVD/ CD) with additional material.

Supervisor at NTNU is professor Carl M. Larsen

Trondheim, January 2011

Carl M. Larsen

Submitted: January 2011

Deadline: June 2011

## Abstract

Vortex induced vibration (VIV) of long flexible riser subjecting to ocean currents is ubiquitous in offshore industry. Although significant efforts have done to understand this complicated fluid structure interaction problem, the numerical modeling and predicting is still a big challenge.

The primary objective of this thesis is to characterize the frequency components of VIV response measured in flexible riser model tests under shear current, and try to establish a general frequency competition system for semi-empirical model VIVANA. As the base of present work, experimental data from Norwegian Deepwater Programme (NDP) and Hanoytangen tests are studied.

Wavelet analysis method is applied to reveal the frequency components included in measured signals, time-varying intensity of each active frequency will be present as wavelet result. Peak frequency and frequency range defined as two key parameter of wavelet result for further studying.

In experiment, the neighbored locations on the riser often display same time-varying peak frequency, rather the whole riser length as assumed by VIVANA. In the other word, the time sharing method maybe better to perform in different zones separately. Based on the observation above, an ideal model combined time sharing and space sharing are proposed. In addition, by observations of VIVANA results, energy limit and excitation length are attempted to limit the active frequency range in VIVANA.

The frequency components in measured signal are compared with eigenfrequencies in still water and eigenfrequencies calculated by Riflex, the differences are stated after discussion. Displacement histories corresponding to single participating mode are composed by modal analysis method, the frequency components of these signals are analyzed by wavelet, an unexpected observation that all decomposed signals have similar frequency components is found, Rayleigh-Ritz method and mono-frequency response are proposed as explanation.

Some other study like high harmonic effects and coexistence of chaotic and stationary signals in NDP are included in this thesis, these can induced more interesting topics for future research.

## Acknowledgements

This master thesis is written by Msc student Ziguang Zhao during the spring semester of 2011 at Department of Marine Technology of Norwegian University of Science and Technology.

First of all, I wish to thank my supervisor Professor Carl Martin Larsen for guiding me through this study. I benefit a lot by his valuable ideas and suggestions. His patience and encouragement are specially appreciated.

I wish to thank Decao Yin and Jie Wu for patient explanation of basic principles, for providing new ideas and for spending time to discuss my problems, it is really important for my study.

I'm graceful to Dr. Zhiyong Huang at CESOS for providing MATLAB code and helpful support regard the code. Thanks also given to MARINTEK for providing confidential test data and correlative reports.

Last but not the least, I thank my parents, friends and classmates for priceless contribution and encouragement during this year.

Ziguang Zhao

赵子光

## Index

M.Sc. thesis 2011 .....	1
Abstract.....	4
Acknowledgements.....	5
Symbols .....	10
<b>Chapter 1, Introduction.....</b>	<b>13</b>
<b>1.1, Background and motivation.....</b>	<b>13</b>
<b>1.2, Research methods.....</b>	<b>14</b>
<b>1.3, Thesis outline .....</b>	<b>15</b>
<b>Chapter 2, Vortex induced vibration.....</b>	<b>17</b>
<b>2.1, Vortex shedding.....</b>	<b>17</b>
<b>2.1.1 Flow regimes of flow around a smooth, circular cylinder.....</b>	<b>17</b>
<b>2.1.2, Boundary layer and vortex formation.....</b>	<b>17</b>
<b>2.1.3, Vortex shedding frequency .....</b>	<b>19</b>
<b>2.1.4, Oscillating drag and lift forces.....</b>	<b>20</b>
<b>2.1.5, Correlation length .....</b>	<b>22</b>
<b>2.2, Vortex induced vibration .....</b>	<b>22</b>
<b>2.2.1, Dimensionless parameters.....</b>	<b>22</b>
<b>2.2.2, The general remarks of VIV.....</b>	<b>23</b>
<b>2.3, Experimental methods of VIV .....</b>	<b>25</b>
<b>2.3.1, Free vibration experiments .....</b>	<b>26</b>
<b>2.3.2, Forced oscillation Experiments.....</b>	<b>26</b>
<b>2.3.3, Inverse method .....</b>	<b>27</b>
<b>2.4, Computer program to predict Vortex Induced Vibration .....</b>	<b>27</b>
<b>Chapter 3, VIVANA software.....</b>	<b>29</b>
<b>3.1, introduction .....</b>	<b>29</b>
<b>3.1.1, program structure.....</b>	<b>29</b>
<b>2.1.2 Analysis options.....</b>	<b>30</b>
<b>3.2, Method overview .....</b>	<b>30</b>
<b>3.3, Frequency domain analysis.....</b>	<b>31</b>
<b>3.4, hydrodynamic coefficients.....</b>	<b>32</b>
<b>3.4.1, excitation coefficients.....</b>	<b>33</b>
<b>3.4.2, added mass coefficient .....</b>	<b>34</b>
<b>3.5, space sharing and time sharing.....</b>	<b>35</b>
<b>3.5.1, space sharing method.....</b>	<b>35</b>
<b>3.5.2, time sharing method .....</b>	<b>36</b>
<b>Chapter 4, Experimental data and data analysis methods.....</b>	<b>38</b>
<b>4.1, Norwegian Deepwater Program (NDP) high mode test.....</b>	<b>38</b>
<b>4.1.1, Background.....</b>	<b>38</b>
<b>4.1.2, Experimental Setup.....</b>	<b>38</b>
<b>4.1.3, Instrumentation.....</b>	<b>40</b>
<b>4.1.4, Test program used in present thesis.....</b>	<b>41</b>
<b>4.2, Hanoytangen Test.....</b>	<b>41</b>



4.2.1, Background.....	41
4.2.2, Experimental setup .....	41
4.2.3, Instrumentation.....	42
4.2.4, Test program.....	43
4.3, Wavelet analysis .....	43
4.3.1, Motivation of wavelet analysis .....	43
4.3.2, Brief introduction of wavelet analysis .....	43
4.3.3, Choice of time window and band-pass ranges.....	43
4.4, Modal analysis .....	46
4.4.1, Motivation of modal analysis .....	46
4.4.2, Modal analysis method used in present thesis .....	47
4.4.3, choice of participating modes.....	48
4.5, Key parameters .....	50
4.5.1, the frequency components got by wavelet analysis .....	50
4.5.2, Peak frequency .....	52
4.5.3, Frequency Range.....	53
4.5.4, Excitation Length.....	54
4.5.5, VIVANA parameters .....	54
Chapter 5, Results .....	57
5.1, Overview .....	57
5.2, Category 1, 2, 3.....	58
5.3, Category 4.....	58
5.4, Category 5.....	59
5.5, Category 6 and 7 .....	59
5.6, Category 8.....	60
Chapter 6, Observations based on analysis results .....	61
6.1, Observations for category 1 .....	61
6.1.1, Comparison between wavelet and VIVANA results .....	61
6.1.2, Linear relationship between peak frequency and towing velocity .....	62
6.1.3, Comparison between similar cases for Hanoytangen .....	63
6.1.4, peak frequency shift for different towing velocity.....	64
6.2, Observations for category 2 .....	64
6.2.1, Comparison between wavelet and VIVANA .....	64
6.2.2, Relationship between frequency range and towing velocity.....	66
6.2.3, Linear relationship between frequency range and peak frequency .....	67
6.2.4, Frequency shifting with towing velocity.....	68
6.3, Observations for category 3 .....	68
6.4, Observations for category 4 .....	71
6.5, Observations for category 5 .....	72
6.6, Observations for category 6 .....	75
6.7, Observations for category 7 .....	77
6.8, Observations for category 8 .....	77
Chapter 7, Attempts to improve frequency model .....	79
7.1, defects of VIVANA model.....	79

7.2, Filter active frequencies by energy limit .....	80
7.3, Excitation parameter and excitation length.....	81
7.3.1, Motivation.....	81
7.3.2, Tests to consider excitation parameters with excitation length.....	83
7.4, Method combined time sharing and space sharing strategy .....	86
7.4.1, VIVANA methods VS observations.....	86
7.4.2, overview of the method .....	86
7.4.3, Active frequencies.....	87
7.4.4, dividing the excitation zones.....	87
7.4.5, time sharing in each excitation zone .....	87
7.4.6, Summary .....	88
Chapter 8, Frequency and response mode.....	89
8.1, Frequency gotten from wavelet analysis .....	89
8.1.1, Eigenfrequencies VS wavelet result .....	89
8.1.2, Comparison and some observations .....	90
8.2, Studying of single mode displacement signals .....	92
8.2.1, Motivation.....	92
8.2.2, Decomposition of displacement history .....	92
8.2.3, The frequency components.....	92
8.2.4, Explanation for the result .....	93
8.2.5, Summary .....	95
Chapter 9, High harmonic effect and chaotic response .....	98
9.1, High harmonic components in VIV .....	98
9.1.1, Defining of high harmonic frequency range .....	98
9.1.2, Power spectrum density .....	100
9.1.3, Observations .....	101
9.2, Chaotic response signals in NDP test.....	103
9.2.1, The signal.....	103
9.2.2, Analysis of signals.....	104
9.2.3, Switching between chaotic and stationary VIV .....	106
Chapter 10, Conclusion and future work.....	107
10.1, Conclusion.....	107
10.2, Future Works.....	109
Reference.....	111
Appendix A .....	113
Result of category 1.....	113
Results of category 2 .....	115
Results of category 3 .....	117
Results of category 5 .....	119
Results of category 6 & 7.....	135
Results of category 8 .....	147
Appendix B .....	157
Appendix C .....	161
Appendix D .....	167





<b>High harmonic effects</b> .....	167
<b>Chaotic and Stationary Signals</b> .....	180

# Symbols

## Abbreviation

CF	Cross flow
CFD	Computational fluid dynamics
FEM	Finite element method
IL	In line
NDP	Norwegian Deepwater programme
RMS	Root mean square
VIV	Vortex induced vibration

## Roman symbols

A	Amplitude, Fourier transformed of acceleration signal
$\left(\frac{A}{D}\right)_{IL/CF}$	Amplitude ratio for IL or CF
$\left(\frac{A}{D}\right)_{C_e=0}$	Amplitude when excitation equal to zero
C	Damping coefficient matrix
$C_a$	Added mass coefficient
$C_d$	Drag coefficient
$C_{e,CF/IL}$	Excitation parameter
$C_l$	Lift coefficient
$c(t)$	Measured curvature history
C	Linear damping coefficient
D	Cylinder diameter
$D_H$	Diameter
d	Displacement history in modal analysis
$d_i$	Decomposed displacement signal corresponding to single mode
E	Elastic modulus
$E_i$	Excitation parameter
F	New parameter for ranking frequency components
$F_{e,CF/IL}$	Excitation force on an unit length element
K	Stiffness matrix
F	Force, New parameter for ranking of active frequencies
$F_D$	Drag force
$F_l$	Lift force
$F'_D$	Oscillating drag force
$F'_L$	Oscillating lift force
f	Frequency

$f_{osc}$	Oscillation frequency
$f_{n,tension}$	Eigen frequency for tensioned string without bending in still water
$f_{n,bending}$	Eigen frequency for nontensioned beam in still water
$f_n$	Eigen frequency in still water
$f_v$	Vortex shedding frequency in units of hertz
$\hat{f}$	Non-dimensional frequency
$g$	acceleration of gravity
$H$	A term $H = (\Theta^T \Theta)^{-1} \Theta^T$
$I$	Area moment of inertia
$KC$	Keulegan-Carpenter number for oscillatory flow
$k$	Characteristic size of roughness
$L$	Model length, Correlation length
$L_{e,i}$	Excitation length
$M$	Mass matrix, Number of measurement points
$M_o$	Bending moment
$m$	mass
$\bar{m}$	mass ratio
$N$	Integer number
$q_i$	unknown weighting
$R$	Radium, Excitation load matrix
$Re$	Reynolds number
$R(z)$	Correlation coefficient
$r$	Displacement
$St$	Strouhal number
$T$	Tension, Eigen period, Time
$T_i$	time duration of frequency No.i
$t$	time
$U$	Velocity
$U_N$	Current flow velocity
$z$	spatial parameter

### Greek Symbols

$\nu$	Viscosity parameter
$\delta$	Thickness of boundary layer
$\omega$	frequency
$\omega_n$	modal weight of mode n
$\omega(t)$	Modal weights
$u_n(t)$	relative parameter $u_n(t) = -\left(\frac{n\pi}{L}\right)^2 \omega_n(t)$
$\varphi$	Known mode shape
$\varphi_n$	Known mode shape of mode n
$\varphi_n''$	Second spatial differential of known mode shape



$P$	density
$\kappa$	curvature
$\varepsilon$	strain
$\theta_n$	curvature mode with unit value
$\Theta$	curvature mode matrix
$\Psi$	Known Mode shape

# Chapter 1, Introduction

## 1.1, Background and motivation

When current flow through slender structures, current will lead to separated flow and vortex shedding. These vortices will again lead to periodic forces on structures that may result in horizontal and vertical oscillation. This phenomenon is known as vortex-induced vibration (VIV), and the horizontal and vertical oscillations are in-line (IL) and cross-flow (CF) respectively. Observations of marine riser response show that vortex-induced vibration (VIV) to be a widely occurring phenomenon, which may lead to accumulation of fatigue damage. With the increasing requirement of fossil energy, offshore exploration and production is trend to deeper area. Prediction of vortex-induced-vibration and relevant damage will be increasingly important in the coming years.

MARINTEK have conducted extensive research on VIV in last several decades, which covers rigid riser, flexible risers, free spanning pipelines, etc. The main approach method can be roughly characterized into two categories:

- The experimental methods for investigation of VIV
- Numerical models for prediction of VIV

Norwegian Deepwater Program (NDP) test and Hanoytangen test are two high qualified experiments to explore the VIV phenomenon conducted by MARINTEK. Large number of time-scaled parameters are measured and recorded for research. Based on previously experimental work and Finite Element Method (FEM), semi-empirical model VIVANA is published to predict VIV of slender marine structures subjected to ocean currents. The original VIVANA is only available for pure CF response, and the hydrodynamic coefficients for pure IL and combined IL and CF are implemented in the program since version 3.7.

In VIVANA, an excitation parameter based on energy considerations has been defined [6]:

$$E_i = \int_{L_{e,i}} U_N^3(s) D_H^2(s) \left(\frac{A}{D}\right)_{C_e=0} ds \quad (1.1)$$

The integral for excitation parameter is taken over the excitation zone  $L_{e,i}$  for each frequency, and the frequency with largest  $E$  is referred to as “the dominating response frequency”.

The definition and interpretation of the excitation zones  $L_{e,i}$  and parameters  $E_i$  has two different options depending on the assumption for multiple frequency response. The two assumptions are:

- Simultaneously acting frequencies, that is space sharing method
- Time sharing between frequencies, that is time sharing method

For space sharing method, the excitation zones never overlap, but occupy different length along the riser. Oppositely, the time sharing allow the overlap of frequencies, and assume that one active frequency will dominate the whole riser, that is the excitation zones are same for all active frequencies; the time duration for each active frequency are defined by using of excitation parameter. For detail of VIVANA see chapter 3.

As a semi-empirical model based on frequency response method, the spacing sharing and time sharing methods cannot predict competition between frequencies and modes well. The aim of present thesis is to analyze data from NDP and Hanoytangen experiments and try to find models to improve frequency completion model of VIVANA.

## 1.2, Research methods

The work presented in this thesis is based on analysis of experimental data, several methods are applied to get requisite results. The most important methods are:

- Wavelet analysis.  
The wavelet analysis is used to study how frequency content of signals varies with time. One result of wavelet analysis is shown in Fig. 1.1; the color in the figure represents the intensity of excited frequencies. Assume that the frequency with maximum intensity will dominate the structure response in transient moment, and the dominate frequencies can be found varies with time. For details see chapter 4.
- Modal analysis.  
The modal analysis is used to get the continuous expression of riser response. Strain and acceleration history in some locations along the riser are measured and saved, the limited data from measurement restrict research. Assuming that the response can be express as modal shape multiply by weight factor, modal analysis will give a continuous expression of riser response. With results of modal analysis, further analysis can be performed. For details see chapter 4.

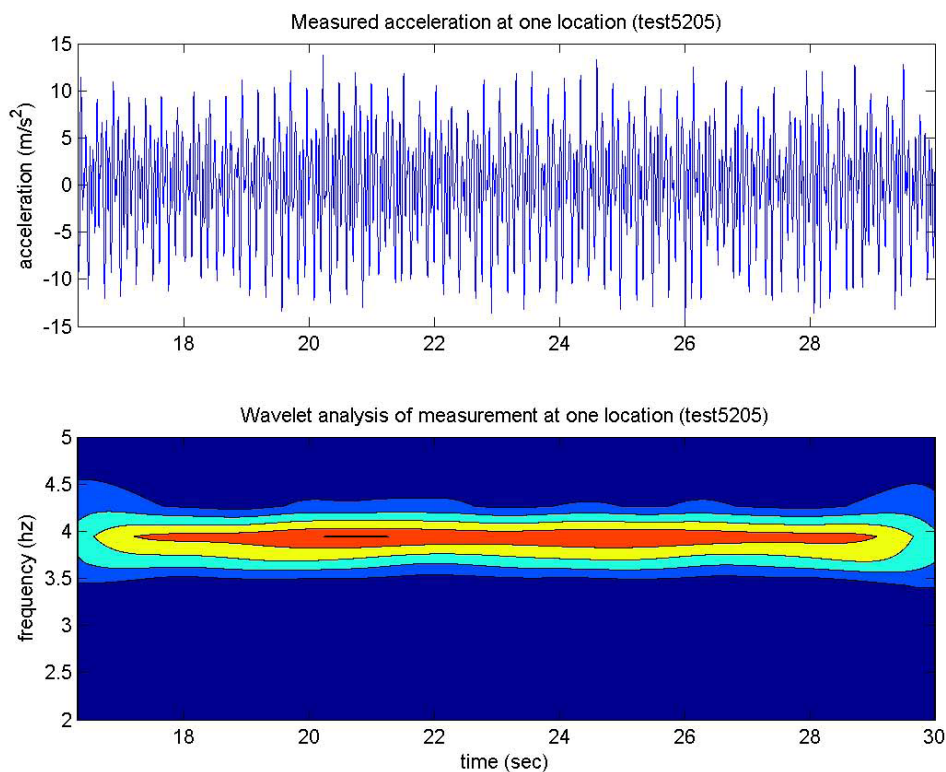


Figure 1.1, wavelet analysis of a measured acceleration signal

### 1.3, Thesis outline

The thesis is divided into the following chapters:

Chapter 2 gives a brief overview of the VIV phenomenon and defines some of the key parameters used in the study. Several experimental methods for investigation of VIV are addressed, and an introduction of numerical methods for VIV is given in the last. In Chapter 3, a detailed description of the semi-empirical model VIVANA is given; controlling parameters, time sharing and spacing sharing methods are described.

Chapter 4 gives an overview of the NDP and Hanoytangen experiments and the data used for study. A detail description of wavelet analysis and modal analysis methods are also addressed in this chapter.

Chapter 5 presents the results from data analysis in several categories.

Chapter 6 presents the comparison between experimental results and VIVANA results, some observations are described.

Chapter 7 presents the defects of VIVANA, several ideas to improve the frequency competition model are described.

In Chapter 8, the frequency components contained in measured signals are compared with eigenfrequencies. In addition, the response is divided into many components corresponding to each modal, wavelet analysis is performed to get the active frequency of each component; and the results are compared with natural frequency in still water.

In Chapter 9, high mode components of VIV are studied by using of power spectrum density of VIV signals. Chaotic and stationary signals found in NDP tests will also be discussed.

Chapter 10 presents the conclusions and observations by highlighting the contribution from the thesis, and discusses further work later.



## Chapter 2, Vortex induced vibration

### 2.1, Vortex shedding

#### 2.1.1 Flow regimes of flow around a smooth, circular cylinder

Vortex shedding from a smooth circular cylinder in a steady subsonic flow is a function of Reynolds number,

$$Re = \frac{\text{inertia force}}{\text{friction force}} = \frac{UD}{\nu} \quad (2.1)$$

The Reynolds number is based on free stream velocity  $U$  and cylinder diameter  $D$ , and  $\nu$  is the kinematic viscosity of the fluid.

A crude division of the flow regimes is given by Blevin[12]:

- $300 < Re < 1.5 * 10^5$  Subcritical regime
- $1.5 * 10^5 < Re < 3.5 * 10^5$  Transitional regime
- $Re > 3.5 * 10^5$  Supercritical regime

A more detail classification is given in figure 2.1.

One should be aware that the division of flow regimes into Reynolds number ranges is not definite. Disturbances may have a profound effect on the flow and change the  $Re$  ranges for where the various regimes are seen. Disturbances that may influence the flow can be surface roughness, inflow turbulence and shape imperfections of the cylinder.

#### 2.1.2, Boundary layer and vortex formation

The boundary layer is the layer in which the flow velocity is increased from zero at the body surface to the free stream velocity at some distance away from the surface, see Figure 2.2. The fluid field can then be divided into two parts:

1. Near the body surface where the velocity gradient normal to the body surface is large, and the shear stress can't be neglected.
2. Outside the boundary layer where the viscosity can be neglected and the flow can be determined by potential theory, i.e. the Bernoulli equation is valid.

The boundary layer thickness, in the case of laminar boundary layer, is

$$\frac{\delta}{D} = O\left(\frac{1}{\sqrt{Re}}\right) \quad (2.2)$$

And it is seen that  $\frac{\delta}{D} \ll 1$  for  $Re$  larger than  $O(100)$ .


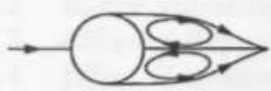




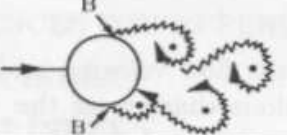
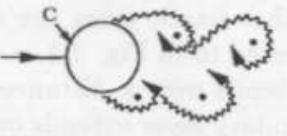
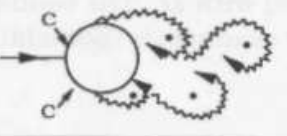
a)		No separation. Creeping flow	$Re < 5$
b)		A fixed pair of symmetric vortices	$5 < Re < 40$
c)		Laminar vortex street	$40 < Re < 200$
d)		Transition to turbulence in the wake	$200 < Re < 300$
e)		Wake completely turbulent. A: Laminar boundary layer separation	$300 < Re < 3 \times 10^5$ Subcritical
f)		A: Laminar boundary layer separation B: Turbulent boundary layer separation; but boundary layer laminar	$3 \times 10^5 < Re < 3.5 \times 10^5$ Critical (Lower transition)
g)		B: Turbulent boundary layer separation; the boundary layer partly laminar partly turbulent	$3.5 \times 10^5 < Re < 1.5 \times 10^6$ Supercritical
h)		C: Boundary layer com- pletely turbulent at one side	$1.5 \times 10^6 < Re < 4 \times 10^6$ Upper transition
i)		C: Boundary layer comple- tely turbulent at two sides	$4 \times 10^6 < Re$ Transcritical

Figure 2.1 Regimes of flow around a smooth, circular cylinder in steady current

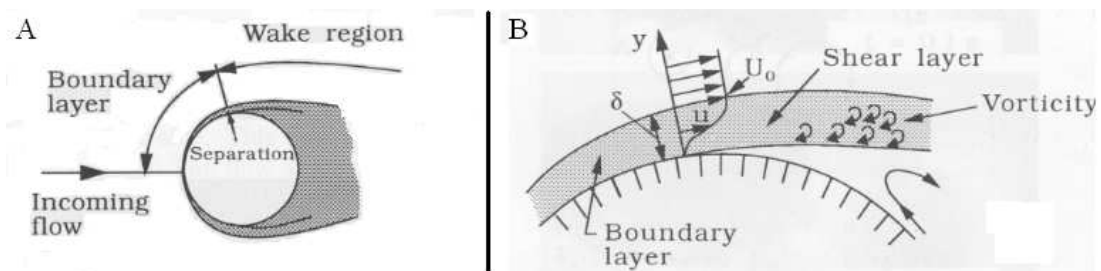


Figure 2.2 Boundary layer

In a viscous flow the particles close to the cylinder will lose energy due to friction, that is the kinetic energy of the water particles in the boundary layer is not high enough overcome the downstream pressure field, the flow will separate from the cylinder, shown in Figure 2.2B. The point of separation is referred as separation point.

From Figure 2.2B, the boundary layer formed along the cylinder contains a significant amount of vorticity. The vorticity is fed into the shear layer formed downstream of separation point and causes the shear layer to roll up into a vortex with a sign identical to the incoming vorticity. Likewise, a vortex, rotating in the opposite direction, is formed at the other side of the cylinder. See figure 2.3a.

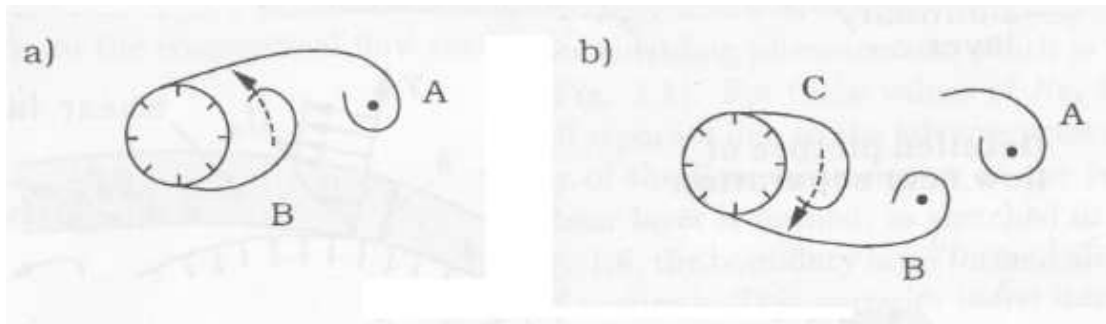


Figure 2.3 Vortex shedding

One vortex will grow larger than the other if  $Re > 40$ . The larger vortex (Vortex A in Figure 2.3a) presumably becomes strong enough to draw the opposing vortex (Vortex B) across the wake. The vorticity in Vortex A is in the clockwise direction (Figure 2.2B), while that in Vortex B is in the anti-clockwise direction. The approach of vorticity of the opposite sign will then cut off further supply of vorticity to Vortex A from its boundary layer. This is the instant where Vortex A is shed. Being a free vortex, Vortex A is then convected downstream by the flow.

Following the shedding of Vortex A, a new vortex will formed at the same side of the cylinder namely Vortex C (Figure 2.3 B). Vortex B will now play the same role as Vortex A, namely it grow in size and strength so that it will draw Vortex C across the wake. This will lead to the shedding of Vortex B. This process will continue each time a new vortex is shed at one side of cylinder where the shedding will continue to occur in an alternative manner between the sides of the cylinder [13].

### 2.1.3, Vortex shedding frequency

The Strouhal number is used to address the vortex shedding frequency.

$$St = \frac{f_v D}{U} \quad (2.3)$$

- U: free stream flow velocity approaching the cylinder
- D: cylinder diameter
- $f_v$ : vortex shedding frequency in units of hertz

The Strouhal number of a stationary circular cylinder in a subsonic flow is a function of Reynolds number, shown in Figure 2.4.

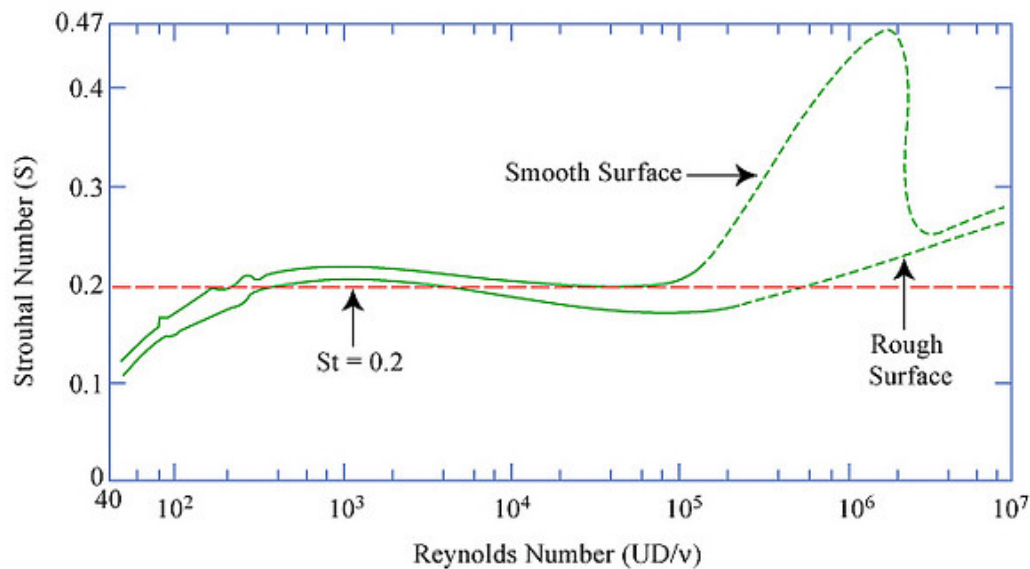


Figure 2.4, relationship between Strouhal number and Reynolds number for circular cylinder

Many different aspects give effect on vortex shedding frequency, the main aspects include

1. Effect of surface roughness
2. Effect of cross-sectional shape
3. Effect of incoming turbulence
4. Effect of shear in the incoming flow
5. Effect of wall proximity

More detail discussion can be found from Sumer and Fredsoe [13].

The shedding of vortices generates time varying pressure over the cylinder. Integrated over the cylinder surface will give a time varying force both in-line (IL) and cross-flow (CF). The frequency of CF direction is given by the vortex shedding frequency, while the oscillation frequency in IL direction has frequency twice the vortex shedding frequency

#### 2.1.4, Oscillating drag and lift forces

A cylinder which is exposed to a steady flow experiences oscillating forces if  $Re > 40$ , where the wake flow becomes time-dependent. The origin of the oscillating forces is the vortex shedding. The pressure distribution around the cylinder undergoes a periodic change as the vortex shedding progresses, which result in a periodic variation in the force (Figure 2.5).

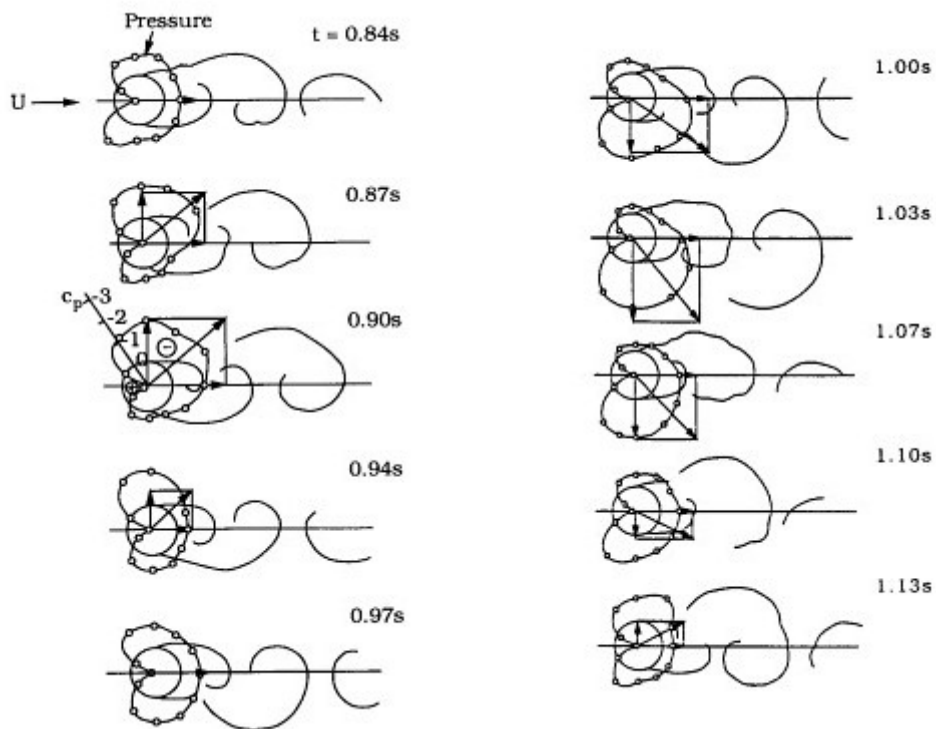


Figure 2.5, time varying pressure displacement [13]

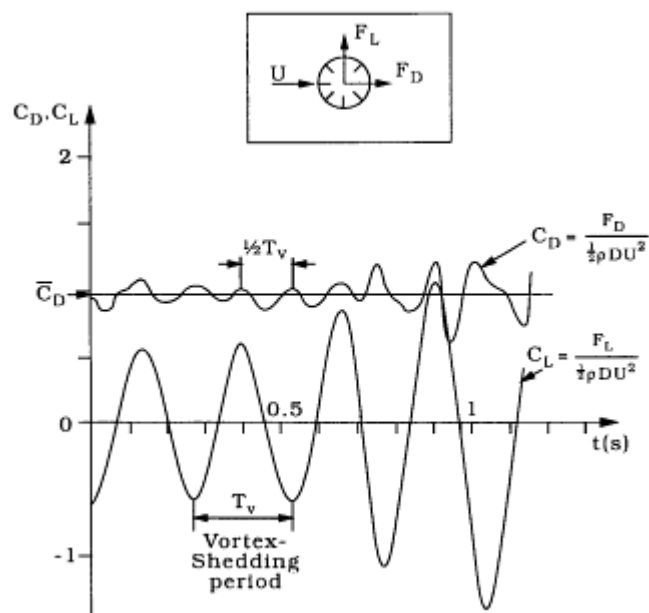


Figure 2.6, drag and lift force traces obtained from the measured pressure distribution

As seen from Figure 2.6, the lift force on the cylinder oscillates at the vortex shedding frequency, while the drag force oscillates at a frequency which is twice the vortex-shedding frequency. Moreover, the amplitude of the oscillations is not a constant process; it varies from one period to another.

The oscillating force of cylinder can be defined by following equations as function of force coefficients

$$F'_D = \frac{1}{2} \rho C'_D U^2 \quad (2.4)$$

$$F'_L = \frac{1}{2} \rho C'_L U^2 \quad (2.5)$$

In which  $F'_D$  is the oscillating part of the drag force

$$F'_D = F_D - \overline{F_D} \quad (2.6)$$

And  $F'_L$  is the oscillating lift force

$$F'_L = F_L - \overline{F_L} = F_L - 0 = F_L \quad (2.7)$$

### 2.1.5, Correlation length

Vortex shedding in the turbulent wake regime occurs in cells along the cylinder, that is, vortex shedding does not occur uniformly along the length of the cylinder, but rather in the cells. Consequently, the maximum resultant force acting on the cylinder over its total length may be smaller than the force acting on the cylinder over the length of a single cell.

The average length of the cells may be termed the correlation length. The correlation length  $L$  is defined by the integral

$$L = \int_0^{\infty} R(z) dz \quad (2.8)$$

Where  $R(z)$  is the correlation coefficient, which is got from experimental measurement.

## 2.2, Vortex induced vibration

### 2.2.1, Dimensionless parameters

The vortex induced vibration can be described in terms of dimensionless parameters. These parameters are useful for scaling flow-induced vibration and estimating the important fluid phenomena.

#### Reynolds Number, $Re$ :

This parameter defines the ratio of inertia force to friction force acting on the body. Reynolds number at a position  $s$  along the structure is defined as

$$Re(s) = \frac{\text{inertia force}}{\text{friction force}} = \frac{UD}{\nu} \quad (2.9)$$

**Roughness ratio:**

This parameter describes the cylinder surface

$$\frac{k}{D} \quad (2.10)$$

K is characteristic size of roughness and D is cylinder diameter.

**Mass ratio:**

This parameter can be defined:

$$\bar{m} = \frac{\text{mass per unit length of model}}{\text{fluid density} * \text{model width}^2} = \frac{m}{\rho D^2} \quad (2.11)$$

The mass ratio is a measure of the relative importance of buoyancy and added mass effects on the model. It is often used to measure the susceptibility of lightweight structures to flow-induced vibration. As the ratio of fluid mass to structural mass increases, so does the propensity for flow-induced vibration.

**Dimensionless amplitude:**

It is used to describe the oscillation amplitude in forced oscillation experiments and response amplitude in free vibration experiments. The subscript indicates the direction of the oscillation.

$$\left(\frac{A}{D}\right)_{IL/CF} \quad (2.12)$$

**Dimensionless frequency:**

The non-dimensional frequency  $\hat{f}$  is used as controlling parameters for added mass and excitation force coefficients. The non-dimensional frequency is defined by

$$\hat{f} = \frac{f_{osc} D}{U} \quad (2.13)$$

Where  $f_{osc}$  is the actually oscillation frequency.

**Reduced velocity,  $U_r$ :**

The reduced velocity is defined as the ratio between the path length in flow direction per circle and the cylinder diameter

$$V_r = \frac{U_N T}{D} = \frac{U_N}{f_0 D} \quad (2.14)$$

$f_0$  is the natural frequency in still water.

**Strouhal number, St:**

As was introduced in section 2.1, the Strouhal number is a parameter to address the vortex shedding frequency for a fixed cylinder in constant flow.

**2.2.2, The general remarks of VIV**

The vibrations which caused by the vortex shedding from both sides of the cylinder is called vortex induce vibration. The vortex shedding frequency is related to a full

periodic cycle for the shedding process. Forces will develop, and these are defined in local in-line (IL) and cross-flow (CF) direction, referring to the direction of the undisturbed incoming flow (shown in Figure 2.7). CF response has traditionally attracted more interest than IL due to their larger amplitudes. However, for several reasons more attention has been given to IL response during the latest years.

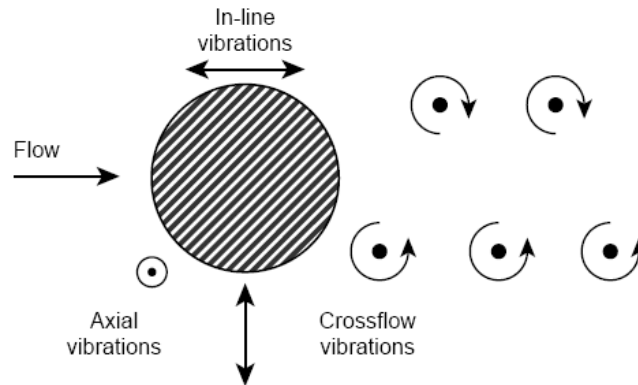


Figure 2.7, Vibration of cylinder due to vortex shedding [14]

The vortex shedding frequency will increase for increasing current velocity. A flexible structure with identical eigenfrequencies in CF and IL direction will therefore have IL response at a lower current velocity than CF. As shown in section 2.2.1, the reduced vibration is proportional to velocity. Figure 2.8 shows observed trajectories at the midpoint of a free spanning pipeline for increasing flow velocity, represented by the reduced velocity  $V_r$  [8].

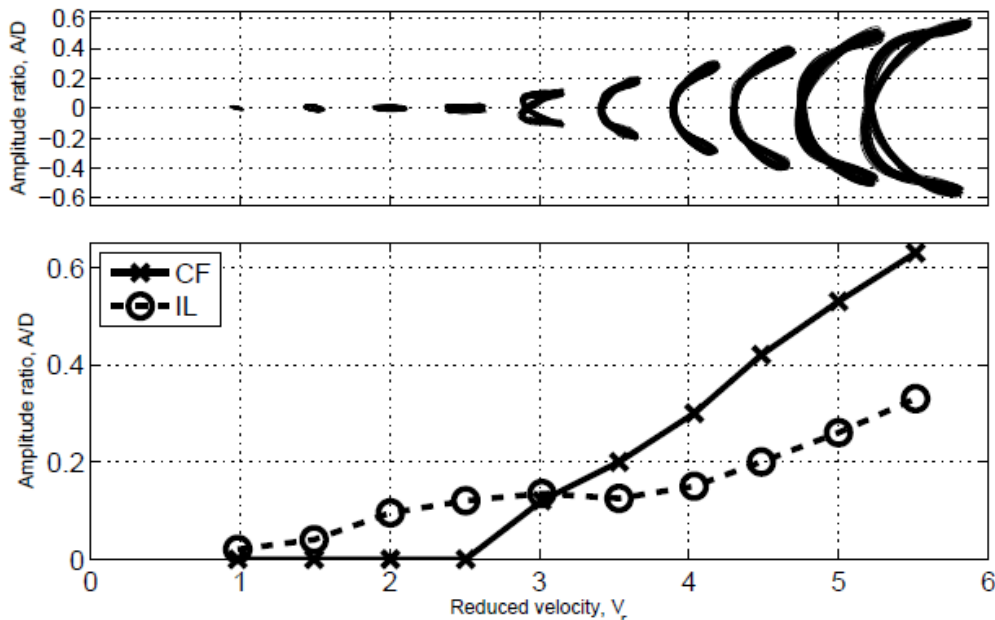


Figure 2.8, trajectories for vibrations at the midpoint of flexible beam for increased flow velocity



## Self-Limited process

VIV is normally defined as a self-limited type of response. If the amplitude exceeds a certain level, the vortex shedding process will no longer transfer energy from the fluid flow to the structure, but reverse the energy transfer process and hence lead to damping. For increasing flow velocity the oscillation amplitude will increase until some maximum value is reached. This value is typically  $1D$  for purely transverse oscillations at subcritical flow conditions and  $Re < 15.000$ ,  $1.2D$  for  $Re > 15.000$ , and up to  $1.5D$  for a body free to oscillate both in-line with and transverse to the flow.

## Lock-in

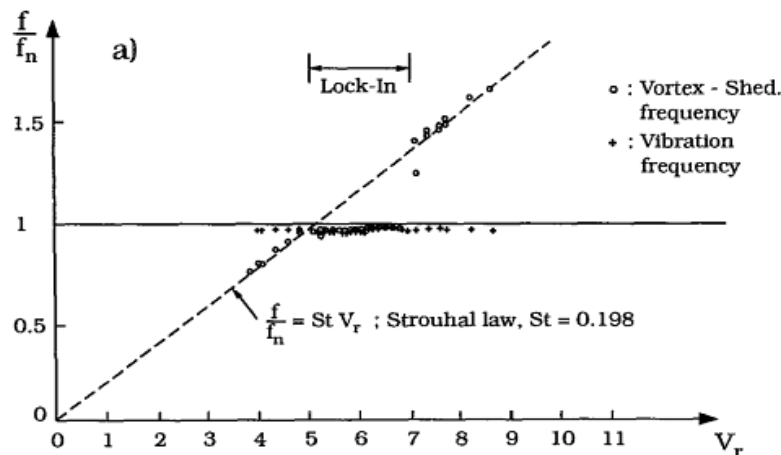


Figure 2.9, Lock in

From Figure 2.9, the vortex shedding frequency locks into the natural frequency of the system at reduced velocity interval 5-7. This implies, in this region, the vortex shedding is controlled not by the Strouhal law; rather the cylinder vibration itself has an important influence as well. This phenomenon is known as the lock-in phenomenon. The lock in region will vary for different conditions.

## Cross-Flow & In-line interaction

The traditional VIV researches are concentrated on pure CF and IL vibration, but the correlation between the responses in these two perpendicular directions plays an important role in fatigue life estimation, because of its relation to the stress statistics of the structure. The nonlinear correlation should be considered when performing response analysis of slender marine structures exposed to currents [15].

## 2.3, Experimental methods of VIV

The research methods of VIV include Numerical method and Experimental method. In this section, a brief introduction of various methods will be given.

### 2.3.1, Free vibration experiments

The free vibration experiments can be divided into two groups based on how the eigenfrequency of the system is generated. These are:

- Rigid cylinder tests where the test cylinder is supported by springs in the oscillation direction, and the eigenfrequency is controlled by the spring stiffness and mass of the oscillating parts.
- Flexible beam tests where the eigenfrequencies are controlled by the mass, bending stiffness, axial tension and length of the beam.

#### **Rigid cylinder test**

In this type of test, oscillations can be restrained in either CF or IL direction, or the cylinder may be free to oscillate in both degrees of freedom. It is assumed that the flow conditions are constant over the length of the cylinder. End plates are used to ensure that there are no 3D effects at the two ends of the cylinder.

#### **Flexible beam experiment**

This kind of experiment is often performed as scaled models of real slender marine structures. The eigenfrequency of these structures are associated with eigenmodes or modeshapes. Hence, when the structure oscillates the oscillation amplitude varies over the length of the structure. Stationary response for experiments with uniform flow along the beam is reached when there is a balance between excitation from forces in zones with low and moderate oscillation amplitudes, damping in zones with high oscillation amplitudes and structural damping.

### 2.3.2, Forced oscillation Experiments

In a forced oscillation experiment the test cylinder is given a prescribed motion. The wake behind the cylinder responds to this motion, and the force from the wake acting on the cylinder can be measured. In order for this method to provide valid data for a cylinder subjected to VIV, the prescribed motions must be follow specified oscillation pattern. This pattern is normally harmonic motion in CF or IL direction, or a combination of CF and IL motions. The result from a forced oscillation experiment is knowledge of the hydrodynamic force acting on the cylinder under the tested conditions. Figure 2.10 is some pattern of forced oscillation.

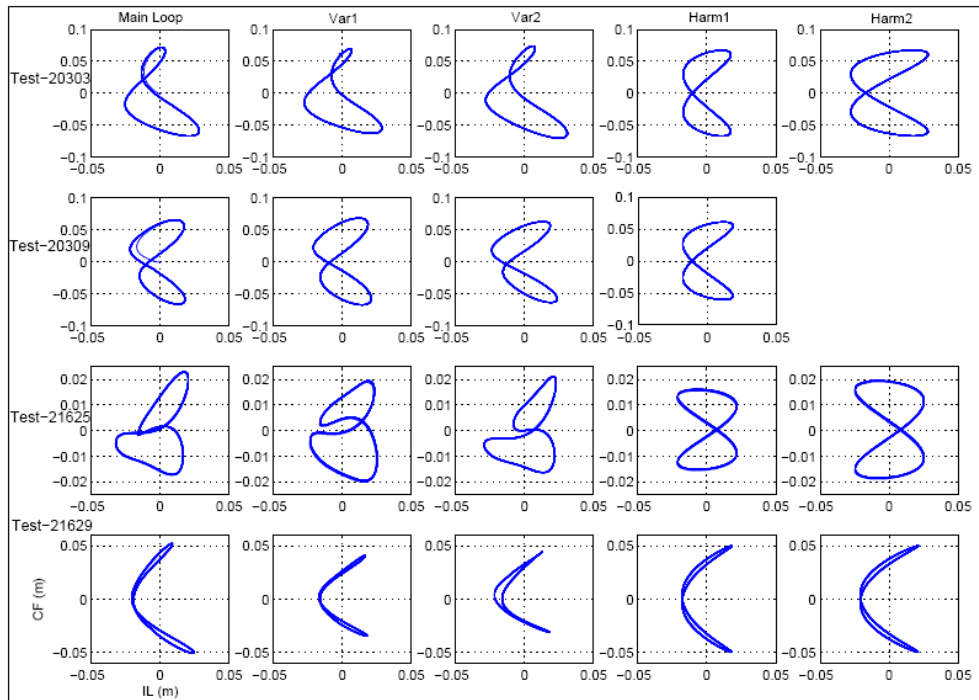


Figure 2.10, forced oscillation patterns [17]

### 2.3.3, Inverse method

A large number of laboratory and ocean tests with long slender beams or cables have been reported. Key results from such experiments have been response frequencies and amplitudes, but also information on mode composition and traveling waves. Due to the difficulty of direct force measurement, accelerometer and bending strain measurement are used in such experiments. Formally, it should be possible to identify the forces that have created the measured response. An inverse force estimation method is to construct the unknown hydrodynamic forces from measured dynamic response data. Detail about the inverse method can be found from Jie Wu [16].

## 2.4, Computer program to predict Vortex Induced Vibration

Computer programs to predict VIV may be based on two different principles [18]:

1. A combined simulation of fluid motions (CFD) and structural response (usually by FEM). The Navier-Stokes equation describes the physics of the fluid, and is solved by a finite element or finite difference method. The result is a detailed description of velocities and pressure in the fluid, which means that the resulting force on the cylinder surface can be found. By this principle, a long computing time is expected.
2. Use of empirical model for hydrodynamic forces in combination with a conventional model for the structure (usually based on FEM). This approach is

the basis for standard engineering tools for prediction of VIV. Computing time is normally three to five orders of magnitude lower than the computational method, since the time consuming in CFD was saved by applying of empirical hydrodynamic coefficients.

With the development of computer technology, the numerical methods are expected to be more accurate and faster. However, it needs time. The design analyses of VIV will continuous based on empirical method in the near future.

VIVANA is a program developed by MARINTEK, which is based on empirical model and frequency analysis. Detail description of VIVANA can be found in Chapter 3.

## Chapter 3, VIVANA software

### 3.1, introduction

#### 3.1.1, program structure

The purpose of VIVANA is to calculate VIV of slender marine structures such as risers, free span pipelines and cables subjected to ocean current. Depend on the length of the structures, cross-section variations and current profiles, the riser may experience single or multi-frequency response. Both response types can be analyzed.

VIVANA is linked to RIFLEX (shown in Figure 3.1), which is developed by MARINTEK and tailor-made for static and dynamic analysis of slender marine structures. The two RIFLEX modules INPMOD and STAMOD are always a part of VIVANA program system, while other RIFLEX modules are not needed. RIFLEX will give a description of the structure and its static shape in a specific file format, which enable VIVANA to analysis a large variety of slender marine structures.

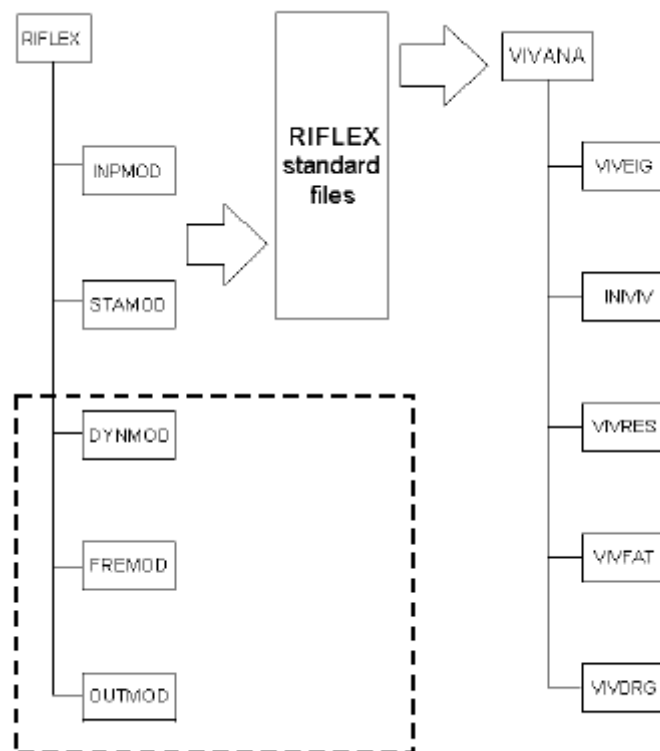


Figure 3.1, The overall structure of VIVANA [6]

A complete VIV analysis consistent of [18]:

- An initial RIFLEX analysis using the INPMOD and STAMOD modules.

- The VIVEIG module computes normal modes and eigenfrequencies.
- Some initial key parameters are calculated in INIVIV. The VIVRES module carries out the dynamic response analysis according to the method described herein. Cross-flow (CF) and/or in-line (IL) response can be calculated.
- The VIVFAT module calculates fatigue damage based on the results from VIVRES
- Finally VIV magnified drag coefficients are calculated in VIVDRG.

### 2.1.2 Analysis options

Three analysis options are offered.

1. Cross-flow(CF) response only  
This option based on hydrodynamic coefficients found from experiments.
2. Pure in-line(IL) response  
This option based on hydrodynamic coefficients found from forced IL motion tests. This response type take place for current velocity lower than the on-set of CF vibrations, that is the reduced velocity related to the fundamental eigenfrequency is lower than 2.5, see in Figure 2.8. This type of responses gives significant contribution to fatigue of structures.
3. Combined CF and IL response  
The response is calculated in two steps. First is the CF response analysis and applies the same method and hydrodynamic coefficient as potion 1. IL response analysis is performed in step2, which is assumed to take place at two times of CF frequency. Analysis method is same as for pure IL, but hydrodynamic coefficient is different.

## 3.2, Method overview

VIVANA is using an iterative procedure for performing dynamic analysis of response dependant loads in frequency domain. A brief outline of the analysis procedure in VIVANA is given in the following.

### Step 1, Static analysis

The static shape of the structure needs to be found. The procedure will depend on the actual case and how it is modeled in REFLEX.

### Step 2, Eigenvalue analysis

The eigenfrequencies and mode shapes of the structure are found. Added mass is initially applied as for a non-responding riser in still water according to data given by the user. A sufficient number of eigenvalues will be found so that all possibly active frequencies can be found when considering the maximum vortex shedding frequency along the structure.

### **Step 3, Identification of possible excitation frequencies**

Added mass under VIV conditions will differ from the still water values, which is found from Step 2. Hence, iterations must be performed for each eigenfrequency that is considered as candidate for being excited by vortex shedding.

### **Step 4, Identification of excitation zones**

Each response frequency will be associated to an excitation zone where vortex shedding may excite the structure at the actual frequency. The zone is defined by an interval for the local non-dimensional frequency. In VIVANA, two different methods are available to define excitation zones

- space sharing method
- Time sharing method

### **Step 5, analysis of the responses**

The frequency response method is used to calculate the dynamic response at the response frequencies found from Step 3 within excitation zones defined in Step 4. The response analysis applies an iteration that converges when the response is in accordance with the nonlinear models for excitation and damping forces. In VIVANA, two different iteration strategies are offered

- Fixed point iteration
- Newton Raphson iteration

### **Step 6, Calculation of fatigue damage**

Fatigue damage is calculated on the basis of user defined SN curves and the calculated response from previous steps. The Miner-Palmgren rule for damage accumulations is applied. Rain-flow cycle counting is used for space sharing case, while an analysis solution can be used for the time sharing cases.

## **3.3, Frequency domain analysis**

The response method is used to calculate the dynamic response at the dominant frequency identified in the previous steps (shown in section 3.2). Frequency response method implies a linear relationship between dynamic and static response, this limitation will normally not be a problem since VIV amplitudes are small relative to global dimensions of the structures, which mean that the structural behavior is linear [19].

Another assumption is that the VIV takes place at discrete frequencies. Laboratory test and large-scale experiment support this assumption. The frequency response method is well suited for this application due to the assumption. Use of the finite element method will give the dynamic equilibrium equation as

$$M\ddot{r}(t) + C\dot{r}(t) + Kr(t) = R(t) \quad (3.1)$$

Where  $M$  is the mass matrix,  $C$  is the damping matrix and  $K$  is the stiffness matrix.  $\ddot{r}$ ,  $\dot{r}$  and  $r$  are the acceleration, velocity and displacement respectively. The external loads here will be harmonic, but loads at all degrees of freedom are not necessarily in phase. It's convenient to describe this type of load pattern by a complex load vector  $X$  with harmonic time variation at known frequency  $\omega$

$$R(t) = Xe^{i\omega t} \quad (3.2)$$

The response vector  $r$  will also be given by a complex vector  $x$  and a harmonic time variation

$$r(t) = xe^{i\omega t} \quad (3.3)$$

BY introducing the hydrodynamic mass and damping matrix and damping matrix, dynamic equilibrium can now be expressed as:

$$-\omega^2(M_S + M_H)x + i\omega(C_S + C_H)x + Kx = X_L \quad (3.4)$$

Where

$M_S$       Structural mass matrix

$M_H$       Hydrodynamic mass matrix

$C_S$       Structural damping matrix

$C_H$       Hydrodynamic damping matrix

$X_L$       Excitation force vector, Non-zero terms are present within an excitation

zones. The excitation force must always be in phase with the local response velocity.

The response vector  $x$  is complex. The vector describes a harmonic response at all nodes, but the responses may have different phase. This means that the response will not necessarily appear as a standing wave, but may have contributions from travelling waves. From a mathematical point of view,  $x$  is equivalent to a complex mode found from the damped eigenvalue problem.

Since the load vector  $X$  depends on the response vector  $x$ , the dynamic equilibrium function must be solved by iteration. The aim of this iteration is to identify a load vector that gives a consistent response vector in the sense that both amplitudes and phases are correct at all positions, and also consistent with the local flow conditions.

When the VIV response analysis is completed, we are left with  $N$  complex response vectors  $x_1, x_2, \dots, x_n$ . These are used in combination with the element stiffness matrices and cross-section properties to derive the time series of stresses. Hence, a multifrequency response at discrete time increments is obtained.

### 3.4, hydrodynamic coefficients

The analysis model is based on empirical coefficients for lift force, added mass and damping. All coefficients will depend on the non-dimensional frequency,

$$\hat{f} = \frac{f_{osc}D}{U} \quad (3.5)$$



Where  $f_{osc}$  is the oscillation frequency,  $D$  is the diameter and  $U$  is the flow velocity. Both  $D$  and  $U$  may vary along the riser, which means that all coefficients also vary.

### 3.4.1, excitation coefficients

The excitation force in CF and IL direction at a give position on the structure is defined as the component of the hydrodynamic force that is in phase with the response velocity at the same position and for the CF and IL respectively. The force on an element with unit length is given by

$$F_{e,CF/IL} = \frac{1}{2} \rho C_{e,CF/IL} D_H U_N^2 \quad (3.6)$$

Instead of defining the excitation force coefficients as a two-parameter function of amplitude and frequency (shown in Figure 3.2), VIVANA’s built-in model applies a set of parameters that defines the coefficient as a function of the amplitude. The parameters are in turn given as functions of the frequency.

From Figure 3.2, the positive excitation coefficient, which can give excitation to marine slender structures, is found in the interval 0.125-0.3 and 0.2-0.9 for non-dimensional frequency. That is, the non-dimensional interval 0.125-0.3 and 0.2-0.9 are the excitation ranges.

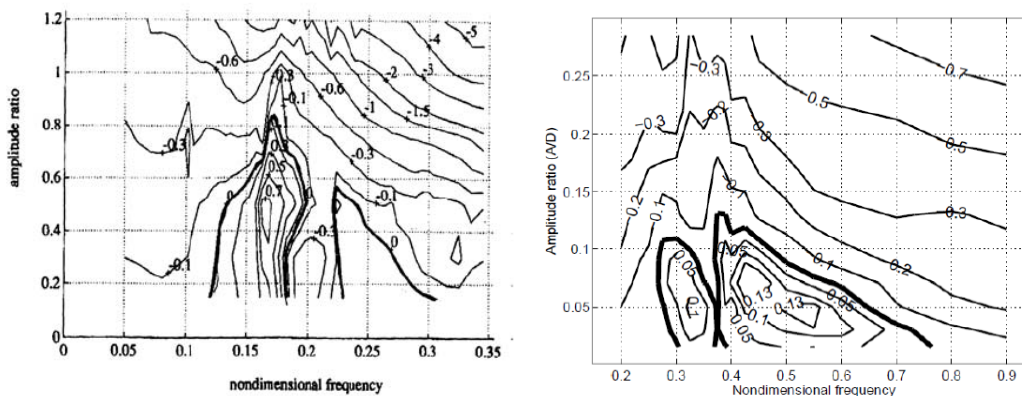
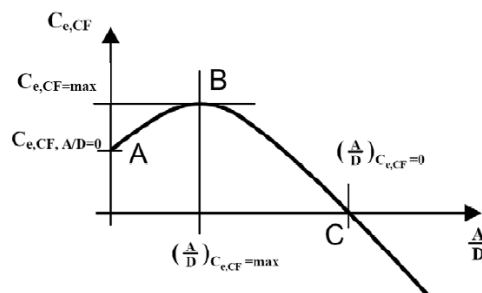


Figure 3.2 contour plots of excitation force for CF and IL oscillation

Left: CF oscillation, Gopalkrishnan (1993)[20]

Right: IL oscillation, Aronsen (2007) [8]

Figure 3.3 show how the CF and IL excitation coefficient are defined as a function of  $\hat{f}$  for a given non-dimensional response frequency.



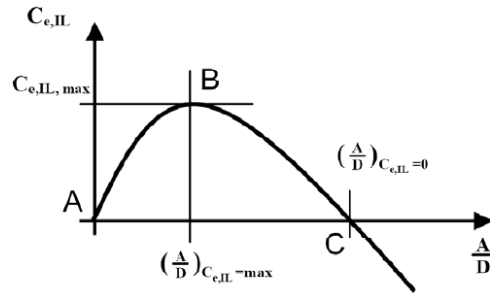


Figure 3.3, The excitation coefficient curve for CF and IL

As discussed before, the VIV is a self-limiting process, which is easy to understand by realizing that  $C_e$  becomes negative if the response amplitude exceeds a certain value. Excitation force will hence change from being an excitation force to become a damping force.

### 3.4.2, added mass coefficient

Figure 3.4 shows the contour plots, which define combinations of amplitudes and frequencies that have equal value of the added mass coefficient.

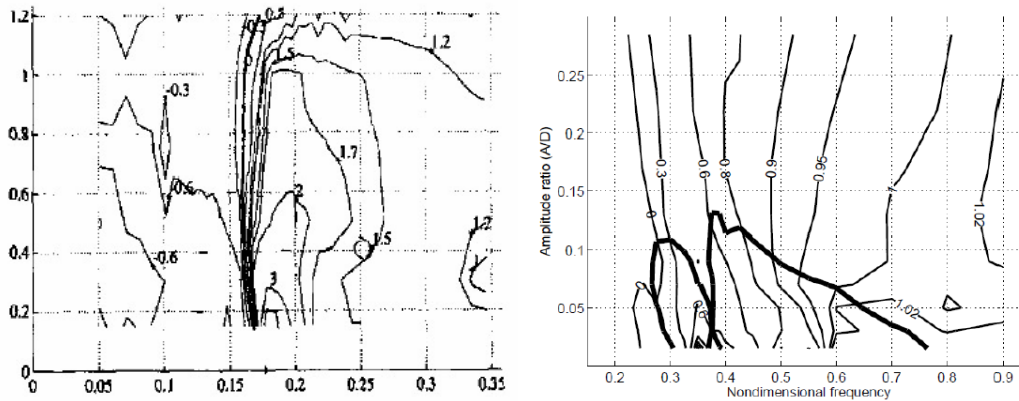
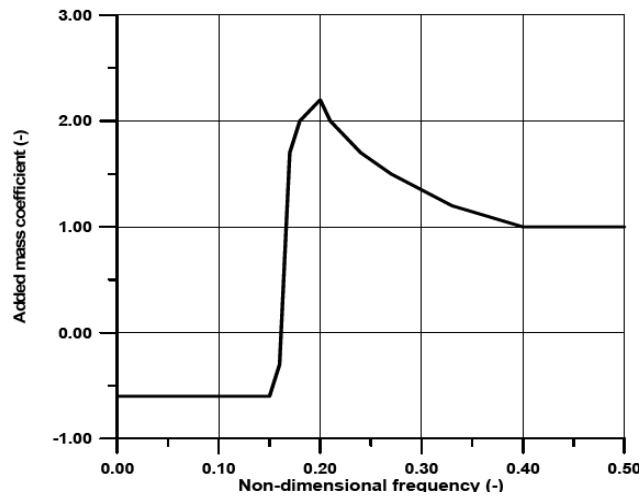


Figure 3.4, Contour plots of added mass coefficients for CF and IL oscillation

By observation of Figure 3.4, it is assumed that the added mass coefficient is independent of the amplitude and is therefore given as a simple function of the frequency, see Figure 3.5.

Added mass as function of non-dimensional frequency (from Gopalkrishnan)



Added mass as function of non-dimensional frequency (from Aronsen).

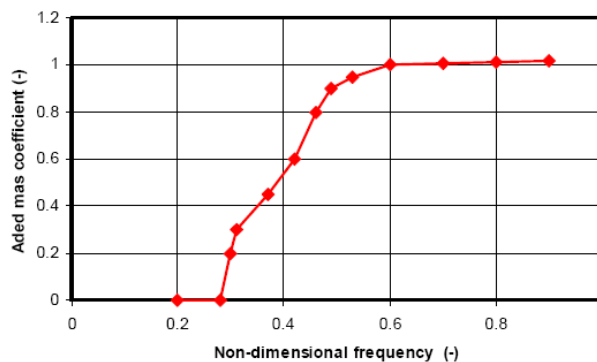


Figure 3.5, the VIVANA model for added mass coefficient of CF and IL

### 3.5, space sharing and time sharing

Multi frequency VIV can be analysed in two different ways, which both have been implemented in the VIVANA.

#### 3.5.1, space sharing method

The response take place at a selected set of eigenfrequencies, and these frequencies act simultaneously. Excitation for each frequency is caused by vortex shedding in defined zones along the structure. No overlap exists between these zones as shown in Figure 3.6. They are defined by specified excitation range for the non-dimensional frequency  $\hat{f}$ , see Figure 3.2 [10].

A new parameter is introduced here

$$E = \int_{L_{e,i}} U_N^3(s) D^2(s) \left( \frac{A}{D} \right)_{C_e, CF=0} ds \quad (3.10)$$

This parameter E will define the priority among all possible acting frequencies. The last term in equation above is defined from the local excitation coefficient curve according to the intersection between the curve and the amplitude axis, see Figure 3.3. The frequency with highest rank will dominate its zones. This approach might be characterized as “space sharing”.

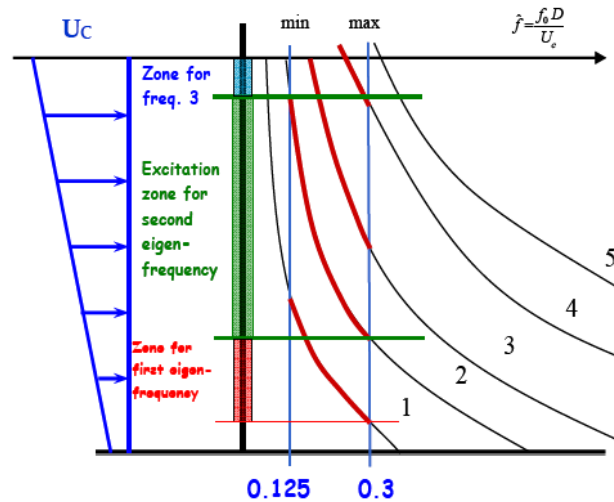


Figure 3.6, excitation zones for simultaneously acting frequencies

The frequency with maximum excitation parameter will take its whole excitation length; the second ranked frequency will take the excitation zone take out of the part overlapped with 1<sup>st</sup> ranked frequency zone; excitation zones of other frequency follow the same order.

### 3.5.2, time sharing method

In this method, the response take place at a selected set of eigenfrequency, but only one frequency will be active a specific time period (shown in Figure 3.7). The response frequencies will be the same as for the time sharing approach, but their excitation zones may now be allowed to overlap, shown in Figure 3.8. The frequencies complete to capture time windows. The duration of time window i,  $T_i$  is found from associated excitation parameter  $E_i$  according to

$$T_i = T \frac{E_i}{\sum_{n=1}^k E_i} \quad (3.11)$$

This approach has been named “time sharing”.

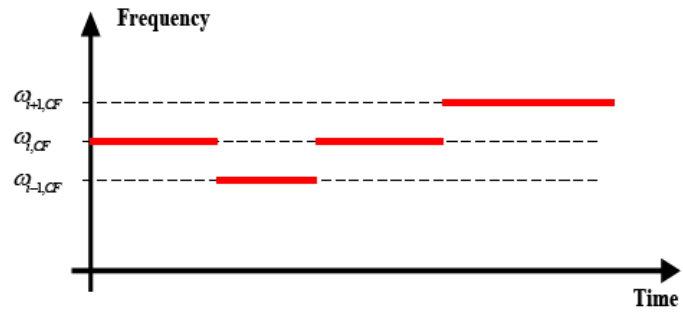


Figure 3.7 Illustration of time sharing

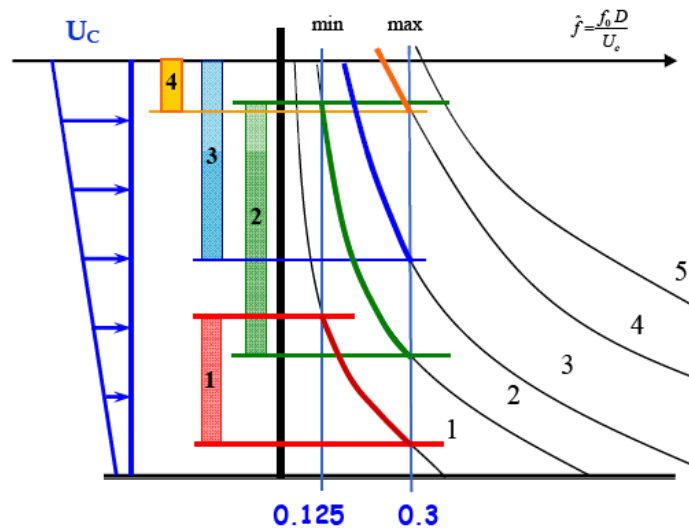


Figure 3.8 Excitation zones according to the time sharing process

# Chapter 4, Experimental data and data analysis methods

The intension of the first two sections of this chapter is to give a brief introduction to the two high qualified tests: NDP (high mode) and Hanoytangen. Data will be used in later study is addressed. For detail reading on these topics, reference is made to reports by MARINTEK.

Background of wavelet analysis method and modal analysis method will be given in last two sections; the purpose is to highlight what kind of information can be extracted from original data, and how to extract useful information from original data. Earlier projects are included in discussion as examples. For more complete overview of these methods is made to review articles by Grossmann&Morlet [7], Mo&Lie [3] and Lie&Kaasen [5].

## 4.1, Norwegian Deepwater Program (NDP) high mode test

### 4.1.1, Background

Norwegian Deepwater Program (NDP) high mode test is a high length-to diameter ratio ( $L/D$ ) riser hydrodynamics testing program. The experimental work this thesis is performed in the MARINTEK Offshore Basin at December 2003. A 38m long riser was towed at different speeds, simulating uniform and triangular shear current. Measurements were made In-Line (IL) and Cross-Flow (CF) of micro bending strain and acceleration along the riser.

Both bare riser configuration and configuration with two types of strakes for VIV suppression were tested. One set of strakes had a pitch  $17.5D$  and a height of  $0.25D$ , and the second set of strakes had a pitch  $5D$  and a height of  $0.14D$ .  $D$  denotes to the outer diameter of the sleeve of strakes, equal to 33mm, the outer diameter of the riser is 27mm. Both strake geometries were tested with 0%, 41%, 62%, 82% and 91% coverage.

In present thesis, only bare riser subjecting to triangular shear current was considered. For detail regard the NDP high mode test can be found in reports by MARINTEK [1].

### 4.1.2, Experimental Setup

The experiment was carried out in the Ocean laboratory at MARINTEK. Dimensions of the tank are 50\*80\*10 meter. The Ocean basin is fitted with an adjustable floor, which enable the depth of the ocean basin adjustable. A horizontal, naturally buoyant

riser model will be located in the Ocean Basin Laboratory. Fig.4.1 presents the Ocean Basin Laboratory at MARINTEK. The 40m riser model, made by a fibre reinforced pipe, will be towed by use of a clump weight spring system and the gondola/transverse crane system. Two different current profiles are proposed to be generated, uniform and triangular. Test principles for uniform and triangular current profiles can be found in Figure 4.2.

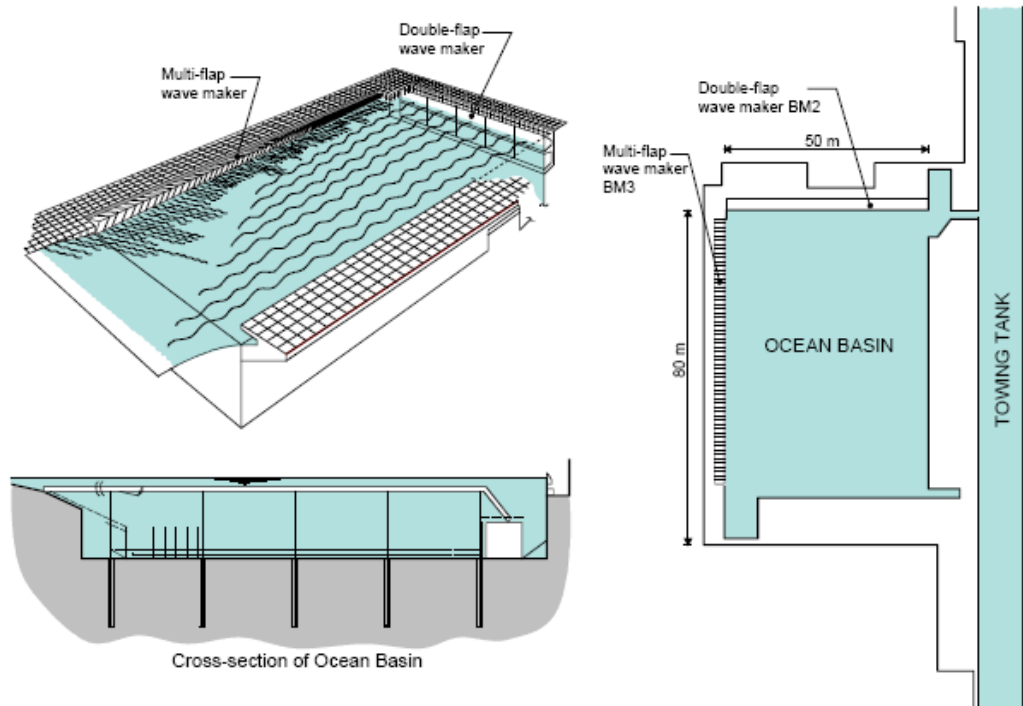


Figure 4.1, Ocean Basin laboratory [1]

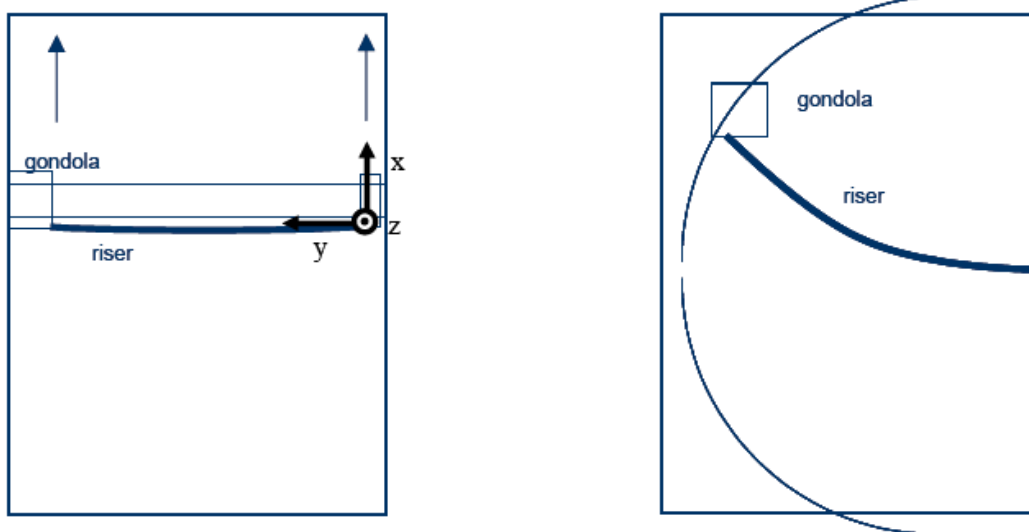


Figure 4.2, Test principles and coordinate systems [1]

The ideal experimental condition require that the riser to be towed in constant velocity and to be fixed in the end of riser. This was achieved by use of a mass-dominated test rig that has natural frequencies well below the lowest responding frequency. The principle sketch of test rig is shown in Figure 4.3.

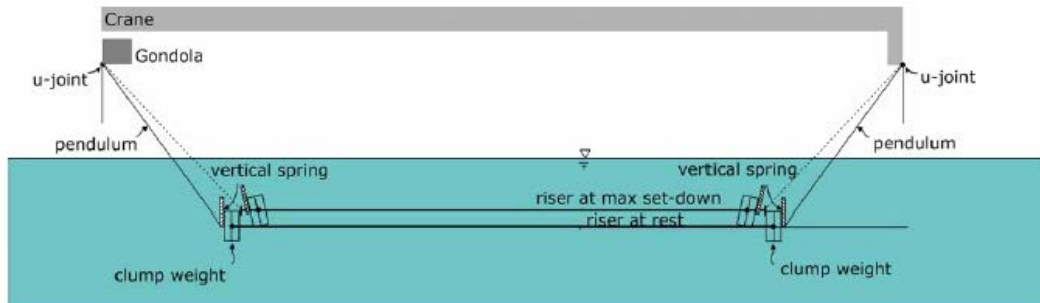


Figure 4.3, principle sketch of test rig [1]

### 4.1.3, Instrumentation

In order to measure all parameters needed, the apparatus was equipped with strain gauge transducer and accelerator.

#### Instrumentation Plan

The number of transducers on the riser model is limited by the internal space of the riser model and the diameter of the instrument cables. The table 4.1 below shows the instrumentation plan of the riser model. The transducers are non-equally located along the riser, riser instrumentation locations can be found in NDP test main report [1].

Table 4.1, number of transducers

Signal	In-line	Cross-flow
Bending moments	40	24
Accelerations	8	8

In addition to the transducers on the riser model, the following instrumentation is included:

Table 4.2, additional instrumentations

Signal	Direction	Transducer
Accelerations of lest clump weight	x, y and z	Linear acceleration
Accelerations of right clump weight	x, y and z	Linear acceleration
Riser force left end	x, y and z	Strain gauge transducer
Riser force right end	x, y and z	Strain gauge transducer
Towing velocity	x and y	Potentiometer

Since the acceleration is measured, it's convenient to get the displacement history by second integral. 9 equally located sections were chosen to calculate displacement history in both IL and CF direction. Accelerations, strains and displacements are



saved into 120 channels, and the complete channel list is present in NDP test main report [1].

## **Data Acquisition**

Six MGCplus units were connected with synchronization cables in a daisy chain. This makes the first unit the master and the other units as slaves. The first five units in the chain were equipped with 16 bridge amplifiers ML10B, while the sixth and last unit was equipped with 15 bridge amplifiers ML10B and an eight channel analog to digital converter ML801.

Based on estimation of the maximum response frequency for the riser model and data and observations from previous VIV tests, a sampling frequency of 1200 Hz was chosen. All signals were filtered with a 250Hz Butterworth filter intrinsic to the MGCplus modules.

### **4.1.4, Test program used in present thesis**

In present thesis, data measured from bare riser subjected to shear current will be analyzed. 22 different flow velocities were tested, from 0.3m/s to 2.4m/s with 0.1m/s as step. The data were saved in file TEST2310 to TEST2520 respectively. Full test program of NDP test can be found in main report of NDP test [1].

## **4.2, Hanoytangen Test**

### **4.2.1, Background**

Hanoytangen test is large scale model test of a tensioned riser which was performed at Hanoytangen, outside Bergen on the west coast of Norway in 1997. The riser model was attached to a floating vessel with constant tension. By moving the vessel at a constant speed, the riser was exposed to a nearly triangular current profile. Tests with one and two risers were carried out.

5 different types of tests were performed:

- Towing tests, parallel quai, single riser
- Towing tests, parallel quai, risers in tandem
- Towing tests, semicircle, single riser
- Damping tests, single riser
- Surface current tests, single riser

In present thesis, only tests of the first type were analyzed.

### **4.2.2, Experimental setup**

The test set-up is illustrated in Figure 4.4. The test site is a deep water quay. The water depth is 97m. The riser model was attached to a floating vessel that was pulled by a rope system and a vehicle on the quay. By moving the vehicle at a constant speed, the riser was exposed to a nearly triangular current profile.

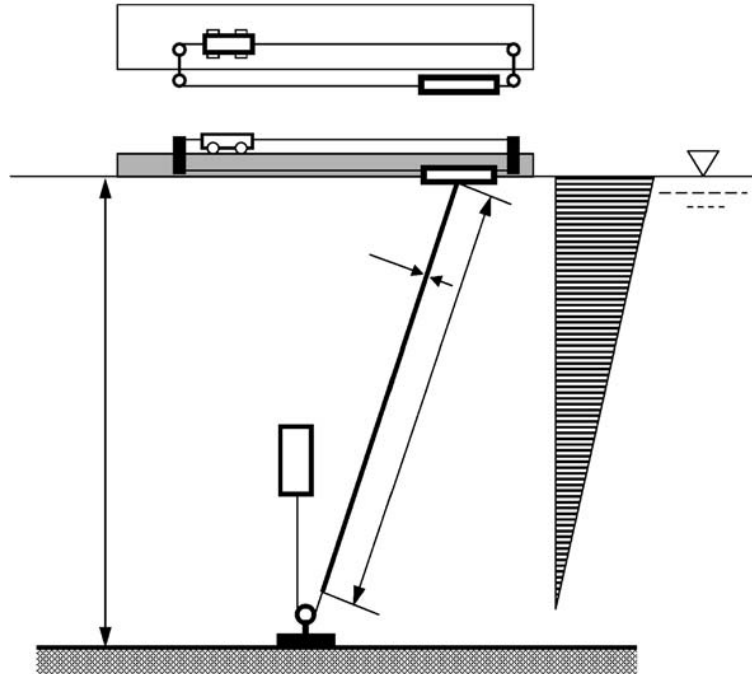


Figure 4.4, Test set-up at Hanoytangen [11]

Riser model used here was instrumented for measuring bending moments in two directions at altogether 29 levels. The 90m long riser model was made of stainless steel pipe with outer diameter 30mm and 2mm wall thickness. The riser model was suspended from the catamaran at its midship position. At the top end the riser was terminated in a universal joint, which allowed angular motion, free from bending X and Y direction, but constrained in torsion. The vertical position of the universal joint was 0.75 m above the free water surface. Above the universal joint the riser was fixed to the catamaran by a special mechanism that allowed the riser to be rotated 180 degree around axis [4].

### 4.2.3, Instrumentation

The bending moment transducers were made from 100 mm long pieces of the same steel pipe as used in the riser models. These pieces were fitted with flanges and strain gauges. Each transducer unit had 4 strain gauges, glued inside the pipe at 90 degrees intervals. The transducers were fitted for measuring bending moments in two directions at exactly 3 m intervals down the riser. The complete channel list can be found in main report of Hanoytangen test [4].

Of total 58 bending moment measuring channels, a total of 7channels failed, and

therefore should be removed from the test data. The missing channels are (referring to the complete channel list mentioned above): N11, N18, S3, S7, S11, S18 and S19.

#### **4.2.4, Test program**

For first type of tests, total 66 tests were carried out. In this thesis, data from test 33 to 66 were used. For complete test condition can be found in main report of Hanoytangen [4].

### **4.3, Wavelet analysis**

#### **4.3.1, Motivation of wavelet analysis**

As stated in the beginning of the thesis, the aim of the present works is to establish general models that can describe the frequency competition in a convenient way. However, frequency information is not included within the original data from experiments. Thus a data-processor has to be introduced here to reveal the frequency content included in measured signals.

#### **4.3.2, Brief introduction of wavelet analysis**

Wavelet analysis is a common tool for analyzing localized variation for the power with a time series. By decomposing a time series into time-frequency space, one is able to determine both the dominate frequency of signals and how those dominate frequency vary in time.

Basically the analysis consists of three parts:

1. Band-pass filtering the stochastic signals into a large number of narrow-banded components
2. Finding the time-varying envelope of narrow-banded signals
3. Algebraic sum of narrow-banded envelopes and get time-varying envelope of stochastic signal.

The further details on wavelets analysis are given by Grossmann and Morlet [7], the present application of the method referred to MARINTEK's report by Mo and Lie [3].

#### **4.3.3, Choice of time window and band-pass ranges**

##### **Time window**

Each single test was performed as following:

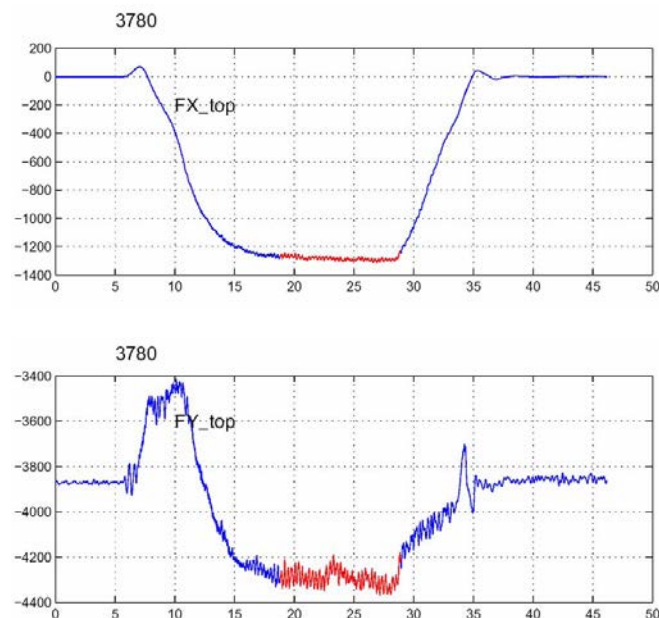
- Zero setting performed on all channels

- Start-up of the tow-carriage and the velocity increasing
- Tow carriage accelerated to the specified two velocity
- Period of constant tow velocity
- The towing velocity starts decreasing

In order to find the principles of VIV, the signals used to study have to under steady condition, that is the phenomena is fully developed and the external condition don't change with time. Thus it is very important to choose time window for further research.

The time window is based on the towing velocity. The stop time coincide with the instant the towing velocity starts decreasing. The start time has to be chosen more carefully, keeping initial transients in mind. First, a nominal start time is chosen, which coincides with the instant the towing velocity reaches its maximum. The period between the nominal start time and the stop time is denoted the nominal time-window. A sufficient interval has to be excluded immediately after the nominal start time, where the behavior is more or less dominated by transients. In general, the interval is in the order of 1/3 of the total period available, which is considerably longer than expected. Figure 4.5 is a great example for time window, the last 2/3, indicated in red, seems to be stationary [1].

Chosen time-windows for both Hanoytangen and NDP tests were determined and were shown in Tale 4.3 and Table 4.4.



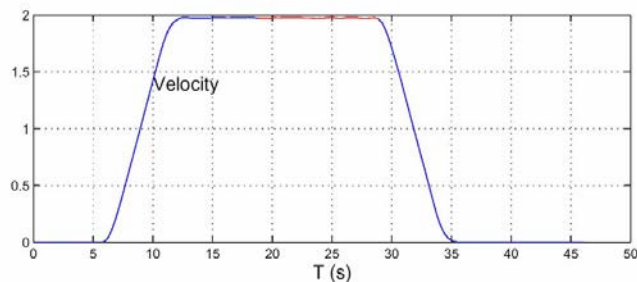


Figure 4.5, example of time window. Chosen time window is indicated in red [1]

### Band pass

In the present thesis, most work is focus on first order VIV. The raw signals from the original model test are band-pass filtered in order to reduce high mode and ultimate low-frequency noise. For NDP test, the data are already band-pass filtered. And the band pass ranges for Hanoytangen tests can be found in Table 4.3.

Table 4.3, band pass range and time window for Hanoytangen tests

test number	freq. filtrate	time window
33	0,5-5	110-180
34	0,5-5	140-180
35	0,5-5	75-125
36	0,5-5	80-115
37	0,5-5	75-110
38	0,5-5	60-90
39	0,5-5	45-75
40	0,5-5	50-80
41	0,5-5	40-65
42	0,5-6	40-70
43	0,5-6	40-65
44	0,5-6	33-58
45	0,5-7	35-60
46	0,5-7	35-60
47	0,5-7	35-60
48	0,5-8	10-50
49	0,5-8	10-50
50	0,5-8	20-50
51	0,5-10	10-40
52	0,5-10	15-45
53	0,5-10	20-40
54	0,5-10	20-40
55	0,5-10	10-37
56	0,5-10	10-35
57	0,5-10	15-35
58	0,5-10	15-35

59	0,5-10	10-30
60	0,5-10	10-30
61	0,5-10	10-30
62	0,5-10	10-30
63	0,5-10	5-30
64	0,5-12	10-27
65	0,5-12	5-25
66	0,5-12	5-25

Table 4.4, time window and active modals for NDP tests

test number	time window	velocity	modals
test2310	60-160	0,3	2--7
test2320	50-120	0,4	2--7
test2330	40-100	0,5	2--7
test2340	35-80	0,6	3--7
test2350	30-70	0,7	3--7
test2360	30-65	0,8	3--8
test2370	25-55	0,9	3--8
test2380	25-55	1	5--10
test2390	25-48	1,1	5--10
test2400	23-45	1,2	5--10
test2410	23-42	1,3	5--12
test2420	21-40	1,4	6--13
test2430	21-38	1,5	6--13
test2440	21-37	1,6	9--16
test2450	20-35	1,7	10--16
test2460	19-33	1,8	10--16
test2470	19-32	1,9	9--16
test2480	18-30	2	9--17
test2490	18-28	2,1	10--17
test2500	18-27	2,2	9--17
test2510	18-27	2,3	10--18
test2520	17-26	2,4	10--18

## 4.4, Modal analysis

### 4.4.1, Motivation of modal analysis

From limit number of transducers, signals from limit number of locations are measured. A lot of studying can be performed based on those data, but studying

concerning about the continuous variation along the whole riser length cannot be carried out. The purpose of modal analysis here is to establish continuous displacement history at everywhere along the riser.

#### 4.4.2, Modal analysis method used in present thesis

The modal analysis is based on the assumption that the shape of the riser may be expressed as a sum of eigenfunctions, or modal shapes, at any instant time. The processing of modal analysis formulation was explicit explained in report by MARINTEK [2] and Lie&Kassen [5]. Here, only theory behind modal analysis using a curvature signals is applied.

#### Transformation between strain & bending moment and curvature

For NDP tests, the strain was measured, while bending moment was measured for Hanoytangen tests. To carry out modal analysis in convenient way, the first step is to transfer the measured signals to curvature signals.

For strain, the relationship between curvature  $\kappa$  and  $\varepsilon$  is:

$$\kappa = \varepsilon/R \quad (4.1)$$

where R is the outer radius of riser.

For bending moment, the curvature can be got by:

$$\kappa = \frac{M_0}{EI} \quad (4.2)$$

where the M is bending moment, E and I denote to elastic modulus and inertia moment respectively.

#### Modal analysis with curvature signal

Assuming that the time varying shape of the riser can be composed as a series of mode shapes:

$$x(t, z) = \sum_{n=1}^{\infty} \omega_n(t) \varphi_n(z) \quad (4.3)$$

where z denotes the position along the riser with local coordinate,  $\omega_n(t)$  are the modal weights and  $\varphi_n(z)$  are the mode shapes.

It's well known that the curvature can be expressed as second spatial derivative, the time varying signals of curvature can be shown in term of mode shapes,

$$\kappa = \sum_{n=1}^N \omega_n(t) \varphi_n''(z) \quad (4.4)$$

where the second spatial derivative is denoted  $\kappa = x''$ .

If the mode shapes of displacement are sinusoidal,

$$\varphi_n(z) = \sin \frac{n\pi}{L} z \quad (4.5)$$

Equation 4.4 can be written as:

$$\kappa = \sum_{n=1}^N -\left(\frac{n\pi}{L}\right)^2 \omega_n(t) \varphi_n(z) = \sum_{n=1}^N v_n(t) \varphi_n(z) \quad (4.6)$$

Information about curvature is only acquired for a finite number of spatial locations,  $z = z_i$ , and  $i = 1, 2, \dots, M$ . In the present analysis,  $M_K^{CF} = 24$  for NDP tests and  $M_K^{CF} = 23$  for Hanoytangen tests.

Equation 4.5 can be expressed in vector notation: first form the vectors of mode shape curvatures evaluated at the points of measurement

$$\theta_n = [\theta_n(z_1), \theta_n(z_2), \dots, \theta_n(z_M)]^T, n=1,2,\dots,N: \quad (4.7)$$

Then form the  $M * N$  matrix

$$\Theta = [\theta_1, \theta_2, \dots, \theta_N] \quad (4.8)$$

The vector of curvature measurements and modal weights

$$c(t) = [c_1(t), c_2(t), \dots, c_M(t)]^T \quad (4.9)$$

$$\omega(t) = [\omega_1(t), \omega_2(t), \dots, \omega_M(t)]^T \quad (4.10)$$

Equation 4.6 can now be written as

$$c(t) = \Theta \omega(t) \quad (4.11)$$

If the number of unknown modal weight equals to the number of measurement ( $N=M$ ), the weight factor can be written as

$$\omega(t) = \Theta^T c(t) \quad (4.12)$$

If the number of unknown modal weight fewer than  $M$ , the system can be solved by least-square method. In this case ( $N < M$ ) the estimate of modal weight becomes

$$\omega(t) = (\Theta^T \Theta)^{-1} \Theta^T c(t) = Hc(t) \quad (4.13)$$

For each time instant, the modal weights are obtained from. Thus the time-varying displacement and curvature for the entire riser are found.

#### 4.4.3, choice of participating modes

For each case, the modes participating modal analysis has to be chosen individually. The number of modes,  $N$ , should not larger than the number of measurements that is available for the analysis. In this thesis, the number of measurement available is the number of curvature channels, i.e. 24 for NDP and 23 for Hanoytangen.

Results among different set of participating modes have been compared, it shows that the choice of modes is very important for modal analysis. Figure 4.6-4.8 shows three modal analysis results (displacement and maximum envelope) for NDP test2400. 1-18, 5-18 and 10-18 three sets of modes are selected for study.



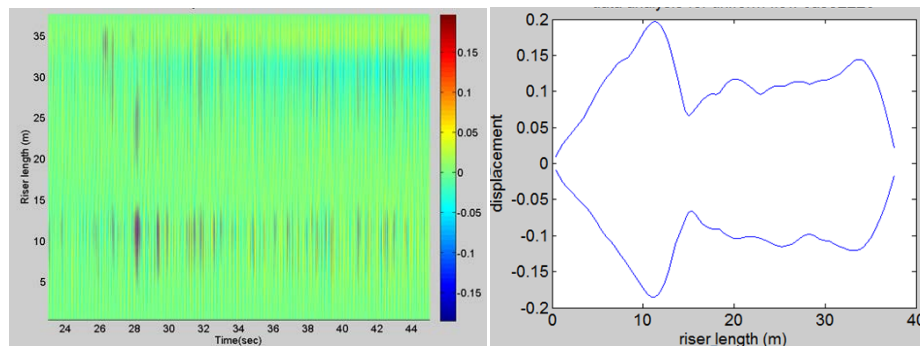


Figure 4.6, result with participating mode 1-18

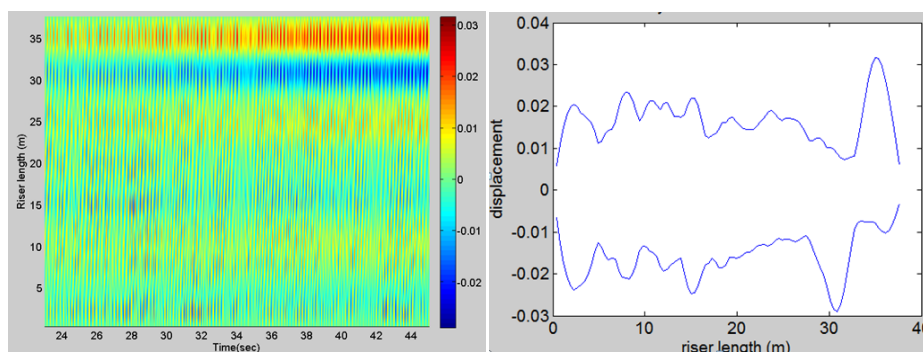


Figure 4.7, result with participating mode 5-18

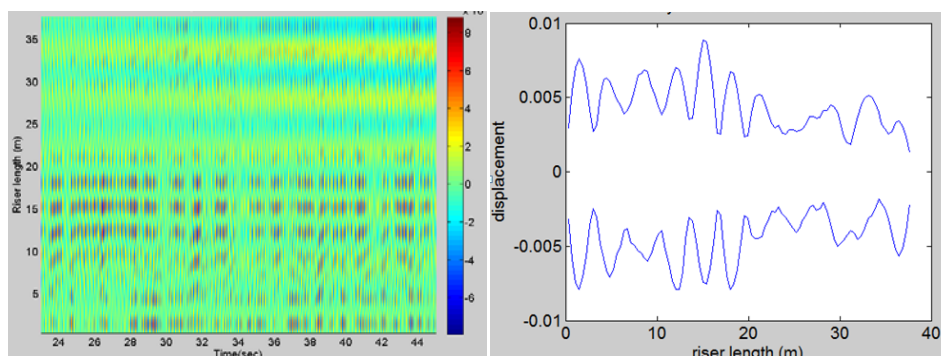


Figure 4.8, result with participating mode 10-18

By error and identifiably analysis, two options are introduced for choice of modes [5]:

1. Modal weight that fall below the noise level or are not physical with regard to frequency content are discarded. The criterion for the former case is that the r.m.s value of the modal weight must be significantly exceed the corresponding noise level; and for the latter case is that the responding frequencies lie far below or far above reasonable vortex shedding frequency.
2. Modes that are likely to be present according to prior judgment based on current speed and spectral analysis of measurements.

In present thesis, the option 1 was chosen for choice of participating modes. First of all, by error and identifiably analysis, the low modes have relevant higher error and the high modes error can't be ignored compare with corresponding weight factor. Figure 4.9 shows the relationship between error and modal weights. Secondly, modes

with high modal weight are included in modal analysis, and modal weight for each case can be found in modal analysis report by MARINTEK [2].

Choice of participating modes in present thesis is shown in Table 4.2.

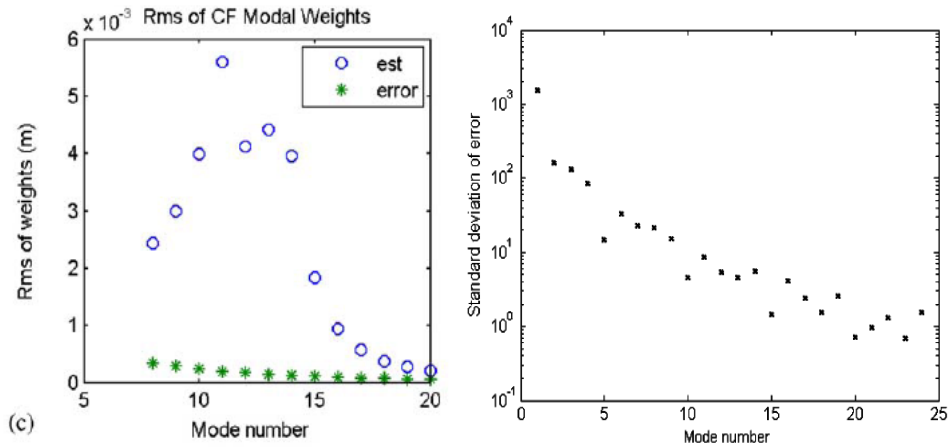


Figure 4.9, error of estimates of modal weights VS modal weights [5]

## 4.5, Key parameters

To find a general frequency competition model, some parameters are selected for observations and comparison. In this section, some key parameters are defined and the purposes of these parameters are stated.

### 4.5.1, the frequency components got by wavelet analysis

Shown in section 4.3, the wavelet analysis was to reveal frequency components contained in signal varying with time and intensity. But first of all, definitions and purposes of these frequencies have to be claimed.

#### Eigenfrequencies and mode shapes in still water

Some key features of riser dynamics can be illustrated by inspecting the eigenfrequencies and mode-shapes. starting with the eigenfrequencies for a tensioned string without bending stiffness and a nontensioned beam of equal length  $L$  and mass per unit length  $m$ :

$$f_{n,tension} = \frac{n}{2} \sqrt{\frac{T}{mL^2}} \quad (4.14)$$

$$f_{n,bending} = \frac{n^2\pi}{2} \sqrt{\frac{EI}{mL^4}} \quad (4.15)$$

Here,  $n$  is the mode number,  $T$  is the tension and  $I$  represents the moment of inertia of the beam.

The mode-shape for eigenfrequency  $n$  is given by

$$\varphi_n(z) = A * \sin\left(\frac{n\pi}{L}z\right) \quad (4.16)$$

$A$  is the amplitude of the motion. This mode shape will give identical modal mass for all modes, also for string and beam case. Hence the  $n$ th eigenfrequency for tensioned beam can be found by

$$f_n = \sqrt{f_{n,tension}^2 + f_{n,bending}^2} \quad (4.17)$$

Figure 4.10 shows an example of eigenfrequency. Each eigenfrequency corresponding to a mode shape of riser, the first, second and third order displacement mode shape can be found in Figure 4.11.

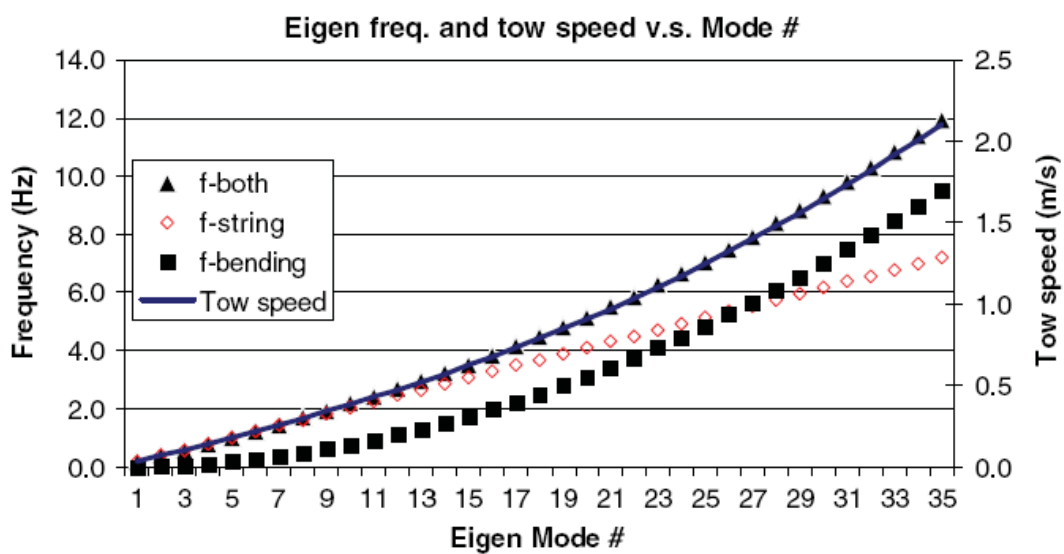


Figure 4.10, Simplified CF eigenfrequencies as a function of mode number

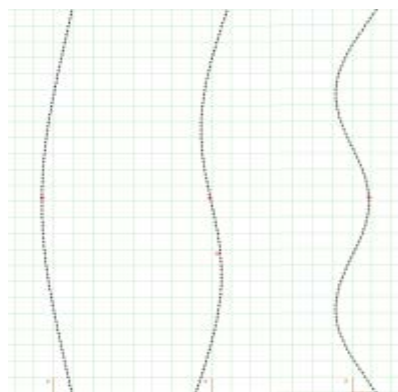


Figure 4.11, First, Second and third order mode shapes

### Frequency components decomposed by wavelet analysis

By wavelet analysis, the frequency component contained in signals from one cross section can be found. Known that the signals was response, curvature or acceleration of the cross section, which means the decomposed frequencies represent the

frequency of oscillation of the cross section. Figure 4.12 shows an oscillation period of a cross section.

Meanwhile, as a part of response of whole riser length, the composed response also corresponding to the eigenfrequency for riser oscillating subjected to current load. This can be verified by modal analysis results. But the eigenfrequency here is different with the one calculated by analytical equation mentioned above, it is the eigenvalue of mode shape which is weighting sum of known mode shapes. The difference will be shown in Chapter 8.

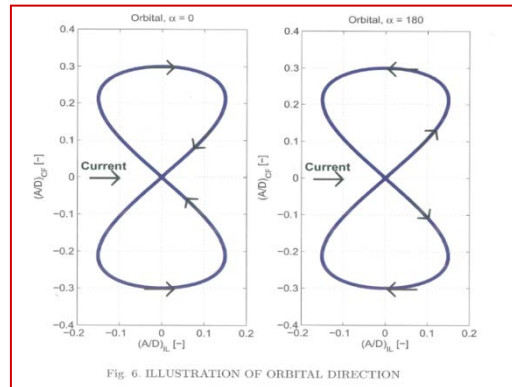


Figure 4.12, the trajectory of a oscillation period

#### 4.5.2, Peak frequency

As stated in Chapter 3, time sharing method assume that active frequencies dominate the response of whole riser in a time duration, that is during this duration, one mode will dominate the response of the whole riser. By wavelet analysis, frequency components included in VIV response signals (from a cross section) can be decomposed. As temporal variations in the frequency content of a signal was gotten, assume that the frequency with largest intensity will dominate the response of VIV in that time instant. Figure 4.13a denotes the result from wavelet analysis of Hanoytangen test0045, and the color in the figure represents the intensity of the excited frequencies; in each time instant, the frequency with maximum intensity is defined as dominate frequency at that moment, time varying dominate frequencies can be found in Figure 4.13b.

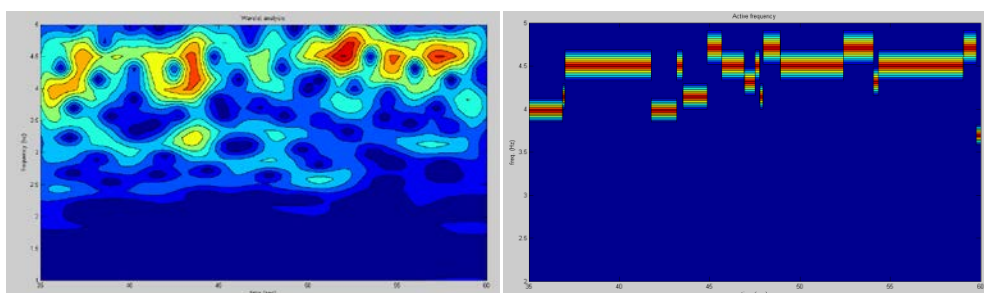


Figure4.13, Wavelet analysis results, figure 4.13a in left and figure 4.13b in right

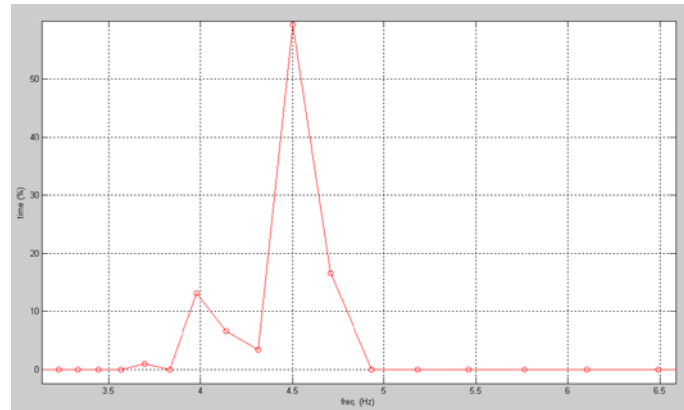


Figure 4.14, the contribution of time duration of active frequencies

Obviously, it's easy to get the percentage of time duration for each active frequency. Distribution of time duration for active frequencies is shown in Figure 4.14. Here, the one with longest time duration was defined as peak frequency.

As stated in Chapter 3, the duration of active frequency for VIVANA is based on excitation parameter  $E$ , and the time duration for each frequency is defined by the energy percentage of total energy. By wavelet analysis and VIVANA (time sharing method); two sets of peak frequencies can be gotten. Based on assumption above, the distribution of time duration for each frequency can found by wavelet analysis, this time duration distribution is seen as true value in present thesis. By comparison between two sets of time duration, some ideas to improve VIVANA model were discussed.

### 4.5.3, Frequency Range

By revising of scale factor for wavelet analysis, more frequency components will be tested by wavelet analysis. Figure 4.15 shows the difference from different scale factors. Blue curve is the time duration distribution for scale factor 0.25, and the red one was for scale factor 0.005. It's found that the frequency ranges in this example keep the same under different scale factors.

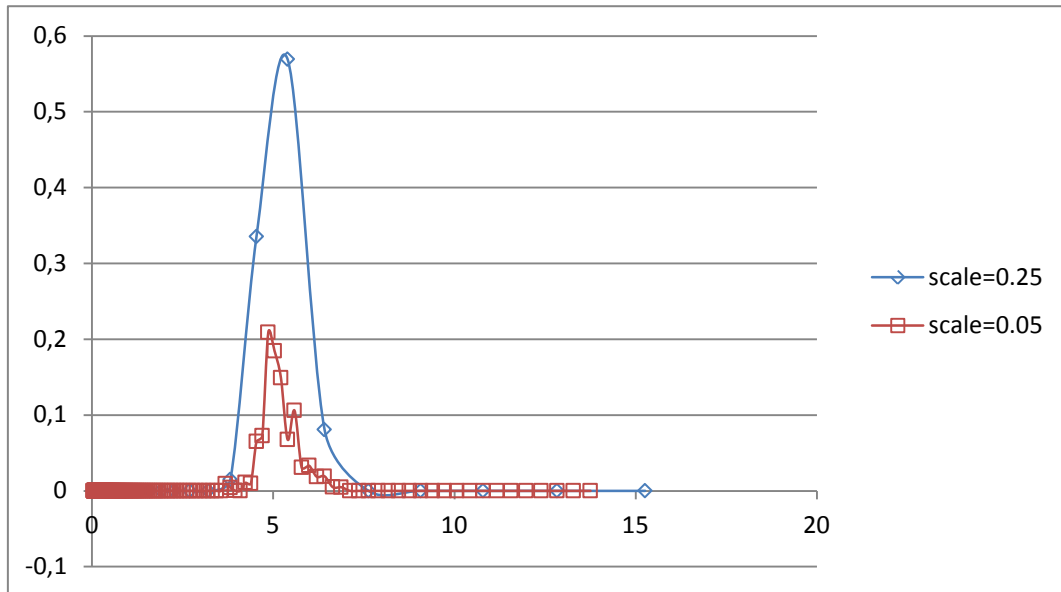


Figure 4.15, scale test of wavelet analysis

After adequate scale tests, it can be concluded that the frequency ranges in wavelet analysis do not change with scale factor. Similar test can be carried out for peak frequencies, it's found that the value difference always appearing acceptable and peak frequency value can be seen as stationary.

In present thesis, the frequency range which contains major active frequencies is defined and studied. Take Hanoytangen test0045 as an example, the distribution of time duration for active frequencies was shown in Figure 4.14 and the corresponding frequency range is 3.85Hz to 4.9Hz. To avoid infinitesimal and high mode frequencies in the range, two limits were set in MATLAB code:

1. The time duration of corresponding frequency have to larger than 0.75%.
2. The active frequency has to smaller than two times peak frequency.

#### 4.5.4, Excitation Length

In present thesis, the peak frequency and frequency range was studied together with excitation length to establish a general frequency competition model. In VIVANA, the excitation length corresponding to each active frequency was defined for time sharing and space sharing method respectively, for details in Chapter 3.

#### 4.5.5, VIVANA parameters

Parameters have to be specified to run VIVANA analysis, the key parameters include:

- Towing Velocity
- Tension

In present thesis, the mean values of velocity and tension during selected time window was specified. The two parameters for NDP and Hanoytangen test can be found in Table 4.5 and 4.6.

Table 4.5, velocity and tension for VIVANA

Case	Velocity	Tension
2310	0.3	4500
2320	0.4	4500
2330	0.5	4500
2340	0.6	4500
2350	0.7	4500
2360	0.8	4500
2370	0.9	4500
2380	1	4400
2390	1.1	4400
2400	1.2	4350
2410	1.3	4350
2420	1.4	4300
2430	1.5	4325
2440	1.6	4300
2450	1.7	4350
2460	1.8	4325
2470	1.9	4335
2480	2	4375
2490	2.1	4540
2500	2.2	4425
2510	2.3	4590
2520	2.4	4640

Table 4.6, mean values during select time windows

test No.	mean tension	mean tow velocity	velocity in report
33	3694.30	0.2592	0.26
34	3734.70	0.2582	N/A
35	3737.20	0.3790	0.38
36	3737.10	0.3796	0.39
37	3764.60	0.4348	0.44
38	3760.40	0.5369	0.54
39	3759.00	0.6435	0.64
40	3750.70	0.6222	0.63
41	3751.50	0.7397	0.74
42	3764.70	0.7309	0.73
43	3781.20	0.7601	0.76



44	3778.00	0.8342	0.83
45	3783.30	0.8389	0.84
46	3770.80	0.8415	0.84
47	3681.80	0.9510	0.95
48	3685.80	0.9388	0.95
49	3687.90	1.0504	1.05
50	3751.20	1.0276	1.04
51	3665.30	1.1477	1.14
52	3744.30	1.1339	1.14
53	3773.70	1.2604	1.26
54	3779.80	1.2591	1.26
55	3745.90	1.3464	1.35
56	3712.40	1.3636	1.36
57	3746.30	1.3441	1.35
58	3767.90	1.4530	1.45
59	3682.20	1.4500	1.45
60	3758.00	1.5590	1.56
61	3758.50	1.5359	1.55
62	3773.80	1.6431	1.65
63	3694.40	1.6336	1.65
64	3786.40	1.7155	1.75
65	3737.50	1.7452	1.86
66	3745.10	1.7525	1.96



# Chapter 5, Results

## 5.1, Overview

In this chapter, only pure cross-flow (CF) VIV of bare riser under shear current is studied, analysis results concerning the frequency competition were classified and introduced in categories below:

1. Peak frequency for wavelet at one cross section
2. Frequency range for wavelet at one cross section
3. Percentage of time duration in VIVANA based on wavelet frequency range
4. Excitation length for VIVANA
5. Frequency components for all measurement locations, varying with time
6. Peak frequency for all measurement locations
7. Frequency range for all measurement locations
8. Modal analysis for NDP test

For the first two categories, only signals from a specified measurement location were analyzed, the measurement location is vertical position No. 5 (1/4 riser length below the water plane) for Hanoytangen and vertical position No. 12 (19.997m below the water plane) for NDP; besides of wavelet, the VIVANA analysis was also performed.

For category 3, the summation of time durations of VIVANA frequencies below, within and above the wavelet frequency range was calculated for further studying, see Figure 5.1. It was performed for all cases, both Hanoytangen and NDP.

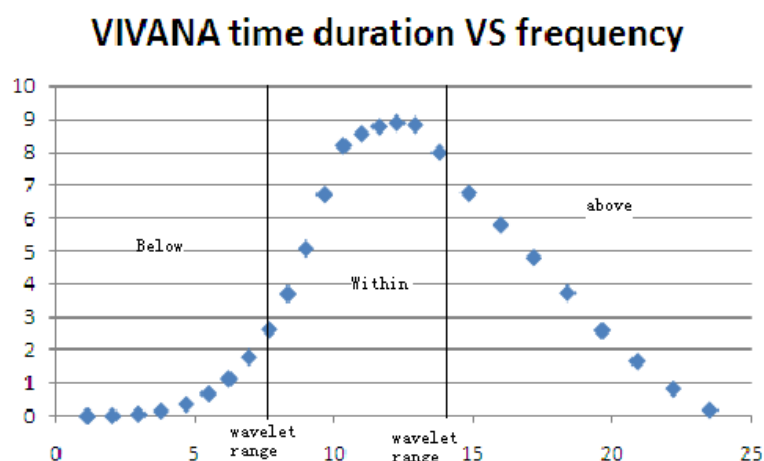


Figure 5.1, three zones for VIVANA frequencies below, within and above wavelet frequency range

Category 4 was only available for VIVANA analysis, excitation length from both time

sharing and space sharing method were recorded (space sharing time duration is only available for Hanoytangen tests). Information about category 1, 2 and 4 can be found in Table 5.1.

Table 5.1, introduction of three results

category	Location (below the water plane)	VIVANA		Wavelet Analysis
		timesharing	spacesharing	
Peak frequency	1/4 length of model	√	×	√
Frequency range	1/2 length of model	√	×	√
Excitation length	×	√	√	×

In category 5, test0051 (from Hanoytangen) and test4200 (from NDP) was selected for studying, wavelet results from all measurement locations (23 locations for Hanoytangen and 24 for NDP) were recorded for studying.

For category 6 and 7, the peak frequency and active frequency range of every test case at all measurement locations are analyzed, for both NDP and Hanoytangen. Time duration distributions for some of those tests were also recorded.

Category 8, only NDP tests are analyzed by modal analysis. Displacement history of 100 equal distanced points were gotten and be plotted, envelope of maximum displacement history is also plotted.

## 5.2, Category 1, 2, 3

For category 1, signals from No.5 vertical measurement point for all Hanoytangen test and signals from half position of riser for all NDP test were analyzed by wavelet. Corresponding VIV processes were also simulated by VIVANA. The results were shown in Table A1 and A2 in Appendix A, for NDP and Hanoytangen respectively.

For category 2, wavelet analysis and VIVANA have different frequency ranges of selected signals (same as category 1), the result can be found in Table A3 and A4 in Appendix A, for NDP and Hanoytangen respectively.

For category 3, summation of time durations for VIVANA frequency below, within and above the wavelet frequency range can be found in Table A5 and A6, for NDP and Hanoytangen cases respectively.

## 5.3, Category 4

In VIVANA, each active frequency has its own excitation zone. The length of excitation zone is defined as excitation length here. Take test2420 as an example, the

active frequencies and corresponding excitation lengths were shown in Table 5.2. The excitation lengths are recorded, but not be shown in this thesis because data is too much.

Table 5.2, Excitation length

Fre. No.	Fre.	length
1	1.1051	3.84
2	1.8478	6.476
3	2.8203	9.537
4	3.5681	12.223
5	4.2542	14.609
6	4.921	17.09
7	5.5427	19.181
8	6.1224	21.141
9	6.6936	21.393
10	7.3086	19.997
11	7.8522	18.736
12	8.439	17.155
13	9.2864	15.19
14	10.2376	12.707
15	11.2316	10.285
16	12.2396	7.835
17	13.2635	5.226
18	14.3084	2.82

## 5.4, Category 5

In this category, curvature signals from 23 measurement points of Hanoytangen test51 and from 24 measurement points of NDP test4200 are analyzed by wavelet. The plot of wavelet result which shows the temporal varying frequency components' intensities is recorded, the frequency time duration distribution were also saved. Those plots can be found in Appendix A.

## 5.5, Category 6 and 7

The peak frequency and active frequency range for all cases at every measurement point was analyzed, results can be found in Appendix A. Table A7 and A8 are the peak frequency and frequency range for NDP; table A9 and A10 are the peak frequency and frequency range for Hanoytangen.

## 5.6, Category 8

Modal analysis was carried out based on NDP signals, displacement history at 100 equal distanced points along the riser was calculated, it's impossible to show the displacement history in thesis and hereby the displacement history was plotted in a coordinate system with length and time. The result was shown in Appendix A; the maximum displacement envelopes were also available.

## **Chapter 6, Observations based on analysis results**

The purpose of the chapter is to describe some observations based on results in Chapter 5, the observations will be stated in following 8 categories:

9. Peak frequency for wavelet at one cross section
10. Frequency range for wavelet at one cross section
11. Percentage of time duration in VIVANA based on wavelet frequency range
12. Excitation length for VIVANA
13. Frequency components for all measurement locations, varying with time
14. Peak frequency for all measurement locations
15. Frequency range for all measurement locations
16. Modal analysis for NDP test

### **6.1, Observations for category 1**

In present section, the peak frequencies of signals from one specified location were studied. The observations can be classified as following:

- a) Comparison between wavelet and VIVANA results
- b) Linear relationship between peak frequency and towing velocity
- c) Comparison between Hanoytangen cases
- d) Peak frequency shift for different towing velocity

#### **6.1.1, Comparison between wavelet and VIVANA results**

Figure 6.1 and 6.2 show the peak frequency values varying with test numbers for Hanoytangen and NDP. It's easy to have two observations:

1. For Hanoytangen test, the peak frequencies value from VIVANA and wavelet are very close; while for NDP test, the peak frequency values are close when the velocity is small, while the differences goes larger for high towing velocity cases.
2. For Hanoytangen test, most of peak frequency values from VIVANA are smaller than from wavelet; while for NDP test, the peak frequency values from VIVANA are always larger than wavelet.
3. Several groups of test share a same peak frequency by wavelet results.

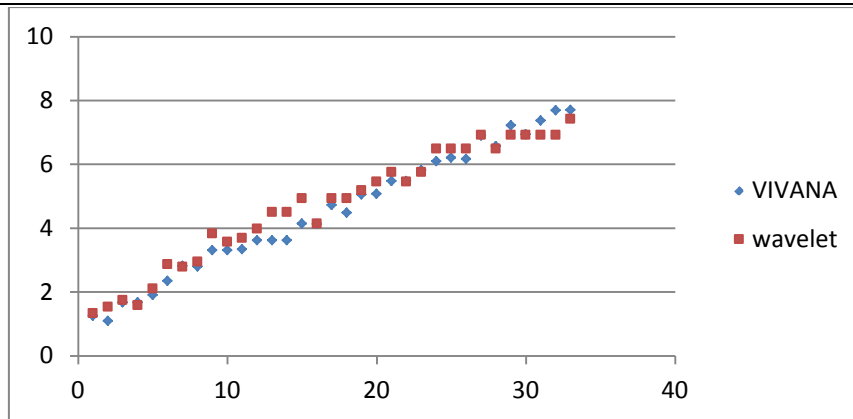


Figure 6.1, Peak frequency values comparison of Hanoytangen

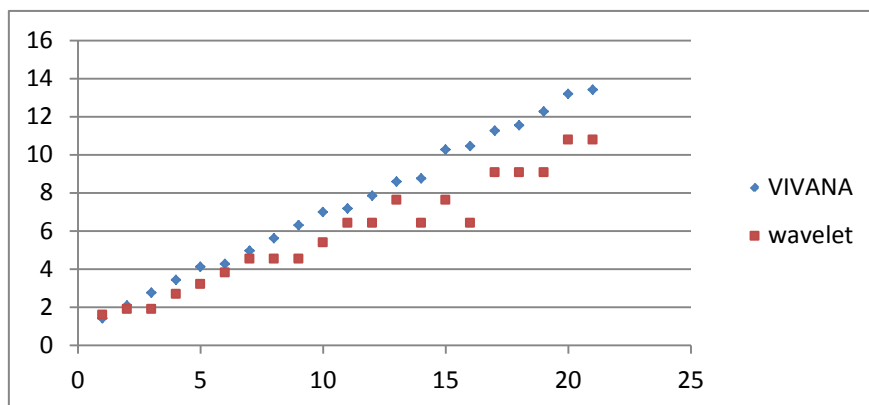


Figure 6.2, Peak frequency values comparison of NDP

### 6.1.2, Linear relationship between peak frequency and towing velocity

Figure 6.3 and 6.4 represent the peak frequency varying with towing velocity, the horizontal axis presents towing velocity and the vertical axis represents peak frequency. Strouhal Frequency ( $St=0.2$ ) was also plotted for controller. Four observations were found from the two figures:

1. The peak frequency always smaller than Strouhal Frequency
2. The VIVANA peak frequencies appear very good linear relationship with towing velocity.
3. For low velocity cases, the wavelet peak frequencies appear good linear relationship with towing velocities; and the estimated peak frequencies are very close to wavelet results; but as the velocity increasing, the difference between wavelet and VIVANA peak frequency becomes larger.
4. For wavelet peak frequencies, several cases with different towing velocity may share a same peak frequency, this observation are very common for VIV with any towing velocity.

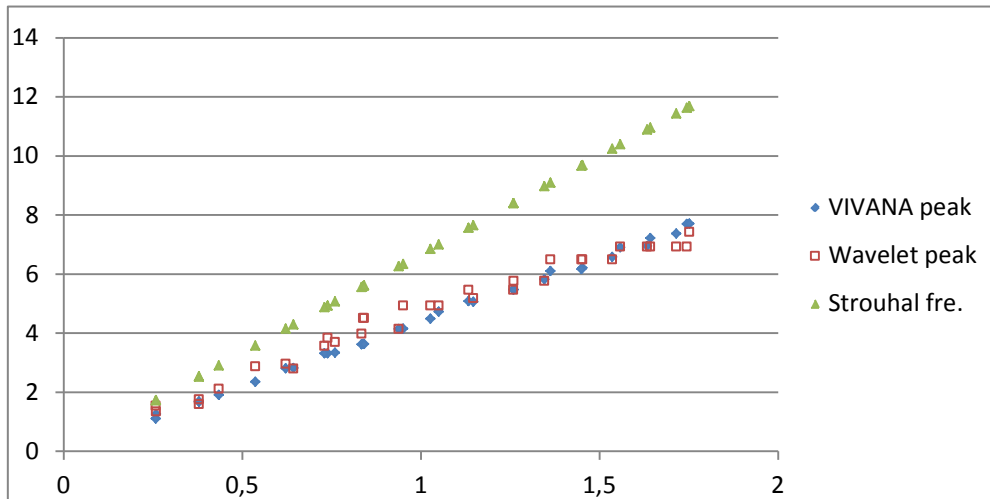


Figure 6.3, peak &amp; Strouhal frequency VS towing velocity-Hanoytangen

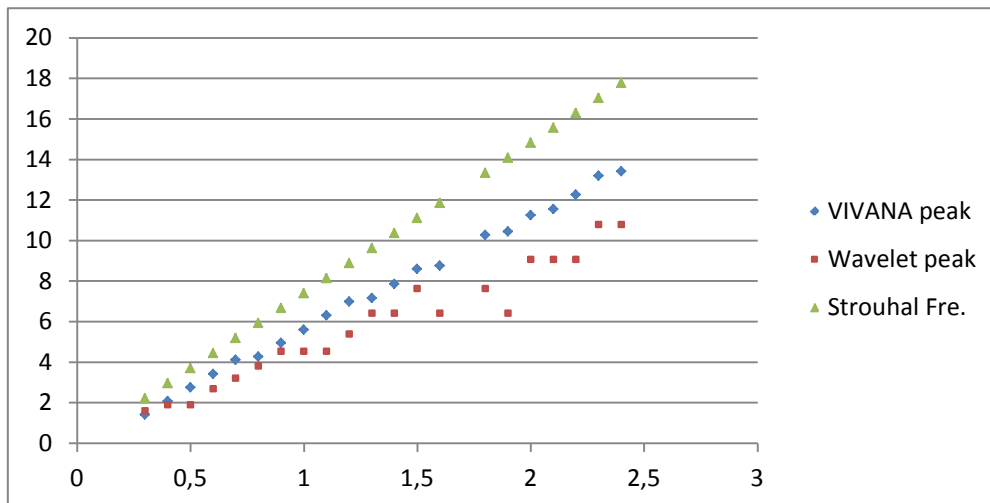


Figure 6.4, peak &amp; Strouhal frequency VS towing velocity-NDP

### 6.1.3, Comparison between similar cases for Hanoytangen

Hanoytangen tests can be sorted into many groups depending on the similarity of velocity and tension value. These groups were shown in Table 6.1, the first column is the group number and column 2 to 4 represents the test number included in the group; “X” means empty.

Table 6.1, classification of Hanoytangen cases

group No.	mem. 1	mem.2	mem.3	vivana	wavelet
1	33	34	X	d	d
2	35	36	X	s	d
3	37	38	X	d	d
4	39	40	X	s	d
5	41	42	43	s	d
6	44	45	46	s	d

7	47	48	X	s	d
8	49	50	X	d	s
9	51	52	X	s	d
10	53	54	X	s	d
11	55	56	57	d	d
12	58	59	X	s	s
13	60	61	X	d	d
14	62	63	X	d	s
15	65	66	X	s	d

The cases in same group have similar tension and velocity value, and thus assumed to be tested under same condition. As stated in Chapter 4, the Hanoytangen test is a large scale test carried out in true ocean environment, which means the parameters like Reynold, current profiles cannot be controlled, but they were ignored here.

In fifth and sixth column of table 6.1, the peak frequency values in a same group were compared; “s” means same and “d” means different. Obviously, most cases by VIVANA analysis get the expected peak frequency (same peak frequency), while only a few of group has same peak frequency for wavelet analysis.

This indicated that the VIV phenomena under real condition is a complex process, the effect factor are much more than tension and towing velocity.

#### 6.1.4, peak frequency shift for different towing velocity

In figure 6.1-6.4, some cases with different towing velocity share the same peak frequency (for wavelet analysis). As known, the active frequency decomposed from wavelet analysis has its corresponding response mode shape. Therefore, this represents the shift of dominating response mode of riser.

## 6.2, Observations for category 2

In present section, the frequency ranges of signals from one specified location were studied. The observations can be classified as following:

- a) The comparison between wavelet and VIVANA
- b) The relationship between frequency range and towing velocity
- c) Linear relationship between frequency range and peak frequency
- d) Frequency range shifting with towing velocity

### 6.2.1, Comparison between wavelet and VIVANA

Figure 6.5&6.6 (NDP) and 6.7&6.8 (Hanoytangen) represent the start and end of



frequency range varying with case number. It can be found that:

1. The frequency range calculated by VIVANA is much wider than wavelet result.
2. The frequency ranges are completely different, and the wavelet range are included in the VIVANA range.
3. The start frequency of frequency range by VIVANA do not vary too much, it is a stable term which is always smaller than wavelet start.
4. The end frequency of frequency range by VIVANA always larger than wavelet, and the difference increase as the increase of velocity.

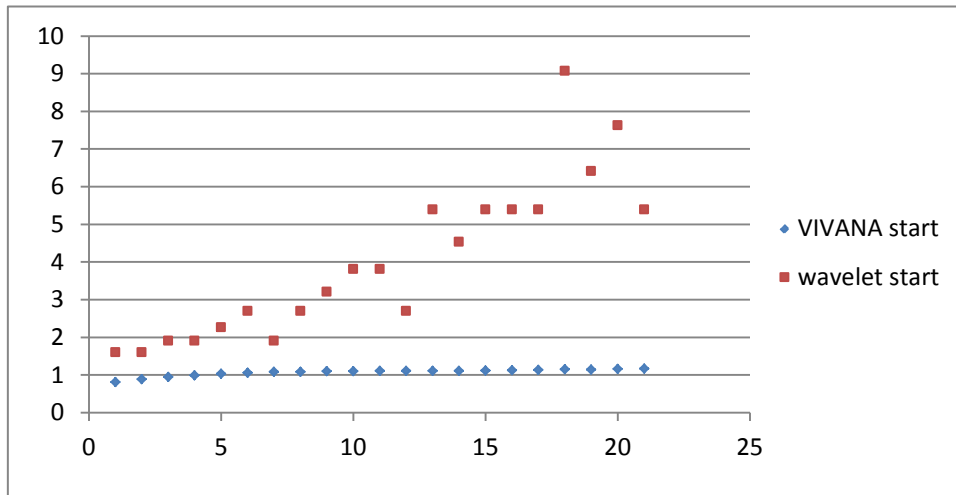


Figure 6.5, start of frequency range varying with case number (NDP)

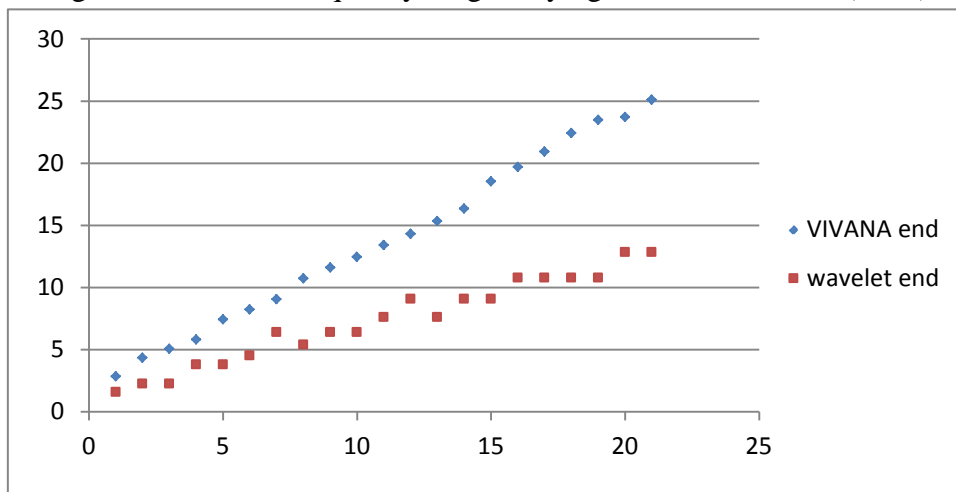


Figure 6.6, end of frequency range varying with case number (NDP)

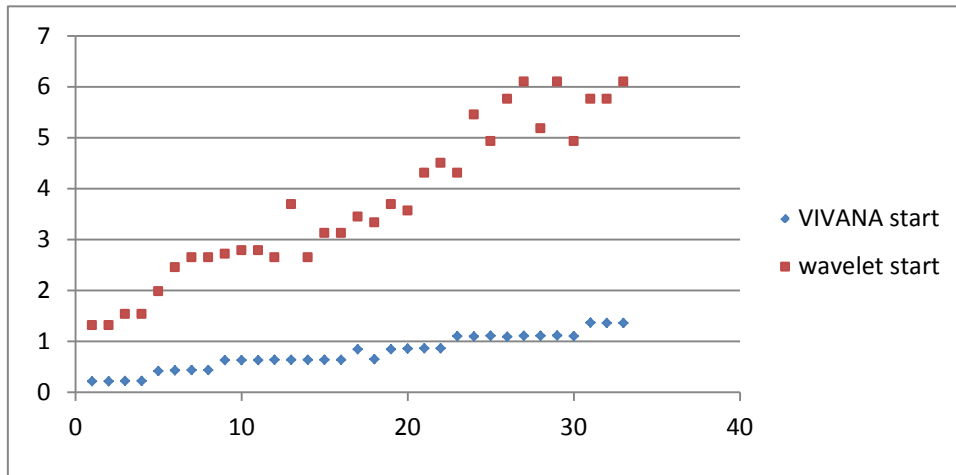


Figure 6.7, start of frequency range varying with case number (Hanoytangen)

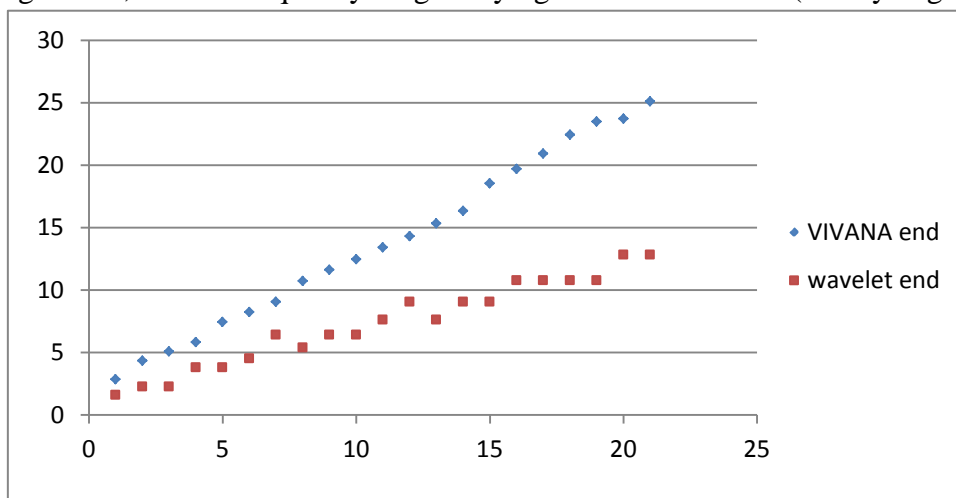


Figure 6.8, end of frequency range varying with case number (Hanoytangen)

### 6.2.2, Relationship between frequency range and towing velocity

Figure 6.9 and 6.10 represent the frequency range varying with towing velocity, some observations were found:

1. The start frequencies of frequency ranges calculated by VIVANA do not vary with towing velocity; while the end frequencies of frequency ranges calculated by VIVANA vary linearly with the increasing of towing velocity.
2. Relationship between towing velocity and frequency range calculated by wavelet is not perfect linear, but the frequency range tends to increase with towing velocity.
3. For start frequencies of frequency ranges calculated by wavelet, several neighboring tests may have the same value; the end frequencies have the same phenomenon. But the value shifting is not synchronous. This exists for both NDP and Hanoytangen.
4. The frequency range goes wider as the increasing of towing velocity.

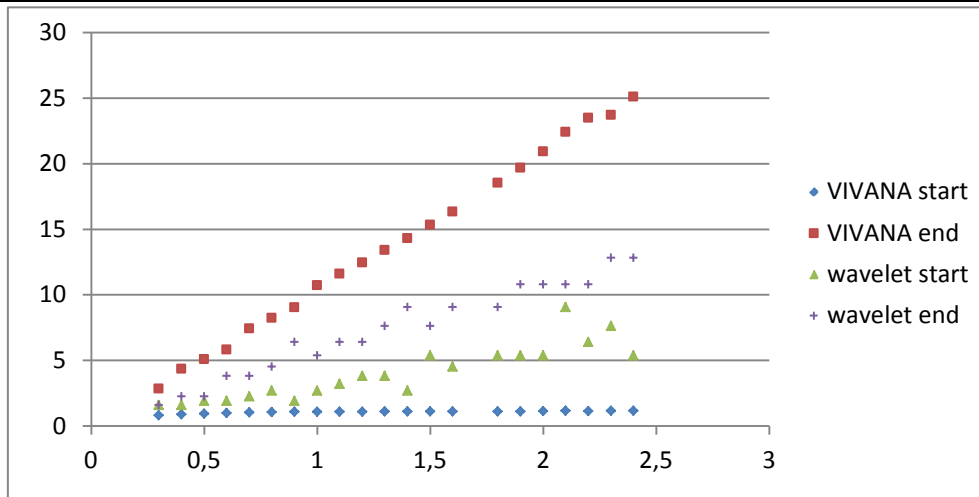


Figure 6.9, frequency range varying with towing velocity (NDP)

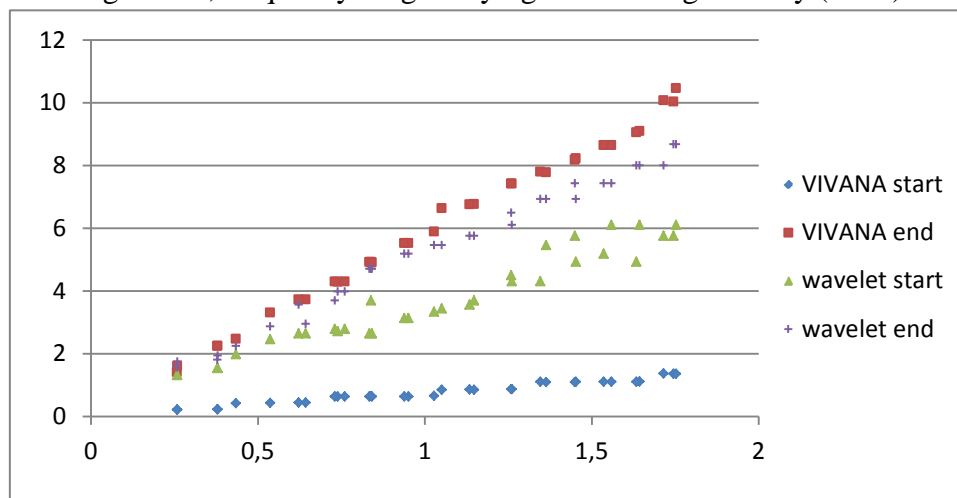


Figure 6.10, frequency range varying with towing velocity (Hanoytangen)

### 6.2.3, Linear relationship between frequency range and peak frequency

In figure 6.11 and 6.12, the wavelet frequency range was plotted varying with corresponding peak velocity. Two observations may be summarized:

1. The start and end frequencies of frequency ranges follow a trend close to linear relationship.
2. The slopes of the start frequencies are different with slopes of the end frequencies, but the difference is not very large.

This observation is only an algebraic relationship, which do not have any theoretical support. But it provides a way to limit frequency range in VIVANA.

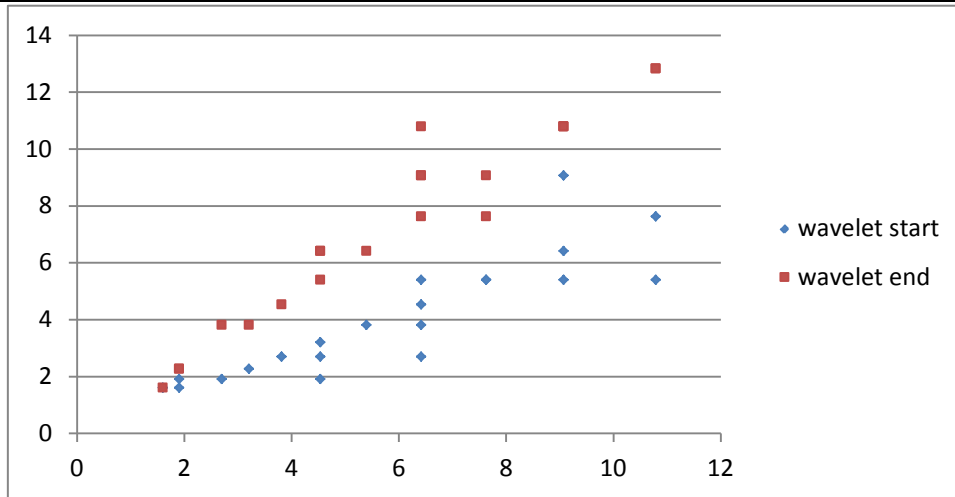


Figure 6.11, frequency range varying with peak frequency for NDP (wavelet)

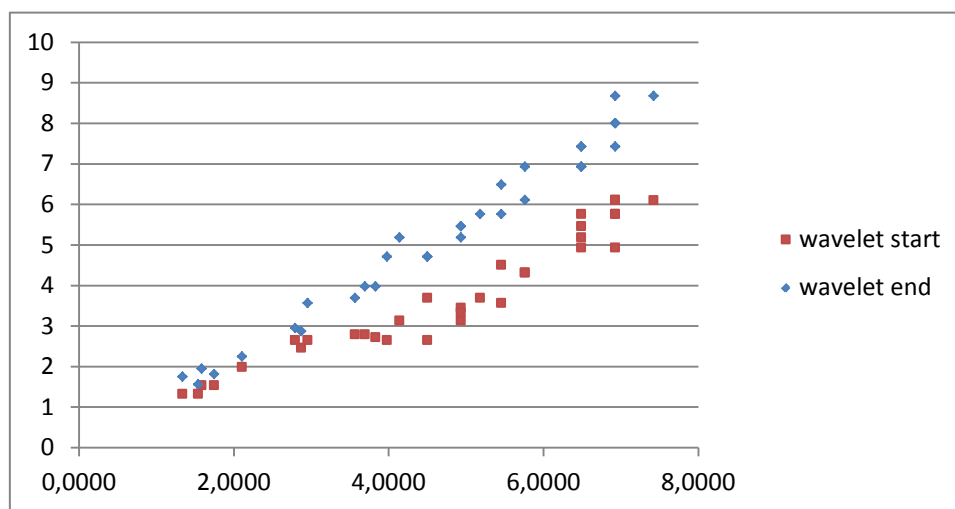


Figure 6.12, frequency range varying with peak frequency for Hanoytangen (wavelet)

### 6.2.4, Frequency shifting with towing velocity

In Figure 6.9 and 6.10, some cases with different towing velocity share the same start or end frequency (for wavelet analysis). As known, the active frequency components of signal from wavelet analysis have its corresponding displacement mode shape. Therefore, this can represent the shift of participating mode.

## 6.3, Observations for category 3

In present thesis, the wavelet results are seen as the true results. Thus, the perfect frequency competition mode should give frequency range as same as the wavelet result, but the VIVANA model is far from perfect.

A test was carried out to evaluate the accuracy of VIVANA frequency competition model. The summations of time durations for VIVANA active frequencies below,

within and above the wavelet frequency range (see Figure 5.1) were calculated for further studying. This test was performed for both Hanoytangen and NDP (same signals as category 1 and 2); the result was shown in Table 6.2 and 6.3, and the percentage varying with case number was plotted in Figure 6.13 and 6.14.

Table 6.2, Percentage based on wavelet frequency range (NDP)

No.	velocity	range wavelet		down(%)	within(%)	up(%)
2310	0.3	1.6043	1.6043	x	x	x
2320	0.4	1.6043	2.2688	20.33	37.96	41.7
2330	0.5	1.9078	2.2688	8.84	24.93	66.22
2340	0.6	1.9078	3.8156	4.43	62.06	33.51
2350	0.7	2.2688	3.8156	2.28	44.92	52.01
2360	0.8	2.6981	4.5376	4.85	46.66	48.5
2370	0.9	1.9078	6.4171	0.67	83.78	15.56
2380	1	2.6981	5.3961	1.77	40.01	58.21
2390	1.1	3.2085	6.4171	1.22	59.91	38.87
2400	1.2	3.8156	6.4171	2.74	33.72	63.54
2410	1.3	3.8156	7.6312	2.03	52.16	45.81
2420	1.4	2.6981	9.0751	0.08	68.83	31.09
2430	1.5	5.3961	7.6312	5.42	32.72	61.86
2440	1.6	4.5376	9.0751	1.95	50.86	47.19
2460	1.8	5.3961	9.0751	2.56	37.33	60.11
2470	1.9	5.3961	10.7922	2.12	51.81	46.07
2480	2	5.3961	10.7922	1.79	46.75	51.46
2490	2.1	9.0751	10.7922	19.05	18.71	62.24
2500	2.2	6.4171	10.7922	2.43	28.11	69.46
2510	2.3	7.6312	12.8342	3.74	49.65	46.61
2520	2.4	5.3961	12.8342	0.46	56.27	43.27

Table 6.3, Percentage based on wavelet frequency range (Hanoytangen)

Test no.	velocity	start	end	down(%)	within(%)	Up(%)
33	0.2592	1.322	1.7487	71.05	28.95	0
34	0.2582	1.322	1.5628	77.52	22.49	0
35	0.379	1.5395	1.8102	36.28	19.3	44.42
36	0.3796	1.5395	1.9472	36.03	38.05	25.92
37	0.4348	1.9847	2.2444	54.6	17.77	27.63
38	0.5369	2.4588	2.8702	51.76	28.01	20.23
39	0.6435	2.6486	2.9525	37.27	12.26	50.47
40	0.6222	2.6486	3.5663	41.08	54.56	4.35
41	0.7397	2.7186	3.98	21.46	64.19	14.36
42	0.7309	2.7923	3.6943	22.5	54.24	23.24
43	0.7601	2.7923	3.98	19.84	63.89	16.26
44	0.8342	2.6486	4.7082	9.06	86.65	4.27

45	0.8389	3.6943	4.7082	57.66	37.8	4.55
46	0.8415	2.6486	4.7082	8.79	86.45	4.75
47	0.951	3.1322	5.1823	11.65	83.58	4.73
48	0.9388	3.1322	5.1823	12.19	83.65	4.15
49	1.0504	3.4469	5.457	11.17	70.14	18.68
50	1.0276	3.3352	5.457	12.77	74.26	12.97
51	1.1477	3.6943	5.7625	14.09	62.26	23.66
52	1.1339	3.5663	5.7625	15.01	53.61	21.36
53	1.2604	4.3136	6.1043	16.5	53.58	29.93
54	1.2591	4.5023	6.4891	21.47	56.86	21.67
55	1.3464	4.3136	6.9258	12.79	71.14	16.07
56	1.3636	5.457	6.9258	33.28	49.22	17.51
58	1.453	4.9339	6.9258	16.32	50.69	32.99
59	1.45	5.7625	7.4254	33.67	56.09	10.23
60	1.559	6.1043	7.4254	33.99	40.2	25.81
61	1.5359	5.1823	7.4254	17.06	58.46	24.46
62	1.6431	6.1043	8.0027	28.22	54.54	17.25
63	1.6336	4.9339	8.0027	10.56	72.15	17.26
64	1.7155	5.7625	8.0027	14.62	60.71	24.67
65	1.7452	5.7625	8.6773	13.63	73.79	12.56
66	1.7525	6.1023	8.6773	17.02	69.3	13.68

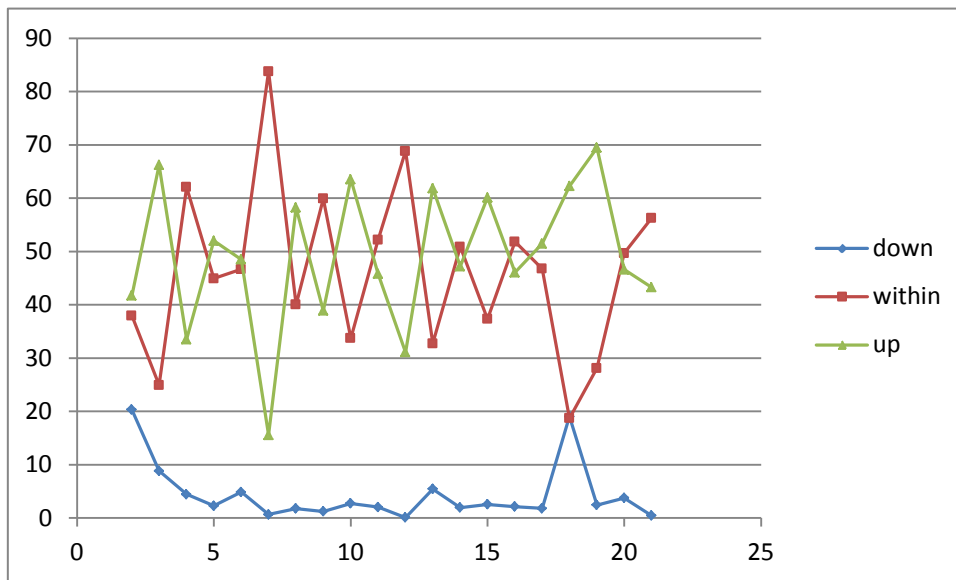


Figure 6.13, percentage varying with case number (NDP)

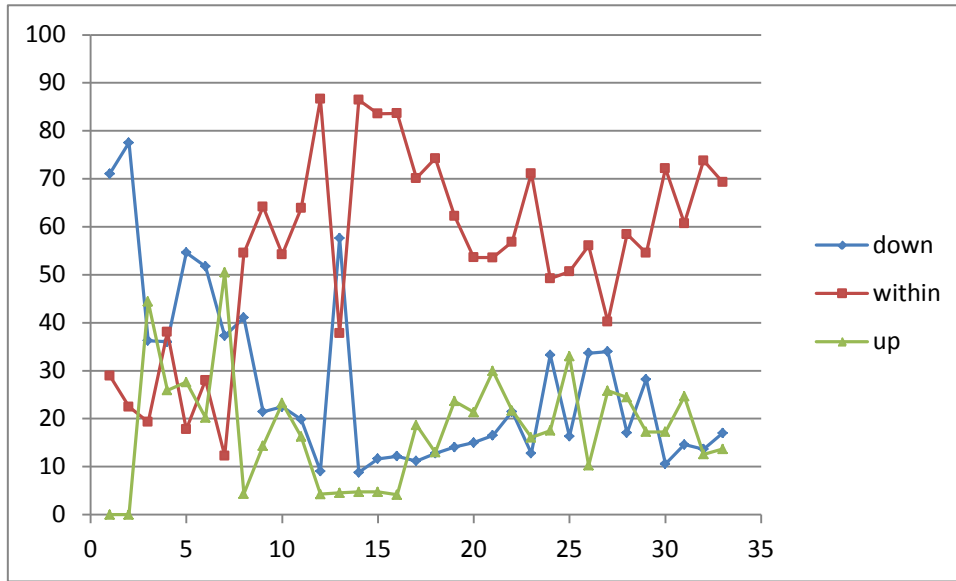


Figure 6.14, percentage varying with case number (Hanoytangen)

The observations can be summarized as below:

1. The average of percentage of time within frequency range is about 50% for NDP and 60% for Hanoytangen, which means that considerable percent of VIV is simulated by wrong frequency.
2. The percentage of time durations under the frequency range is much smaller than the percentage within or above frequency range.
3. The percentage of time duration above the frequency range is quite large for NDP simulation and relatively small in Hanoytangen calculation.
4. The percentage of time durations below, within and above frequency can keep in a stable standard for different cases.

By the calculation equation of time duration:

$$T_i = T \frac{E_i}{\sum_{n=1}^k E_n} \quad (6.1)$$

The time duration represents the energy share of specified frequency. In this case, pretty much of energy was allocated to the frequency which do not participate real response, especially the frequencies above true frequency range. Limiting the top side of frequency range is more important than low side.

## 6.4, Observations for category 4

Excitation length can be gotten by both time sharing and space sharing methods, the available results can be shown in table below.

Table 6.4, excitation lengths

Data	Time sharing method	Space sharing method
NDP	√	×
Hanoytangen	√	√

In present thesis, the purpose of time sharing excitation length is to build a general frequency competition model (time sharing) cooperating with excitation parameter E. Excitation lengths calculated by space sharing method were also recorded for further studying.

### Time sharing

Wavelet frequency range was seen as aim for frequency model, so that the excitation lengths will be discussed in three classes: lengths corresponding to active frequencies (VIVANA result) below, within and above true frequency range. Observations can be summarized below:

1. The excitation lengths increase with the active frequencies; and it turn to going down once the excitation length get the peak value.
2. The active frequency within true frequency range has relatively larger excitation length than the other two set of frequencies. The frequency corresponding to longest excitation length normally locates within true frequency range.
3. The active frequency outside of true frequency range normally has the shorter excitation lengths than frequency within true frequency range.
4. Some excitation length is even shorter than 5% of riser length, which mean it's impossible to dominate the displacement of riser.

### Space sharing

The observations found are:

1. The frequency with largest excitation parameter occupies the whole length of its excitation length, and it's much larger than excitation length of other frequencies.
2. The excitation length corresponding to the frequency with largest excitation parameter always takes the top side of the riser, and it is up to 40% of whole riser.

## 6.5, Observations for category 5

Signals from all measurement point for one specified case were analyzed by wavelet, the test 2420 was selected for NDP and test 51 for Hanoytangen. The Hanoytangen test is large scale experiment under true ocean environment, it can be seen as real response; the NDP test is experiment conducted under lab condition, it's an ideal response. In present section, the observations of NDP and Hanoytangen will be



described respectively.

### NDP test

1. The wavelet results from the first three locations on the top side of riser are completely different with the other locations; and these three results are almost same with each other, see Figure 6.15.
2. Except the first three results, time depended peak frequency are very similar for the other signals. It means that the different cross sections along the riser will oscillate in same peak frequencies simultaneously, see Figure 6.16.
3. Although the time depended peak frequency varying simultaneously, the intensities of the wavelet results are different, and this can be told by color.
4. The dramatic peak frequency shifting do not exist, which may indicate that this VIV response is mono-frequency.
5. The signal of NDP test can be divided into two types, chaotic and stationary. For most of cases, the signals are dominated by chaotic type or combined type. See Figure 6.17.

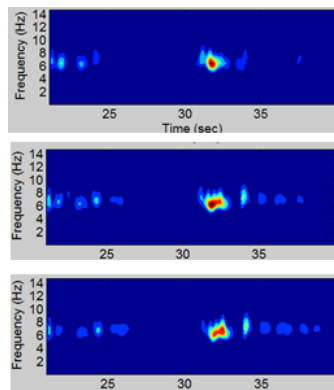


Figure 6.15, the wavelet result from first three measurement locations

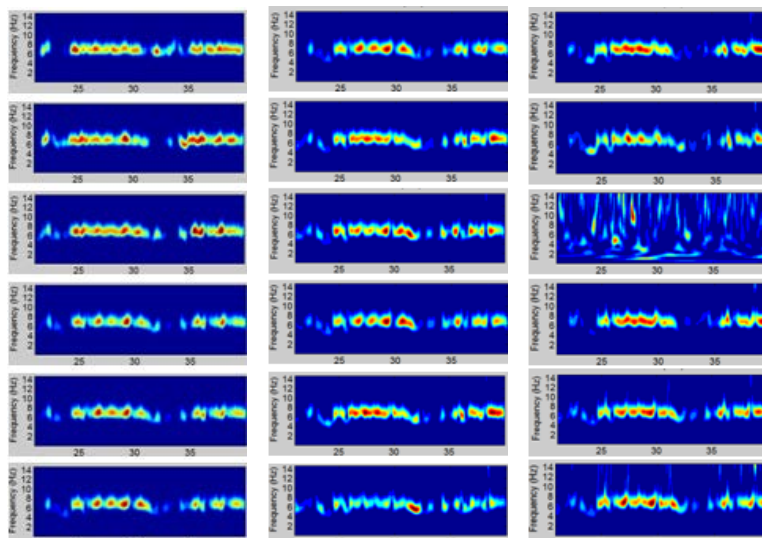


Figure 6.16, wavelet result for measurement locations lower than No.3

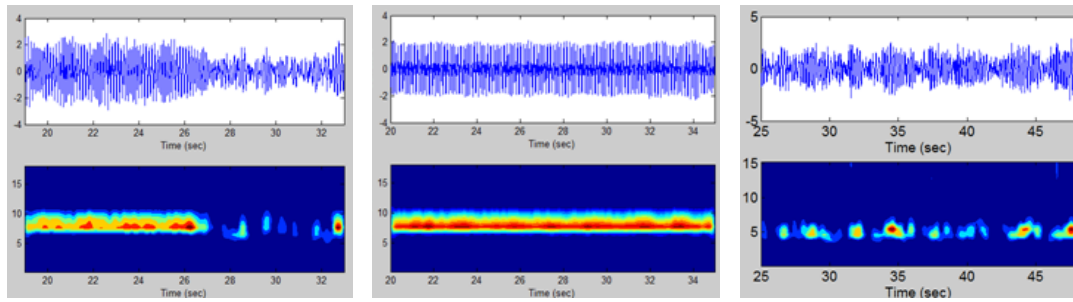


Figure 6.17, chaotic and stationary signals

### Hanoytangen test

1. Different with NDP test, the time depended peak frequencies at different locations are very different.
2. Dramatic peak frequency shifting can be observed, and it often happens. See Figure 6.18.
3. It can be observed that some neighbored measurement points share the same peak frequency history. In other words, these cross sections will oscillations with same peak frequency simultaneously. Figure 6.19 shows this phenomenon.
4. The signals for Hanoytangen test do not contain stationary part, this mean the Hanoytangen test is dominated by chaotic response.

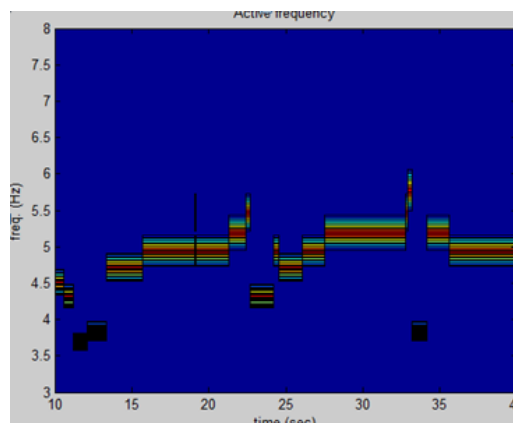


Figure 6.18, peak frequency shifting for Hanoytangen test

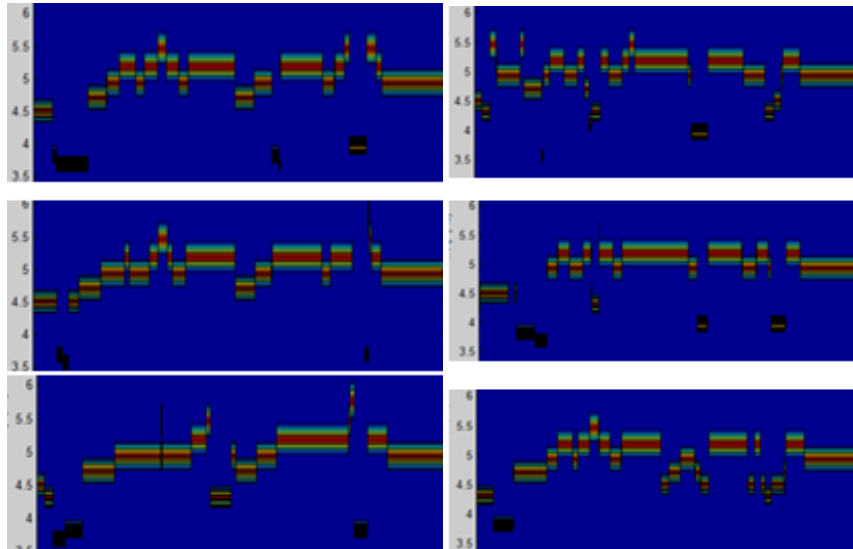


Figure 6.19, wavelet result from two groups of neighbored measurement points

## 6.6, Observations for category 6

The signal at every measurement point of all test cases are analyzed by wavelet analysis, the peak frequency of each signal was detected. In this section, the observations will be discussed in two categories, towing velocity and measurement location.

Mean values and standard deviations of peak frequencies at different measurement points of test are calculated. Figure 6.20 and 6.21 shows the mean peak frequencies of tests vary with towing velocity, and Figure 6.22 and 6.23 shows the standard deviation of peak frequencies vary with tests' towing velocity.

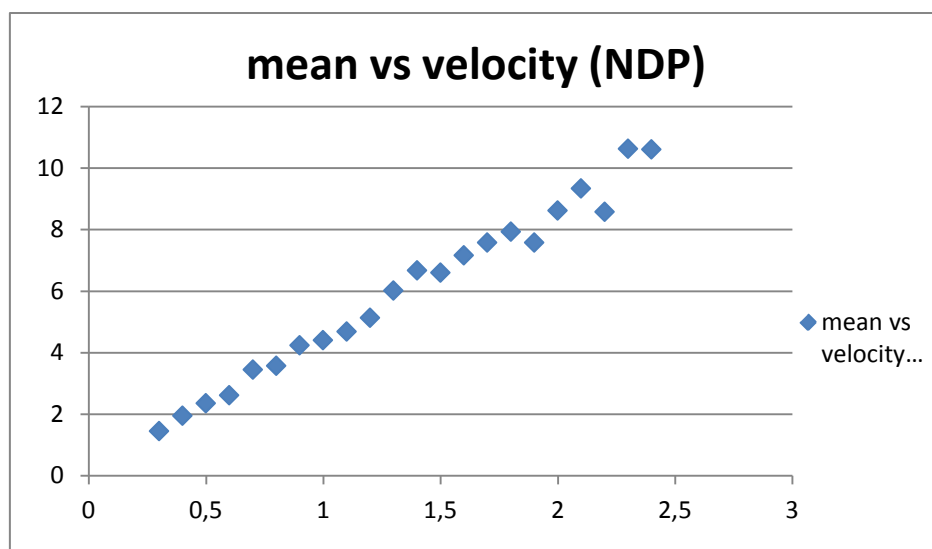


Figure 6.20, mean peak frequency vary with towing velocity

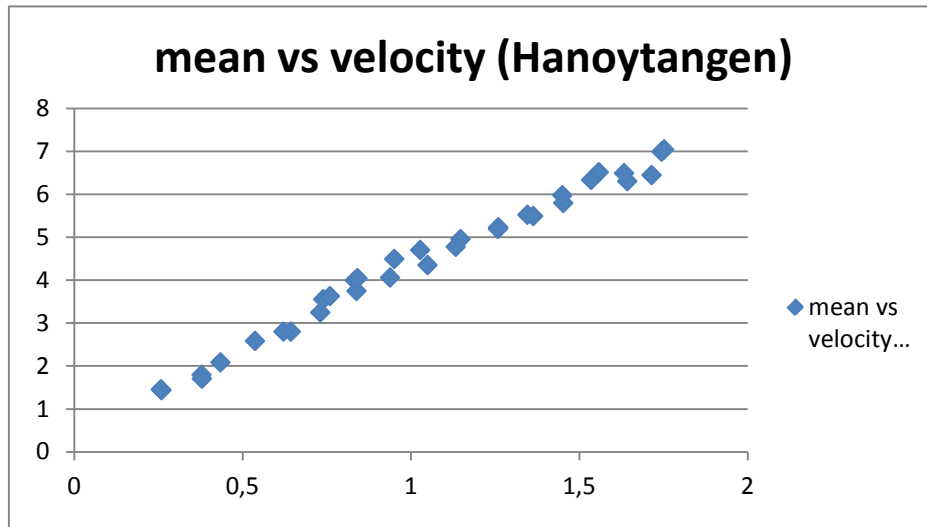


Figure 6.21, mean peak frequency vary with towing velocity

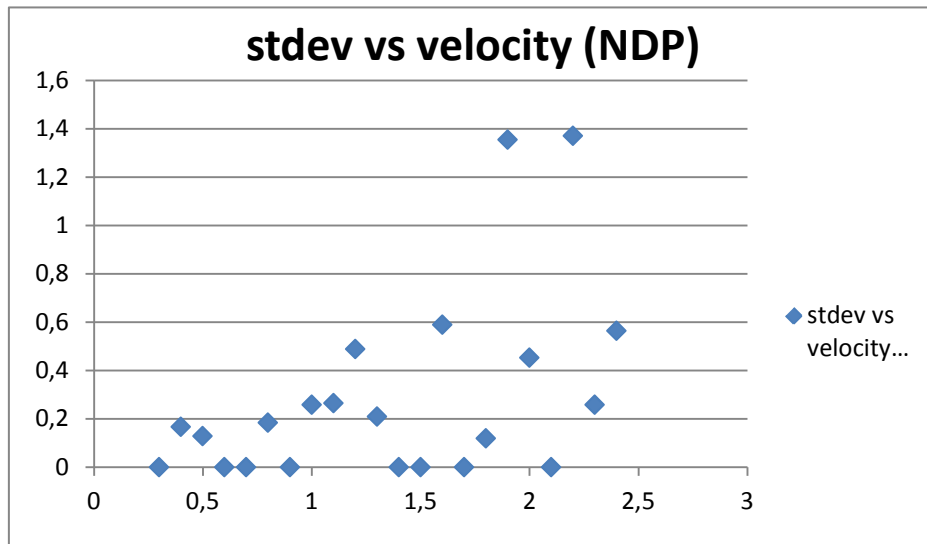


Figure 6.22, standard deviation of peak frequencies vary with towing velocity

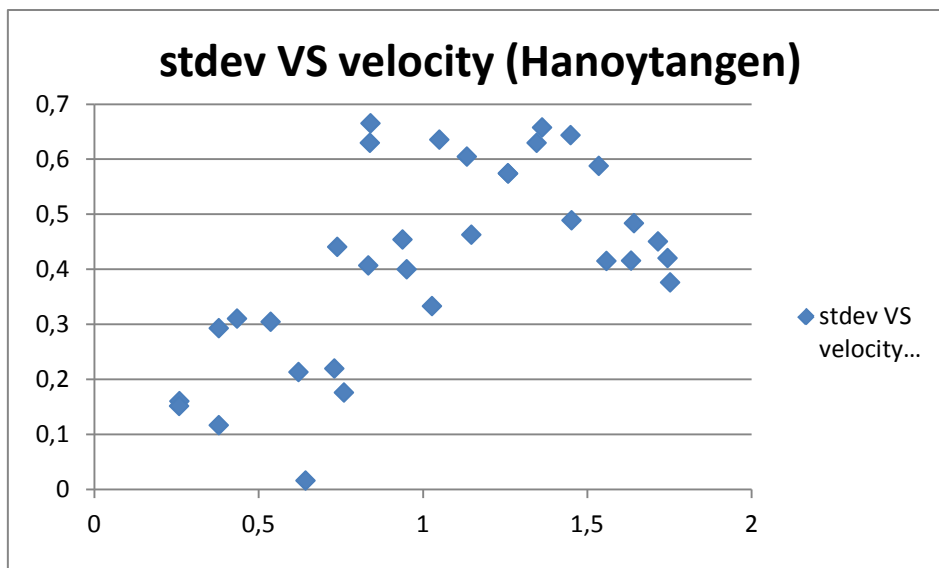


Figure 6.23, standard deviation of peak frequencies vary with towing velocity

### **Compared location by location**

1. In some test, most of locations have the same peak frequency, higher peak frequencies are normally happened at top side of riser, the lower peak frequencies are normally appeared at bottom side.
2. In some case, the peak frequency appears step-like descent with the depth increasing. In other word, several neighbored measurement points have some peak frequency.
3. In several cases, all measurement points on the riser share the same peak frequency.
4. In a few case, the peak frequency decrease with the depth linearly.

### **Compared by towing velocity**

The average value and standard deviation of peak frequencies of all measurement locations under same towing velocity was calculated, and then compared with with towing velocity. The observations are list below:

1. The average peak frequency increasing linearly as the increasing of towing velocity.
2. For test under higher towing velocity, the standard deviation of peak frequencies from different measurement points is larger. In other word, high towing velocity may cause high variation at different locations.

## **6.7, Observations for category 7**

The signal at every measurement point of all test cases are analyzed by wavelet analysis, the frequency range of each signal was detected. The start frequency and end frequency range was studied separately.

The start frequencies and end frequencies were processed in the same way as peak frequency in section 6.6, same observations can be found. Same types of figures are plotted and they can be found in Appendix B Figure B1-Figure B8.

In addition, the frequency range tends to wider as the increasing of towing velocity; and the widths in different location of one test do not have a specified order, the widths are close to each other and vary around one value.

## **6.8, Observations for category 8**

Through displacement history and maximum displacement envelope, observations can



be found as below:

1. The displacement along the riser length shows clear mode when the towing velocity is small.
2. As the increase of towing velocity, the displacement along the riser becomes complicated.
3. Travelling wave dominate most of test, and standing wave and normally found in case with low towing velocity.
4. The displacement of riser is dominated by one major mode during the time of stationary signals, while the displacement modes become complicated once the response shift to chaotic.

# Chapter 7, Attempts to improve frequency model

In this chapter, defects of VIVANA model will be stated first; some ideas from observations in Chapter 6 will be discussed then; some attempts were performed in order to improve frequency competition model.

Although the frequency competition model cannot be established in present thesis, some useful advice will be given in the last of the chapter.

## 7.1, defects of VIVANA model

Both time sharing and space sharing method were carried out. Therefore, defects of VIVANA will be stated in the two methods separately.

### Time sharing method

In section 6.1 and 6.2, the peak frequencies and frequency ranges calculated by VIVANA and wavelet were compared. In present thesis, wavelet results were seen as true value. Based on observations in section 6.1 and 6.2, the defects of VIVANA time sharing method are listed below:

1. Estimated peak frequency is not same as experimental result. In the other word, the time duration based on power cannot estimate peak frequency precisely.
2. VIVANA results contain too many active frequencies than experiments. Most of the active frequencies are too far from estimated vortex shedding frequency.

### Space sharing method

The response frequencies and excitation lengths of space sharing method were measured; the results were compared with wavelet results. Although the wavelet analysis is designed to improve time sharing method, some observation cans found by comparison of frequency components.

1. Too many active frequencies (the value smaller than peak frequency) were included in calculation, most of them are impossible to happen.
2. The frequencies larger than calculated peak frequency (the frequency with largest excitation parameter E) was excluded. The larger frequency represents larger displacement mode, which may cause larger curvature and larger fatigue.

## 7.2, Filter active frequencies by energy limit

As stated in section 7.1, too many frequencies were included in time sharing calculation, and some of them are impossible to happen. These extra frequencies do not participate in the real VIV phenomenon, it's necessary to found a way to filtrate these frequencies.

Time duration calculation for VIVANA time sharing method was introduced in Chapter 3. The time duration represents the percentage of excitation parameter of the sum of all excitation parameters, in other word, the time duration can be seen as the scale of energy content in the active frequency.

By observation of VIVANA, the time durations of active frequencies in the beginning or ending of active frequency range are normally very small. In addition, these frequencies are too far from true frequency range and do not participate true vortex. Therefore, it's feasible to set a limitation to filtrate these frequencies.

Figure 7.1 and 7.2 is a typical time duration distribution varying with frequency. Obviously, lots of active frequencies are concentrated in the beginning side of frequency range, and the limitation 2% was selected to filtrate these frequencies.

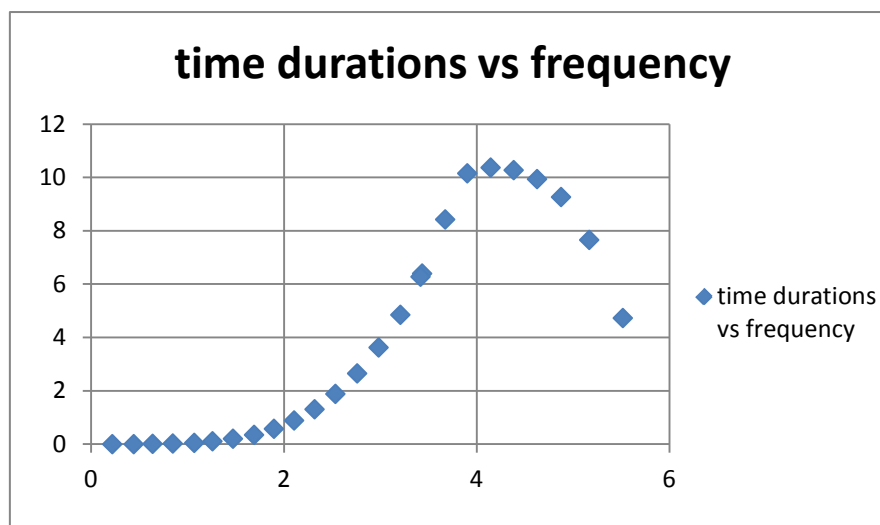


Figure 7.1, the time duration distribution of test 47 calculated by VIVANA



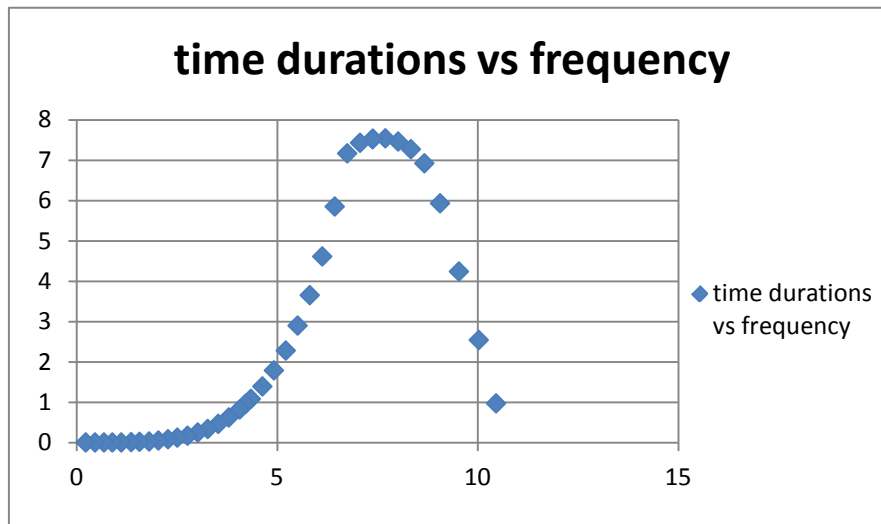


Figure 7.2, the time duration distribution of test 66 calculated by VIVANA

The frequencies with time duration less than 2% will be ignored in future calculation, and this limitation will reduce considerable number of active frequencies, some frequencies in larger side of frequency range will also be filtrated. For test under slow towing velocity, the reduced frequencies are about 1/4 of overall calculated frequencies; for test under high towing velocity, the reduced frequencies may up to 1/2 of active frequencies,

By calculation of several cases, the sum of time durations corresponding to reduced frequencies are normally less than 10%, that is the excitation power contained in these frequencies are not important.

The reduced frequencies represent low mode response, which means the curvature generated by these active frequencies are quite small, thus they do not contribute too much to fatigue. Once these frequencies were ignored, the time durations corresponding to other frequencies have to be reallocated based on excitation length). Time durations for other frequencies will increase, which will take higher mode response and increase the fatigue estimation.

By energy limit, the extra active frequencies with small values and extreme high values will be avoided. By observation of Figure 6.12 and 6.13, the sum of time durations below true frequency range is small compared with the sum of time durations above true frequency range. So the limit at the top side is more important.

## 7.3, Excitation parameter and excitation length

### 7.3.1, Motivation

Excitation parameter is defined as:

$$E_i = \int_{L_{e,i}} U_N^3(s) D^2(s) \left(\frac{A}{D}\right)_{C_e,CF=0} ds \quad (7.1)$$

Where  $L_{e,i}$  is the excitation length, and the  $E$  is integral value along the excitation length  $L_{e,i}$ . In VIVANA, the  $E$  is the only parameter to scale the time duration:

$$T_i = T \frac{E_i}{\sum_{n=1}^k E_i} \quad (7.2)$$

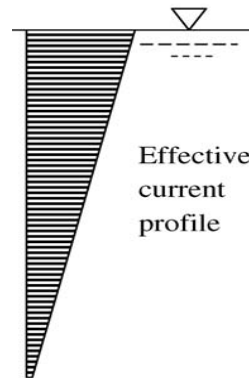


Figure 7.3, Shear current profile

However, this may induce a new issue. For riser subjected to linearly shear current (Figure 7.3), the water flow velocity change with depth linearly. So that the reduced velocity along the riser varying with velocity. Which means that the parameters  $U_N$  and  $\left(\frac{A}{D}\right)_{C_e,CF=0}$  will varying with depth. Therefore, it's possible that the frequency with shorter excitation length may have higher excitation parameter than frequencies with much longer excitation length. However, it's also possible that the excitation length is too short to dominated whole riser. This indicate that the excitation length have to be considered as an important parameter for frequency model.

Take NDP test2500 as an example. Table 7.1 shows the response frequencies, corresponding excitation lengths and time durations estimated by VIVANA. The frequencies with yellow color belong to the frequency range calculated by wavelet (true range), red numbers represent the true peak frequency, and the one with green color is the peak frequency calculated by VIVANA.

The frequency No. 16 (VIVANA peak) has maximum  $E$  by VIVANA, but its excitation length is not longest. In contrast, the frequency No. 12 (true peak frequency) has the smaller  $E$ , but the excitation length is longer. Although the difference between the two lengths is not too large, but it indicates that the excitation length should be considered together with excitation parameter.

Table 7.1, NDP test2500 by VAVINA

test2500	Fre.	time dur.	length
1	1.14	0	2.539
2	2.0473	0.01	4.374
3	2.9763	0.06	6.483
4	3.7881	0.16	8.306
5	4.6895	0.37	10.236
6	5.4847	0.69	11.947
7	6.2251	1.14	13.656
8	6.9489	1.79	15.298
9	7.6586	2.63	16.811
10	8.338	3.71	18.359
11	8.9938	5.08	19.988
12	9.6516	6.72	21.397
13	10.3351	8.2	21.66
14	10.9899	8.56	20.673
15	11.6127	8.78	19.748
16	12.2611	8.89	18.736
17	12.9056	8.83	17.682
18	13.7754	7.99	16.452
19	14.8314	6.76	14.685
20	15.978	5.8	12.949
21	17.1716	4.81	11.012
22	18.3856	3.74	9.168
23	19.6225	2.6	7.062
24	20.8853	1.67	5.226
25	22.1739	0.84	3.084
26	23.4911	0.19	0.767

### 7.3.2, Tests to consider excitation parameters with excitation length

Known that the excitation length may influence the active frequencies, it's necessary to create a new way to consider excitation length and excitation parameter together. Lots of ideas were considered and some were attempted; all of the tests are only based on available values, they cannot be taken as an available model because the lack of theoretical support. But it's helpful to present these ideas here.

The purpose of these tests is to narrow the active frequencies range calculated by VIVANA. Energy limit mentioned in section 7.2 can reduce the most of extra frequencies in the lower side, and the tests here were expected to limit the higher side.

### Multiplication

A new parameter F was attempted to rank the frequency instead of excitation parameter  $E_i$ :

$$F = E_i * L_{e,i} \quad (7.3)$$

Several cases from Hanoytangen and NDP test were selected and calculated. Test 50 and test 2500 are taken as examples here.

Test2550 (NDP) is shown in Table 7.2, the fifth column represent the F; and the sixth column is the value in column 5 divided by sum of column 5. Elements in 2<sup>nd</sup>, 3<sup>rd</sup> and 4<sup>th</sup> column marked in yellow are belong to true frequency range (calculated by wavelet), true peak frequency was marked in red.

Table 7.2, Test 2500 by VIVANA

test2500	Fre.	Time dur.	length	F.	perc
1	1.14	0	2.539	0	0
2	2.0473	0.01	4.374	0.04374	2.59E-05
3	2.9763	0.06	6.483	0.38898	0.00023
4	3.7881	0.16	8.306	1.32896	0.000787
5	4.6895	0.37	10.236	3.78732	0.002244
6	5.4847	0.69	11.947	8.24343	0.004884
7	6.2251	1.14	13.656	15.56784	0.009223
8	6.9489	1.79	15.298	27.38342	0.016222
9	7.6586	2.63	16.811	44.21293	0.026192
10	8.338	3.71	18.359	68.11189	0.040351
11	8.9938	5.08	19.988	101.539	0.060153
12	9.6516	6.72	21.397	143.7878	0.085182
13	10.3351	8.2	21.66	177.612	0.10522
14	10.9899	8.56	20.673	176.9609	0.104835
15	11.6127	8.78	19.748	173.3874	0.102718
16	12.2611	8.89	18.736	166.563	0.098675
17	12.9056	8.83	17.682	156.1321	0.092495
18	13.7754	7.99	16.452	131.4515	0.077874
19	14.8314	6.76	14.685	99.2706	0.05881
20	15.978	5.8	12.949	75.1042	0.044493
21	17.1716	4.81	11.012	52.96772	0.031379
22	18.3856	3.74	9.168	34.28832	0.020313
23	19.6225	2.6	7.062	18.3612	0.010877
24	20.8853	1.67	5.226	8.72742	0.00517
25	22.1739	0.84	3.084	2.59056	0.001535
26	23.4911	0.19	0.767	0.14573	8.63E-05
Sum				1687.958	1

The percentage larger than 1% in sixth column was marked in yellow color, and the frequencies with relatively large value are marked in blue. Some observations can be

found:

1. The active frequencies with relatively large value of F (marked in blue, No.12 to 17) are deviate from the true frequency range (No.8 to 14).
2. If the frequencies with ignorable F (value smaller than 1%) were filtrated, the frequency range left was still much larger than true range.
3. After filtration of ignorable F, the frequency range at top side still include too much active frequencies.

Test 50(Hanoytangen) is shown in Table7.3, and the content of each column is same as Table 7.2. The relatively large percentages in sixth column are marked in blue, and the elements larger than 1% in sixth column are marked in yellow.

Table 7.3, Test50 by VIVANA

test50	frequency	duration	length	x	perc.
1	0.2264	0	1.62	0	0
2	0.4502	0	3.6	0	0
3	0.6522	0.01	5.04	0.0504	2E-05
4	0.859	0.02	6.66	0.1332	5.29E-05
5	1.0926	0.04	8.64	0.3456	0.000137
6	1.2804	0.08	10.26	0.8208	0.000326
7	1.507	0.16	12.24	1.9584	0.000778
8	1.7203	0.28	14.22	3.9816	0.001583
9	1.9246	0.44	15.84	6.9696	0.00277
10	2.1399	0.68	17.64	11.9952	0.004768
11	2.3611	1.01	19.44	19.6344	0.007804
12	2.5839	1.45	21.24	30.798	0.012241
13	2.8081	2.03	23.04	46.7712	0.01859
14	3.0376	2.79	24.84	69.3036	0.027545
15	3.273	3.78	26.82	101.3796	0.040294
16	3.4551	4.72	28.44	134.2368	0.053353
17	3.5116	5.05	28.98	146.349	0.058167
18	3.745	6.58	30.96	203.7168	0.080969
19	3.9891	8.56	33.3	285.048	0.113294
20	4.2321	10.03	32.76	328.5828	0.130597
21	4.4815	10.2	29.34	299.268	0.118946
22	4.7305	10.11	25.92	262.0512	0.104154
23	4.9808	9.81	22.5	220.725	0.087729
24	5.2402	9.2	18.9	173.88	0.06911
25	5.5355	7.87	14.94	117.5778	0.046732
26	5.8936	5.1	9.9	50.49	0.020068
sum				2516.067	1

By observation of Table 7.3:

1. The frequencies with relatively large  $F$  in sixth column are included in true frequency range.
2. If the ignorable frequencies were filtrated, the remaining frequency range is very close to true frequency range.
3. The filtrated frequency range at the top side is similar with true value. However, because the estimation of frequency range at top side is pretty good for Hanoytangen test, this cannot prove that  $F$  is feasible parameter.

In sum, the  $F$  is not a feasible parameter to limit the frequency range.

## 7.4, Method combined time sharing and space sharing strategy

By observations of wavelet results of VIV response signals, it's easy to found that VIVANA model is far from representing all features of VIV. It's found that the features regard time sharing and space sharing are observed in real VIV responses. Thus, it's possible to propose a method combined both methods.

### 7.4.1, VIVANA methods VS observations

It's necessary to state observations in real condition, which can represent the features of both time sharing and space sharing method. This will be described in time sharing and space sharing.

#### Space sharing

As stated in Chapter 6, the peak frequency (dominate modes) at different location along the riser often appear step-like descent with increasing of depth. That is, some neighbored points have same peak frequency (dominating mode); and from top to bottom along the riser, the peak frequency tend to decrease.

#### Time sharing

Stated in section 6.5, signals from neighbored measurement point may have the same time depended peak frequency simultaneously. This can be assumed that this part of riser (corresponding to neighbored points mentioned above) is totally dominated by peak frequency, and the shifting of the frequency at different location of this part is synchronous.

Based on these observations, a new approach combined time sharing and space shearing method may be considered.

### 7.4.2, overview of the method

In this method, Active frequency calculated by VIVANA will be filtrated by energy limit first; then excitation lengths will be defined base on space sharing method; within each excitation zones, response will be simulated by time sharing method.

The energy limit (see section 7.2) will be performed to reduce the frequency range. Because the excitation zones are divided based on space shearing method, active frequencies (by VIVANA) which is larger than peak frequency (the frequency with maximum excitation parameter) will be ignored. However, in order to estimate the higher mode donation, the higher frequencies will be considered in the excitation zone corresponding to peak frequency (at the top of the riser).

Because some frequencies, which have excitation zones at bottom of riser, were filtrated by energy limit, part of riser will be out of excitation zone as a result. Here, the missed part was emerged by the lowest excitation zone (the excitation zone at the lowest part).

Then, time sharing method will be used in every excitation zone.

### **7.4.3, Active frequencies**

By VIVANA, the active frequencies can be got. The number of active frequencies is normally too large, a method have to chosen to limit the participating frequencies.

Energy limit is a possible candidate, although it is not good enough. The frequency will be deleted if its time duration (based on excitation parameter) smaller than 2%. See section 7.2 for more detail.

### **7.4.4, dividing the excitation zones**

The excitation zone will be divided based on space sharing method. As some small frequencies were filtrated by energy limit, bottom side of the riser will be out of excitation zones. Thus, this part will be emerged with lowest excitation zone, and dominated by smallest active frequencies (after filtrating). After all, the excitation zone at top and bottom will be relatively longer than the others.

### **7.4.5, time sharing in each excitation zone**

For different excitation zones, that part of riser is assumed to oscillating independently. Time shearing method was selected for estimation.

To carry out the time sharing method, active frequencies corresponding to each zone have to be defined. Because frequencies which is larger than peak frequency (the frequency with maximum excitation parameter) are ignored by space sharing method

when dividing the excitation zones, so that the higher mode responses were missed in calculation. It will cause the under-estimation of response. Here, the active frequencies will define by:

1. For the excitation zone at top side of riser, only frequencies larger or equal than peak frequency (with maximum excitation parameter) were included.
2. For other excitation zones, the all frequencies (frequencies belong to filtrated range and smaller than peak frequency) were included.

#### **7.4.6, Summary**

This is only frame of new method, and lots of problems have to be solved for further work. Also, no result is available for comparison in present thesis. It's possible that this approach is infeasible or goes against theory.



## Chapter 8, Frequency and response mode

In this chapter, two tests were conducted to study the frequencies gotten from wavelet analysis. The relationship between cross section oscillation frequency and eigenfrequency of whole riser length response will be studied.

### 8.1, Frequency gotten from wavelet analysis

The purpose of this section is to find the relationship between the frequencies gotten from wavelet analysis and eigenfrequencies (for basic mode shapes). From the VIVANA theory manual, the active frequencies are gotten by iteration based on eigenfrequency in still water, and it is another interesting result for comparison. In present thesis, the wavelet analysis results were compared with the active frequencies and eigenfrequencies (in still water). It is expected that the wavelet result and eigenfrequency in real condition are equivalent, and the wavelet results not only represent the oscillation frequency of cross sections, but also related with response of global riser.

Now, it's interesting to know the difference among eigenvalues in still water, eigenvalue in still water and eigenvalue by iteration. NDP data was used in present section.

#### 8.1.1, Eigenfrequencies VS wavelet result

The wavelet result contains many frequency components, one have to be chosen for comparison. In this test, the peak frequency was considered to dominate the response. The results are available from previous works.

Each basic eigenmode has an eigenfrequency in still water, and the eigenfrequency corresponding to dominating response mode will be selected for comparison. The dominating displacement mode can be found by root-mean-square of displacement history (by modal analysis method, see Chapter4) along the riser. Therefore the eigenfrequency in still water can be gotten.

The response frequency corresponding to the dominating displacement mode can be found in VIVANA result file. If the dominated displacement mode is  $n$  (by rms of displacement history), the iterated eigenfrequency frequency is No. $n$  active frequency.

Several cases with clear displacement mode in root mean square result were chosen for studying. The results were shown in Table 8.1; Table 8.2 shows the value difference between these values.

The first column is test number; the second is the towing velocity of case; the third column represents the dominating displacement mode observed from RMS of displacement history along the riser; the fourth column is the peak frequency found by wavelet analysis; the fifth column is the iterated response frequency for dominating mode; the last column is the eigenfrequency estimated under still water.

Table 8.1, Eigenfrequency VS wavelet result

test No.	velocity	Dom. Mode	wavelet	VIVANA	eigen. Freq.
2340	0.6	4	2.6981	2.9364	3.6257
2350	0.7	5	3.4388	3.6045	4.5333
2380	1	8	4.8632	5.6075	7.2409
2410	1.3	9	6.0109	6.61	8.104
2420	1.4	10	6.6627	7.3	8.95
2460	1.8	11	7.92	8.4701	9.88
2500	2.2	12	9.0751	9.6516	10.91

Table 8.2, differences with true value

test No.	velocity	Dom. Mode	VIVANA	eigen freq.
2340	0.6	4	0.2383	0.6893
2350	0.7	5	0.1657	0.9288
2380	1	8	0.7443	1.6334
2410	1.3	9	0.5991	1.494
2420	1.4	10	0.6373	1.65
2460	1.8	11	0.5501	1.4099
2500	2.2	12	0.5765	1.2584

### 8.1.2, Comparison and some observations

Assume the free oscillating system without damping, the dynamic equations is:

$$m\ddot{u} + ku = 0 \quad (8.1)$$

Then the eignefrequency of the system can be simplified as:

$$\omega^2 = \frac{k}{m} \quad (8.2)$$

Assuming the stiffness  $k$  keep the same, with increase of mass (due to added mass), the eigenfrequency will decrease. Figure 8.1 shows the three sets of results in table 8.1.

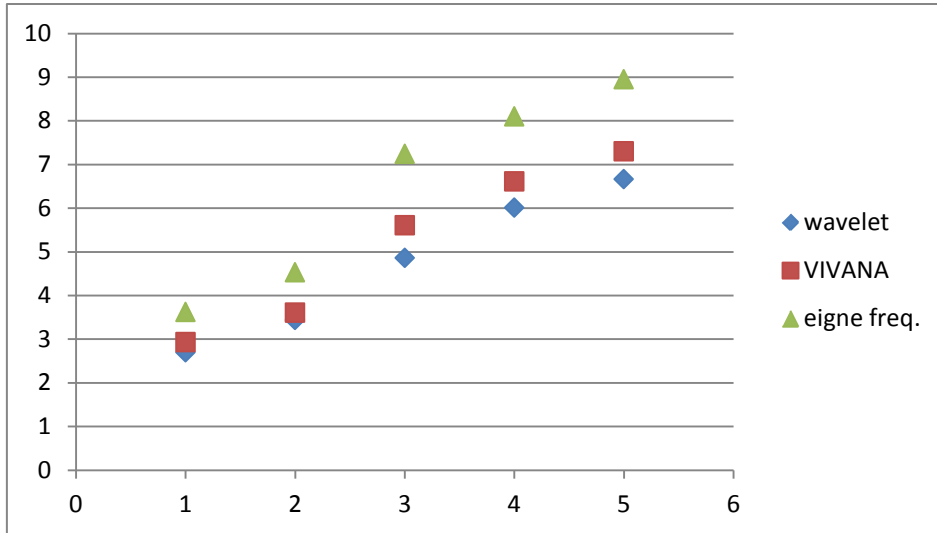


Figure 8.1, Eigenfrequencies

The added mass was related with frequency. Figure 8.2 shows 2-D added mass for circular with axis in the mean water plane varying with oscillation frequency. The  $A_{33}$  shows the added mass in sway direction, and added mass coefficient  $A_{33}$  goes to infinite when frequency is very small, and goes to 1 when frequency goes to infinite (linearly).

Obviously, the added mass coefficient in VIV does not follow Figure 8.2 by observations of Table 8.2. It represents the complicity of VIV.

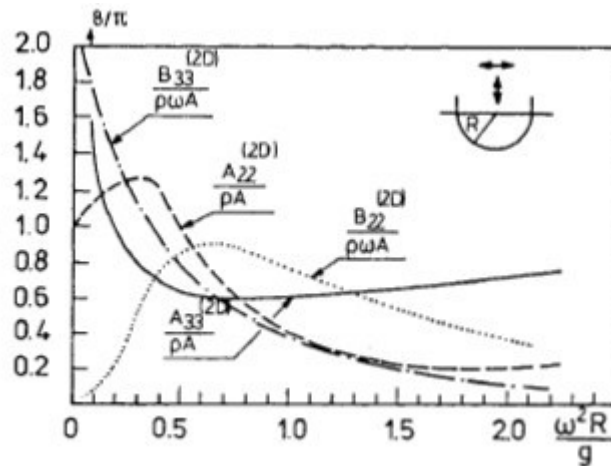


Figure 8.2, two dimensional added mass and damping in heavy and sway for circular cylinder with axis in the mean water plane.

Some observations can be gotten from Table 8.1 and 8.2:

1. The eignefrequencies from iteration of VIVANA always higher than peak frequency in wavelet result. But the difference is reasonable.
2. The difference between eigenfrequency in still water and true response value are quite different, which mean the added mass is very important for VIV

## 8.2, Studying of single mode displacement signals

The response history gotten from modal analysis will be decomposed into several response histories, which corresponding to each participating mode. These response histories will be analysis by wavelet tool to check the frequency components. Some advice will be given by observations.

### 8.2.1, Motivation

At the beginning, the decomposed signals corresponding to single response mode was supposed to have only one frequency component, which is the eigenfrequency corresponding to the response mode (real condition). The eigenfrequencies can be found by spectrum analysis and wavelet analysis for further study.

However, the result is completely opposite. More than one frequency components are contained in decomposed signals.

### 8.2.2, Decomposition of displacement history

Modal analysis method is stated in Chapter 4, the displacement history can be found by:

$$d = \sum_{n=i}^j \omega_n(t) \varphi_n(z) \quad (8.3)$$

Where  $\omega_n(t)$  is the weight factor, and  $\varphi_n(z)$  is the known modal shapes; modes between  $i$  and  $j$  ( $i, j$  included) are participating modes.  $\omega_n(t)$  and  $\varphi_n(z)$  can be written as:

$$\omega(t) = [\overline{\omega_1(t)}, \overline{\omega_{i+1}(t)}, \dots, \overline{\omega_j(t)}] \quad (8.4)$$

$$\varphi(z)^T = [\overline{\varphi_1(z)}, \overline{\varphi_{i+1}(z)}, \dots, \overline{\varphi_j(z)}] \quad (8.5)$$

And the decomposed displacement signals are:

$$d_i = \omega_i(t) \varphi_i(z) \quad (8.6)$$

$$d_{i+1} = \omega_{i+1}(t) \varphi_{i+1}(z) \quad (8.7)$$

.....

$$d_j = \omega_j(t) \varphi_j(z) \quad (8.8)$$

Decomposed displacement signals  $d_i$  to  $d_j$  can be analyzed by wavelet to get the peak frequency and power spectrum density.

### 8.2.3, The frequency components

Test 2420 was selected as an example. Information of the test is shown in table 8.3.

Table 8.3, information of test 2420

number	Time	velocity	modes
test2420	21-40	1.4	6 to13

8 mode shapes are selected to simulate the displacement, from mode 6 to mode 13. Thus, eight decomposed displacement were available, both wavelet analysis and power spectrum density analysis are performed on the eight data. The results can be found in Appendix C.

The results are completely different with expectation, more than one frequency components were found, and the frequency components included in each decomposed signal are similar.

#### 8.2.4, Explanation for the result

This unexpected result, there are two possible explanations, one is by Rayleigh-Ritz method, and another is that the response is a mono-frequency. It cannot determine which one is correct and the ideas behind the two explanations are shown below.

##### Rayleigh-Ritz

The Rayleigh-Ritz method is a good way to explain the results gotten above. For Rayleigh-Ritz method, it's not necessary to know the mode shape itself, but it's possible to calculate it. The shape functions are expressed as a weighted sum of known base functions. The weighting for each base function is unknown, but it can be calculated by iteration.

Assume that a good estimate of a mode shape can be written as [9]:

$$\Psi(x) = \sum_{i=1}^N \varphi_i(x)q_i \quad (8.9)$$

Here the  $\varphi_i(x)$  is known shape functions (basic mode shapes) and  $q_i$  is an unknown weighting. The weighting determines the contribution from each known shape function, and it will be calculated such that the sum gives the best possible approximation to the mode shape. Figure 8.3 shows how 3 known base shapes contribute to the mode shapes.

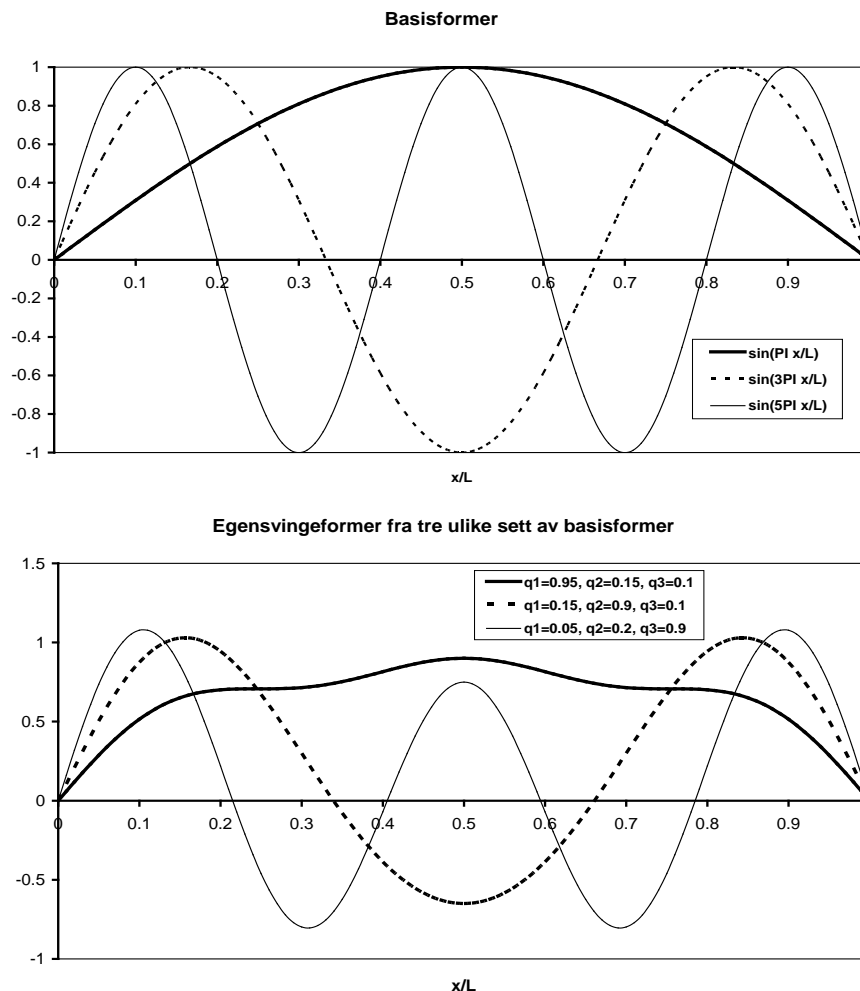


Figure 8.3, base shapes and shape function for 3 different sample of weighting [9]

In a general expression, the displacement of riser is:

$$d(x, t) = \sum_{i=1}^{N_w} \sum_{j=1}^{N_\varphi} \varphi_j(x) q_{i,j}(t) \quad (8.10)$$

Where  $N_\varphi$  represents the number of known based mode shapes, and  $N_w$  represents of number of eigenvalues. The mode shape can be shown as:

$$d_i(x) = \sum_{j=1}^N \varphi_j(x) q_{i,j}(t) \quad (8.11)$$

The  $d_i(x)$  is the same as the decomposed displacement history mentioned above, and  $i$  means the corresponding displacement mode. The  $d_i(x)$  was suppose to be  $\varphi_j(x)$  incorrectly at the beginning, that is why the wavelet and spectrum results are opposite with expectation.

## Mono-frequency

The principle idea for this explanation is that the VIV response is actually mono-frequency phenomena for this signal. Figure 8.4 is the wavelet result for test2420. Obviously, the clear mode shifting phenomena found in Hanoytangen test do not exist here, and the active frequencies appear like narrow band process

It's possible that the VIV response is actually a mono-frequency response, therefore the VIV is totally dominated by one mode. This indicate that the response cannot simulated by weighting sum of several response mode.

But the frequency components of the signal cover the range from 5Hz to 10Hz, which is too large for one single mode. More work should do for this question.

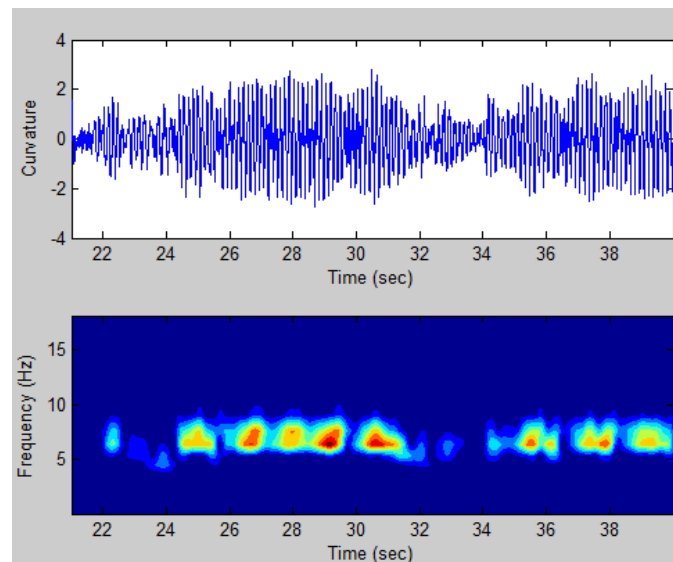


Figure 8.4, signal and wavelet result

### 8.2.5, Summary

From the theory of Rayleigh-Ritz method, the decomposed displacement signals is actually the mode shape  $\Psi(x)$ , which is a combination of known mode shape  $\varphi_j(x)$  with weighting factor  $q$ . The mode shape  $\Psi(x)$  must have an eigenvalue; and the known mode shape  $\varphi_j(x)$  also have its own eigenvalue, it's interesting to know the difference between the two eigenvalues.

The known mode shape  $\varphi_j(x)$  can be written as:

$$\varphi_j(x) = \sin\left(\frac{n\pi}{L}z\right) \quad (8.12)$$

The eigenfrequency for this mode are:

$$f_n = \sqrt{f_{n,tension}^2 + f_{n,bending}^2} \quad (8.13)$$

However, the eigenfrequency of mode shape  $\Psi(x)$  cannot be found by analysis equation. It can be calculated by:

$$\mathbf{Kq} - \omega^2 \mathbf{Mq} = \mathbf{0} \quad (8.14)$$

This eigenfrequency is corresponding to the  $\Psi(x)$ , in other word, it is the eigen frequency corresponding to composed displacement.

By wavelet analysis, the decomposed displacement signal contains many different frequency components. Also, the decomposed displacement (mode shape  $\Psi(x)$ ) is a combination of numbers of known mode shapes. So, it can be assume that the frequency components found by wavelet are just the eigenfrequencies corresponding to participating known mode shapes.

This assumption was test by available data. Figure 8.5 is the wavelet result of decomposed signal, and all active frequency can be found. Take test2420 as an example, the frequency components appear in decomposed displacement covers the range from 5Hz to 10Hz.

The eignefrequencies for known mode shapes were shown in Figure 8.6. In the frequency range 5Hz to 10Hz, mode 6 to mode 11 can be found. From Table 4.2, the modal analysis is carried out with participating mode 6 to 13, which is similar as 6 to 11.

The discussion above indicated that the eigenfrequency gotten from still water for known mode shape ( $\varphi_j(x)$ ) is different with the eigenfrequency of decomposed displacement ( $\Psi(x)$ ). That is why the eigenfrequency (still water) is much larger than wavelet peak frequency and eigenfrequency iterated by VIVANA.

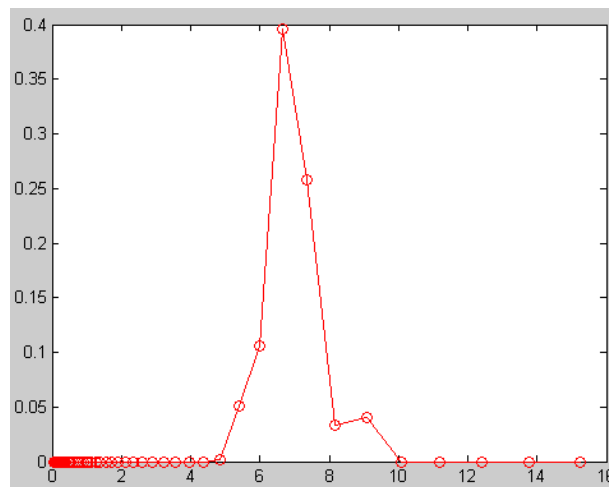


Figure 8.5, time duration VS frequency components from wavelet



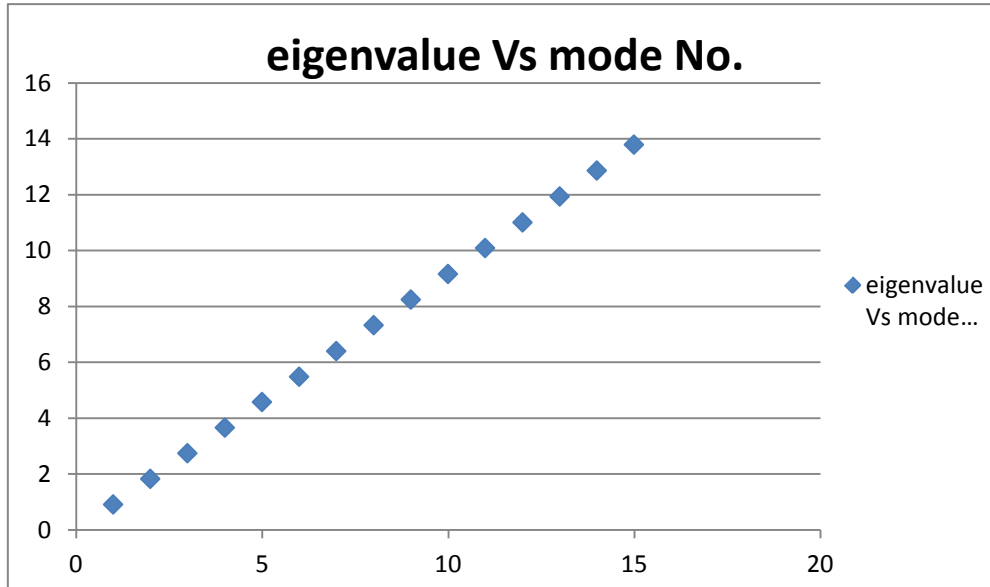


Figure 8.6, eigenvalue for known mode shapes from mode1

## Chapter 9, High harmonic effect and chaotic response

In previous chapters, only first harmonic VIV was studied. The high harmonic components of VIV normally were filtrated by band pass. In this chapter, based on NDP and Hanoytangen data, the effect of high harmonic components will be evaluated. As stated in Chapter 6, chaotic and stationary signals are found in NDP test, but this has never been observed in Hanoytangen test.

The section 9.1 will discuss about the high harmonic effect of VIV, and the section 9.2 shows some studying on chaotic response signals.

### 9.1, High harmonic components in VIV

In this section, high harmonic response of cross flow (CF) VIV was studied. Through the study of power spectrum density, the percentage of power contained in different range of frequency can be found. The powers for first harmonic, second harmonic and higher harmonics are calculated. Some observations will be given.

#### 9.1.1, Defining of high harmonic frequency range

To study the high harmonic components, the frequency range corresponding to high harmonic components has to be defined. It is known that the first harmonic cross flow (CF) frequency is half of first harmonic in line (IL) frequency; the second harmonic CF frequency is three time of its first harmonic frequency, and the second harmonic IL frequency is two times of its first harmonic frequency. Based on this, the frequency range for first harmonic, second harmonic and higher harmonic are shown in table 9.1 and 9.2.

Table 9.1, frequency range for high harmonic components (NDP)

Case No.	velocity	1st order	3rd order
2310	0.3	0.3-3	3-6
2320	0.4	0.3-4	4-8
2330	0.5	0.3-4	4-8
2340	0.6	0.3-5.5	5-11
2350	0.7	0.3-7	7-14
2360	0.8	0.3-8	8-16
2370	0.9	0.3-8	8-16
2380	1	0.3-9	9-18
2390	1.1	0.3-9	9-18
2400	1.2	0.3-10	10-20

2410	1.3	0.3-12	21-24
2420	1.4	0.3-12	21-24
2430	1.5	0.3-14	14-28
2440	1.6	0.3-14	14-28
2450	1.7	0.3-16	16-32
2460	1.8	0.3-16	16-32
2470	1.9	0.3-16	16-32
2480	2	0.3-18	18-36
2490	2.1	0.3-20	20-40
2500	2.2	0.3-20	20-40
2510	2.3	0.3-20	20-40
2520	2.4	0.3-22	22-44

Table 9.2, frequency range for high harmonic components (Hanoytangen)

test No.	velocity	1st range	3rd range
33	0.2592	0,5-3	3,0-6
34	0.2582	0,5-3	3,0-6
35	0.3790	0,5-3,2	3,2-6,5
36	0.3796	0,5-4	4,0-8
37	0.4348	0,5-4	4,0-8
38	0.5369	0,5-5,5	5,0-11
39	0.6435	0,5-6	6,0-12
40	0.6222	0,5-6	6,0-12
41	0.7397	0,5-6	6,0-12
42	0.7309	0,5-6	6,0-12
43	0.7601	0,5-7	7,0-14
44	0.8342	0,5-8	8,0-16
45	0.8389	0,5-8	8,0-16
46	0.8415	0,5-8	8,0-16
47	0.9510	0,5-9	9,0-18
48	0.9388	0,5-9	9,0-18
49	1.0504	0,5-8	8,0-16
50	1.0276	0,5-9	9,0-18
51	1.1477	0,5-10	10,0-20
52	1.1339	0,5-10	10,0-20
53	1.2604	0,5-10	10,0-20
54	1.2591	0,5-10	10,0-20
55	1.3464	0,5-10	10,0-20
56	1.3636	0,5-11	11,0-22
58	1.4530	0,5-11	11,0-22
59	1.4500	0,5-11	11,0-22
60	1.5590	0,5-13	13-26
61	1.5359	0,5-13	13-26

62	1.6431	0,5-13	13-26
63	1.6336	0,5-14	14-28
64	1.7155	0,5-14	14-28
65	1.7452	0,5-14	14-28
66	1.7525	0,5-14	14-28

### 9.1.2, Power spectrum density

A Matlab code was composed to find the power spectrum density in present thesis, the power contained in corresponding frequency range was calculated by integral, and percentage that the integral of the sum power were record.

Signals within the selected time window (see Table 4.3 and 4.4) measured at different locations of different tests were calculated, both for NDP and Hanoytangen. Table 9.3 is an example of the result.

Table 9.3, example of result

test2310	1st	3rd	higher
1	0.7542	0.2281	0.0177
2	0.7742	0.2158	0.01
3	0.743	0.2006	0.0564
4	0.7871	0.1992	0.0137
5	0.783	0.1869	0.0301
6	0.6646	0.2761	0.0593
7	0.5074	0.4185	0.0741
8	0.4717	0.4775	0.0508
9	0.9597	0.0189	0.0214
10	0.7451	0.242	0.0129
11	0.6822	0.2981	0.0197
12	0.6986	0.1122	0.1892
13	0.6541	0.1224	0.2235
14	0.2224	0.7158	0.0618
15	0.2837	0.6717	0.0446
16	0.3798	0.5781	0.0421
17	0.861	0.0978	0.0412
18	0.9404	0.0311	0.0285
19	0.6951	0.288	0.0169
20	0.7053	0.282	0.0127
21	0.9121	0.0598	0.0281
22	0.751	0.2157	0.0333
23	0.1403	0.6678	0.1919
24	0.9437	0.0445	0.0118

The first column represent the location number of measurement point; the second

column is the power contained in first harmonic VIV (in percentage); the third column is the power contained in second harmonic VIV (in percentage); and the fourth is the power contained in higher mode VIV (in percentage). The result is available in Appendix D in Table D1-Table D6.

### 9.1.3, Observations

Figure 9.1 shows the second harmonic effects varying with towing velocity for NDP test, and Figure 9.2 shows the same content for Hanoytangen test. The vertical axis represents the power percentage of second harmonic response, and the horizontal axis is the maximum towing velocity (linear shear current); different lines represent the different measurement locations. The high mode effect was studied in two dimensions, velocity and depth.

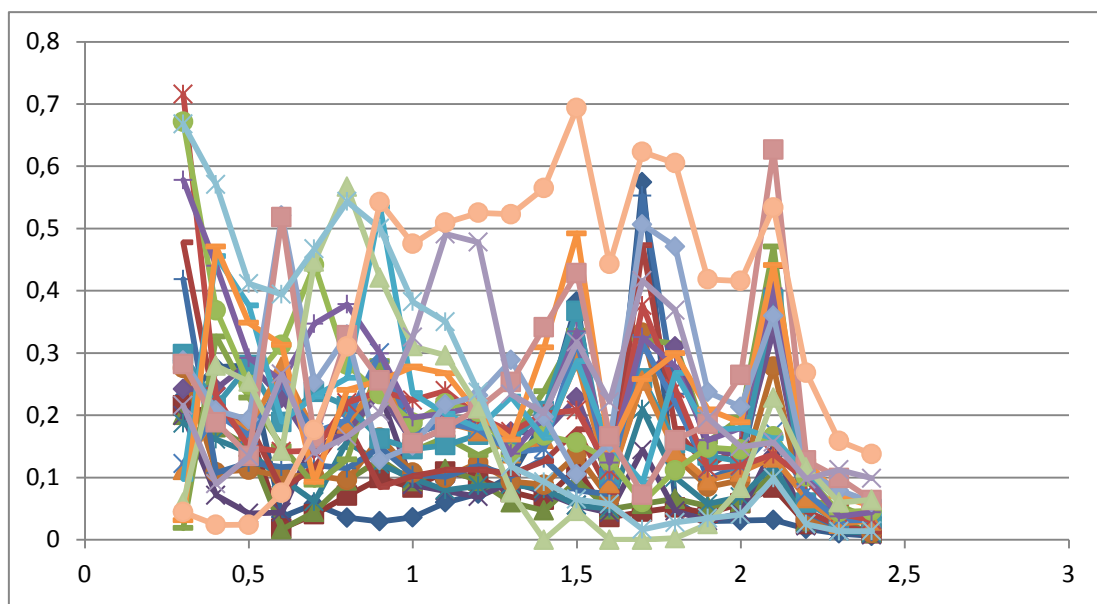


Figure 9.1, Second mode components (NDP)

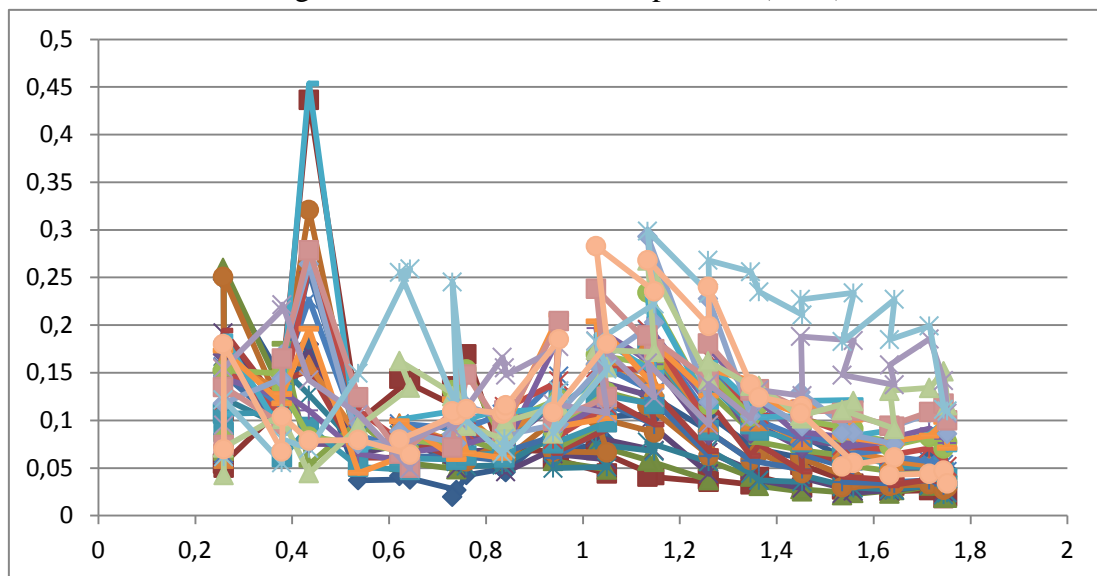


Figure 9.2, Second mode components (Hanoytangen)

## Velocity dimension

For NDP test, the second harmonic components are around 10 to 30 percent of the total signals; the second harmonic component as large as 70 percent of the total signal can be observed in some cases.

For Hanoytange test, the second harmonic effect is not as significant as NDP, the second harmonic components are around 5 to 15 percent of the total signals; and the second harmonic components may up to 45 percent at some locations.

Some observations can be found:

1. The second harmonic components take considerable part of power in measured signals, and the second harmonic components should be ignored.
2. The effects of second harmonic components do not follow a linear trend as the increase of towing velocity.
3. The curves shown in Figure 9.1 or 9.2 are quite similar. This indicates that second harmonic effect may vary with locations in some orders.

## Depth dimension

With the increase of depth, the second harmonic component of total response tends to increase. Figure 9.3 is a typical case for this observation. The vertical axis is the percentage for second harmonic component of total signal, and the horizontal axis is the depth.

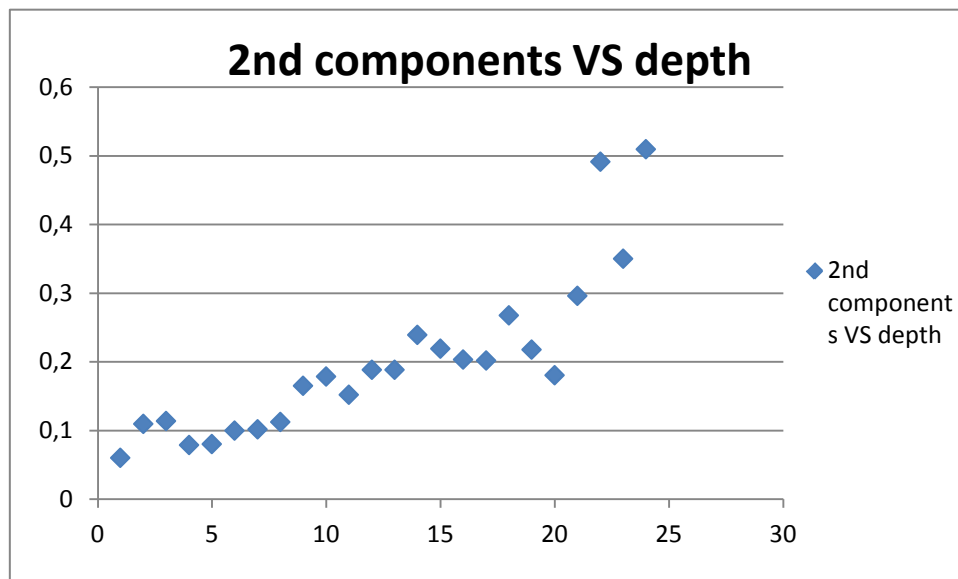


Figure 9.3, the 2<sup>nd</sup> mode components vary with depth

This observation was observed by cases subjected to linear shear current, whose velocities at different locations are different. The velocity may be another impact factor for second harmonic signals.

## 9.2, Chaotic response signals in NDP test

By observation of NDP signal histories, one observation is found. The NDP signals may contain the stationary signal part and chaotic signal part in a same test, which cannot be observed in Hanoytangen test.

The signals mentioned in the first paragraph are all from the selected time window (see Table 4.2), which mean it's happen in the period when the VIV phenomenon has already fully developed. In this section, NDP test 2460 was chosen to be an example, spectrum analysis was performed and some studies about trajectory and oscillation period were also carried out.

### 9.2.1, The signal

The cross flow curvature signals from location No.5 was shown in figure 9.4, the wavelet analysis was performed to detect the chaotic period and stationary period. The first half of the signal, the frequency components are relatively stable and it was seen as stationary part, and the second half part was seen as chaotic part. The time windows for chaotic and stationary can be found in table 9.4

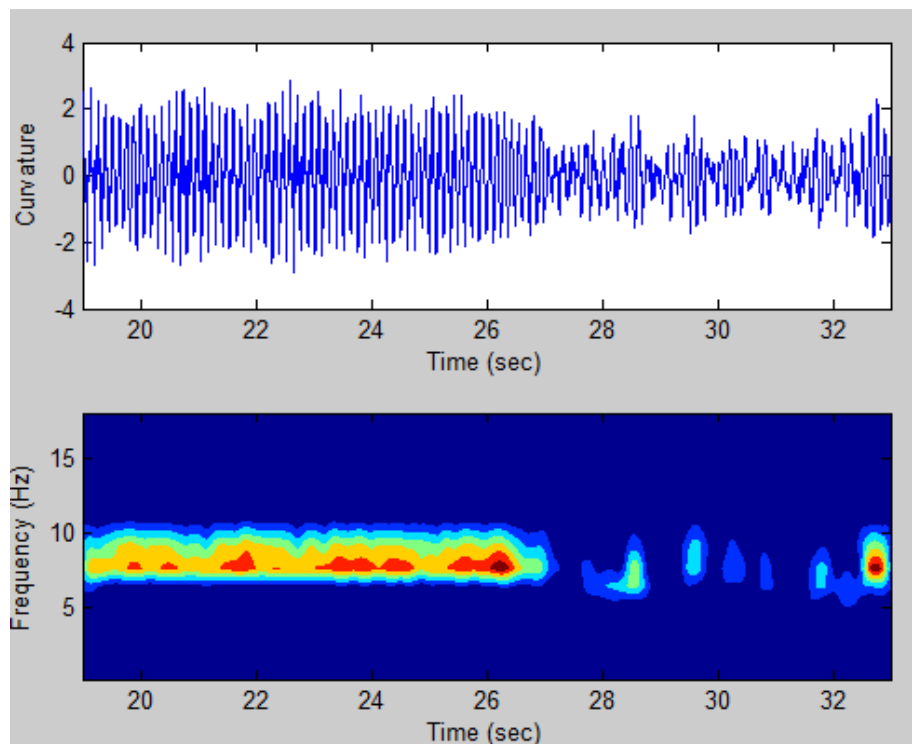


Figure 9.4, signals of test2460 in time window with its wavelet result

Table 9.4, Time window for both type of signals

Type of signals	Chaotic	Stationary
Time window	20-25	28-33

## 9.2.2, Analysis of signals

### Spectrum analysis

The power spectrum density (PSD) of chaotic and stationary signal is found, Figure 9.5 is the PSD for chaotic signal, and Figure 9.6 is PSD for stationary signal.

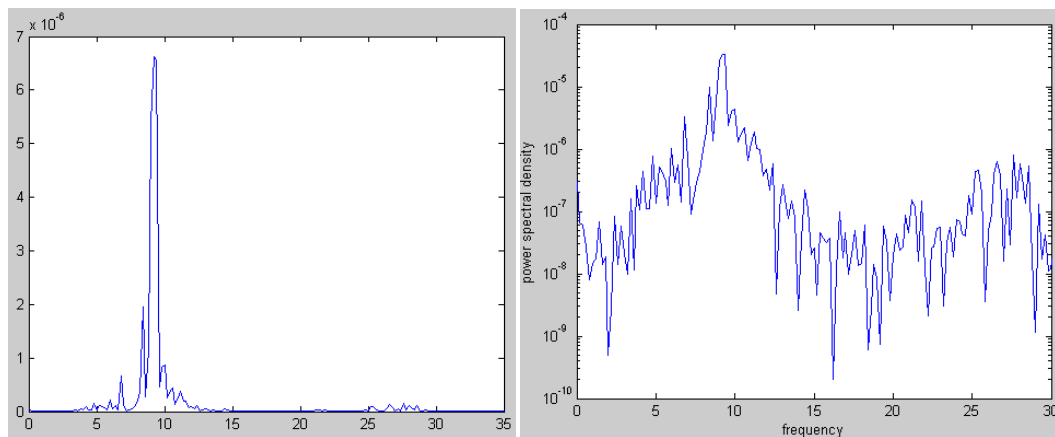


Figure 9.5, power spectrum density for chaotic signal

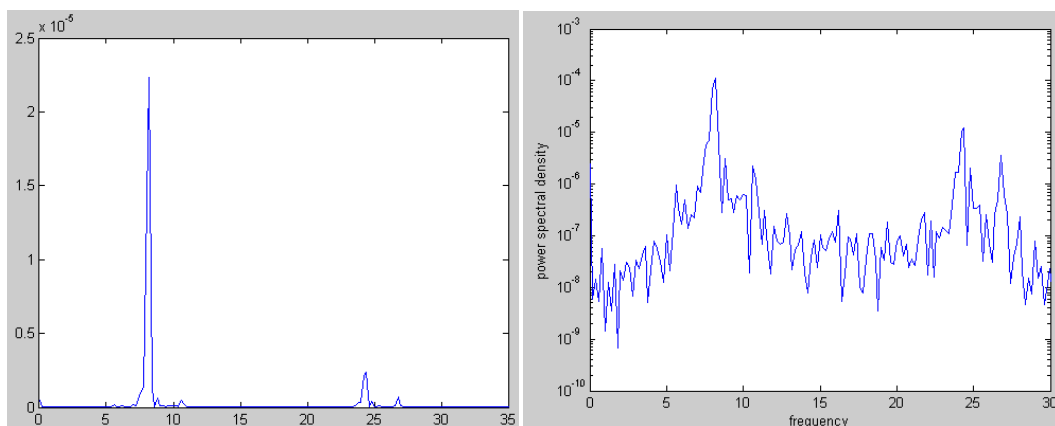


Figure 9.6, power spectrum density for stationary signal

Obviously, the PSD of stationary signal appear as a narrow band, while the chaotic signal contains much more frequency than stationary signal.

### Oscillation period and trajectory

By the displacement histories of inline and cross flow VIV, the trajectory history in two time windows were plotted, shown in Figure 9.7 and 9.8. The trajectories of stationary signal follow the same track, although the trajectories are not exactly same. However, the trajectories from chaotic signals display a disorder condition.



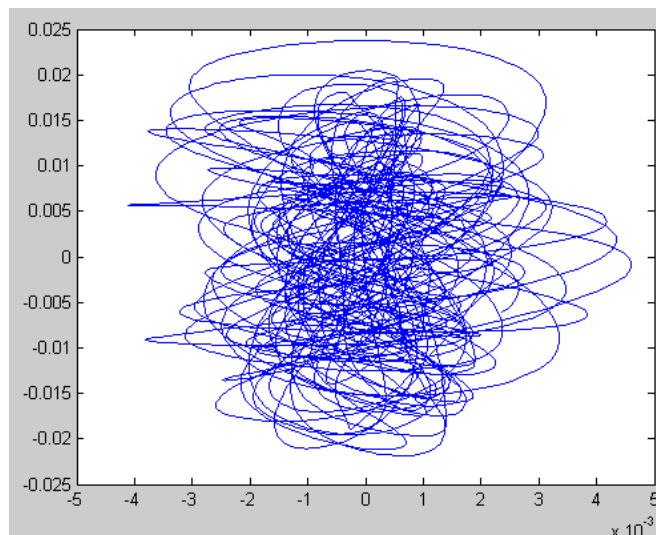


Figure 9.7, Trajectory history in chaotic time window

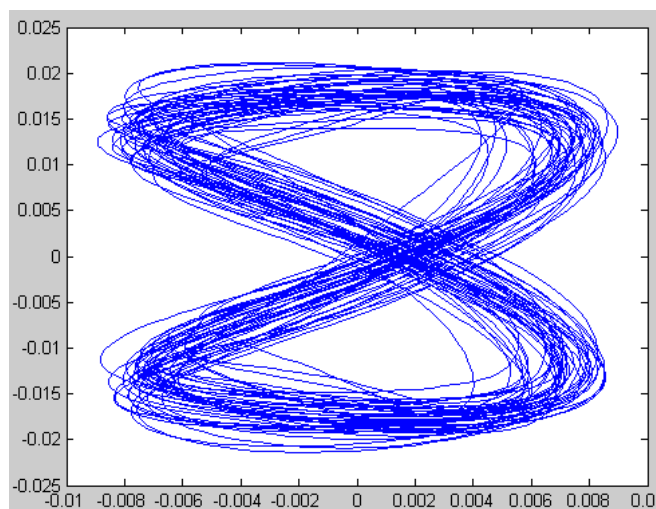


Figure 9.8, Trajectory history in stationary time window

The IL and CF oscillation history were studied then. The value of each IL and CF period was recorded (shown in Appendix D in Table D7-Table D10), the standard deviation and mean values of these periods were calculated.

Table 9.5, standard deviation and average of oscillation periods

type	Standard deviation		Average period	
	IL	CF	IL	CF
chaotic	0.00878	0.014127	0.055449	0.113663
stationary	0.001227	0.00297	0.06175	0.123526

The standard deviation of chaotic signals are much larger than stationary signals, this indicate that the stationary signal represent stable oscillation period. In addition, the average period of chaotic signals is shorter than average period for stationary signals.

### 9.2.3, Switching between chaotic and stationary VIV

By spectrum analysis above, the stationary signal have narrow banded frequency components. Therefore, the wavelet analysis result is good way to determine the chaotic signal and stationary signal.

Wavelet analysis was carried out in Chapter 5 for all NDP tests. These signals can be divided into follow three categories:

1. Signals with pure chaotic oscillation
2. Signals with pure stationary oscillation
3. Signals with both chaotic oscillation and stationary oscillation

Only a few of case was pure chaotic signal, and most of cases are belong to the last two type. NDP test is conducted at laboratory, which proved an ideal experimental condition. If the oscillation is under stable mode in ideal condition, it will expect to oscillate in same mode. However, most of stationary oscillations tend to chaotic.

For Hanoytangen test, which was test in real ocean condition, stationary signal does not exist. But this does not indicate the general mode for VIV is chaotic, because there are too much other factor more than current load in real condition may effects the VIV response.

## Chapter 10, Conclusion and future work

### 10.1, Conclusion

The motivation of the thesis is to establish a general frequency competition model for VIVANA. Wavelet analysis method is applied to reveal the time-depended intensity of frequency components include in experimental data, some observations and ideas are found by comparison between VIVANA estimations and wavelet result. In present thesis, the general model is not found, but several useful observations and advices are proposed and discussed. A brief summary of present thesis was shown below.

1. VIVANA cannot estimate precise frequency result.

The frequency competition model of VIVANA gives too wide frequency range for response calculation, estimated frequency ranges are far beyond true real range and most of active frequencies included do not participate in real VIV.

For time sharing method, the active frequencies out of true frequency range take considerable time durations. The sum of the duration is about 50% for NDP, and about 30% for Hanoytangen.

2. Frequency range varies with towing velocity

Peak frequency and frequency range calculated by wavelet analysis vary with towing velocity, the observations are listed following:

- Peak frequency and towing velocity have an approximately linear relationship, the peak frequency tend to increase with towing velocity. Meanwhile, step-like rise is clearly observed, that is several neighbored test with different towing velocity may have same peak frequency.
- Start frequency and end frequency of frequency range have the same observations as peak frequency stated above. But the changes are not synchronous.
- The width of frequency range tends to increase with the towing velocity, which may indicate that more response modes are included under higher velocity condition.
- It's found that the standard deviations of key values tend to increase with towing velocity. This indicated that the VIV phenomenon is more chaotic under higher towing velocity condition.

3. Frequency range at different location of riser in same test

Signals from numbers of measurement points are measured in same test, wavelet

analysis was performed to detect the frequency components for different place along the riser. Observations are shown below:

- Peak frequencies at different locations tend to decrease as the result of increase of depth.
- Several neighbored locations often have same peak frequency; this phenomenon make the peak frequency along the riser displays step-like descent with depth.
- The start frequency and end frequency of frequency range have same observations as peak frequency. But the changes are not synchronous.
- Instant peak frequency often varies simultaneously for several neighbored locations, and these locations normally have same peak frequency.
- The width of frequency range varies around a value, no specified order can be found.

#### 4. Advices for limiting frequency range

To improve the frequency competition model of VIVANA, several strategies are proposed as below:

- Energy limit: the active frequency with time duration less than 2% will be filtrated. This method can reduce most of extra frequencies at the low side of frequency range.
- The excitation parameter E should not be the only term to determine frequencies, and excitation length should be considered. The frequency with small excitation zone may not be included in frequency range, even though it has considerable excitation parameter.
- A new method which combines time sharing and space sharing are proposed. Excitation zones are defined based on space sharing theory, and the frequency domain dynamic calculation within each excitation zone is based on time sharing method.

#### 5. Frequency components of measured signal and eigenfrequency

Peak frequency (for wavelet) of measured signal is assumed to be the eigenfrequency corresponding to dominating mode in real condition, ideal eigenfrequency corresponding to dominating mode can be found by analytical equation and VIVANA can give another eigenfrequency. By comparison between the three frequencies, observations below were found:

- VIVANA always give higher value than peak frequency calculated by wavelet, but the difference is not too large.
- Eigenfrequency under still water condition always have highest value among the three frequencies; and the difference is relatively large.

In addition, displacement component corresponding to single participating mode in modal analysis is decomposed. Wavelet analysis was performed to study frequency components of decomposed signal, and the frequency components of different decomposed signals are almost same. Two candidates are proposed to explain this phenomenon.

- As described by Rayleigh-Litz method.
- The VIV response is actually a mono-frequency response.

## 6. High mode effect of VIV

By spectrum analysis, the power contained in first, second and higher order frequencies are calculated. Several observations can be found below:

- The first and second harmonic components take most of power contained in measured signals.
- The second harmonic components take considerable percent of total power, and it should not be ignored in calculation.
- The effects of second harmonic components do not follow a linear trend as the increase of towing velocity.
- Second harmonic component of total response tends to increase with depth.

## 7. Chaotic and stationary signals in NDP test

The chaotic signal and stationary signal can be found in a fully developed VIV response signal, which do not exist in Hanoytangen test. Several tests are performed to study this phenomenon. The observations are listed below:

- The stationary signal is a narrow banded process; while the frequency components contained in chaotic signals are much more than chaotic signals.
- The trajectories of VIV oscillation during stationary period follow same track; while the trajectories for chaotic signal appear as a disordered oscillation.
- Oscillation period for VIV during chaotic time is quite mutable; while it is relatively stable during stationary time.
- Average oscillation period of VIV during chaotic time is smaller than average oscillation period during stationary time.
- Chaotic response is general phenomenon for VIV.

## 10.2, Future Works

Except to the work shown in present thesis, some other analysis regard other VIV features have been attempted, but most of these attempts were failed because the lack

of theoretical knowledge and analysis tools. VIV is an extremely complicated phenomenon which can be affected by many factors, and the understanding of VIV is still far from enough. The future works regard to the present thesis is shown below:

1. Establish a more general frequency ranking system, which can consider the effect from excitation length.
2. Verifying the new method proposed in present thesis, which is a combination of time sharing and space sharing method.
3. Travelling wave and standing wave can be observed in displacement history; it's interesting to study the relationship between two types of signals (chaotic and stationary) and travelling & standing wave.
4. The effect of high harmonic response on fatigue life.

## Reference

- [1]. Henning Braaten, Halvor Lie. *NDP Riser High Mode VIV Tests, Main Report*. Marintek.
- [2]. Trygve Kristansen, Halvor Lie. *NDP Riser high Mode VIV Tests – Modal Analysis*. Marintek.
- [3]. Knut Mo, Halvor Lie. *Additional VIV analysis – stationarity study / wavelet analysis*. Marintek.
- [4]. Norsk Hydro A.S. *Large Scale Testing of Riser Models – Main report*. November 1997.
- [5]. H. Lie, K.E. Kaasen. *Modal analysis of measurements from a large-scale VIV model test of a riser in linearly sheared flow*. Journal of Fluids and Structures, March 2006.
- [6]. Carl Martin Larsen, Halvor Lie, Elizabeth Passano, Rune Yttervik, Jie Wu, Gro Baarholm. *VIV Theory Manual*. Marintek, 3.7 version, June 2009.
- [7]. A. Grossmann, J. Morlet. *Decomposition of hardy functions into square integrable wavelets of constant shape*. SIAM. J. MATH. ANAL, Vol.15, No.4, July 1984.
- [8]. Kristoffer H. Aronsen. *An experimental of in-line and combined in-line and cross-flow vortex induced vibrations*. PhD, Norwegian University of Science and Technology, Norway, 2007
- [9]. Carl M. Larsen. *Marine Dynamics*. Department of Marine Technology, Norwegian University of Science and Technology, January 2007.
- [10]. Carl M. Larsen, Jie Wu, Halvor Lie. *On the Understanding of non-stationary VIV of Slender beams*. OMAE 2010.
- [11]. R.D. Blevins. *Flow-Induced Vibration*. Krieger Publishing Company, Florida, Krieger drive, Florida, edition 2, 1990.
- [12]. B.M. Sumer and J. Fredsøe. *Hydrodynamic around cylindrical structures.*, volume 12, *Advanced series on Ocean Engineering*. World Scientific, London, 1997.
- [13]. C.Le Cunff, F.Biolley , E. Fontaine (2002), *Vortex-Induced Vibrations of risers: theoretical, numerical and experimental investigation*, Oil&Gas Science and Technology –Rev. IFP, Vol 57 (2002).
- [14]. J.K. Vandiver, J.-Y. Jong, *The relationship between in-line and cross-flow vortex-induced vibration of cylinders*, Journal of Fluid Structures (1987) 1, 281-299.
- [15]. Soni, P, *Hydrodynamic coefficients for vortex-induced vibration of flexible beams*, PhD , Department of Marine Technology, Norwegian University of Science and Technology, 2008.
- [16]. Jie Wu, Carl M. Larsen, Karl E. Kaasen, *A new approach for identification of forces on slender beams subjected to vortex induced vibration*, OMAE 2008-577550 (2008).
- [17]. Carl M. Larsen, *Vortex Induced Vibration Introduction*, Department of



Marine Technology, NTNU.

- [18]. Carl M. Larsen, Vikestad, K., Yttervik, R. and Passano, E., *VIVANA, Users' Manual*, MARINTEK, Trondheim.
- [19]. G.S. Baarholm, Carl M. Larsen, H. Lie, *On fatigue damage accumulation from in-line and cross-flow vortex-induced vibrations on risers*, Journal of Fluid and Structures 22(2006), 109-127.
- [20]. R. Gopalkrishnan. *Vortex Induced Forces on Oscillating Bluff Cylinders*. PhD thesis, MIT, Dep. of Ocean Engineering, 1993.



## Appendix A

### Result of category 1

Table A1, Peak frequencies of NDP

peak frequency				
No.	velocity	wavelet	vivana	difference
2310	0.3	1.6043	1.4181	0.1862
2320	0.4	1.9078	2.0847	0.1769
2330	0.5	1.9078	2.7569	0.8491
2340	0.6	2.6981	3.4272	0.7291
2350	0.7	3.2085	4.1128	0.9043
2360	0.8	3.8156	4.277	0.4614
2370	0.9	4.5376	4.9579	0.4203
2380	1	4.5376	5.6075	1.0699
2390	1.1	4.5376	6.3026	1.765
2400	1.2	5.3961	6.9869	1.5908
2410	1.3	6.4171	7.1691	0.752
2420	1.4	6.4171	7.8522	1.4351
2430	1.5	7.6312	8.5925	0.9613
2440	1.6	6.4171	8.7633	2.3462
2460	1.8	7.6312	10.2707	2.6395
2470	1.9	6.4171	10.4522	4.0351
2480	2	9.0751	11.2581	2.183
2490	2.1	9.0751	11.5468	2.4717
2500	2.2	9.0751	12.2611	3.186
2510	2.3	10.7922	13.2008	2.4086
2520	2.4	10.7922	13.4173	2.6251

Table A2, Peak frequencies of Hanoytangen

peak frequency				
Test no.	velocity	wavelet	VIVANA	difference
33	0.2592	1.3392	1.2529	0.0863
34	0.2582	1.5395	1.0982	0.4413
35	0.379	1.7484	1.6782	0.0702
36	0.3796	1.5869	1.6787	0.0918
37	0.4348	2.1066	1.9042	0.2024
38	0.5369	2.8702	2.3496	0.5206
39	0.6435	2.7923	2.8204	0.0281
40	0.6222	2.9525	2.8024	0.1501
41	0.7397	3.8318	3.3126	0.5192
42	0.7309	3.5663	3.3109	0.2554
43	0.7601	3.6943	3.3373	0.357
44	0.8342	3.98	3.6197	0.3603
45	0.8389	4.5023	3.6258	0.8765
46	0.8415	4.5023	3.6242	0.8781
47	0.951	4.9339	4.1478	0.7861
48	0.9388	4.1401	4.1379	0.0022
49	1.0504	4.9339	4.726	0.2079
50	1.0276	4.9339	4.4815	0.4524
51	1.1477	5.1823	5.059	0.1233
52	1.1339	5.457	5.0799	0.3771
53	1.2604	5.7625	5.4723	0.2902
54	1.2591	5.457	5.4738	0.0168
55	1.3464	5.7625	5.8132	0.0507
56	1.3636	6.4891	6.1029	0.3862
58	1.453	6.4891	6.2062	0.2829
59	1.45	6.4891	6.1686	0.3205
60	1.559	6.9258	6.8975	0.0283
61	1.5359	6.4891	6.5742	0.0851
62	1.6431	6.9258	7.2196	0.2938
63	1.6336	6.9258	6.9424	0.0166
64	1.7155	6.9258	7.3721	0.4463
65	1.7452	6.9258	7.6943	0.7685
66	1.7525	7.4254	7.705	0.2796

**Results of category 2**
**Table A3, Frequency Range for NDP**

Frequency Range							
No.	velocity	vivana			wavelet		
		peak	start	end	peak	start	end
2310	0.3	1.4181	0.8094	2.8479	1.6043	1.6043	1.6043
2320	0.4	2.0847	0.885	4.3507	1.9078	1.6043	2.2688
2330	0.5	2.7569	0.9455	5.0808	1.9078	1.9078	2.2688
2340	0.6	3.4272	0.9928	5.8246	2.6981	1.9078	3.8156
2350	0.7	4.1128	1.0301	7.44	3.2085	2.2688	3.8156
2360	0.8	4.277	1.0584	8.2391	3.8156	2.6981	4.5376
2370	0.9	4.9579	1.0796	9.0571	4.5376	1.9078	6.4171
2380	1	5.6075	1.0848	10.7299	4.5376	2.6981	5.3961
2390	1.1	6.3026	1.0966	11.6163	4.5376	3.2085	6.4171
2400	1.2	6.9869	1.0995	12.468	5.3961	3.8156	6.4171
2410	1.3	7.1691	1.1059	13.407	6.4171	3.8156	7.6312
2420	1.4	7.8522	1.1051	14.3084	6.4171	2.6981	9.0751
2430	1.5	8.5925	1.112	15.3414	7.6312	5.3961	7.6312
2440	1.6	8.7633	1.112	16.3374	6.4171	4.5376	9.0751
2460	1.8	10.2707	1.1201	18.5424	7.6312	5.3961	9.0751
2470	1.9	10.4522	1.1233	19.6961	6.4171	5.3961	10.7922
2480	2	11.2581	1.1303	20.9372	9.0751	5.3961	10.7922
2490	2.1	11.5468	1.1523	22.428	9.0751	9.0751	10.7922
2500	2.2	12.2611	1.14	23.4911	9.0751	6.4171	10.7922
2510	2.3	13.2008	1.1618	23.7144	10.7922	7.6312	12.8342
2520	2.4	13.4173	1.1697	25.1047	10.7922	5.3961	12.8342

Table A4, Frequency range for Hanoytangen

frequency range							
Test no.	velocity	VIVANA			wavelet		
		VIVANA	start	end	wavelet	start	end
33	0.2592	1.2529	0.22	1.6117	1.3392	1.7487	1.322
34	0.2582	1.0982	0.2215	1.4154	1.5395	1.5628	1.322
35	0.379	1.6782	0.224	2.2442	1.7484	1.8102	1.5395
36	0.3796	1.6787	0.224	2.2438	1.5869	1.9472	1.5395
37	0.4348	1.9042	0.4227	2.4709	2.1066	2.2444	1.9847
38	0.5369	2.3496	0.4327	3.3104	2.8702	2.8702	2.4588
39	0.6435	2.8204	0.4397	3.7232	2.7923	2.9525	2.6486
40	0.6222	2.8024	0.438	3.7286	2.9525	3.5663	2.6486
41	0.7397	3.3126	0.6327	4.2886	3.8318	3.98	2.7186
42	0.7309	3.3109	0.6334	4.2986	3.5663	3.6943	2.7923
43	0.7601	3.3373	0.6369	4.2953	3.6943	3.98	2.7923
44	0.8342	3.6197	0.6417	4.9169	3.9800	4.7082	2.6486
45	0.8389	3.6258	0.6426	4.9175	4.5023	4.7082	3.6943
46	0.8415	3.6242	0.6415	4.91	4.5023	4.7082	2.6486
47	0.951	4.1478	0.6404	5.519	4.9339	5.1823	3.1322
48	0.9388	4.1379	0.64	5.5264	4.1401	5.1823	3.1322
49	1.0504	4.726	0.8506	6.632	4.9339	5.457	3.4469
50	1.0276	4.4815	0.6522	5.8936	4.9339	5.457	3.3352
51	1.1477	5.059	0.8487	6.7718	5.1823	5.7625	3.6943
52	1.1339	5.0799	0.8603	6.7558	5.4570	5.7625	3.5663
53	1.2604	5.4723	0.8691	7.416	5.7625	6.1043	4.3136
54	1.2591	5.4738	0.8699	7.4201	5.4570	6.4891	4.5023
55	1.3464	5.8132	1.1033	7.8003	5.7625	6.9258	4.3136
56	1.3636	6.1029	1.0977	7.7746	6.4891	6.9258	5.457
58	1.453	6.2062	1.1091	8.2214	6.4891	6.9258	4.9339
59	1.45	6.1686	1.0943	8.1721	6.4891	7.4254	5.7625
60	1.559	6.8975	1.1104	8.6412	6.9258	7.4254	6.1043
61	1.5359	6.5742	1.1097	8.6472	6.4891	7.4254	5.1823
62	1.6431	7.2196	1.1163	9.0963	6.9258	8.0027	6.1043
63	1.6336	6.9424	1.1026	9.0516	6.9258	8.0027	4.9339
64	1.7155	7.3721	1.3708	10.0685	6.9258	8.0027	5.7625
65	1.7452	7.6943	1.3635	10.0288	6.9258	8.6773	5.7625
66	1.7525	7.705	1.3655	10.4612	7.4254	8.6773	6.1023

**Results of category 3**

Figure A5, summation of time duration according to frequency range (NDP)

No.	velocity	range wavelet		down(%)	within(%)	up(%)
2310	0.3	1.6043	1.6043	x	x	x
2320	0.4	1.6043	2.2688	20.33	37.96	41.7
2330	0.5	1.9078	2.2688	8.84	24.93	66.22
2340	0.6	1.9078	3.8156	4.43	62.06	33.51
2350	0.7	2.2688	3.8156	2.28	44.92	52.01
2360	0.8	2.6981	4.5376	4.85	46.66	48.5
2370	0.9	1.9078	6.4171	0.67	83.78	15.56
2380	1	2.6981	5.3961	1.77	40.01	58.21
2390	1.1	3.2085	6.4171	1.22	59.91	38.87
2400	1.2	3.8156	6.4171	2.74	33.72	63.54
2410	1.3	3.8156	7.6312	2.03	52.16	45.81
2420	1.4	2.6981	9.0751	0.08	68.83	31.09
2430	1.5	5.3961	7.6312	5.42	32.72	61.86
2440	1.6	4.5376	9.0751	1.95	50.86	47.19
2460	1.8	5.3961	9.0751	2.56	37.33	60.11
2470	1.9	5.3961	10.7922	2.12	51.81	46.07
2480	2	5.3961	10.7922	1.79	46.75	51.46
2490	2.1	9.0751	10.7922	19.05	18.71	62.24
2500	2.2	6.4171	10.7922	2.43	28.11	69.46
2510	2.3	7.6312	12.8342	3.74	49.65	46.61
2520	2.4	5.3961	12.8342	0.46	56.27	43.27

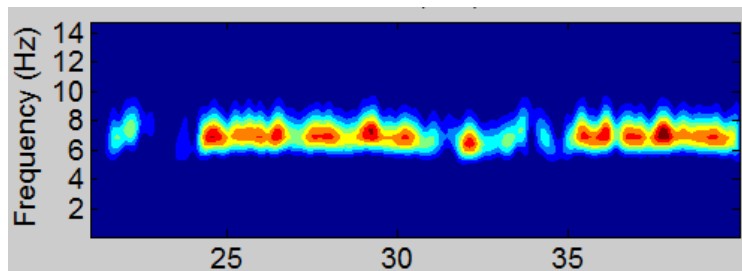
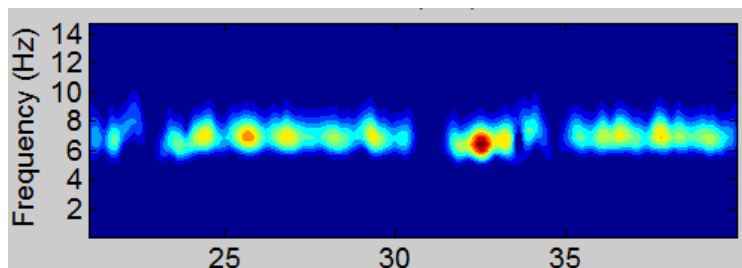
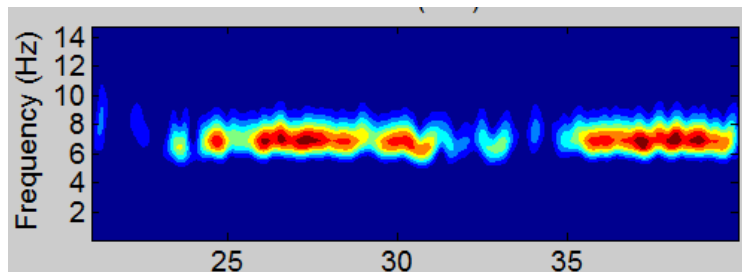
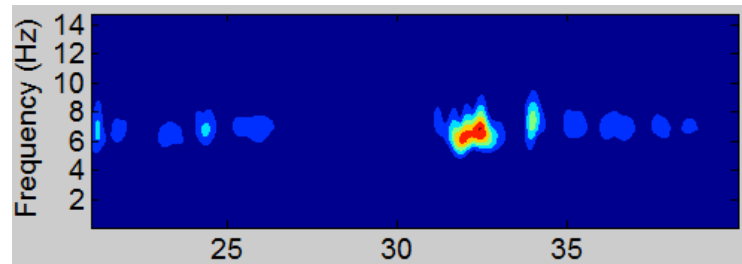
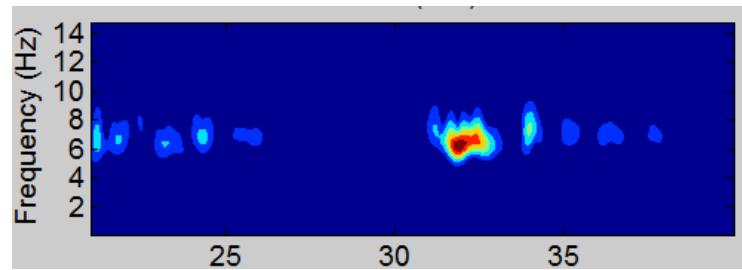
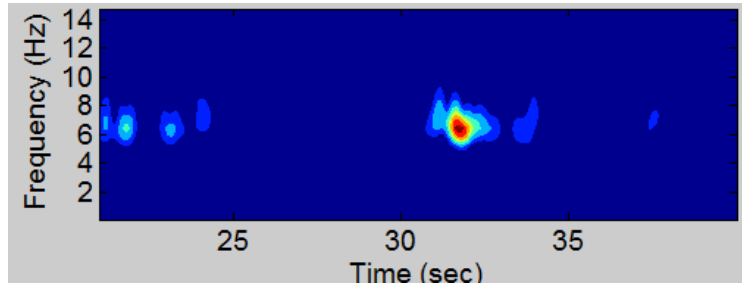
Figure A6, summation of time duration according to frequency range (Hanoytangen)

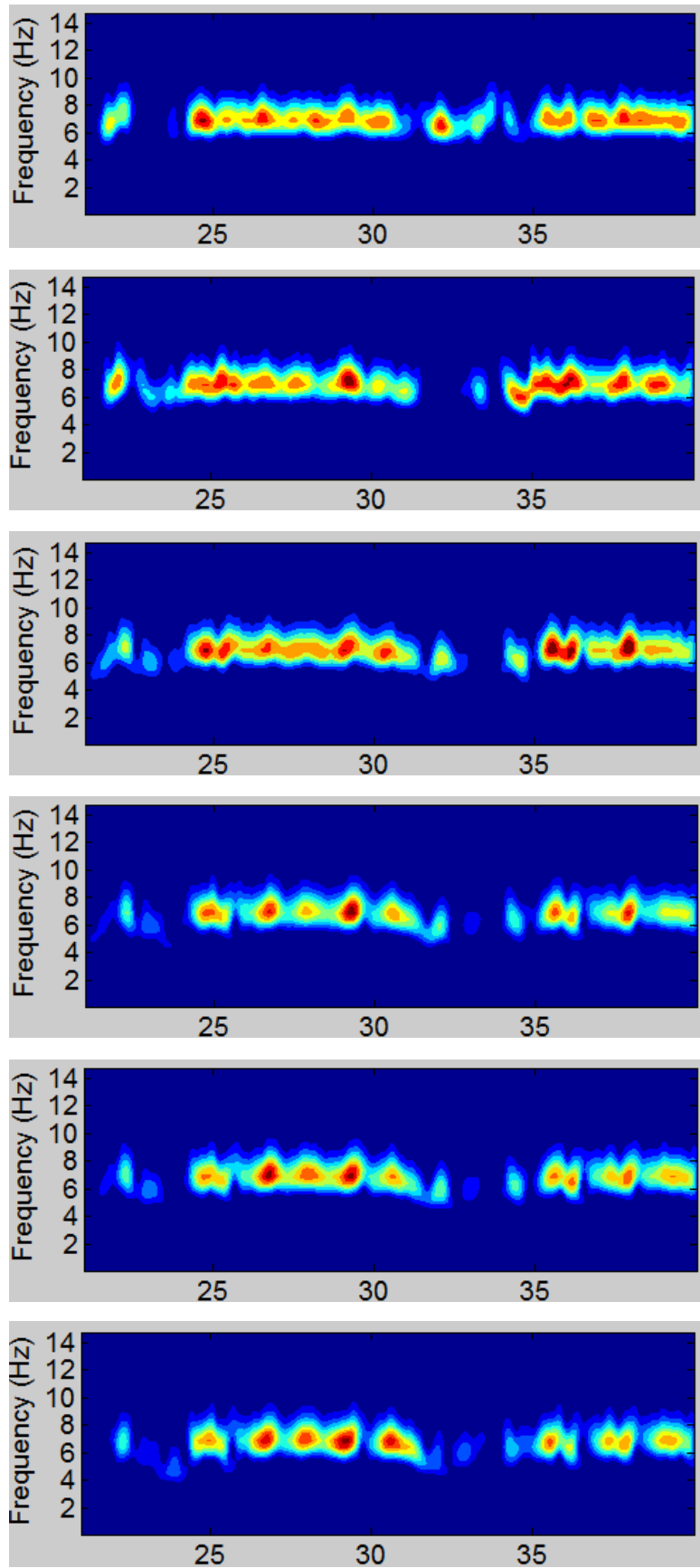
Test no.	velocity	Range wavelet		Down(%)	within(%)	up(%)
33	0.2592	1.322	1.7487	71.05	28.95	0
34	0.2582	1.322	1.5628	77.52	22.49	0
35	0.379	1.5395	1.8102	36.28	19.3	44.42
36	0.3796	1.5395	1.9472	36.03	38.05	25.92
37	0.4348	1.9847	2.2444	54.6	17.77	27.63
38	0.5369	2.4588	2.8702	51.76	28.01	20.23
39	0.6435	2.6486	2.9525	37.27	12.26	50.47
40	0.6222	2.6486	3.5663	41.08	54.56	4.35
41	0.7397	2.7186	3.98	21.46	64.19	14.36
42	0.7309	2.7923	3.6943	22.5	54.24	23.24
43	0.7601	2.7923	3.98	19.84	63.89	16.26
44	0.8342	2.6486	4.7082	9.06	86.65	4.27
45	0.8389	3.6943	4.7082	57.66	37.8	4.55
46	0.8415	2.6486	4.7082	8.79	86.45	4.75
47	0.951	3.1322	5.1823	11.65	83.58	4.73
48	0.9388	3.1322	5.1823	12.19	83.65	4.15
49	1.0504	3.4469	5.457	11.17	70.14	18.68
50	1.0276	3.3352	5.457	12.77	74.26	12.97
51	1.1477	3.6943	5.7625	14.09	62.26	23.66
52	1.1339	3.5663	5.7625	15.01	53.61	21.36
53	1.2604	4.3136	6.1043	16.5	53.58	29.93
54	1.2591	4.5023	6.4891	21.47	56.86	21.67
55	1.3464	4.3136	6.9258	12.79	71.14	16.07
56	1.3636	5.457	6.9258	33.28	49.22	17.51
58	1.453	4.9339	6.9258	16.32	50.69	32.99
59	1.45	5.7625	7.4254	33.67	56.09	10.23
60	1.559	6.1043	7.4254	33.99	40.2	25.81
61	1.5359	5.1823	7.4254	17.06	58.46	24.46
62	1.6431	6.1043	8.0027	28.22	54.54	17.25
63	1.6336	4.9339	8.0027	10.56	72.15	17.26
64	1.7155	5.7625	8.0027	14.62	60.71	24.67
65	1.7452	5.7625	8.6773	13.63	73.79	12.56
66	1.7525	6.1023	8.6773	17.02	69.3	13.68



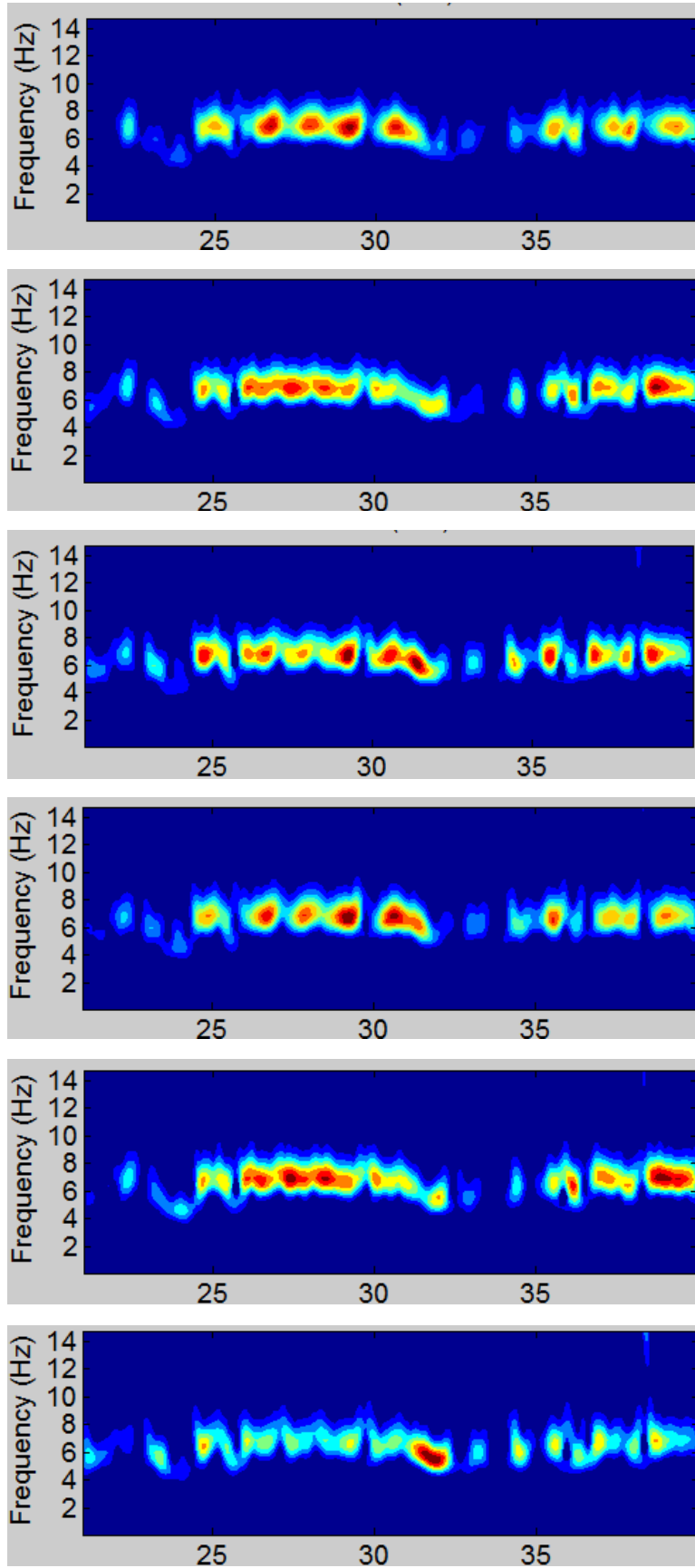
## Results of category 5

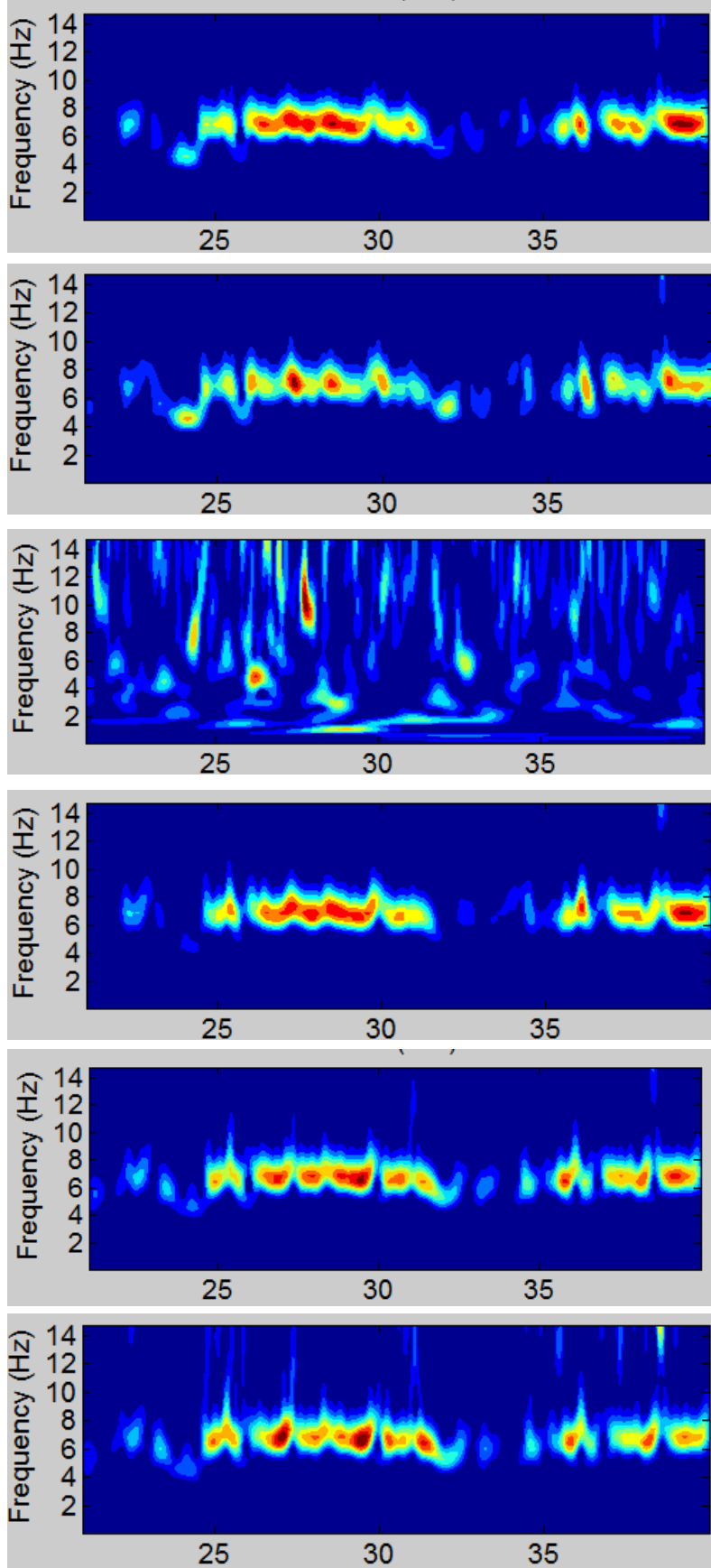
Category 4, wavelet result for NDP test4200 at all 24 measurement point





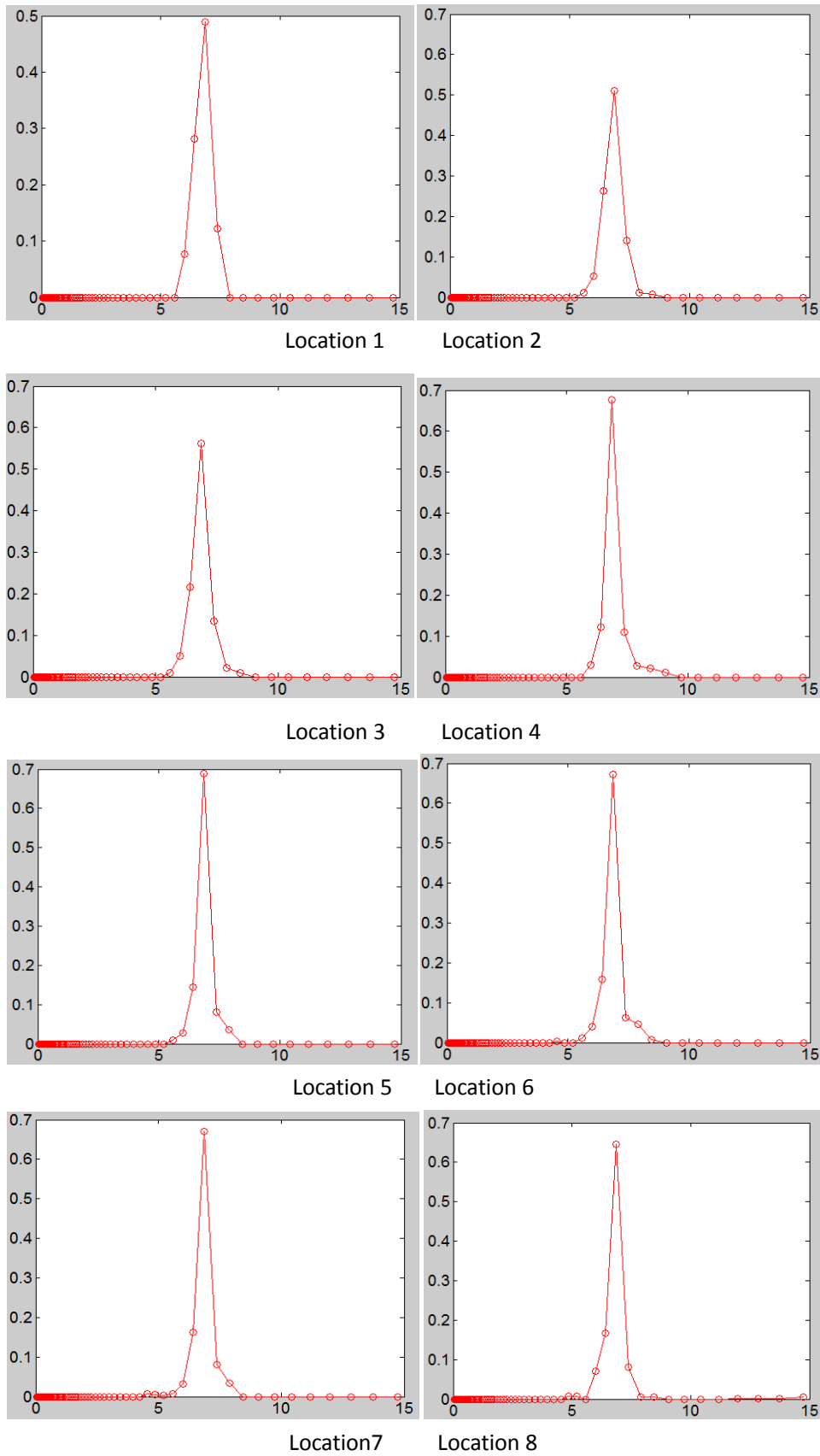


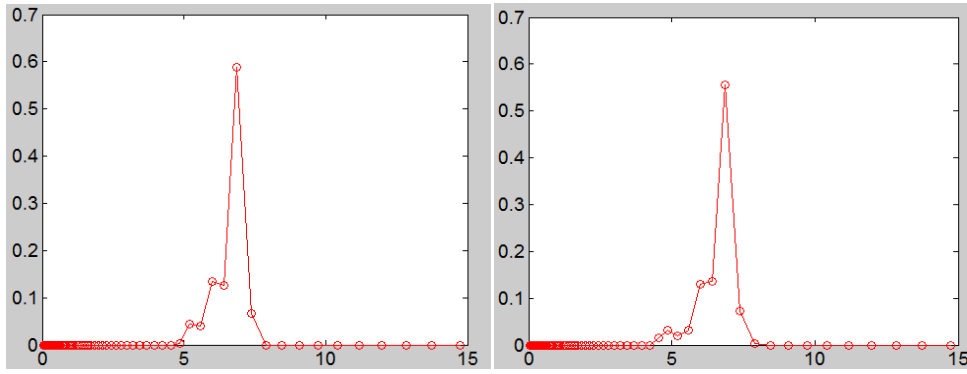




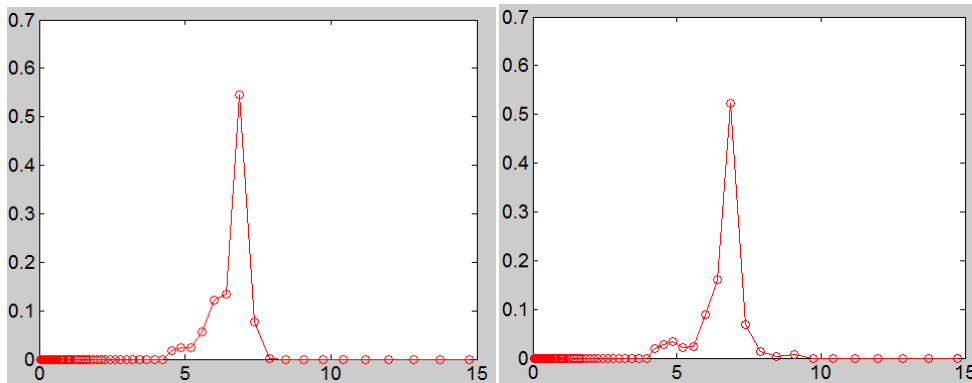


Category 4, Time duration distribution of NDP test4200 at 24 measurement points

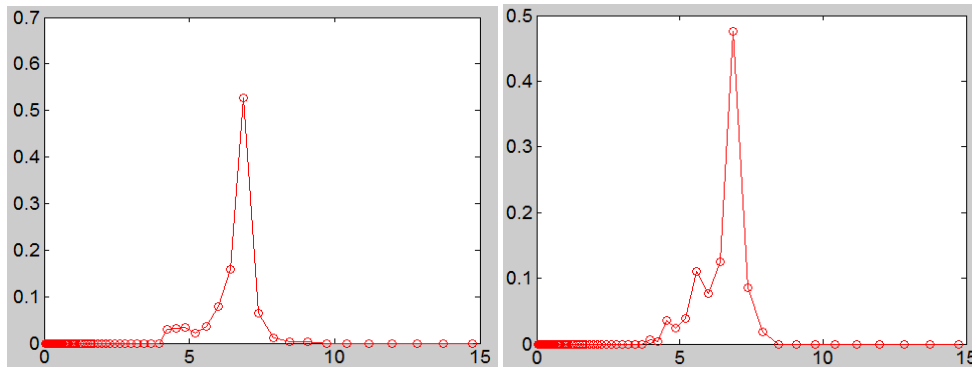




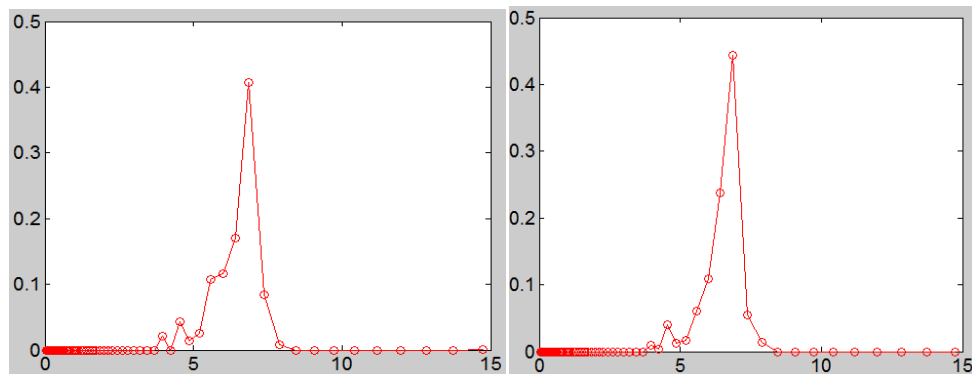
Location 9      Location 10



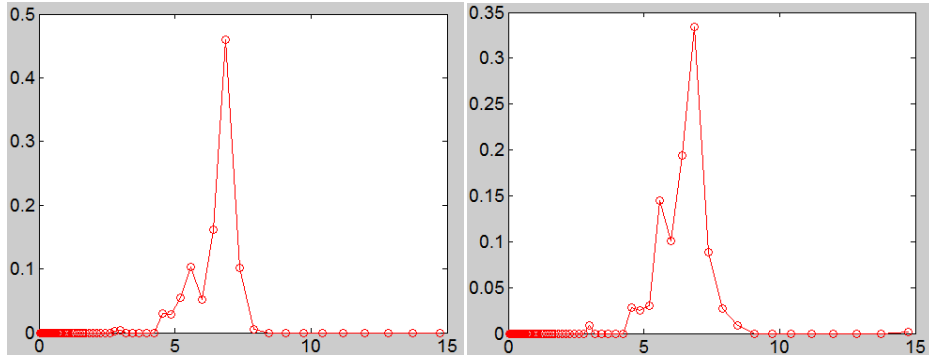
Location 11      Location 12



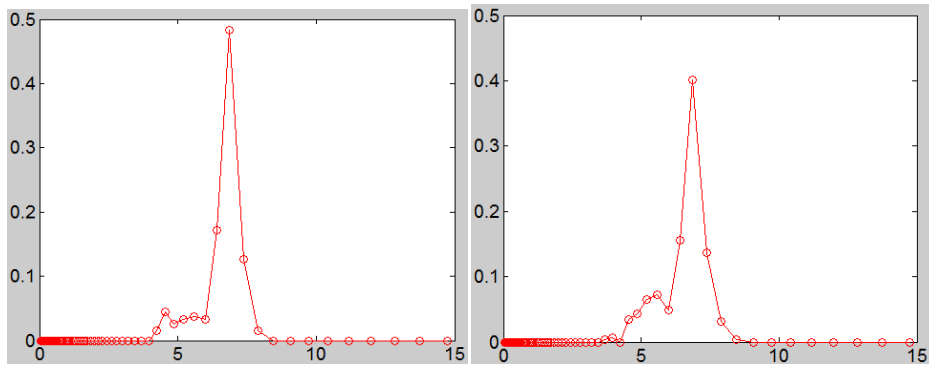
Location 13      Location 14



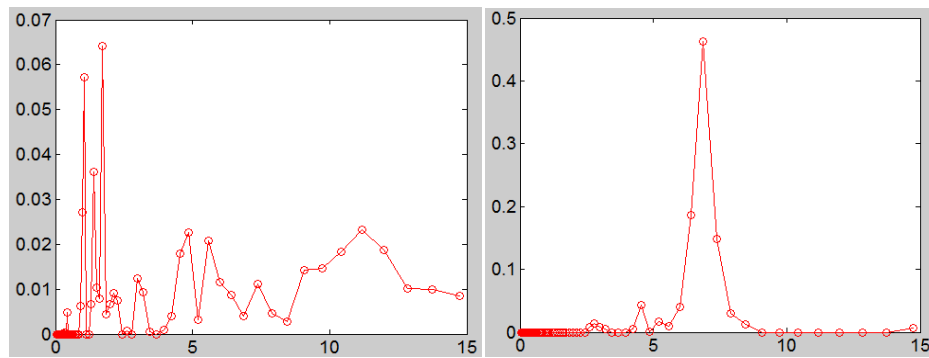
Location 15      Location 16



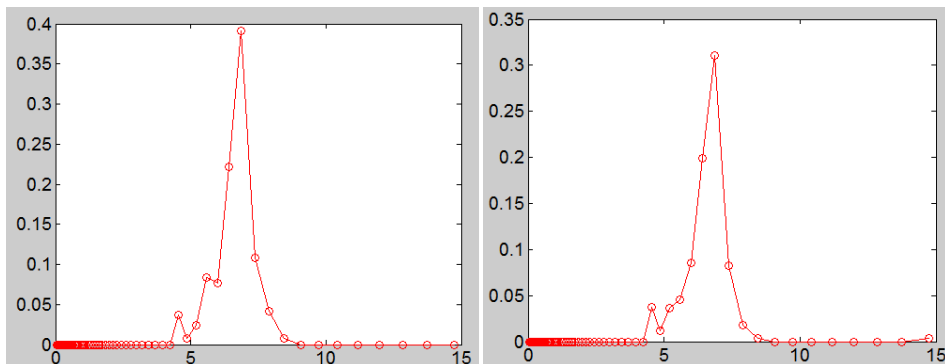
Location 17 Location 18



Location 19 Location 20

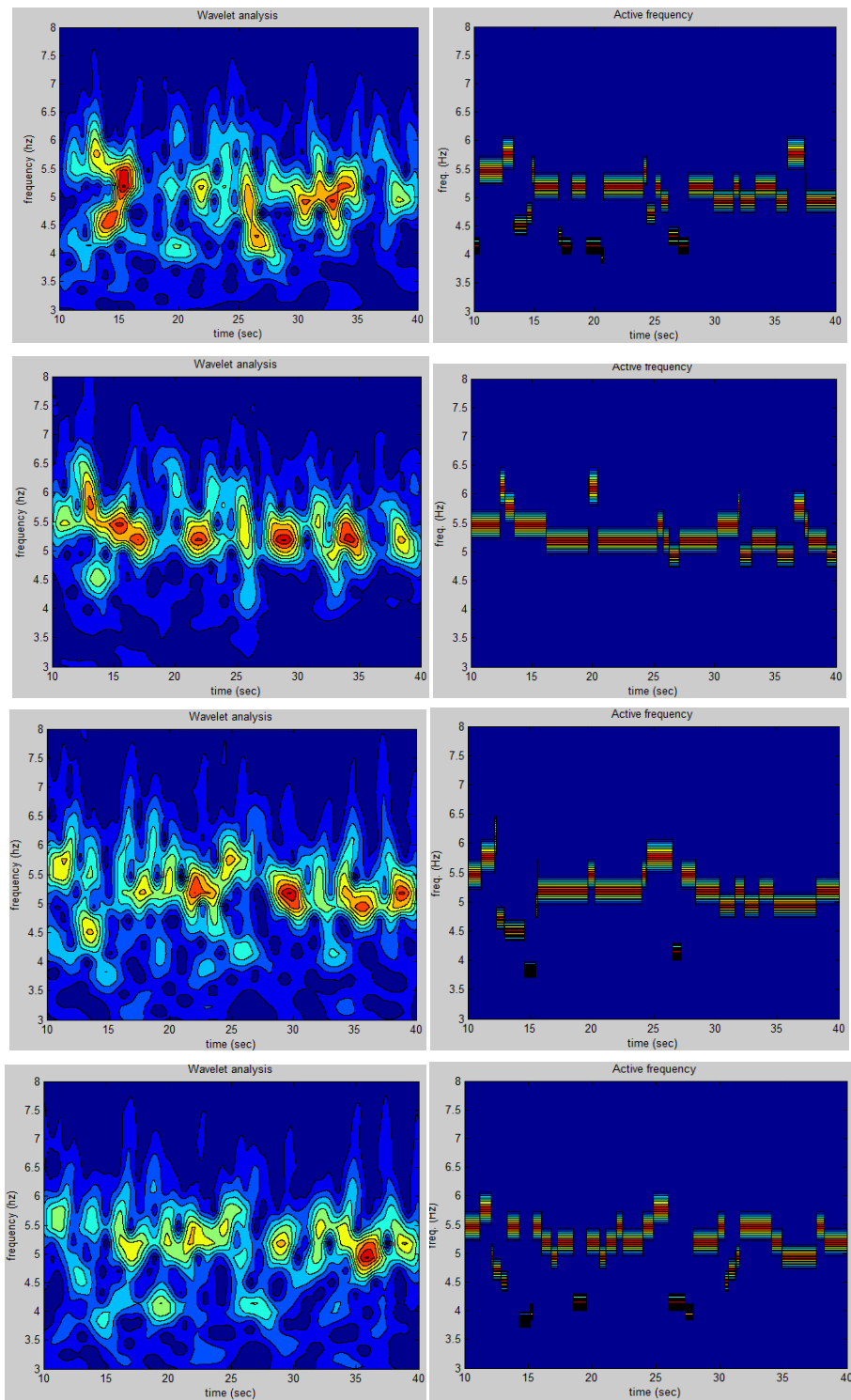


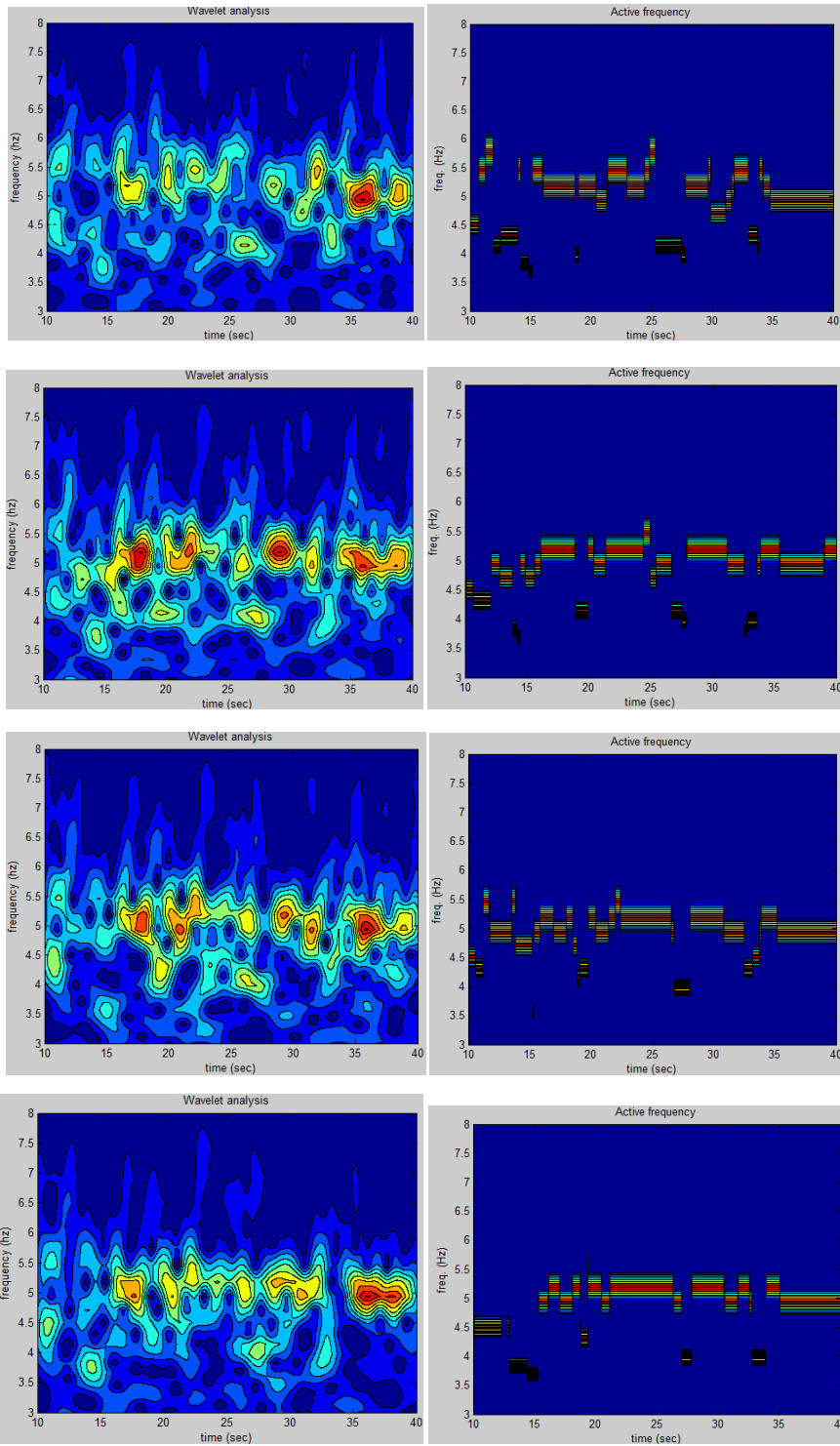
Location 21 Location 22

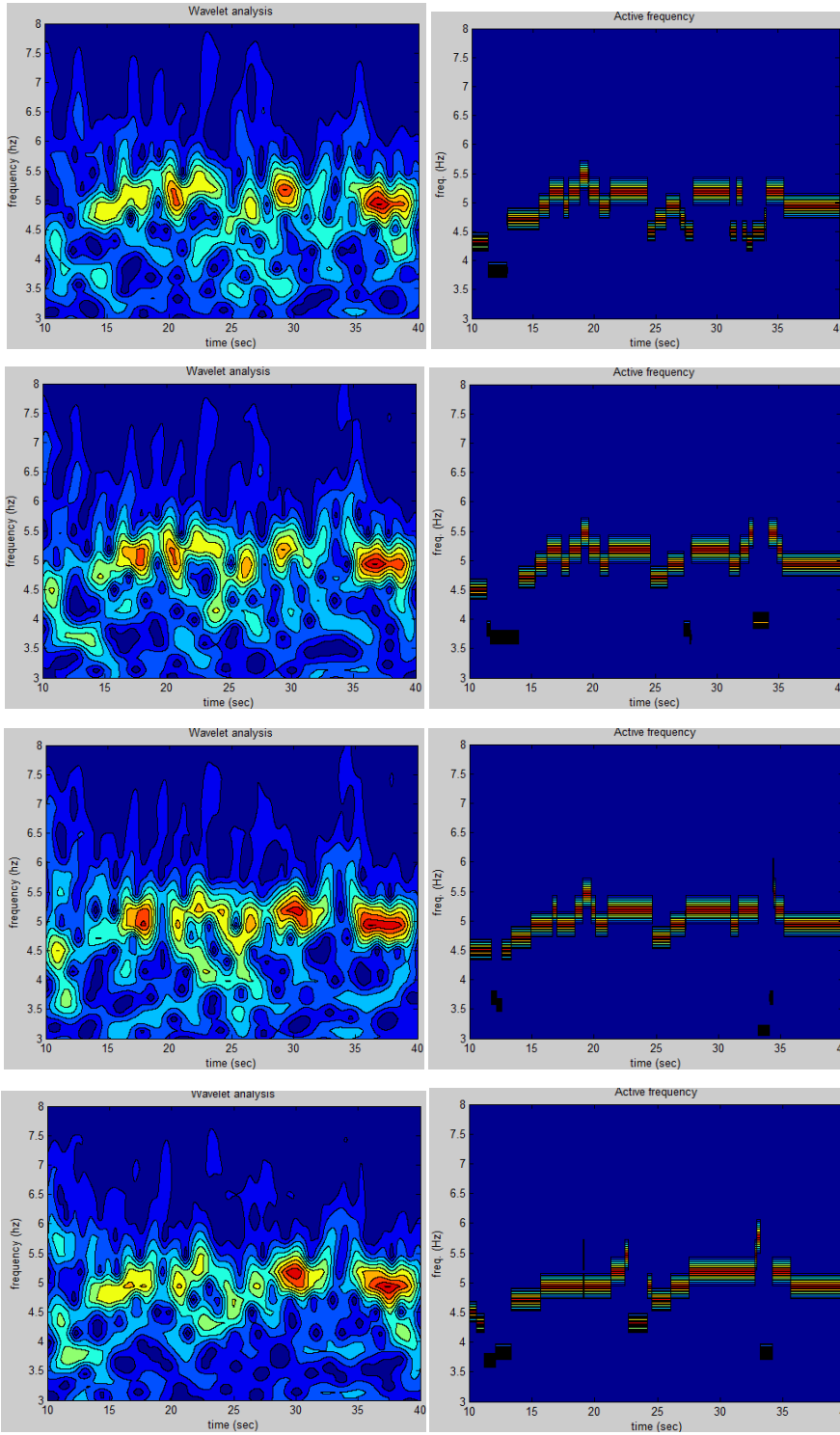


Location 23 Location 24

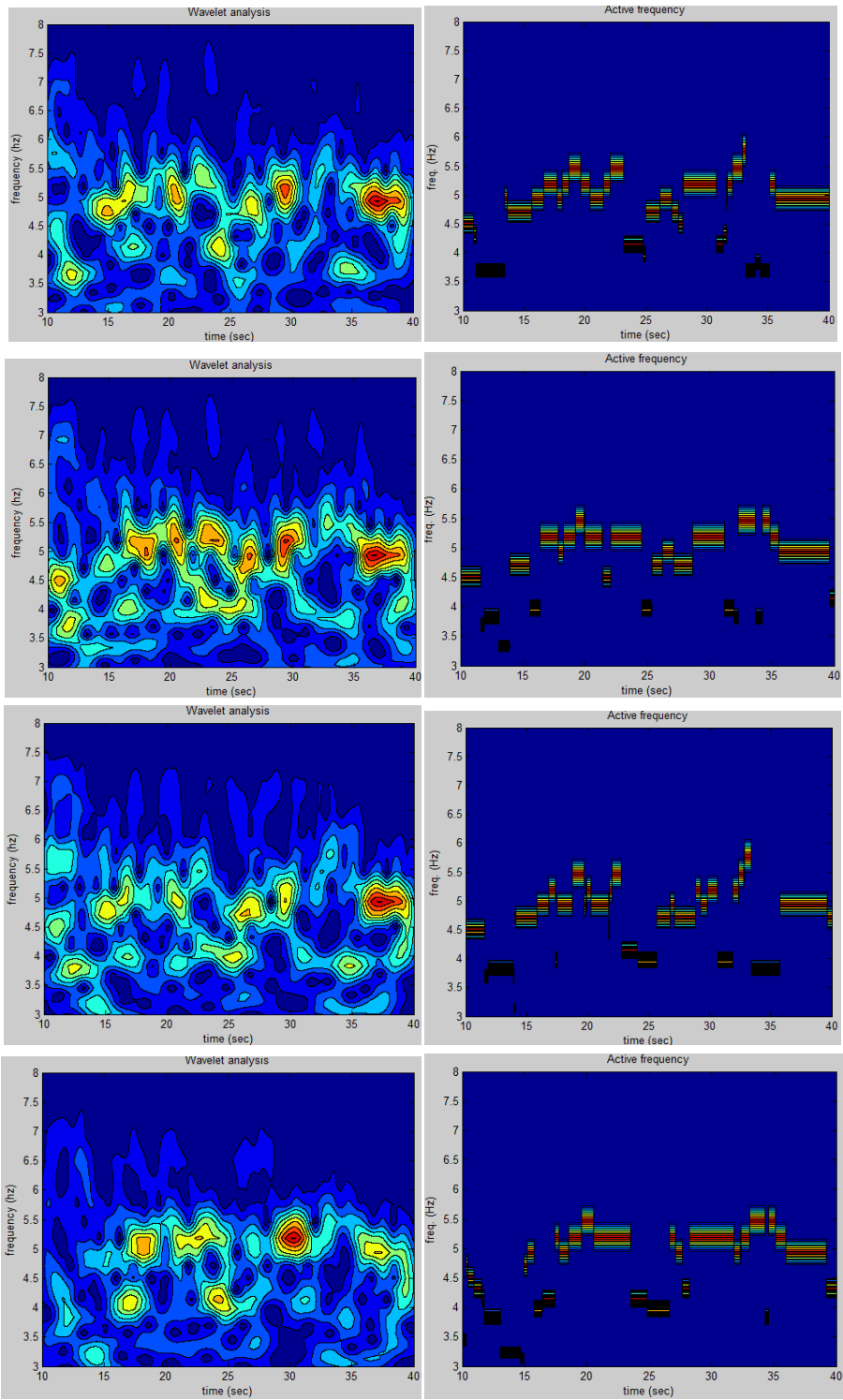
## Category 4, wavelet results of Hanoytangen test51 at 23 measurement points

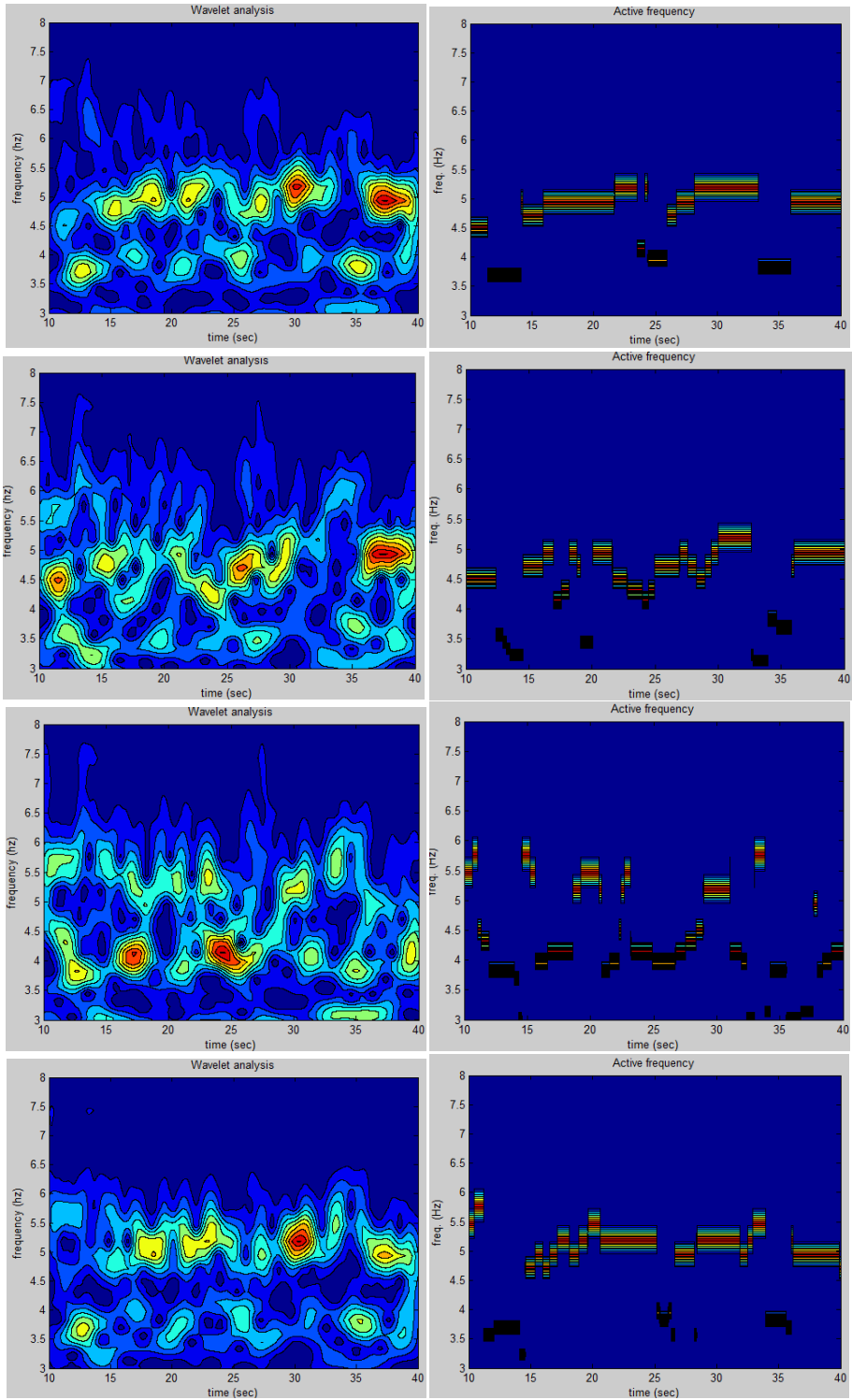


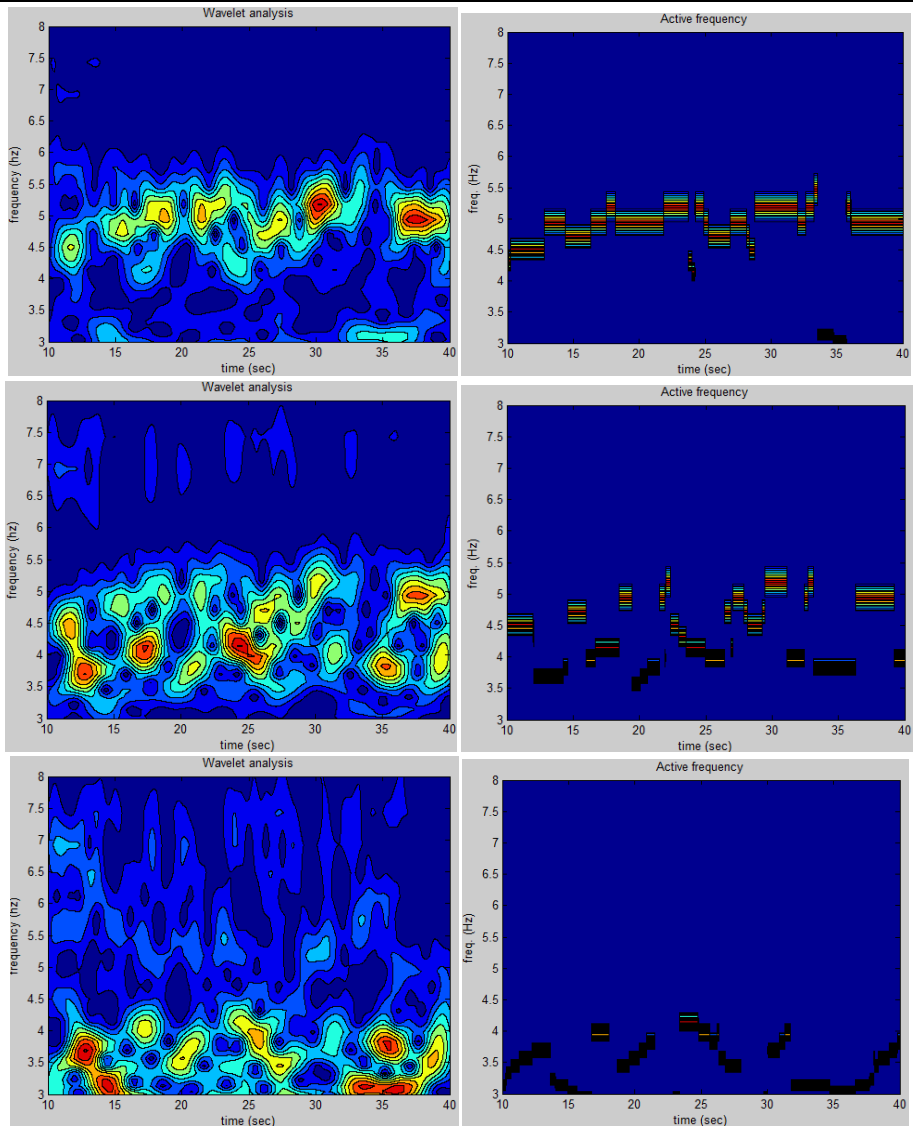




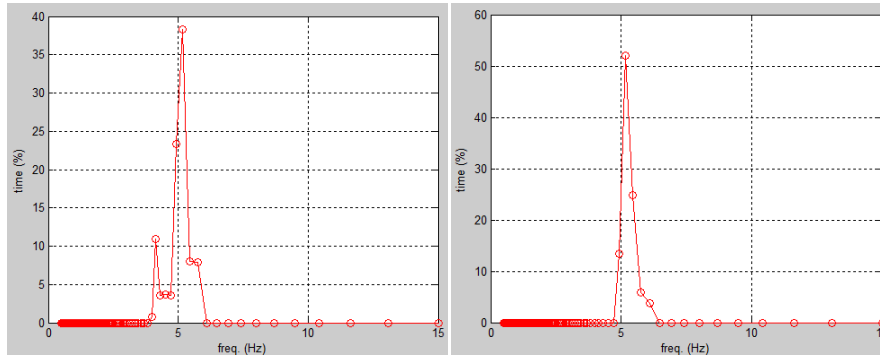




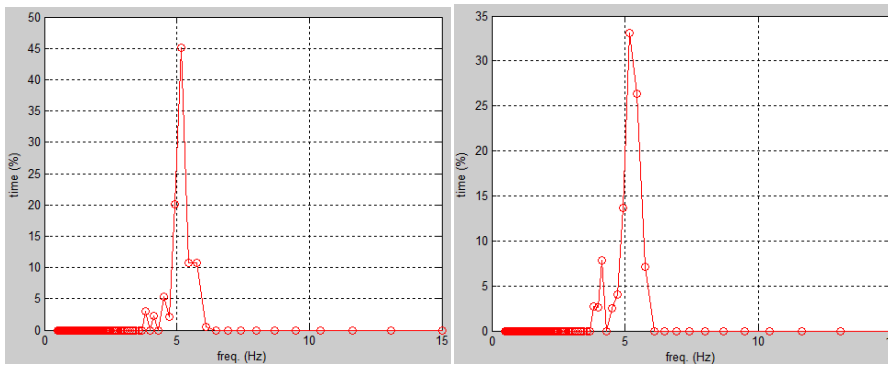




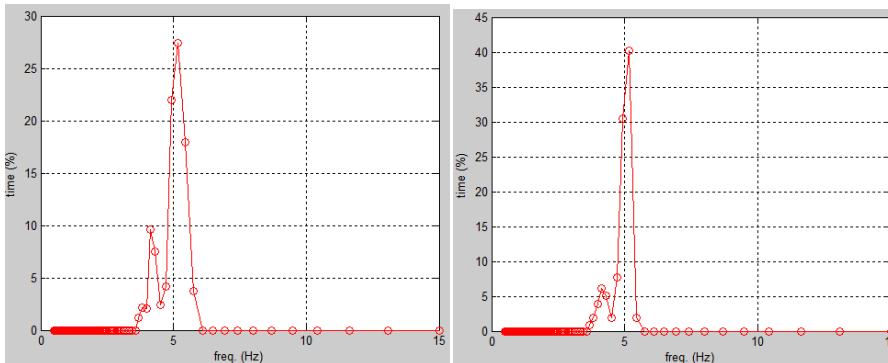
Category 4, time duration distribution of Hanoytangen test51 at 23 measurement points



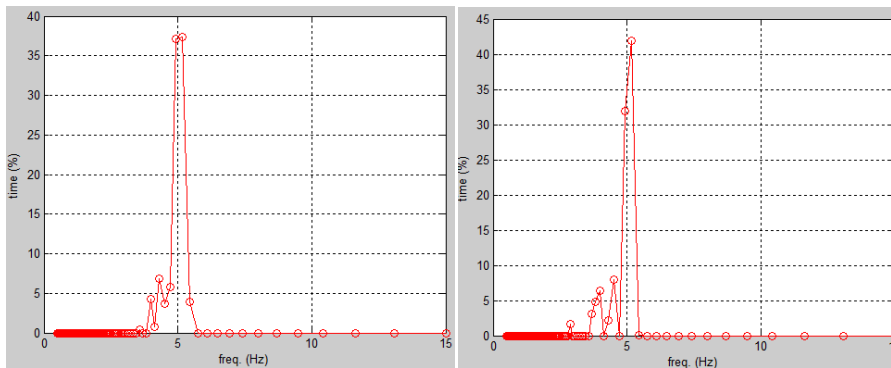
Location 1&Location 2



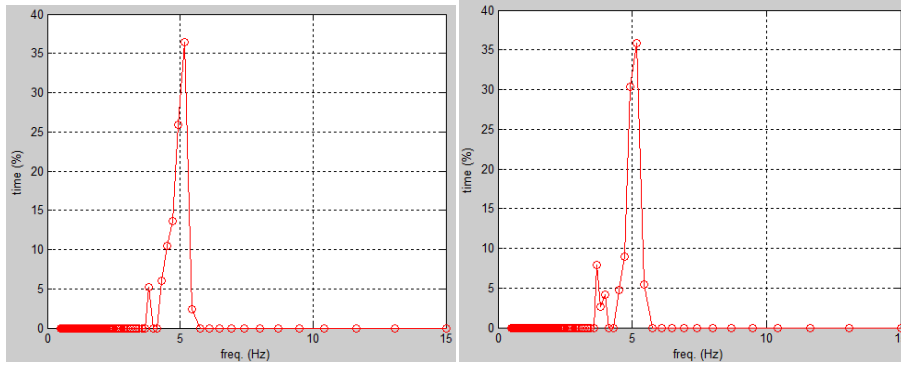
Location 3&Location 4



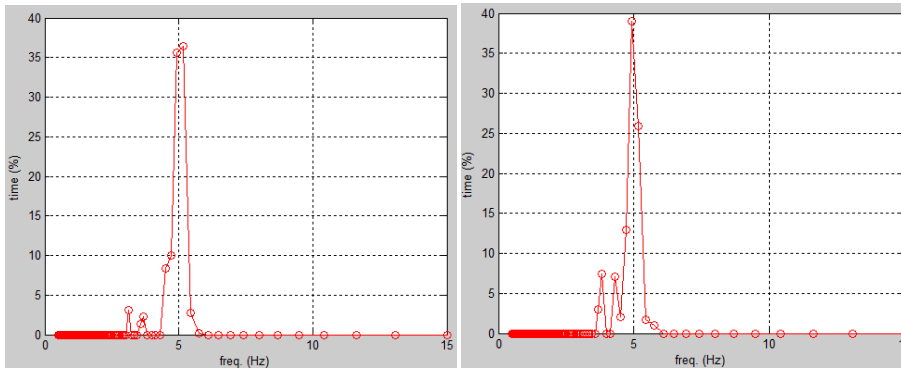
Location 5&Location 6



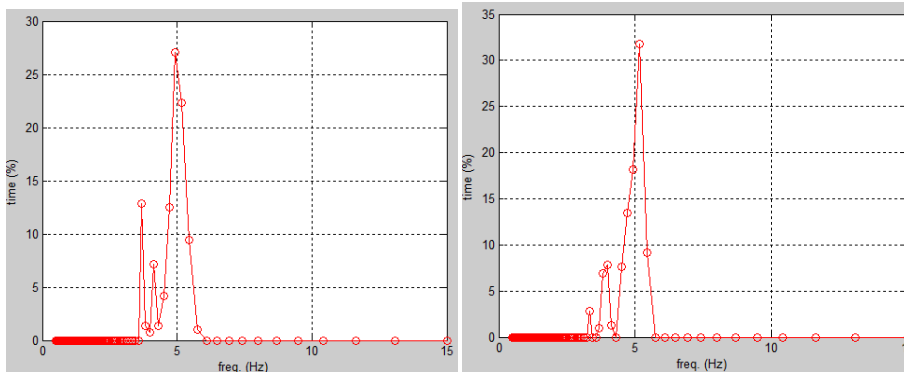
Location 7&Location 8



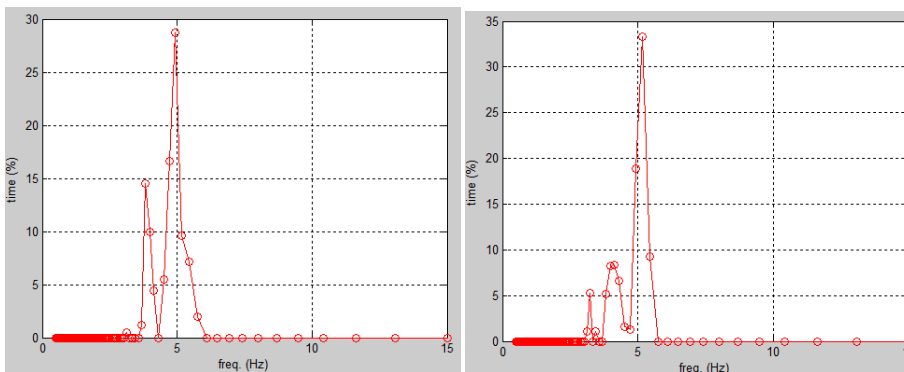
Location 9&Location 10



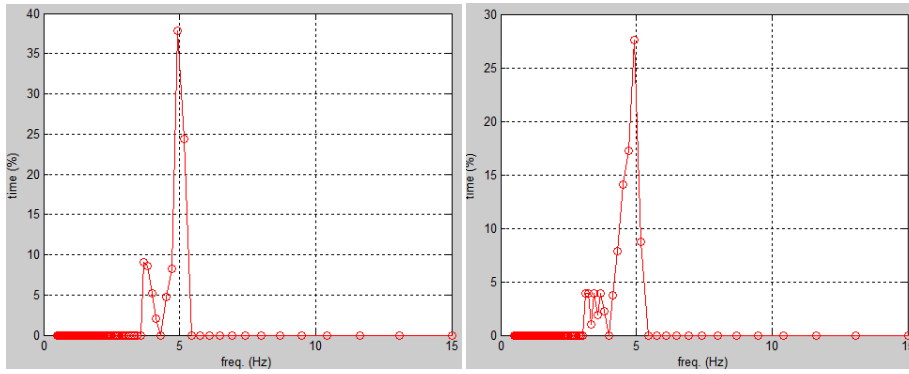
Location 11&Location 12



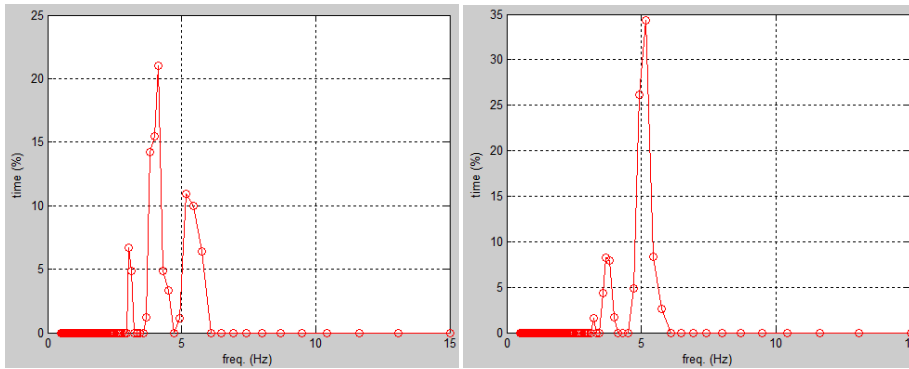
Location 13&Location 14



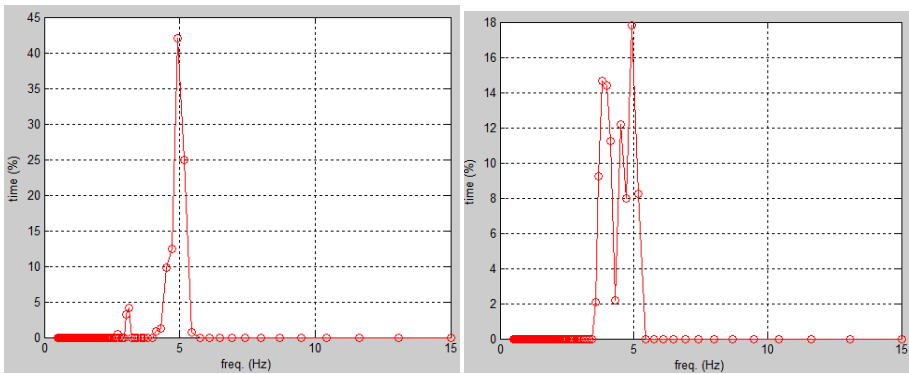
Location 15&Location 16



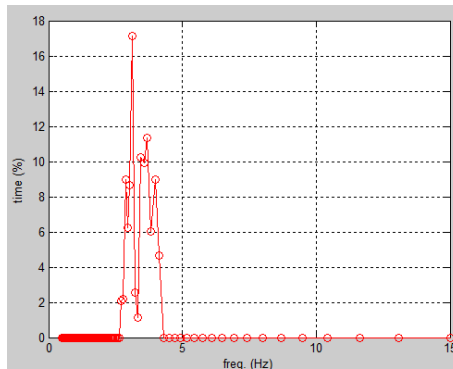
Location 17&Location 18



Location 19&Location 20



Location 21&Location 22



Location 23



Results of category 6 & 7

Table A7, Frequency Peaks for NDP (vertical direction is locations and horizontal is cases)

location	2310	2320	2330	2340	2350	2360	2370	2380	2390	2400	2410
1	1.497	2.269	2.432	2.606	3.439	3.686	4.234	4.863	4.863	5.987	5.987
2	1.497	2.117	2.269	2.606	3.439	3.439	4.234	4.863	4.863	5.586	6.417
3	0.010	2.117	2.269	2.606	3.439	3.439	4.234	4.863	4.863	5.586	6.417
4	1.497	2.269	2.432	2.606	3.439	3.686	4.234	4.863	4.863	6.417	6.417
5	1.497	1.975	2.432	2.606	3.439	3.950	4.234	4.863	5.586	5.987	6.417
6	1.497	2.117	2.117	2.606	3.439	3.950	4.234	4.863	5.212	5.987	6.417
7	1.497	2.117	1.975	2.606	3.439	3.950	4.234	4.863	5.212	5.987	6.417
8	1.497	2.117	2.269	2.606	3.439	3.686	4.234	4.863	5.212	5.586	6.417
9	1.497	1.975	2.117	2.606	3.439	3.439	4.234	4.538	4.863	5.586	6.417
10	1.497	1.975	2.117	2.606	3.439	3.439	4.234	4.234	4.863	4.863	6.417
11	1.497	1.975	2.117	2.606	3.439	3.439	4.234	4.234	4.863	5.212	6.417
12	1.497	1.975	2.117	2.606	3.439	3.439	4.234	4.538	4.863	4.863	6.417
13	1.497	1.975	2.117	2.606	3.439	3.439	4.234	4.538	4.863	4.863	6.417
14	4.538	2.117	2.117	2.606	3.439	3.686	4.234	4.234	4.863	5.212	5.987
15	1.497	2.117	2.117	2.606	3.439	3.686	4.234	4.234	4.538	5.586	5.987
16	1.497	2.117	2.117	2.606	3.439	3.439	4.234	4.234	4.538	4.863	5.987
17	1.497	1.397	2.269	2.606	3.439	3.439	4.234	4.863	4.863	4.863	6.417
18	1.497	1.975	1.975	2.606	3.439	3.439	4.234	4.538	5.212	5.212	5.987
19	1.497	1.975	2.117	2.606	3.439	3.439	4.234	4.538	4.538	4.863	6.417
20	1.497	1.975	2.117	2.606	3.439	3.686	4.234	4.538	4.863	4.863	5.987
21	1.497	1.975	2.117	2.606	3.439	3.439	4.234	0.035	0.044	0.047	0.107
22	1.497	1.975	2.117	2.606	3.439	3.439	4.234	4.234	4.538	4.863	6.417
23	0.010	0.018	6.417	2.606	3.439	3.439	4.234	4.538	4.863	4.863	5.987
24	0.010	1.975	2.117	2.606	3.439	3.439	4.234	4.538	4.538	5.212	5.987



2420	2430	2440	2450	2460	2470	2480	2490	2500	2510	2520
6.878	6.878	8.467	7.900	7.900	9.726	9.075	9.726	10.425	11.173	11.173
6.878	6.878	8.467	7.900	7.900	9.726	9.075	9.726	10.425	11.173	11.173
6.878	6.878	8.467	7.900	7.900	9.726	9.075	9.726	10.425	11.173	11.173
6.878	6.878	7.900	7.900	8.467	9.075	9.726	9.726	10.425	11.173	11.173
6.878	6.878	7.900	7.900	7.900	9.726	9.075	9.726	10.425	11.173	11.173
6.878	6.878	7.900	7.900	7.900	9.075	9.075	9.726	10.425	11.173	11.173
6.878	6.878	7.900	7.900	7.900	9.075	9.075	9.726	10.425	11.173	11.173
6.878	6.878	7.371	7.900	7.900	9.075	9.075	9.726	9.726	11.173	11.173
6.878	6.878	7.371	7.900	7.900	9.075	9.075	9.726	9.075	11.173	11.173
6.878	6.878	7.371	7.900	7.900	6.878	9.075	9.726	9.075	11.173	11.173
6.878	6.878	6.878	7.900	7.900	6.417	9.075	9.726	9.075	11.173	11.173
6.878	6.878	6.878	7.900	7.900	6.878	9.075	9.726	9.075	11.173	11.173
6.878	6.878	6.878	7.900	7.900	6.878	9.075	9.726	6.878	11.173	11.173
6.878	6.878	7.371	7.900	7.900	7.371	9.075	9.726	9.075	11.173	11.173
6.878	6.878	6.417	7.900	7.900	6.417	9.075	9.726	7.900	11.173	11.173
6.878	6.878	6.878	7.900	7.900	6.878	9.075	9.726	6.878	10.425	11.173
6.878	6.878	7.371	7.900	7.900	5.586	9.075	9.726	7.900	11.173	11.173
6.878	6.878	7.371	7.900	7.900	6.878	7.371	9.726	7.371	11.173	11.173
6.878	6.878	7.371	7.900	7.900	7.371	7.900	9.726	7.900	10.425	11.173
1.719	0.071	0.076	0.107	0.071	0.076	0.081	0.107	0.215	0.142	0.142
6.878	6.878	7.371	7.900	7.900	6.878	9.075	9.726	8.467	10.425	8.467
6.878	6.878	6.417	7.900	7.900	6.878	9.075	9.726	6.878	11.173	11.173
6.878	6.878	7.371	7.900	7.900	6.878	9.075	9.726	6.878	11.173	11.173





Table A8, frequency range for NDP (vertical direction is locations and horizontal is cases)

location	case2310		2320		2330		2340		2350		2360		2370		2380	
1	1.497	1.497	2.793	1.604	3.209	1.975	3.686	2.269	4.234	3.209	5.212	3.209	6.878	3.439	6.417	3.950
2	1.497	1.497	2.606	1.719	3.209	1.719	3.686	2.606	3.950	3.209	5.212	3.209	5.586	3.209	5.586	3.686
3	0.010	0.010	2.606	1.719	2.994	1.719	3.439	0.022	3.950	3.209	4.863	0.035	5.586	2.994	5.987	3.686
4	1.497	1.497	2.606	1.604	2.793	1.719	3.439	2.606	3.686	2.994	4.863	3.209	5.586	3.686	6.878	3.439
5	1.497	1.497	2.432	1.303	2.994	1.843	3.439	2.432	4.234	2.994	4.863	2.793	5.586	3.686	5.987	4.234
6	1.497	1.497	2.269	1.397	2.994	1.843	3.439	2.432	3.686	3.209	4.234	3.209	5.212	3.439	5.987	3.686
7	1.497	1.397	2.269	1.397	2.793	1.843	3.439	2.606	3.686	3.209	4.234	3.209	5.212	3.439	5.586	3.686
8	1.497	1.497	2.606	1.303	2.793	1.719	3.209	2.432	3.439	2.994	4.234	2.793	5.586	3.439	5.212	3.686
9	1.497	1.497	2.606	1.303	2.793	1.843	2.994	2.432	3.950	2.994	4.234	3.209	4.863	3.439	5.212	3.439
10	1.497	1.497	2.269	1.397	2.994	1.843	3.209	2.432	4.234	2.994	4.234	2.793	4.538	3.439	5.212	3.439
11	1.497	1.497	2.269	1.497	2.994	1.843	3.209	2.432	4.234	2.994	4.234	2.793	4.863	3.439	5.987	3.439
12	1.497	1.497	2.269	1.719	2.269	1.975	3.686	1.975	3.686	2.269	4.538	2.994	4.863	2.994	5.212	3.209
13	1.497	1.497	2.269	1.719	2.269	1.975	3.686	1.975	3.686	2.269	4.538	2.994	4.863	3.439	5.212	3.209
14	4.538	1.497	2.269	1.719	2.269	1.975	2.793	1.975	3.950	2.117	4.234	2.432	4.863	3.686	5.212	3.439
15	1.497	1.497	2.606	1.303	2.432	1.843	2.793	1.975	4.234	2.269	4.234	2.269	4.538	3.439	5.987	3.439
16	1.497	1.497	2.606	1.303	2.793	1.843	2.994	1.975	4.234	2.269	4.234	2.269	4.538	3.439	5.586	3.439
17	1.497	1.497	2.606	0.860	3.209	1.843	3.439	2.606	3.439	2.994	3.950	2.793	4.863	2.994	5.212	3.209
18	1.497	1.497	2.117	1.303	3.439	1.975	3.439	1.604	3.950	3.209	3.950	2.793	5.212	2.994	5.586	2.994
19	1.497	1.497	2.269	1.397	2.269	1.975	2.994	1.497	4.538	3.209	4.234	2.117	4.863	3.686	5.212	3.439
20	1.497	1.497	2.269	1.303	2.269	1.975	2.793	1.497	4.538	1.719	4.538	1.719	4.863	3.686	5.212	3.686
21	1.497	1.497	2.269	1.397	2.269	1.975	2.793	1.604	3.439	2.269	4.234	2.117	5.212	1.975	0.035	0.035
22	1.497	1.497	2.269	1.397	2.269	1.975	3.209	1.604	3.686	2.269	3.950	2.117	4.538	2.994	5.212	2.793
23	0.010	0.010	0.019	0.018	11.975	2.117	3.209	2.606	4.538	3.209	4.234	2.793	4.863	3.439	5.987	3.439
24	0.010	0.010	2.269	0.018	2.269	1.975	2.793	1.497	3.686	1.719	4.863	0.608	4.863	2.117	5.212	2.432



2390		2400		2410		2420		2430		2440		2450		2460	
7.371	4.538	7.371	4.538	7.900	5.586	7.371	5.987	9.075	6.878	9.726	6.417	8.467	7.371	11.173	6.878
6.878	4.538	7.371	4.538	7.900	5.586	8.467	5.586	9.726	5.987	9.726	5.987	7.900	7.900	10.425	6.417
6.417	3.950	7.371	4.538	7.900	5.212	8.467	5.586	8.467	5.987	9.726	5.987	7.900	7.900	10.425	6.417
7.371	4.234	7.900	4.538	7.900	5.212	9.075	5.987	8.467	6.417	9.075	5.987	8.467	7.900	9.726	7.900
6.417	4.234	7.900	4.538	7.371	5.212	7.900	5.586	7.900	6.878	9.726	6.878	7.900	7.900	10.425	5.586
6.417	3.950	6.878	4.538	7.371	5.212	7.900	5.586	7.900	6.878	9.726	6.417	7.900	7.900	9.726	6.878
6.417	4.234	6.878	4.538	7.371	5.212	7.900	4.538	7.900	6.878	9.726	6.417	7.900	7.900	10.425	5.586
6.417	3.950	6.878	4.538	7.900	5.212	7.371	4.863	8.467	5.987	9.726	5.987	7.900	7.900	10.425	6.417
5.987	3.950	6.878	4.234	7.900	5.212	7.371	5.212	7.371	5.987	9.726	5.212	7.900	7.900	11.173	6.417
6.417	3.686	6.417	3.950	7.900	4.234	7.371	4.538	7.371	4.863	9.075	4.538	7.900	7.900	11.173	0.071
5.987	3.686	6.417	3.950	7.371	4.234	7.371	4.538	7.371	5.212	9.075	4.538	7.900	7.900	11.173	5.987
5.987	2.994	6.417	3.686	7.371	3.950	9.075	4.234	7.371	4.863	8.467	4.538	7.900	7.900	9.075	5.212
5.987	2.994	6.878	4.234	7.371	3.950	7.900	4.234	7.371	4.863	8.467	4.538	7.900	7.900	9.075	5.212
5.987	3.686	6.417	3.950	6.878	4.538	7.900	3.950	7.371	5.212	8.467	4.538	7.900	7.900	11.173	4.863
5.987	3.686	6.417	3.950	7.371	4.234	7.900	3.950	7.900	3.950	7.900	4.538	7.900	7.900	8.467	5.586
6.417	2.793	6.417	3.950	6.878	4.234	7.900	3.950	7.371	4.234	8.467	4.234	7.900	7.900	8.467	5.586
5.987	2.793	6.417	4.234	6.878	4.538	7.371	4.538	7.371	4.863	8.467	4.538	7.900	7.900	9.075	4.234
5.987	2.994	6.417	3.686	6.878	4.863	8.467	2.994	7.371	5.212	8.467	4.538	7.900	7.900	9.726	5.212
5.212	3.686	6.417	3.950	7.371	3.950	7.900	4.234	7.371	4.234	7.900	4.538	7.900	7.900	8.467	4.234
6.878	3.686	6.417	3.950	7.371	3.686	7.900	3.950	7.371	4.538	8.467	4.234	7.900	7.900	9.726	4.234
0.044	0.044	0.047	0.047	0.115	0.107	3.209	0.921	0.142	0.071	0.076	0.071	0.107	0.107	0.076	0.071
6.878	2.793	6.878	2.606	7.900	2.793	8.467	2.606	7.900	3.950	14.743	4.234	7.900	7.900	9.726	3.950
6.878	3.686	7.900	3.686	7.900	4.234	8.467	4.538	7.371	4.234	9.075	4.538	7.900	7.900	9.726	5.212
5.987	2.793	6.878	2.432	7.371	2.793	7.900	4.538	7.371	4.234	14.743	4.538	7.900	7.900	12.834	5.212



2470		2480		2490		2500		2510		2520	
11.173	7.900	12.834	7.371	10.425	7.900	12.834	8.467	12.834	9.075	14.743	9.075
11.173	6.878	11.975	7.900	10.425	9.075	12.834	8.467	12.834	10.425	13.755	10.425
11.173	6.878	11.173	7.900	10.425	9.075	12.834	8.467	13.755	10.425	13.755	9.726
11.173	7.900	11.975	8.467	10.425	8.467	12.834	8.467	11.975	9.075	13.755	9.075
10.425	5.987	12.834	7.371	10.425	9.075	12.834	7.371	13.755	9.726	14.743	9.075
10.425	4.234	11.173	7.900	10.425	9.075	13.755	6.417	13.755	9.726	11.975	9.075
10.425	5.987	11.173	6.878	10.425	9.075	12.834	8.467	13.755	7.371	11.975	8.467
10.425	6.417	11.173	7.371	10.425	9.075	13.755	7.371	13.755	7.900	11.975	7.900
10.425	5.987	10.425	5.212	10.425	9.075	11.975	6.417	11.173	6.417	11.975	7.371
10.425	5.212	10.425	6.878	10.425	9.075	11.173	6.417	11.975	6.878	11.975	6.417
10.425	5.212	10.425	6.878	10.425	9.075	10.425	5.987	11.173	6.417	11.975	6.417
10.425	5.987	10.425	5.586	10.425	9.075	10.425	5.987	11.173	7.371	12.834	5.212
10.425	5.586	10.425	5.586	10.425	9.075	11.173	5.987	11.173	7.900	12.834	5.212
10.425	5.212	10.425	5.212	10.425	9.075	11.975	5.212	11.173	6.417	12.834	6.417
10.425	4.863	9.726	5.586	10.425	9.075	11.975	5.212	11.173	6.878	12.834	5.586
10.425	4.863	10.425	5.586	10.425	9.075	11.173	5.987	11.975	5.586	12.834	5.586
10.425	5.212	9.726	5.212	10.425	9.075	11.173	4.863	11.173	5.586	12.834	5.212
10.425	4.863	11.173	5.212	10.425	9.075	11.975	5.212	11.975	5.586	11.975	5.586
10.425	4.234	10.425	4.538	10.425	9.075	11.173	4.234	11.975	4.863	12.834	5.586
11.173	3.950	11.173	4.538	11.173	9.075	11.975	4.234	11.975	4.863	12.834	5.212
0.115	0.076	0.081	0.081	0.107	0.107	0.215	0.215	0.152	0.142	0.152	0.142
10.425	3.686	14.743	6.417	10.425	9.075	10.425	4.234	11.173	6.878	14.743	7.371
10.425	5.212	11.173	4.538	10.425	9.075	11.173	4.863	11.975	4.863	12.834	5.586
11.173	5.212	13.755	4.538	10.425	9.075	11.975	5.212	22.346	6.417	13.755	5.212



Table A9, peak frequency for Hanoytangen (vertical direction is locations and horizontal is cases)

	33	34	35	36	37	38	39	40	41	42	43	44	45	46	47
1	1.357	1.539	1.947	1.947	2.196	2.582	2.870	2.956	3.288	3.300	3.729	4.020	4.512	4.434	4.761
2	1.339	1.539	1.749	1.911	2.064	2.649	2.792	2.956	3.839	3.574	3.676	4.592	4.592	4.512	4.851
3	1.357	1.172	1.947	1.947	2.151	2.870	2.792	2.901	3.839	3.478	3.676	4.592	4.512	4.434	4.851
4	1.719	1.539	1.947	1.947	2.107	2.870	2.792	2.956	3.912	3.343	3.676	4.592	4.512	4.512	4.851
5	1.339	1.539	1.749	1.587	2.107	2.870	2.792	2.956	3.839	3.526	3.676	4.020	4.512	4.434	4.851
6	1.339	1.172	1.749	1.947	2.151	2.870	2.792	2.956	3.912	3.478	3.676	3.958	4.512	4.512	4.512
7	1.719	1.539	1.749	1.843	2.151	2.649	2.792	2.956	3.839	3.140	3.676	3.958	4.512	4.434	4.512
8	1.339	1.539	1.749	1.587	2.151	2.870	2.792	2.901	3.912	3.140	3.676	3.958	2.550	4.434	4.512
9	1.339	1.339	1.749	1.394	2.151	2.870	2.792	2.746	3.912	3.140	3.676	3.958	4.512	4.512	4.512
10	1.339	1.539	1.749	1.876	2.151	2.196	2.792	2.956	3.839	3.432	3.676	3.958	3.300	3.300	4.287
11	1.539	1.539	1.947	0.811	0.660	2.870	2.792	2.699	2.836	3.140	3.676	4.020	3.259	4.149	4.512
12	1.339	1.691	1.749	1.587	2.151	2.196	2.792	2.956	2.917	3.432	3.625	3.958	3.343	4.512	4.512
13	1.339	1.357	1.749	1.394	2.151	2.196	2.792	2.699	3.839	3.140	3.676	3.958	3.259	3.840	4.359
14	1.339	1.539	1.947	1.947	2.151	2.870	2.792	2.956	2.876	3.432	3.625	4.020	3.432	4.512	4.592
15	1.339	1.539	1.947	1.947	2.151	2.649	2.792	2.699	3.912	2.655	3.625	3.958	3.343	2.655	4.761
16	1.719	1.691	1.749	1.587	2.151	2.649	2.792	2.699	3.397	3.178	3.625	4.020	3.343	3.343	4.083
17	1.339	1.357	1.947	1.947	2.151	2.196	2.792	2.956	3.839	2.994	3.676	3.958	3.958	4.083	4.944
18	1.339	1.539	1.563	1.394	2.151	2.196	2.792	2.699	3.573	3.387	3.625	4.512	3.259	4.512	4.512
19	1.719	1.563	1.749	1.587	2.151	2.870	2.792	2.699	2.876	2.994	3.676	3.958	3.218	2.740	4.287
20	1.719	1.172	1.749	1.947	2.151	2.196	2.792	2.699	3.839	3.178	3.676	3.958	3.259	3.343	3.432
21	1.339	1.357	1.563	1.394	2.151	2.870	2.792	2.699	2.876	2.994	2.830	2.926	3.218	4.512	4.851
22	1.339	1.357	1.749	1.587	2.151	2.196	2.792	2.000	3.912	3.178	3.676	3.958	3.784	4.512	4.512
23	1.339	1.357	1.749	1.947	2.151	2.196	2.792	2.699	2.876	3.387	3.625	2.926	3.387	2.711	3.432



48	49	50	51	52	53	54	55	56	58	59	60	61
4.675	5.141	4.675	5.239	5.346	5.825	5.459	5.825	5.697	5.825	6.559	6.907	6.728
4.592	5.354	4.851	5.239	5.346	5.958	5.575	5.825	6.397	6.559	6.559	6.907	6.728
4.675	4.851	4.851	5.136	5.346	5.958	5.459	5.825	6.397	6.397	6.559	6.907	6.728
4.675	4.851	4.851	5.136	5.239	5.958	5.459	5.958	6.397	6.559	6.559	6.907	6.728
4.149	4.851	4.851	5.239	5.239	5.825	5.575	5.825	6.397	6.559	6.559	6.907	6.728
4.149	4.851	4.851	5.036	5.036	5.825	5.346	5.825	5.958	6.098	6.559	6.907	6.728
4.149	4.851	4.851	5.036	5.239	5.239	5.459	5.825	6.244	6.098	6.728	6.907	6.728
4.217	4.851	4.851	5.036	5.239	5.239	5.575	5.958	5.958	6.098	6.728	6.907	6.397
4.083	3.840	4.851	5.136	4.512	4.760	5.459	5.825	5.459	5.697	5.575	6.244	6.559
4.217	4.851	4.851	4.941	5.136	5.239	5.346	5.239	5.136	5.697	5.575	6.098	6.559
4.083	4.851	4.761	5.036	5.346	5.136	5.136	5.825	5.136	5.825	5.575	6.244	6.397
3.840	3.840	4.851	5.036	5.239	4.941	5.036	5.825	5.036	5.575	5.575	6.244	6.397
4.217	3.676	4.851	5.036	4.153	4.849	5.697	5.825	5.459	5.575	5.575	6.244	6.244
4.083	3.840	4.761	5.239	3.904	5.346	5.346	5.239	4.760	5.575	5.346	6.098	6.244
3.102	3.840	4.761	4.941	3.904	4.849	5.697	5.825	5.459	5.825	5.697	6.907	6.728
4.217	3.898	4.149	5.136	4.153	5.239	4.024	5.346	5.136	5.239	6.397	6.728	6.397
3.784	4.851	4.851	5.136	5.036	4.941	5.036	4.849	5.136	4.941	6.559	6.098	6.397
4.217	3.625	4.761	4.941	4.592	4.849	4.941	5.958	4.674	5.958	5.697	5.958	6.397
4.083	3.840	4.149	4.087	3.904	5.459	5.575	5.825	4.436	5.825	5.575	5.958	6.244
3.784	3.840	4.851	5.136	5.239	5.239	5.575	5.825	5.136	5.697	5.575	5.958	5.575
3.102	4.851	4.851	4.941	5.036	5.346	5.036	4.760	4.760	4.941	4.849	5.958	5.036
4.149	3.840	4.761	4.941	3.904	4.849	3.790	4.512	4.674	4.849	4.512	6.907	4.361
3.102	3.029	3.478	3.111	3.683	3.351	3.735	3.351	6.397	5.825	6.559	6.907	6.559



62	63	64	65	66
6.098	6.728	6.244	7.095	7.095
6.098	6.728	7.095	7.095	7.095
6.907	6.728	7.095	7.294	7.095
6.907	6.728	7.095	7.095	7.294
6.907	6.728	7.095	7.095	7.095
6.907	6.728	6.397	7.294	7.294
6.907	6.728	6.397	7.294	7.294
6.098	6.728	6.397	7.095	7.294
6.098	6.559	6.397	7.294	7.294
5.958	6.559	6.397	7.294	7.294
5.958	6.559	6.397	7.294	7.294
5.958	6.397	6.397	7.294	7.294
6.244	6.397	6.397	7.095	7.095
5.958	6.397	6.397	6.907	7.095
6.728	6.728	5.575	6.728	6.559
6.559	6.559	6.397	6.728	6.397
6.098	6.559	6.397	6.728	6.397
5.958	6.559	6.397	6.244	6.244
5.958	5.825	6.397	5.958	6.244
5.459	5.958	5.575	5.958	7.294
5.459	4.941	5.575	7.294	7.294
6.907	6.728	7.095	7.294	7.294
6.907	6.728	6.559	7.294	7.294



Table A10, Frequency range for Hanoytangen (vertical direction is locations and horizontal is cases)

Location	33		34		35		36		37		38		39		40	
1	2.196	1.322	1.779	1.339	2.151	1.719	2.244	1.539	2.294	0.589	3.231	2.151	3.040	2.719	3.490	2.405
2	1.719	1.322	1.563	1.339	1.985	1.517	2.107	1.394	2.196	0.534	2.953	2.107	3.566	2.401	3.655	2.405
3	2.196	1.145	2.244	0.781	2.401	1.612	2.196	1.911	2.459	1.985	2.953	2.196	3.566	2.649	3.269	2.332
4	1.810	1.289	1.749	0.775	1.985	0.628	2.196	1.749	2.151	1.985	2.953	2.151	3.447	2.649	3.269	2.443
5	1.719	1.322	1.563	1.322	1.810	1.539	1.947	1.539	2.244	1.985	2.870	2.459	2.953	2.649	3.490	2.652
6	1.810	1.158	1.749	1.172	1.985	1.394	1.985	1.394	2.244	2.107	2.870	2.151	3.132	2.649	3.269	2.405
7	1.911	1.432	1.779	1.185	1.810	1.539	2.151	1.563	2.196	2.024	2.953	2.401	3.335	2.649	3.074	2.652
8	2.151	1.158	1.587	1.199	1.947	1.539	2.196	1.539	2.151	2.024	2.870	2.196	3.231	2.649	3.201	2.405
9	1.719	1.322	1.749	1.322	1.843	1.375	1.985	1.357	2.151	2.024	2.870	2.064	3.231	2.649	3.014	2.405
10	1.749	1.133	1.664	1.158	1.947	1.413	2.244	1.375	2.244	2.107	3.040	2.151	3.040	2.582	3.074	2.405
11	1.947	1.158	1.563	1.158	1.985	0.592	1.612	0.793	1.273	0.585	2.870	0.636	3.231	2.347	3.014	0.672
12	1.719	1.289	1.749	1.185	1.947	1.357	2.024	1.563	2.151	2.024	3.040	2.151	3.040	2.582	3.074	2.443
13	1.749	1.305	1.749	1.305	1.911	1.375	2.196	1.357	2.244	2.107	2.870	2.151	3.231	2.294	2.848	2.139
14	1.947	1.133	1.612	1.158	1.985	1.375	1.985	1.563	2.196	2.024	2.870	1.911	3.040	2.649	3.074	2.443
15	1.357	1.305	1.637	1.305	1.947	1.357	1.985	1.357	2.196	2.024	2.719	1.911	3.335	2.519	2.796	2.443
16	1.779	1.172	3.447	1.158	1.843	1.563	1.985	1.587	2.196	1.749	2.870	1.691	3.335	2.347	2.796	2.443
17	1.876	1.158	1.719	1.158	1.985	1.339	2.107	1.375	2.151	2.024	2.870	1.947	3.040	2.649	3.074	2.652
18	1.357	1.257	1.563	1.185	1.779	1.322	2.401	1.357	2.294	2.107	2.649	2.151	3.335	2.294	2.848	2.443
19	1.779	1.339	1.749	1.322	1.911	1.339	1.985	1.563	2.151	1.749	2.953	1.947	3.040	2.649	3.074	2.482
20	2.196	0.799	2.151	0.775	1.947	1.273	2.151	1.587	2.151	2.024	2.582	2.064	3.335	2.244	2.956	2.000
21	1.357	1.158	1.563	1.158	1.749	1.199	2.719	1.063	2.294	2.107	2.953	2.196	3.040	2.649	2.956	2.482
22	1.749	1.242	1.810	1.185	1.947	1.322	2.024	1.394	2.151	1.779	2.582	1.947	3.335	1.664	3.571	1.792
23	1.779	1.273	1.779	1.289	1.947	1.305	2.024	1.563	2.151	2.024	2.953	2.151	3.040	2.649	3.269	2.443



41		42		43		44		45		46		47		48	
3.912	2.724	3.526	2.994	4.359	2.861	4.675	2.740	4.592	3.300	4.592	3.300	5.141	3.478	5.040	3.300
4.321	2.620	3.958	2.769	4.359	2.861	4.675	2.683	4.761	4.149	4.944	2.655	5.141	4.359	5.354	4.149
3.987	2.654	3.729	2.861	4.149	2.799	4.675	2.711	4.761	3.840	4.675	2.683	5.040	4.287	5.245	3.102
3.912	3.288	3.676	3.065	4.083	2.926	4.675	2.711	4.592	3.218	4.675	3.259	4.944	3.300	5.245	3.300
3.987	2.724	3.729	2.799	4.020	2.830	4.592	2.683	4.761	3.729	4.675	2.683	5.245	3.178	5.245	3.102
3.912	2.761	3.526	2.799	3.898	2.861	4.592	2.861	4.761	2.799	4.592	2.501	5.040	3.140	4.944	3.102
4.066	2.689	3.526	2.994	4.020	2.711	4.592	2.655	4.592	2.550	4.512	2.550	5.040	3.178	4.761	3.140
3.987	2.876	3.625	2.385	4.020	2.861	4.592	2.960	4.592	2.525	4.675	2.628	5.040	3.102	4.851	3.065
4.066	2.836	3.625	2.408	3.958	3.065	4.512	3.432	4.675	2.525	4.592	2.453	5.040	3.178	4.761	3.102
3.912	2.836	3.526	2.861	4.020	2.830	4.675	2.628	4.287	3.259	4.512	2.477	5.040	3.140	4.761	2.655
3.912	0.691	3.574	0.843	3.784	3.065	4.592	0.604	4.592	0.539	4.675	0.528	4.761	0.554	5.245	1.194
3.987	2.836	3.526	2.525	4.020	2.830	4.512	2.926	4.512	2.525	4.512	2.550	5.040	3.343	4.675	2.628
3.912	2.654	3.574	2.655	3.840	3.065	4.944	2.683	4.512	3.065	4.434	2.576	5.467	3.102	4.675	3.065
3.987	2.876	3.574	2.385	3.958	2.830	4.512	2.926	4.217	2.926	4.675	2.893	4.851	3.343	5.245	2.711
3.987	2.620	3.526	2.655	3.840	2.655	4.761	2.576	4.149	3.218	4.512	2.576	4.851	2.628	4.675	3.065
3.987	2.464	3.526	2.408	3.729	2.628	4.512	2.430	4.217	3.218	4.512	2.525	5.245	3.102	4.287	3.065
3.912	2.798	3.625	2.655	3.898	2.769	4.761	2.183	4.149	2.112	4.761	2.683	5.141	2.861	5.141	2.628
3.769	2.274	3.574	2.363	3.784	2.453	4.592	2.453	4.761	2.477	4.761	2.550	5.040	3.102	4.675	2.321
3.987	2.798	3.343	2.628	3.840	2.711	4.675	2.926	4.592	2.602	4.592	2.655	5.467	2.501	4.434	2.960
3.987	2.249	3.574	2.363	4.020	2.430	4.020	2.202	4.149	2.363	4.149	2.112	5.245	3.102	5.245	2.280
3.573	2.724	3.387	2.385	3.729	2.628	4.675	2.655	4.592	2.576	4.675	2.655	5.141	2.926	5.040	2.602
3.987	2.274	3.840	2.342	4.217	3.029	4.761	3.300	4.761	3.218	4.592	3.343	4.851	3.387	4.592	3.387
3.912	2.724	3.574	2.363	3.784	2.683	4.020	2.202	3.432	2.453	4.149	2.477	4.217	2.183	4.287	2.576





49		50		51		52		53		54		55		56	
5.467	3.478	5.354	3.526	5.825	4.087	5.825	4.289	6.098	4.592	6.098	4.361	6.559	4.361	6.559	4.087
5.839	4.592	5.839	4.592	6.244	4.941	6.397	4.674	6.244	4.592	6.397	4.941	6.907	5.036	6.559	5.346
5.586	3.729	5.467	4.359	5.697	3.790	5.825	4.361	6.244	4.941	6.397	4.512	7.095	4.760	6.728	4.941
5.467	3.478	5.467	3.840	5.697	3.846	5.958	3.735	6.244	4.436	6.397	4.941	6.728	4.760	6.907	4.849
5.467	3.625	5.467	4.149	5.697	3.735	5.697	4.087	6.244	4.361	6.397	3.904	6.728	4.289	6.907	5.575
5.467	3.178	5.467	3.218	5.346	3.904	5.697	3.790	6.397	4.220	6.397	3.963	6.559	4.849	6.559	4.289
5.354	3.140	5.586	3.300	5.575	3.963	5.958	3.790	6.244	4.289	6.397	4.220	6.559	4.361	6.559	4.289
5.354	3.140	5.245	3.259	5.346	2.871	5.697	3.846	5.958	4.087	6.397	3.904	6.728	4.153	6.397	3.846
5.709	3.102	5.040	3.178	5.346	3.790	5.575	3.439	5.697	3.485	5.697	3.904	6.244	4.024	6.397	4.436
5.354	3.102	5.467	3.218	5.459	3.631	5.575	3.533	5.459	3.439	6.907	3.581	6.559	4.087	6.397	4.220
5.467	2.711	5.040	0.575	5.346	3.111	5.459	3.308	5.958	3.581	6.728	3.790	6.559	4.153	6.397	4.512
5.354	3.029	5.040	3.029	5.346	3.735	5.346	3.226	6.397	3.148	6.907	3.790	6.397	4.024	6.397	4.436
5.467	3.065	5.354	3.102	5.575	3.631	5.575	3.439	5.697	3.533	6.728	3.351	6.397	4.087	6.559	4.512
5.586	2.830	5.467	3.478	5.575	3.308	5.575	3.267	6.244	4.592	6.728	3.904	6.244	4.024	6.728	4.512
5.709	2.861	4.944	3.259	5.697	3.735	5.459	3.790	5.958	4.512	5.825	3.439	6.559	4.024	6.559	4.512
5.586	3.029	5.245	3.300	5.459	3.187	5.575	3.351	5.575	4.087	6.559	3.683	6.559	3.395	6.397	4.361
5.354	2.769	5.040	2.994	5.239	3.631	5.346	2.721	6.397	3.790	6.559	3.581	6.559	3.683	6.559	2.871
4.944	3.029	4.944	3.102	5.136	3.111	5.346	3.308	6.397	4.592	6.559	3.395	6.397	3.395	6.397	4.289
5.709	2.799	5.354	2.994	5.697	3.074	5.697	2.692	6.098	3.904	5.697	3.790	6.244	4.024	6.397	4.361
5.467	3.343	5.354	3.387	5.697	3.581	5.825	3.351	6.098	3.631	5.697	3.581	6.098	3.533	6.098	3.485
5.586	2.799	5.245	2.550	5.346	3.074	5.575	2.721	5.459	4.361	5.697	3.003	5.958	2.903	5.575	4.361
4.944	3.343	4.944	3.625	5.136	3.533	5.346	3.683	5.239	3.846	5.239	3.533	5.036	3.533	6.728	1.728
4.020	2.799	4.512	2.477	4.153	2.721	4.087	2.692	6.244	2.511	5.697	2.903	6.244	2.692	6.907	2.250



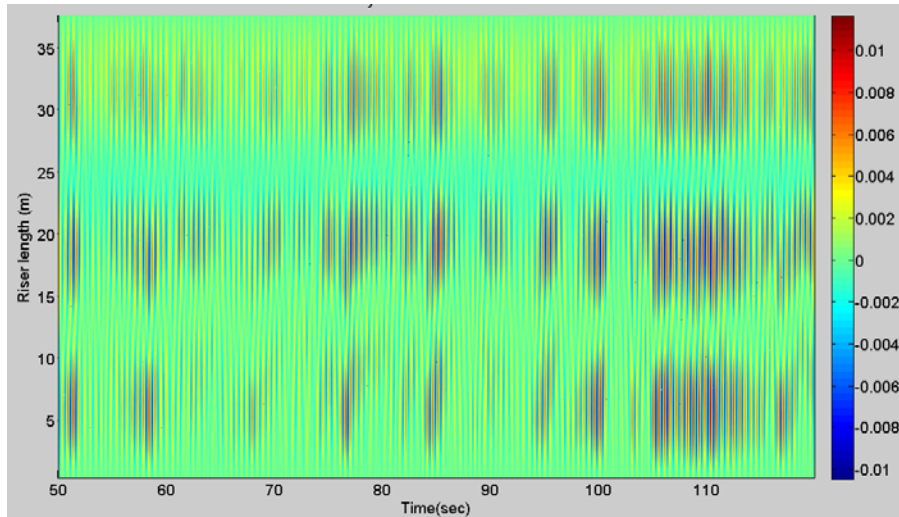
58		59		60		61		62		63		64		65		66	
6.728	4.849	6.728	3.963	7.095	4.674	6.907	0.602	7.095	4.760	7.095	4.941	8.482	4.849	8.482	5.459	7.504	5.346
6.728	4.849	6.728	5.575	7.095	5.697	7.095	5.825	7.726	5.575	8.482	5.459	8.482	5.825	8.767	5.825	9.400	6.397
6.907	4.849	6.907	4.592	7.095	5.958	7.504	5.459	7.726	5.825	8.482	6.397	8.482	5.697	8.767	6.728	8.767	6.559
6.907	4.849	6.907	5.459	7.095	5.958	7.294	5.575	7.963	5.697	8.214	4.941	8.482	5.958	8.482	6.098	8.482	5.459
6.728	4.941	6.907	5.825	7.095	5.958	7.294	5.825	7.726	5.958	8.214	6.244	8.214	5.958	8.482	6.098	8.482	6.244
6.907	4.674	6.907	5.036	7.294	5.697	7.095	5.346	7.095	5.697	8.214	5.036	7.095	6.244	8.482	5.136	7.504	5.697
6.728	4.849	6.907	4.592	7.095	5.575	7.095	4.361	6.907	5.697	8.214	4.941	7.095	6.244	8.482	4.941	7.504	5.697
6.728	5.239	6.907	5.036	7.095	5.825	7.095	5.575	6.907	5.825	8.214	4.849	7.095	6.244	7.726	5.697	7.504	5.459
6.559	4.436	6.907	4.436	7.294	5.239	7.095	4.512	6.907	5.575	7.095	4.849	7.095	6.244	7.726	5.575	7.504	5.697
6.728	4.436	6.728	5.136	7.294	5.459	7.095	4.512	6.907	5.575	7.095	4.849	7.294	5.346	7.294	5.575	7.504	5.459
6.397	4.153	6.907	4.361	7.294	5.459	6.907	5.136	6.907	5.575	8.214	3.581	7.294	5.239	8.767	4.941	7.504	5.459
6.728	3.904	6.907	3.904	7.294	5.459	6.907	4.361	6.907	5.575	8.214	3.351	7.095	5.346	7.294	4.941	7.504	5.459
6.728	4.436	6.559	4.220	7.095	5.459	6.907	4.592	6.907	5.459	8.214	3.395	7.095	5.346	9.073	4.941	7.504	4.153
6.907	4.087	6.559	4.592	7.095	5.346	6.907	4.087	6.907	5.346	8.214	3.308	7.095	5.459	7.294	4.024	7.504	5.239
6.728	4.436	6.728	4.592	7.095	5.575	7.095	4.592	6.907	5.346	7.095	3.735	7.095	5.346	7.294	3.963	7.504	4.674
6.728	4.289	6.728	4.849	7.095	5.239	6.728	4.361	6.907	5.136	7.294	4.849	7.095	4.941	7.504	4.289	7.095	4.087
6.728	4.849	6.728	4.849	6.907	3.683	6.728	4.512	6.728	4.849	6.907	3.631	6.907	4.760	6.728	4.849	6.728	2.935
6.244	4.220	6.728	3.485	6.907	4.592	6.728	4.289	6.559	4.760	6.728	3.267	7.294	4.941	8.482	4.512	10.132	4.153
6.098	4.024	6.397	3.846	6.397	3.963	6.559	4.024	6.559	5.459	8.482	1.661	7.294	5.459	8.767	3.963	7.504	2.935
5.958	3.790	5.958	4.849	7.095	3.790	6.728	3.581	6.244	5.239	8.214	1.933	6.559	4.941	8.767	4.941	8.767	5.036
5.697	4.289	5.825	4.674	7.095	4.512	7.095	4.361	6.098	4.220	8.214	3.395	7.294	4.592	8.767	4.361	8.767	2.935
5.239	3.683	6.907	3.485	7.294	3.735	7.095	3.846	7.504	4.024	8.482	1.651	7.504	3.846	8.767	3.904	8.767	4.024
6.907	2.535	7.294	2.839	7.294	5.825	7.504	3.439	6.907	5.958	7.294	3.226	7.504	6.098	8.767	2.331	9.752	2.935



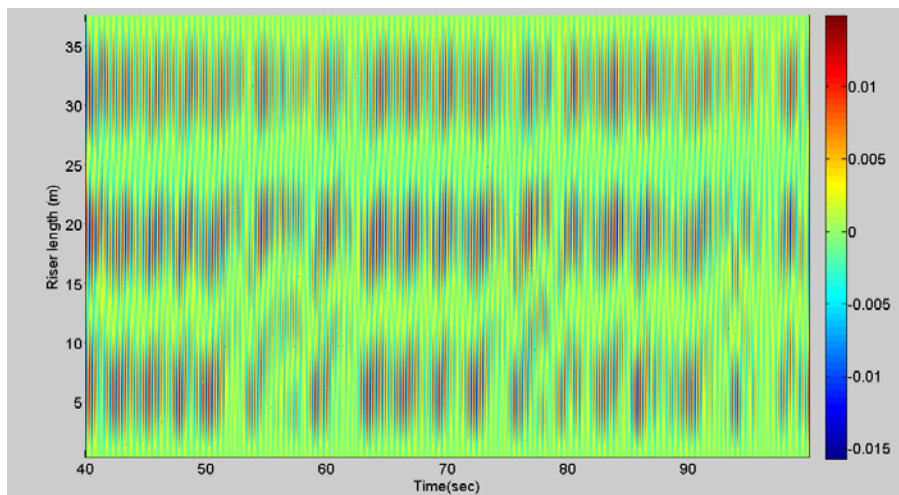
### Results of category 8

Result of category 8, Displacement history of NDP test for bare riser under shear current:

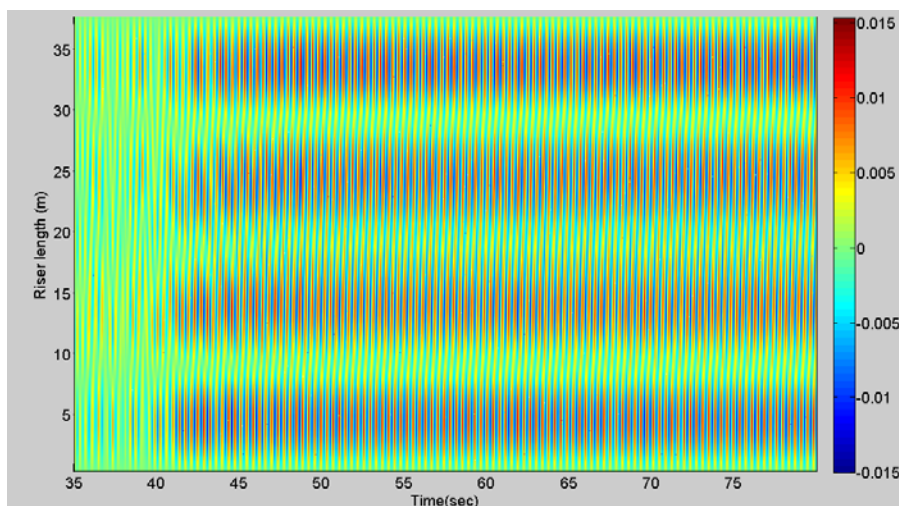
Test2320



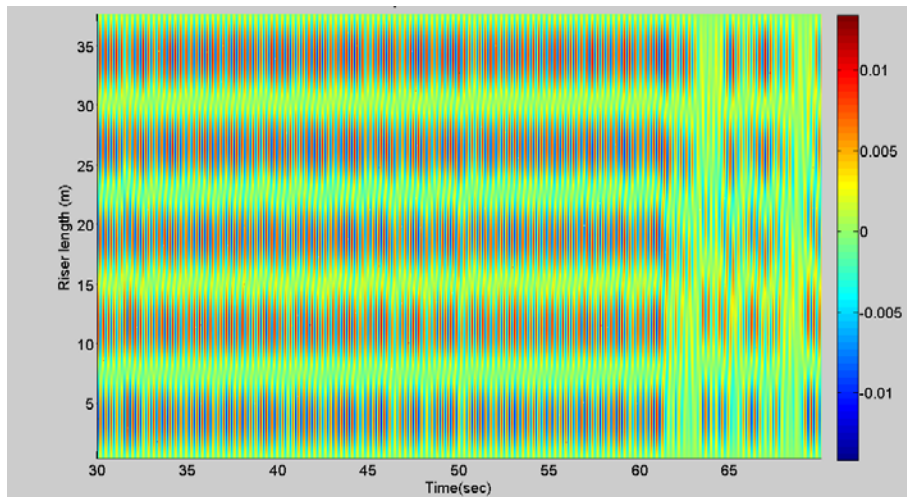
Test2330



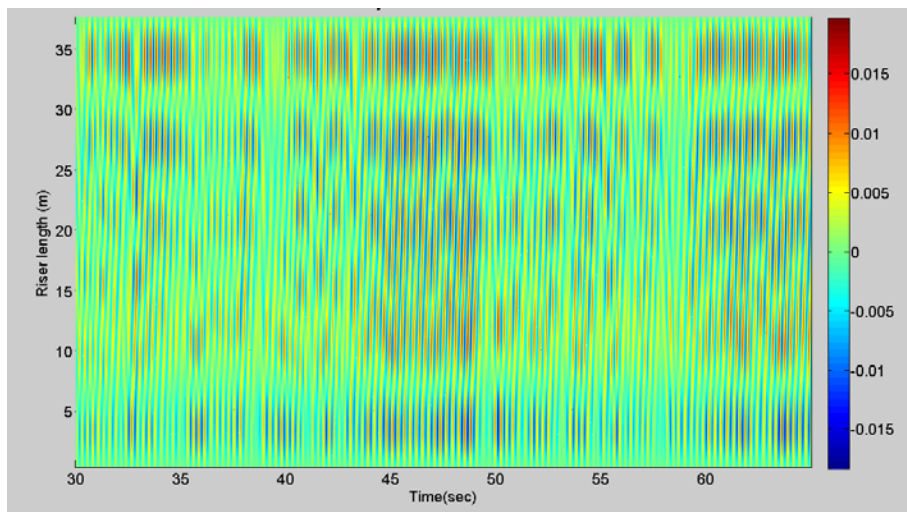
Test2340



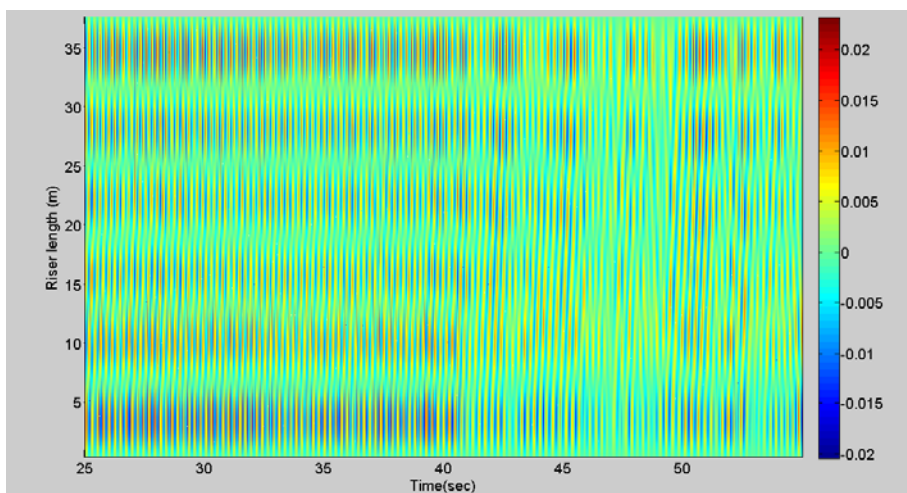
Test2350



Test2360

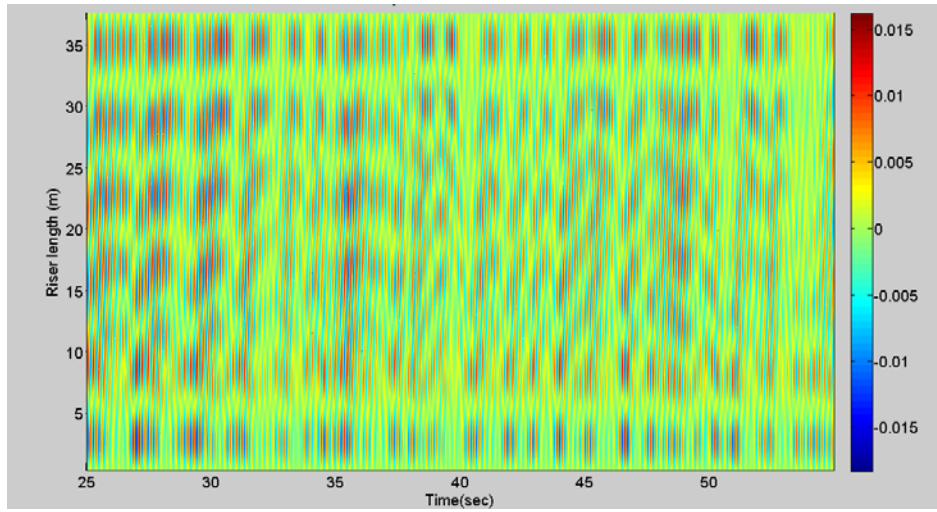


Test2370

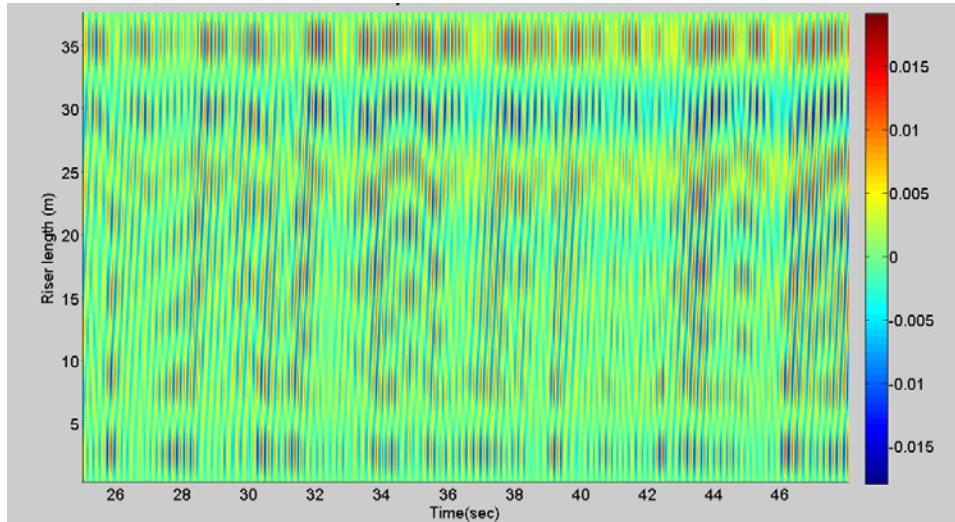




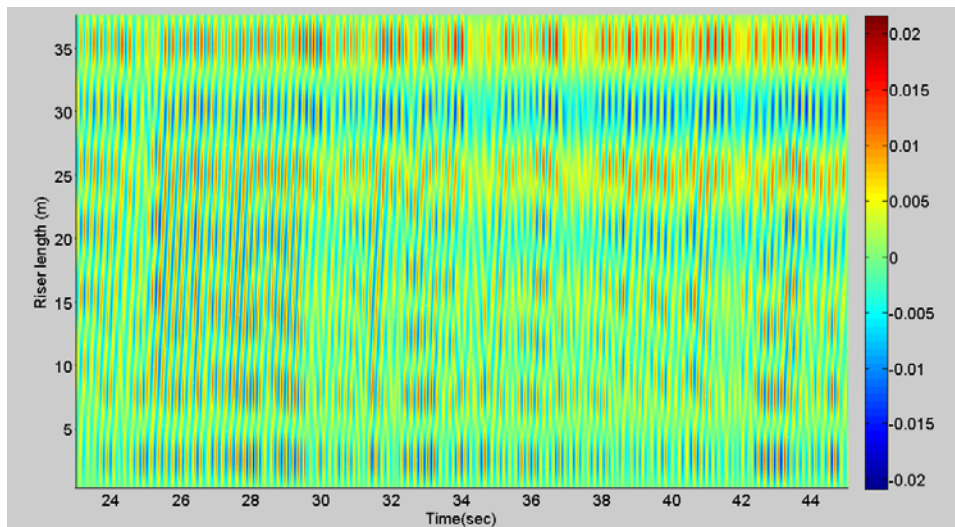
Test2380



Test2390

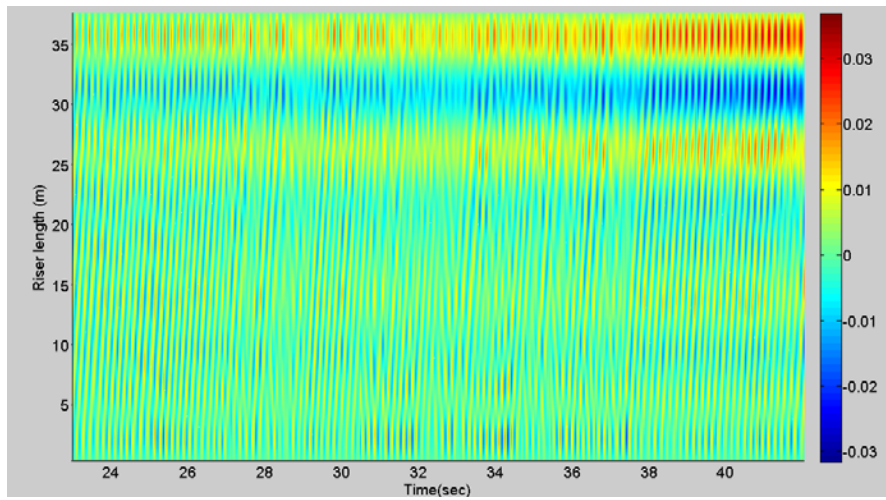


Test2400

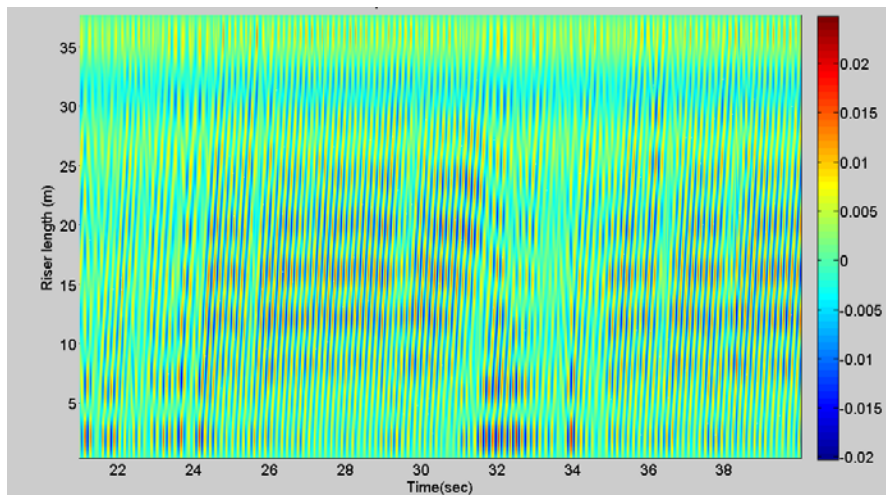




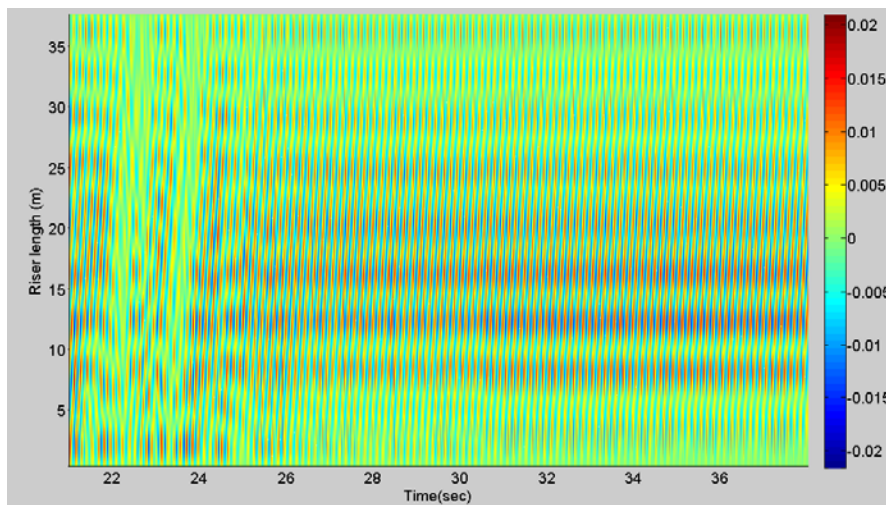
Test2410



Test2420

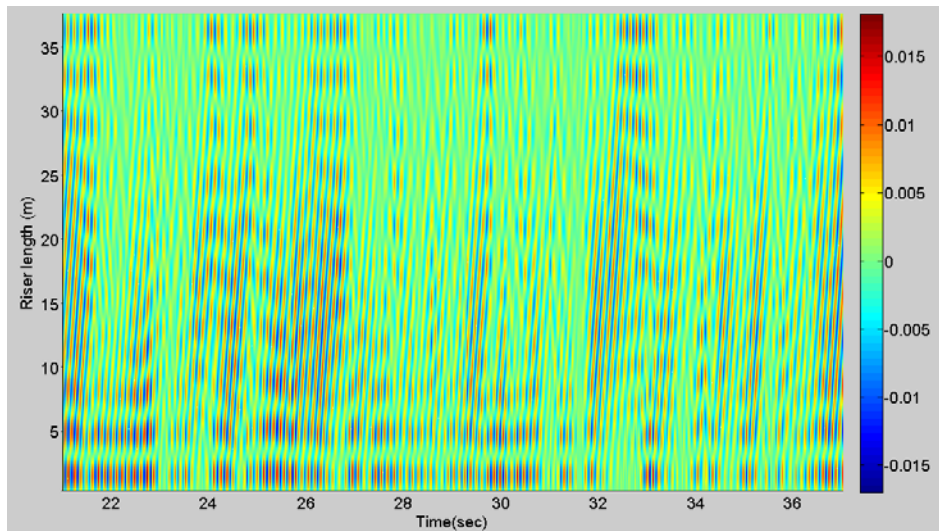


Test2430

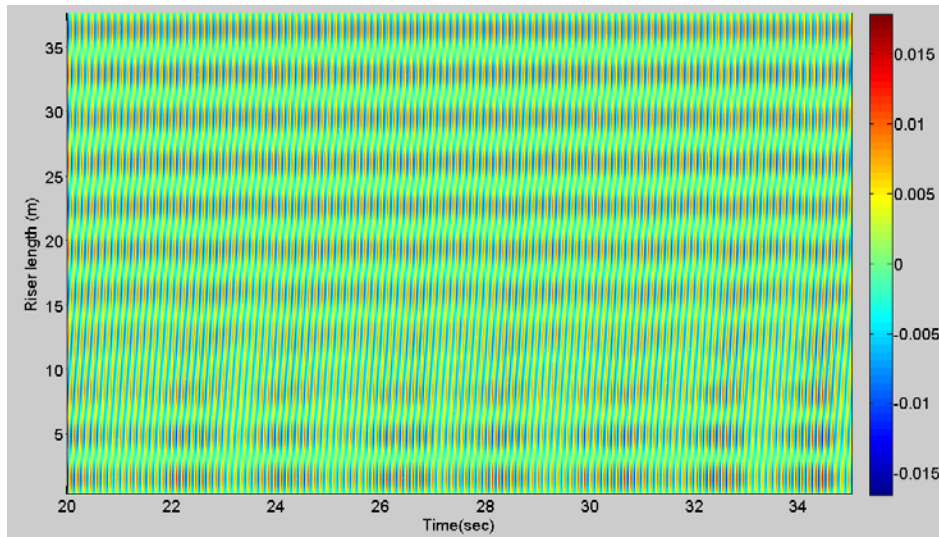




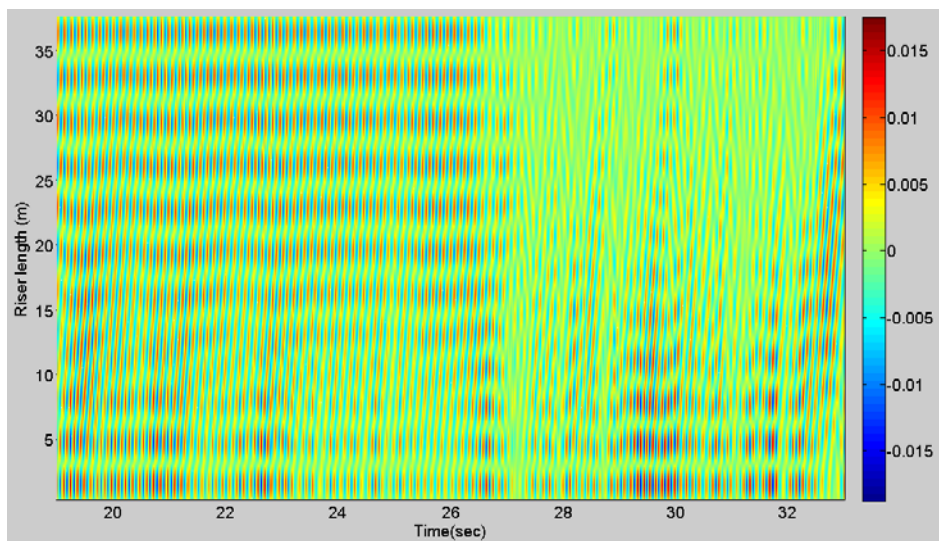
Test2440



Test2450

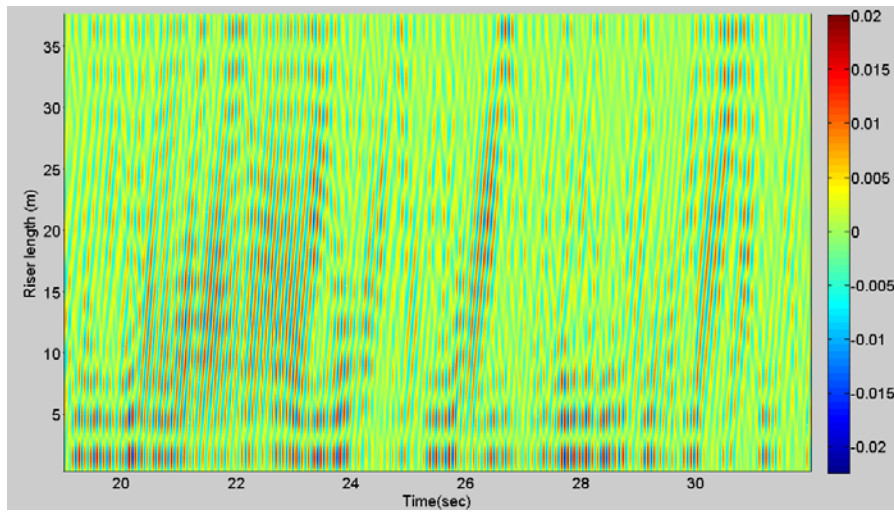


Test2460

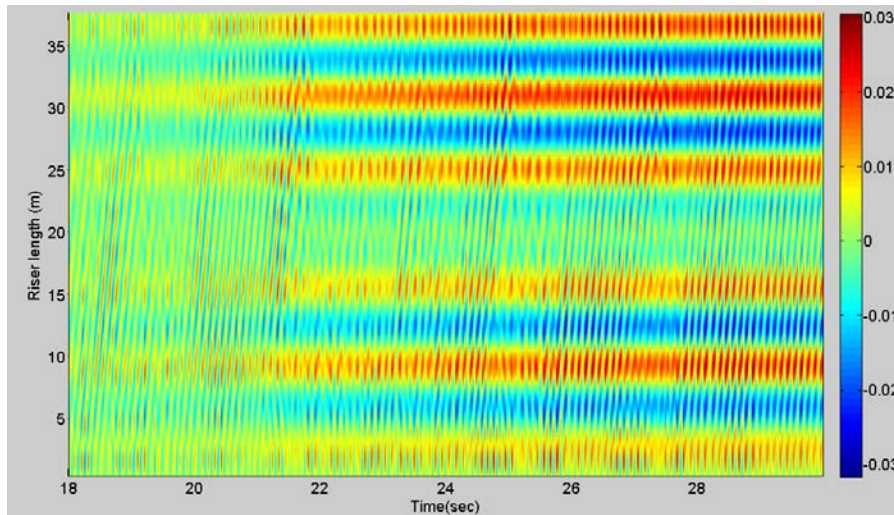




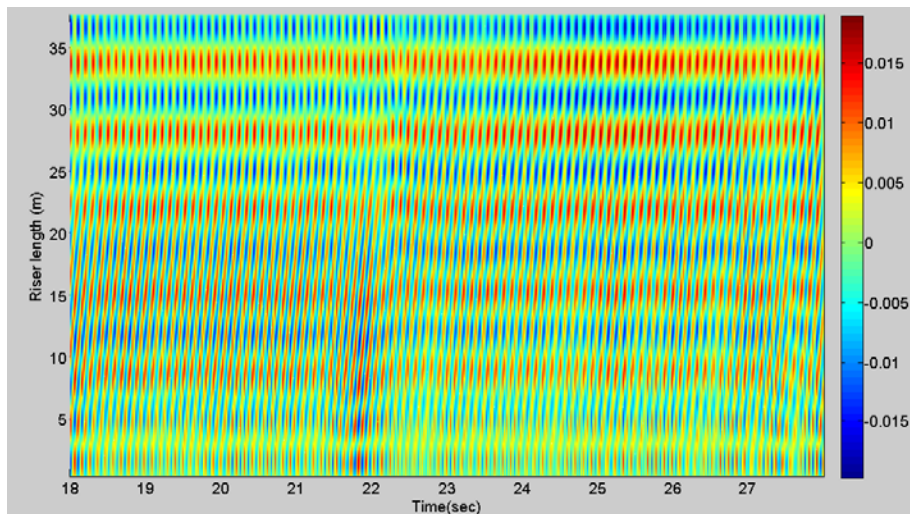
Test2470



Test2480

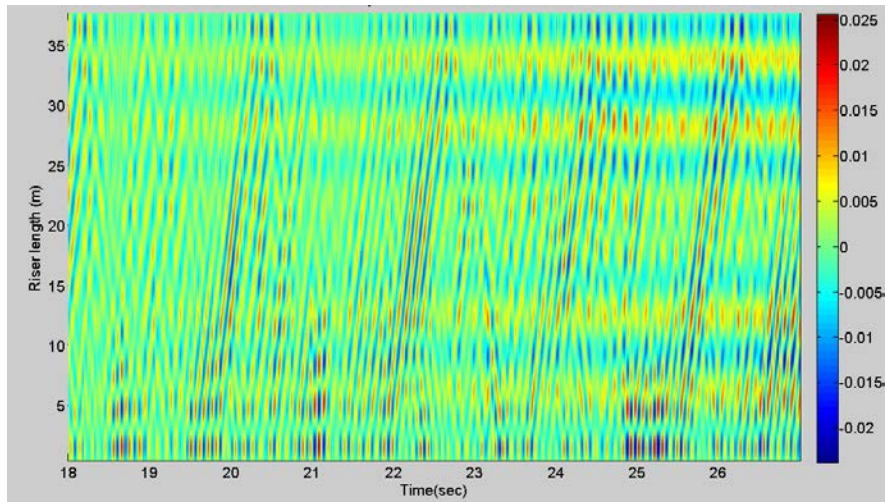


Test2490

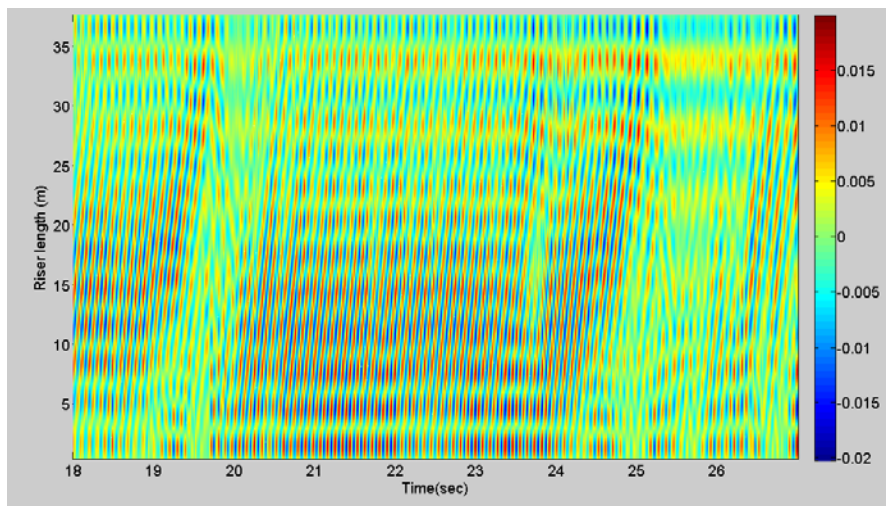




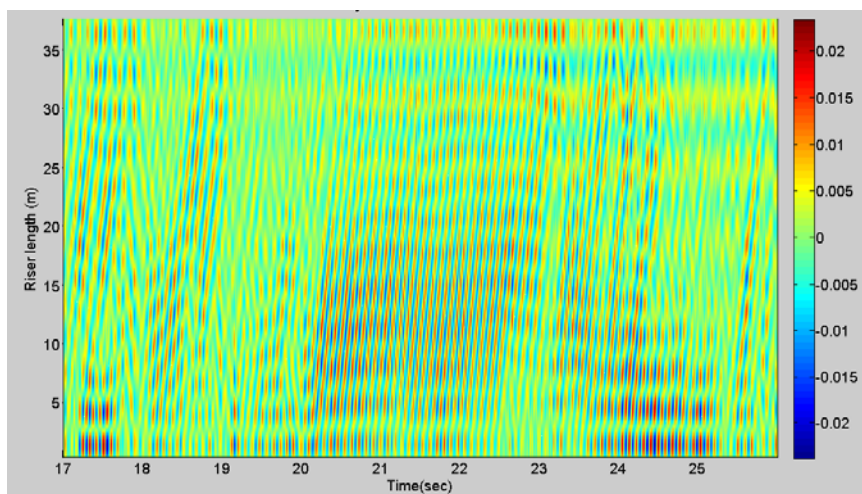
Test2500



Test2510

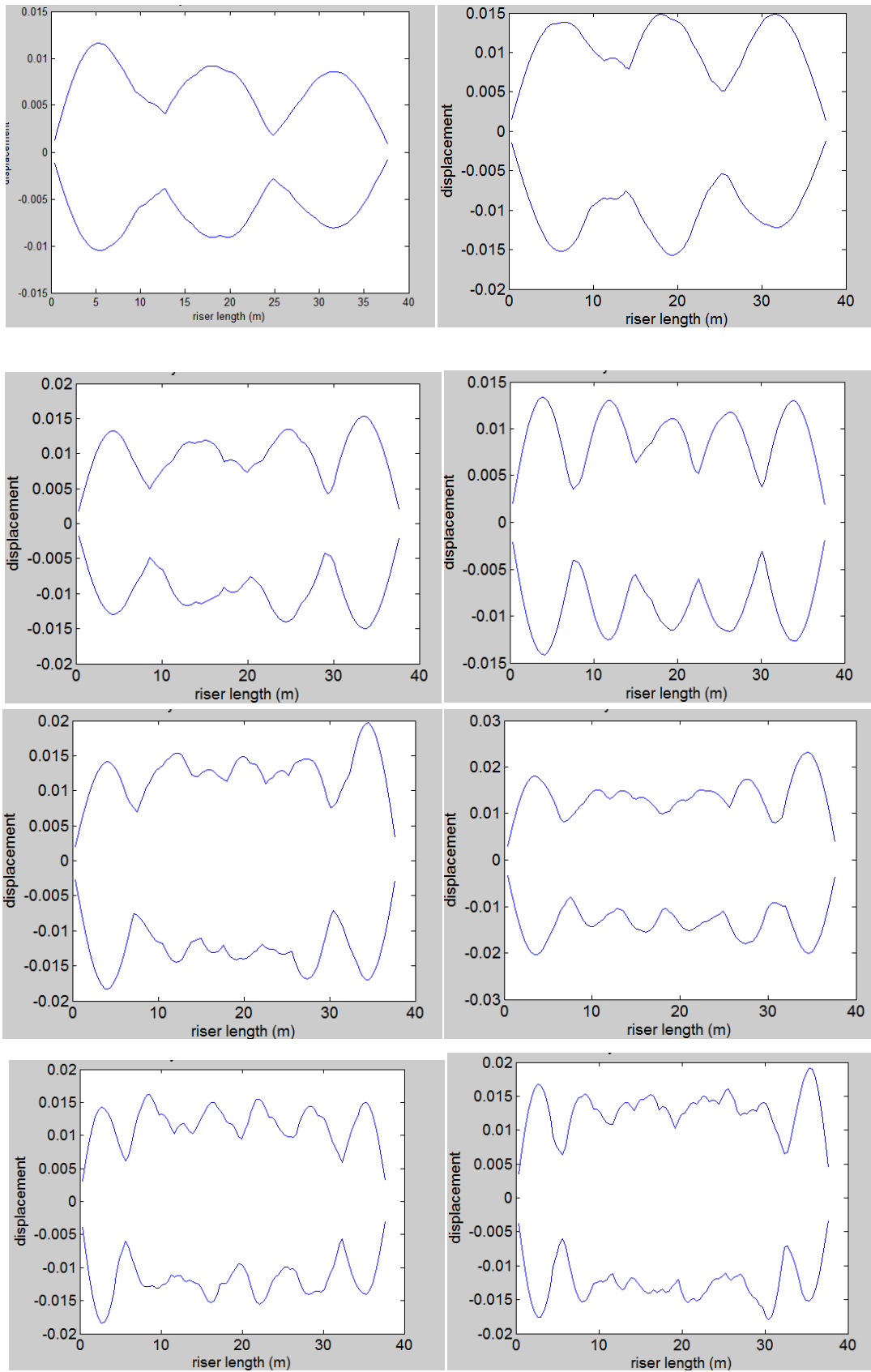


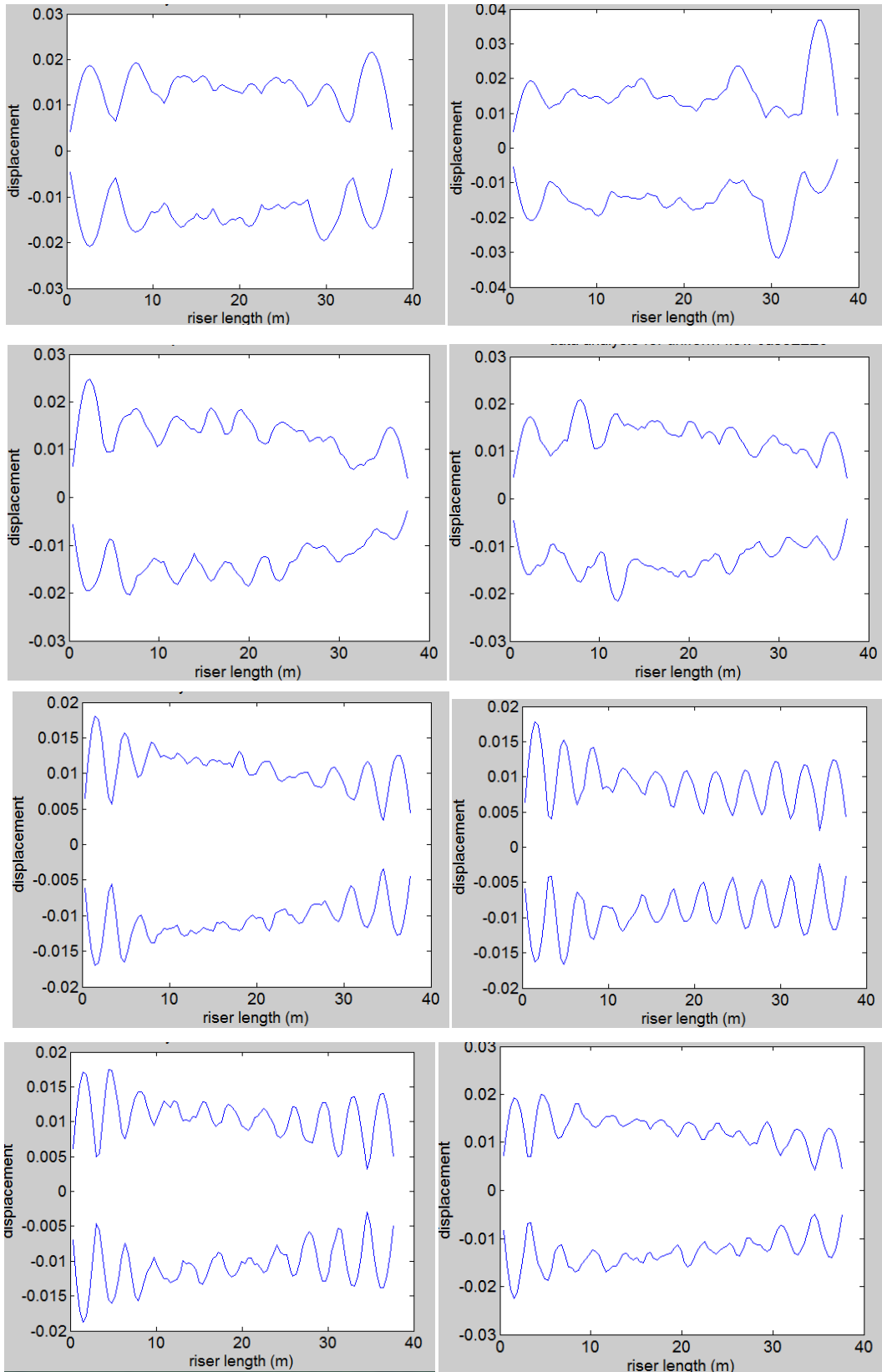
Test2520

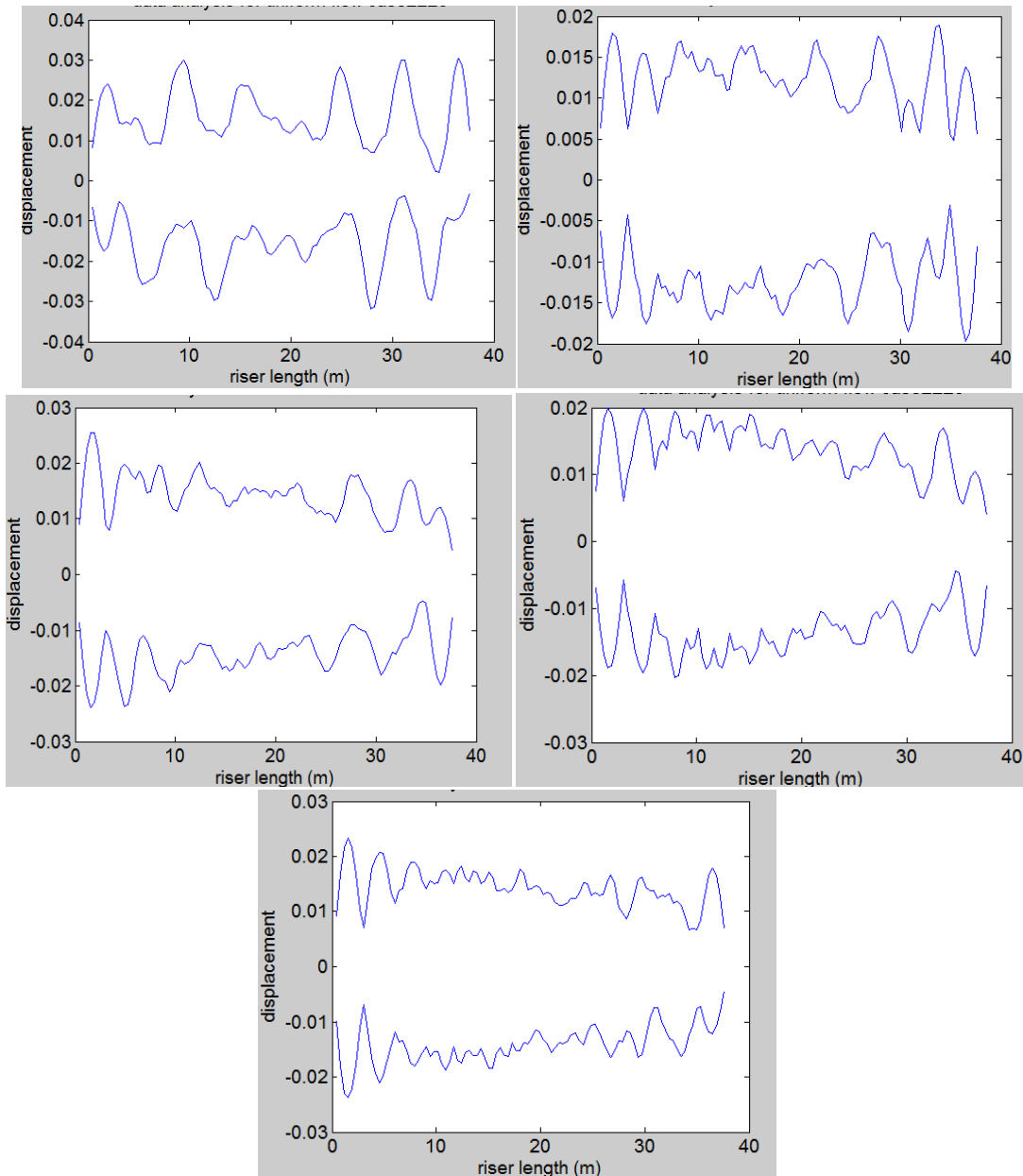




Results of category 8, Envelope of maximum displacement along riser









## Appendix B

Figure B1, mean value of start frequency (at different measurement locations along riser) vary with towing velocity for Hanoytangen tests

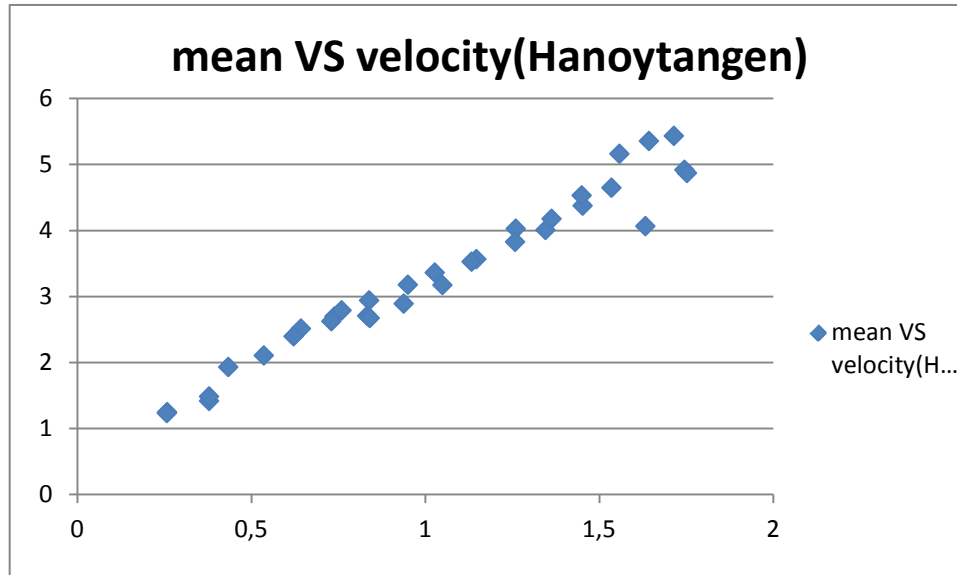


Figure B2, standard deviation of start frequencies (at different measurement locations along riser) vary with towing velocity for Hanoytangen tests

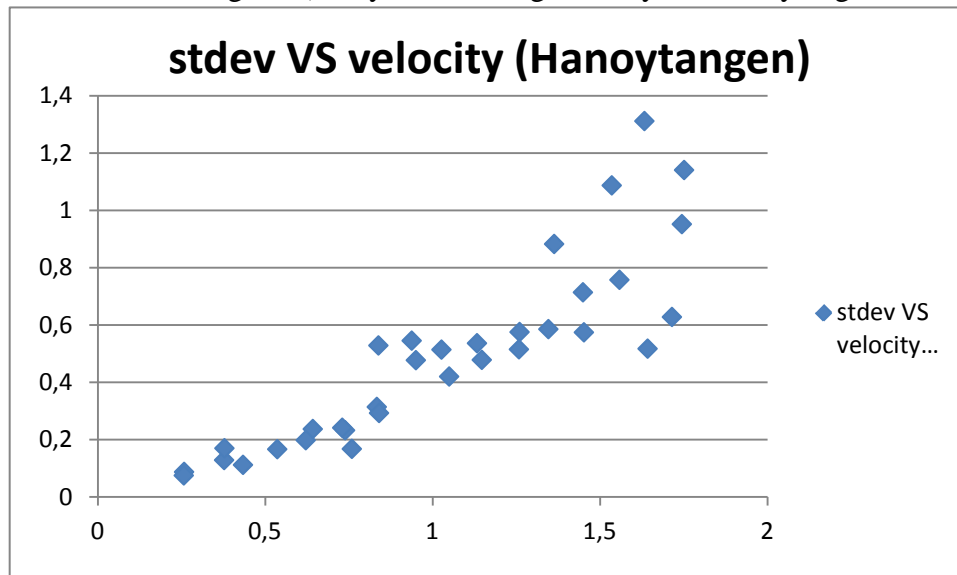


Figure B3, mean value of start frequencies (at different measurement locations along riser) vary with towing velocity for NDP tests

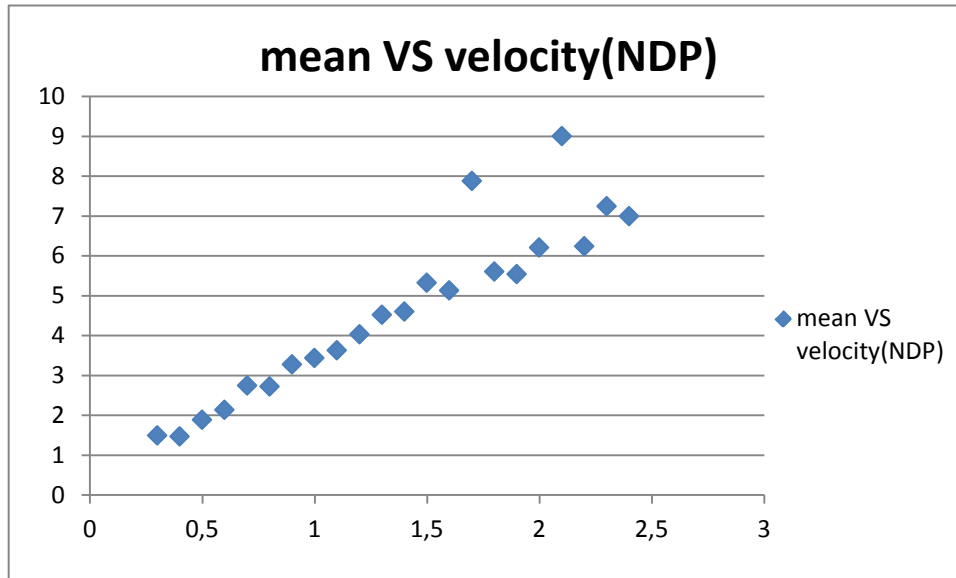


Figure B4, standard deviation of start frequencies (at different measurement locations along riser) vary with towing velocity for NDP tests

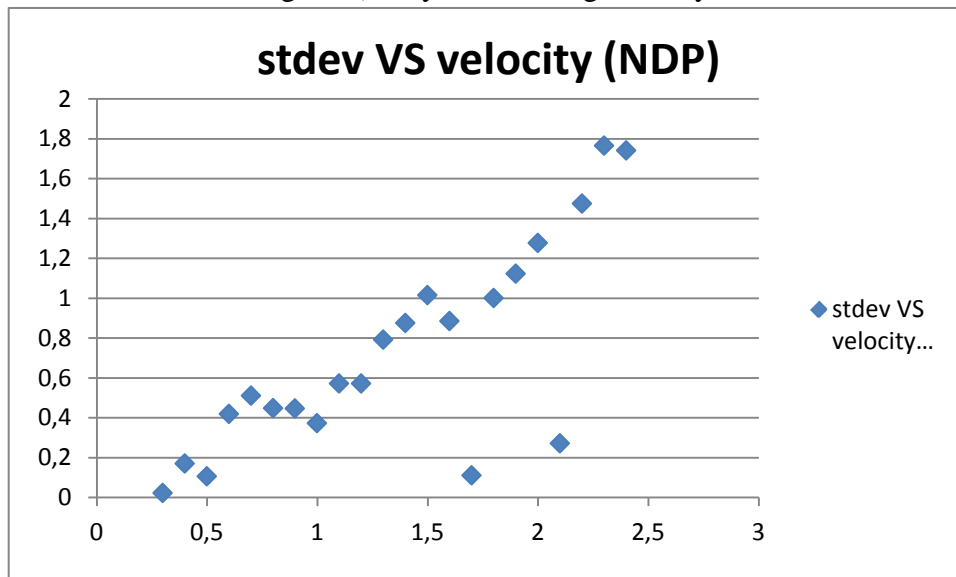


Figure B5, mean value of end frequencies (at different measurement locations along riser) vary with towing velocity for NDP tests

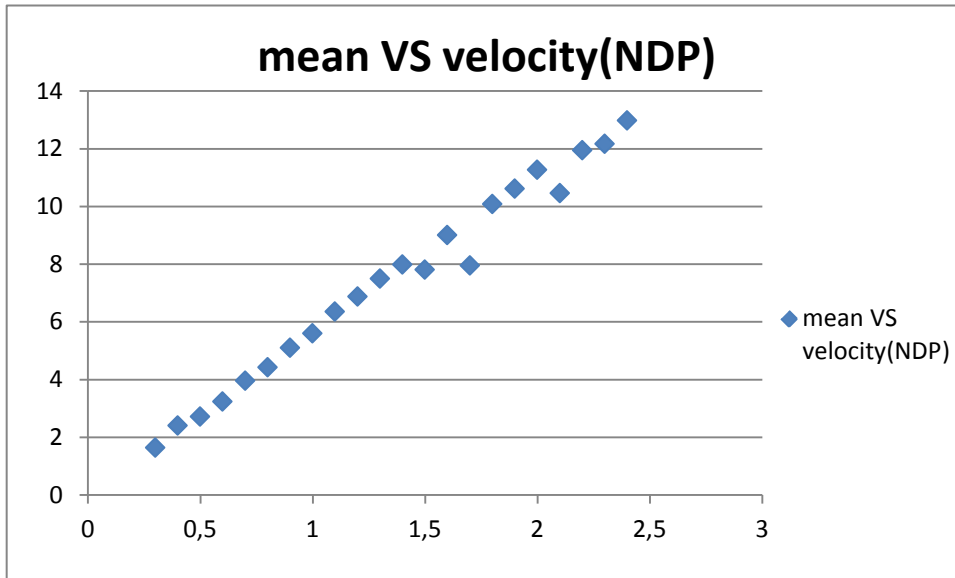


Figure B6, standard deviation of end frequencies (at different measurement locations along riser) vary with towing velocity for NDP tests

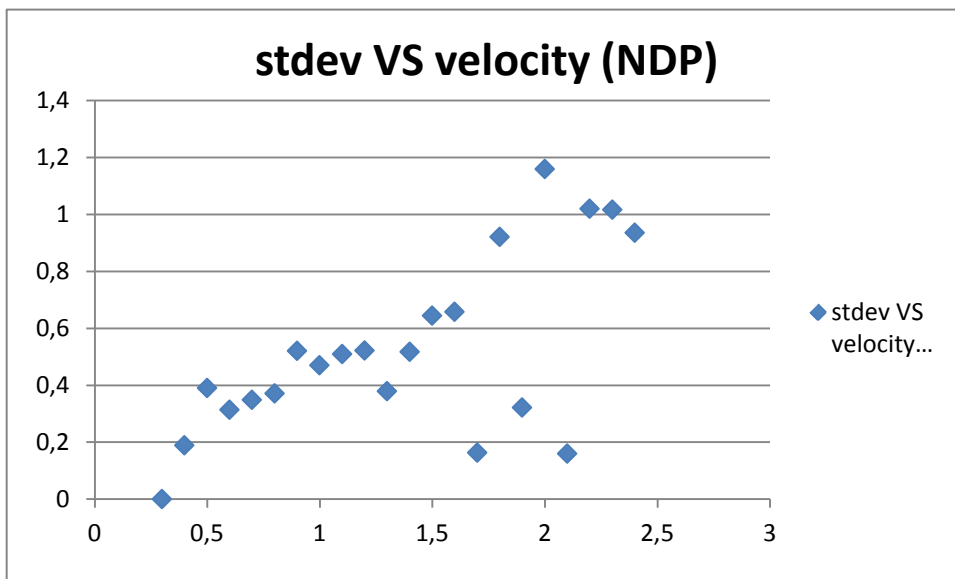


Figure B7, mean value of end frequencies (at different measurement locations along riser) vary with towing velocity for Hanoytangen tests

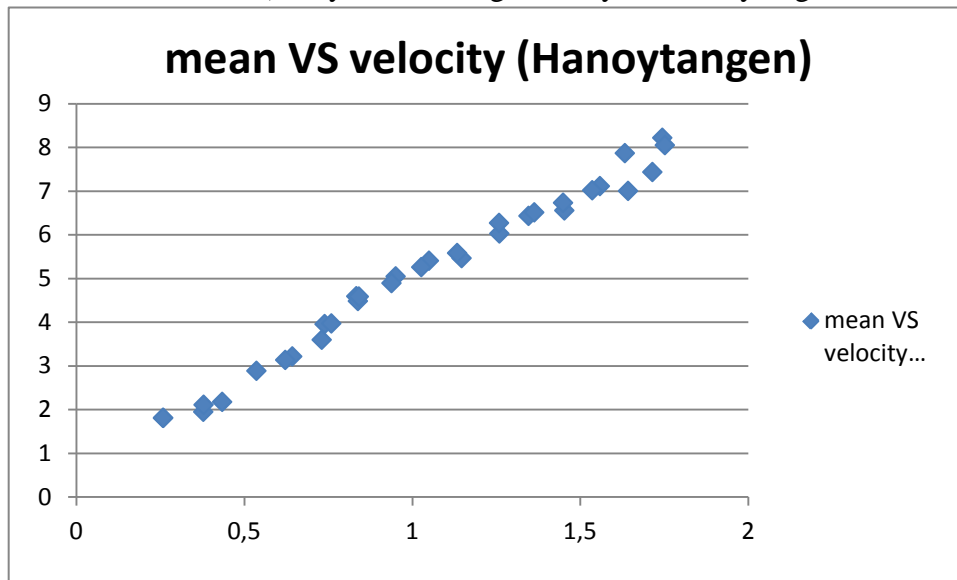
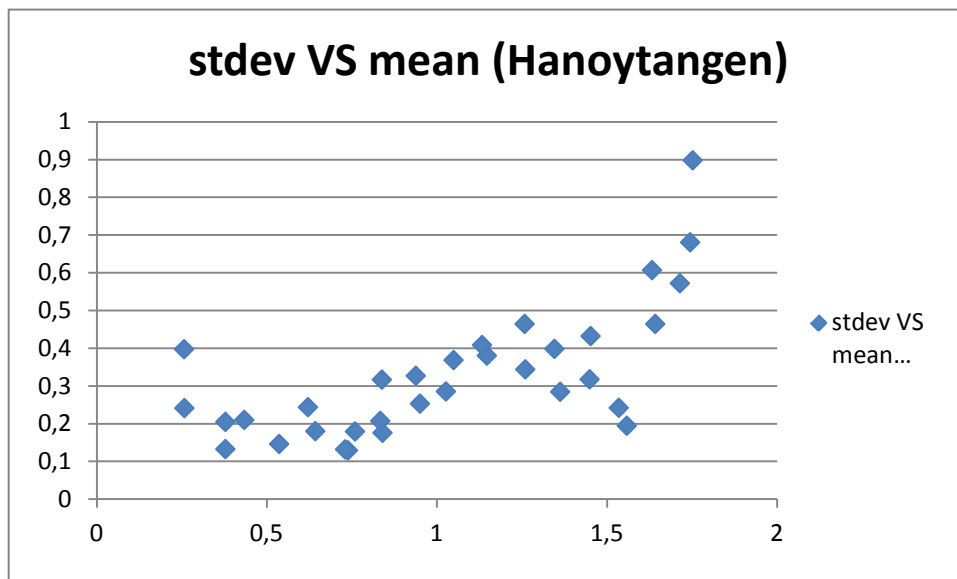


Figure B8, standard deviation of end frequencies (at different measurement locations along riser) vary with towing velocity for Hanoytangen tests





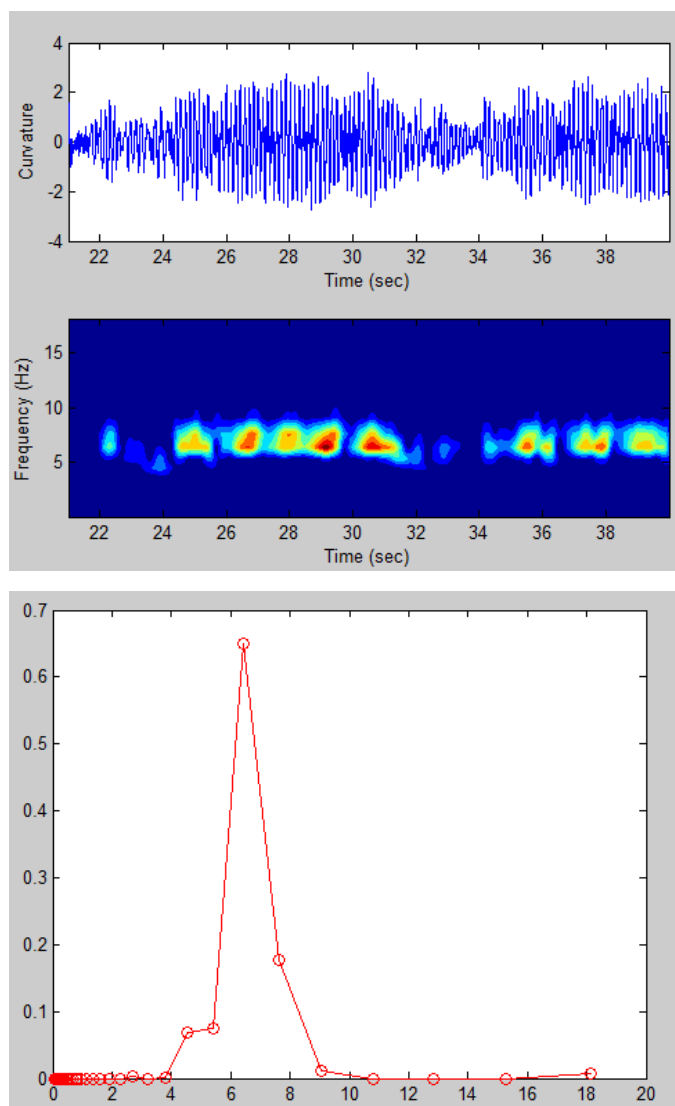
## Appendix C

Here take test2420 as an example, the information of this test is:

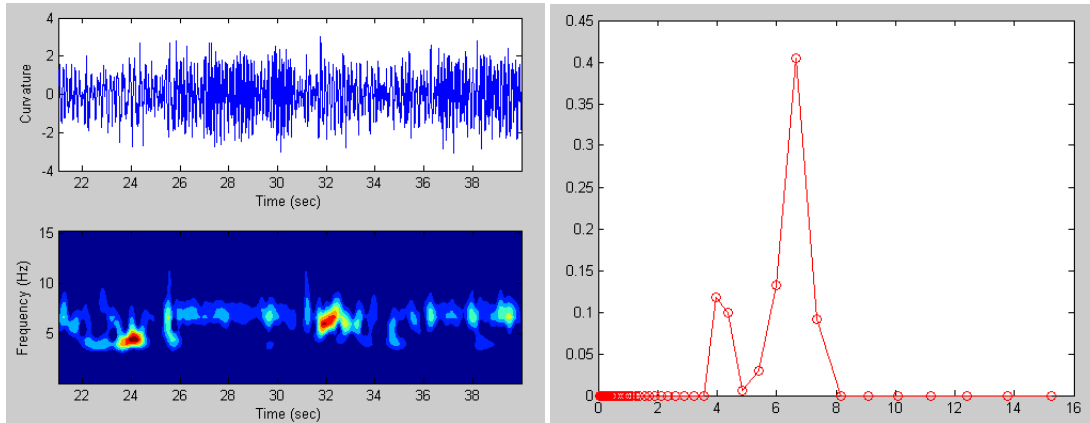
Table C1, information of test2420

number	Time	velocity	modes
test2420	21-40	1,4	6--13

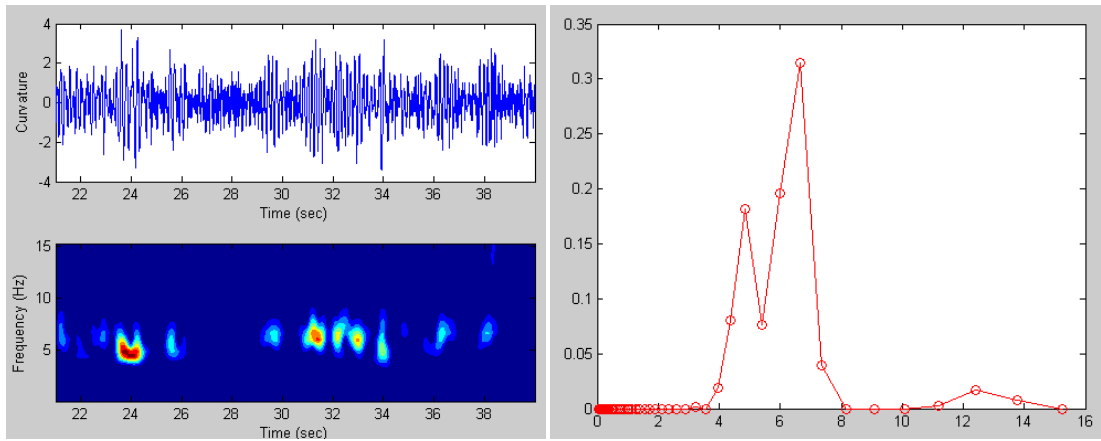
The figures below are the wavelet result and time duration distribution from original signal from measurement.



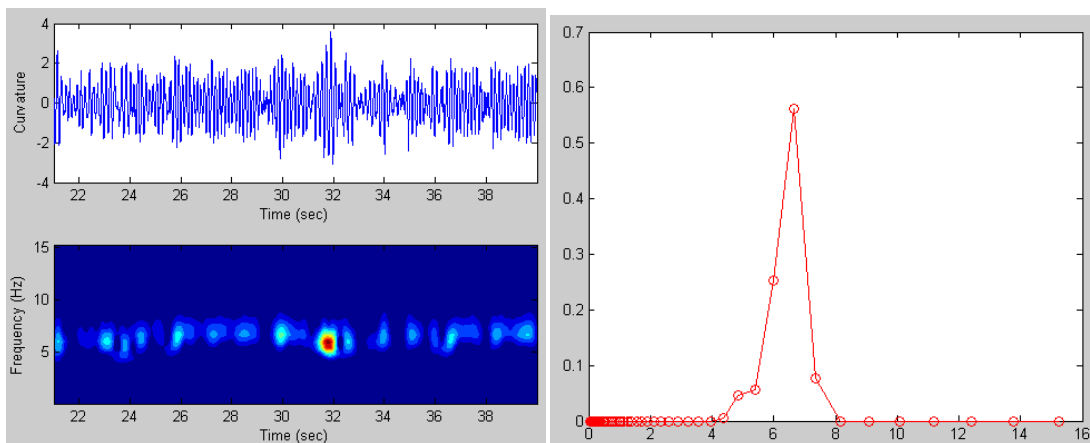
Mode 6:



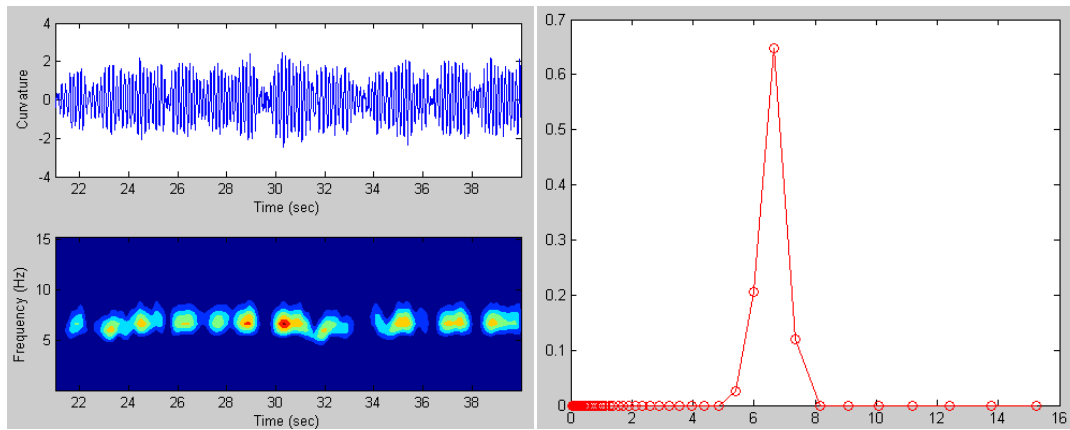
Mode 7



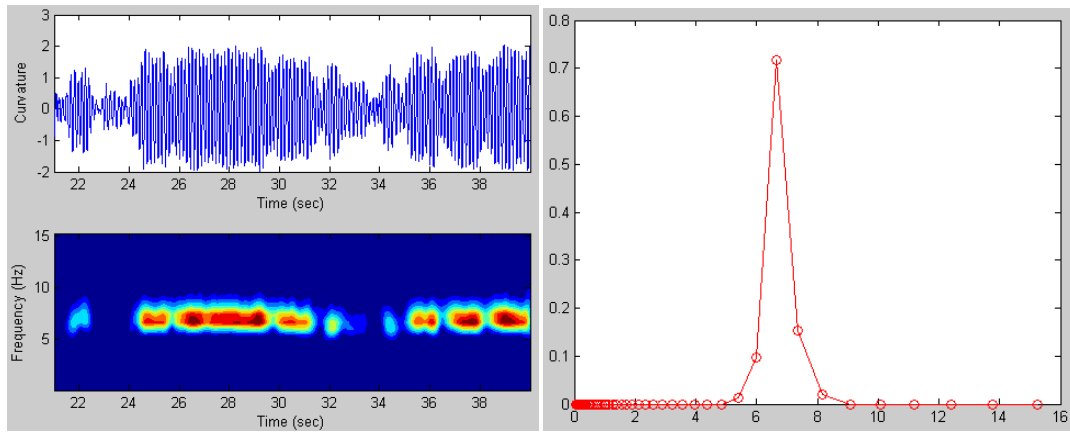
Mode 8



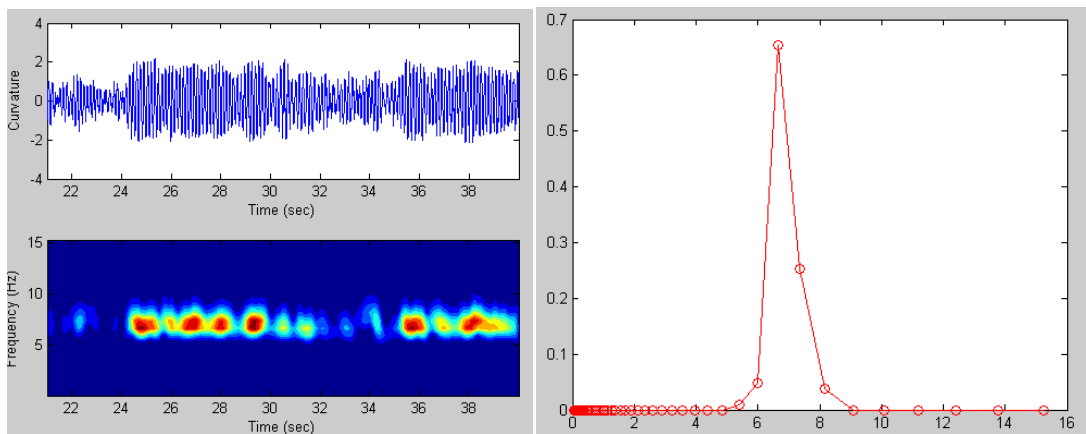
Mode 9



Mode 10

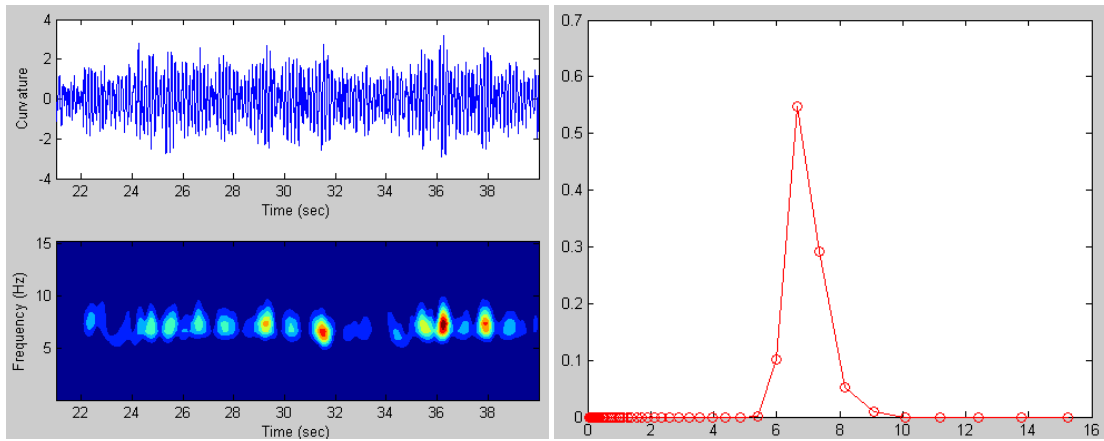


Mode 11

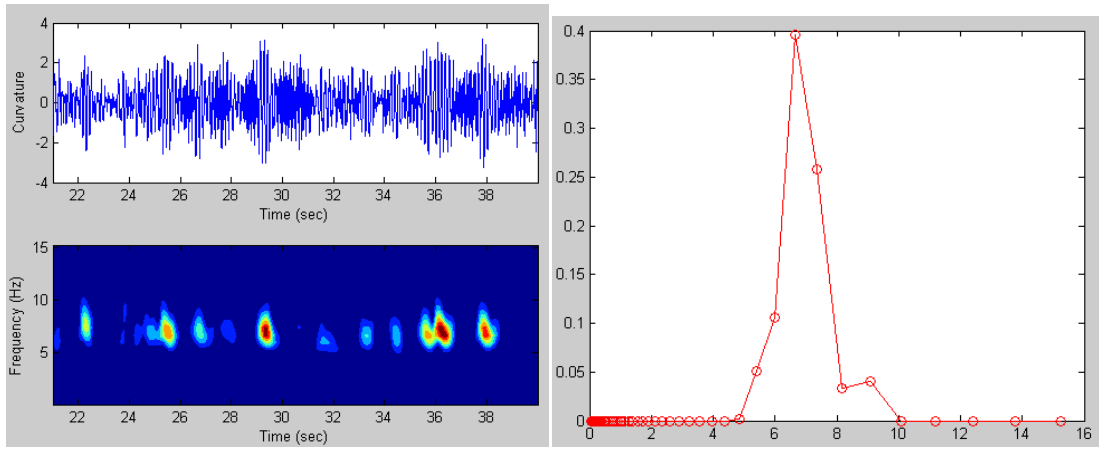




### Mode 12



### Mode 13

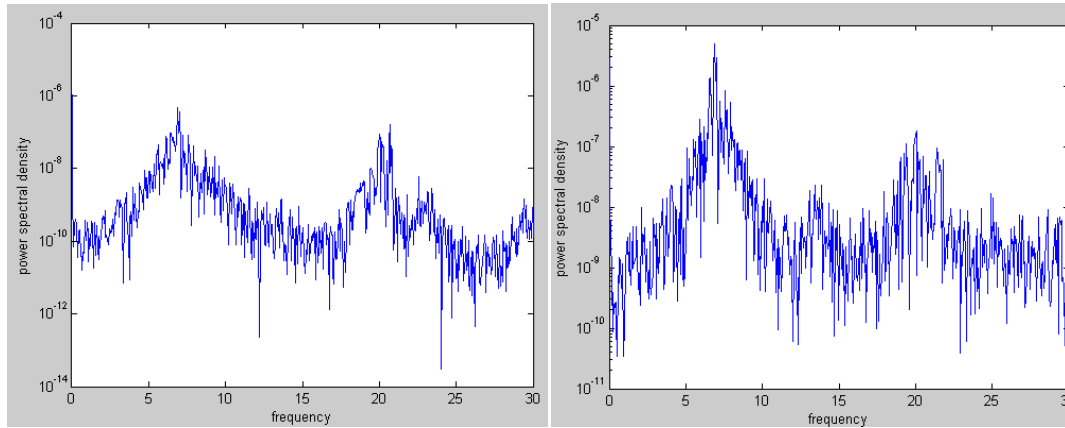


Power Spectral Density of decomposed signal corresponding to single mode, table C2 is the peak frequency corresponding to each decomposed displacement signal.

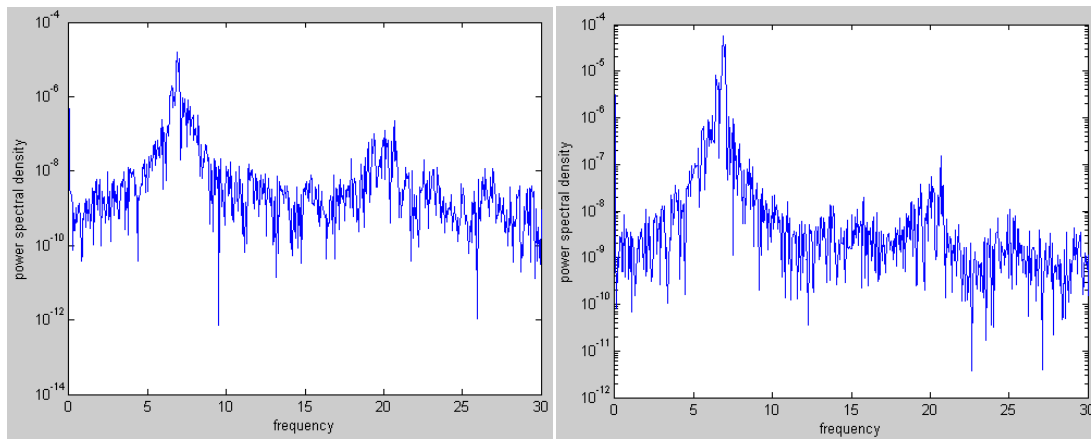
Table C2, peak frequency of each decomposed displacement signal

No.	6	7	8	9	10	11	12	13
Peak	6.895Hz	6.895Hz	6.4Hz	6.895Hz	6.895Hz	6.895Hz	6.895Hz	6.895Hz

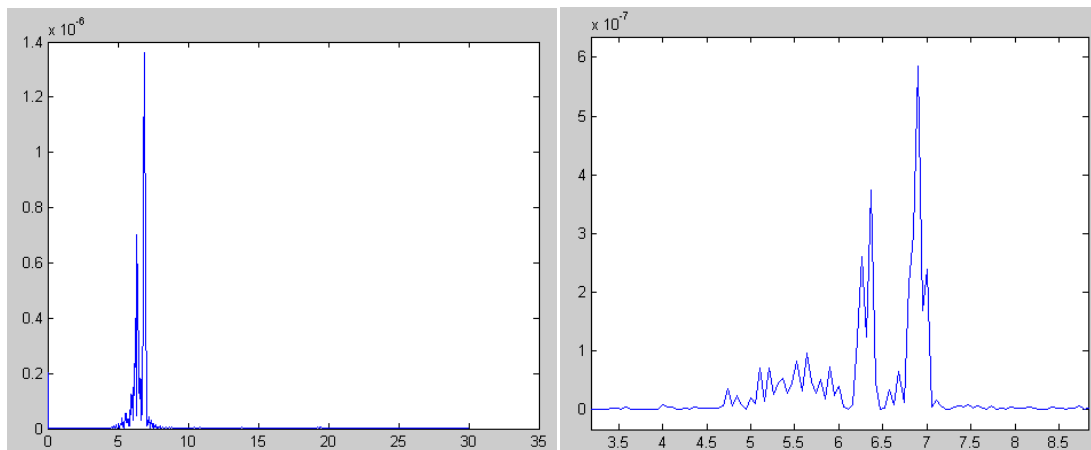
Mode 13 & Mode 12



Mode 11 & Mode 10

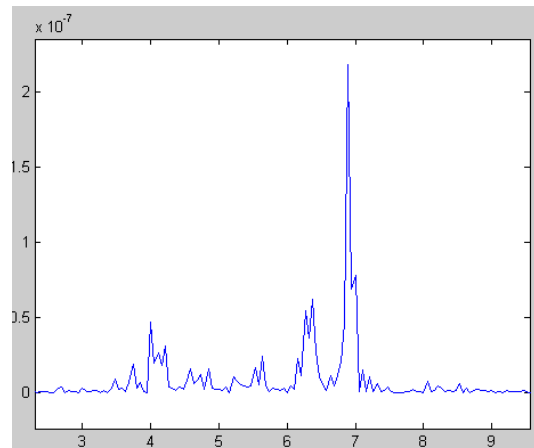
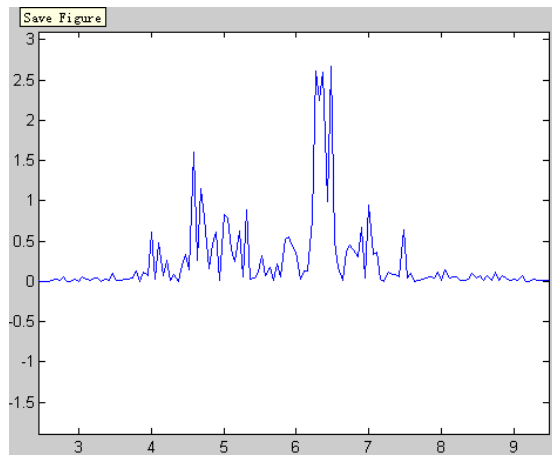


Mode 9 & Mode 8





Mode 7 & Mode 6





## Appendix D

### High harmonic effects

Table D1, First harmonic power of all power in percentage (NDP)

	2310	2320	2330	2340	2350	2360	2370	2380	2390	2400	2410	2420	2430
1	0.7542	0.6531	0.669	0.9351	0.9252	0.9369	0.9423	0.9439	0.9213	0.9136	0.8932	0.7956	0.5978
2	0.7742	0.7776	0.7713	0.84	0.941	0.906	0.8793	0.9057	0.8786	0.891	0.9126	0.921	0.8606
3	0.743	0.8035	0.7844	0.8119	0.9371	0.8823	0.8518	0.8963	0.8735	0.8909	0.9288	0.9385	0.8904
4	0.7871	0.8394	0.8058	0.8303	0.8142	0.7992	0.7194	0.8879	0.8993	0.9141	0.8989	0.9172	0.9406
5	0.783	0.8	0.7844	0.7034	0.919	0.8091	0.8543	0.8817	0.9005	0.8943	0.9036	0.9069	0.9233
6	0.6646	0.8303	0.7556	0.7635	0.8711	0.8772	0.8016	0.8701	0.8789	0.8537	0.8988	0.9007	0.8529
7	0.5074	0.8432	0.715	0.7878	0.8544	0.8566	0.8144	0.8732	0.8775	0.8581	0.8889	0.8587	0.911
8	0.4717	0.6924	0.7025	0.7415	0.8551	0.7774	0.8866	0.8769	0.8664	0.8669	0.8851	0.8639	0.8072
9	0.9597	0.5162	0.5898	0.7488	0.8835	0.8366	0.6675	0.8308	0.8056	0.8373	0.8302	0.7517	0.6519
10	0.7451	0.6599	0.4988	0.6974	0.8035	0.7686	0.7299	0.8138	0.7952	0.7841	0.8166	0.8193	0.7624
11	0.6822	0.6939	0.5049	0.6338	0.7274	0.7339	0.7873	0.8188	0.8119	0.8069	0.8313	0.7855	0.625
12	0.6986	0.7303	0.7238	0.534	0.8071	0.7827	0.6922	0.8024	0.7837	0.8062	0.8546	0.831	0.7062
13	0.6541	0.733	0.7337	0.6257	0.8047	0.7765	0.6533	0.8013	0.7831	0.8022	0.8501	0.8459	0.6756
14	0.2224	0.6347	0.6576	0.5372	0.823	0.7376	0.7204	0.7427	0.7262	0.7779	0.8139	0.7861	0.7861
15	0.2837	0.527	0.6287	0.6193	0.514	0.6544	0.7327	0.7809	0.7473	0.767	0.853	0.8186	0.8305
16	0.3798	0.4489	0.5105	0.566	0.6208	0.5649	0.6713	0.7745	0.7643	0.7565	0.8516	0.7883	0.6545
17	0.861	0.3517	0.3717	0.6694	0.7526	0.7001	0.4294	0.7267	0.7617	0.7924	0.7509	0.8199	0.7051
18	0.9404	0.4078	0.2334	0.4265	0.8878	0.7096	0.6562	0.6802	0.6933	0.7674	0.8238	0.6722	0.4949
19	0.6951	0.7446	0.5063	0.314	0.7117	0.6398	0.8411	0.8187	0.7446	0.7344	0.6879	0.7881	0.8845
20	0.7053	0.7337	0.618	0.3525	0.7435	0.614	0.7038	0.8212	0.7966	0.7573	0.7267	0.6414	0.5647
21	0.9121	0.6648	0.5391	0.7811	0.4927	0.3628	0.4591	0.6352	0.6451	0.7211	0.7969	0.2611	0.0452
22	0.751	0.7533	0.7434	0.5608	0.8299	0.7898	0.7434	0.6329	0.4514	0.4568	0.7427	0.7742	0.6711
23	0.1403	0.0398	0.0554	0.1845	0.4904	0.4143	0.4647	0.6001	0.6335	0.7495	0.8733	0.8953	0.9196
24	0.9437	0.949	0.9296	0.6807	0.7698	0.5777	0.331	0.4029	0.3626	0.3716	0.438	0.3977	0.2859



2440	2450	2460	2470	2480	2490	2500	2510	2520
0.9515	0.4048	0.928	0.9642	0.9548	0.9565	0.965	0.9624	0.9489
0.9587	0.9503	0.9437	0.9496	0.9279	0.9093	0.9537	0.9154	0.9244
0.9449	0.9387	0.9292	0.9389	0.9293	0.8863	0.9521	0.9061	0.9366
0.9518	0.8462	0.9477	0.9634	0.9382	0.8112	0.9548	0.9354	0.9285
0.9444	0.7817	0.8933	0.9339	0.914	0.8363	0.9436	0.8935	0.9097
0.9282	0.6573	0.8524	0.9058	0.8875	0.6833	0.9243	0.769	0.8743
0.9201	0.4327	0.7493	0.8933	0.8606	0.6094	0.9008	0.7878	0.8679
0.9168	0.5165	0.8087	0.873	0.8266	0.5246	0.9018	0.8037	0.8341
0.8962	0.6643	0.673	0.8287	0.7848	0.5022	0.8797	0.7759	0.801
0.8959	0.7342	0.6807	0.8429	0.8467	0.6444	0.8988	0.8476	0.8612
0.8925	0.732	0.8351	0.8528	0.8571	0.6004	0.9041	0.9005	0.879
0.9007	0.7363	0.8501	0.8936	0.8764	0.8523	0.901	0.9152	0.9069
0.8918	0.6758	0.7705	0.873	0.8661	0.8036	0.888	0.9065	0.8957
0.8772	0.6091	0.7411	0.8698	0.8637	0.8405	0.8593	0.8607	0.8792
0.8615	0.9294	0.8768	0.8374	0.8363	0.8165	0.8524	0.8651	0.8509
0.8653	0.661	0.7133	0.8211	0.7967	0.5729	0.8414	0.8713	0.855
0.8347	0.8843	0.7154	0.8054	0.7973	0.8154	0.8424	0.8475	0.796
0.841	0.7321	0.6927	0.7735	0.7872	0.5261	0.8227	0.8567	0.8436
0.8292	0.4876	0.5199	0.739	0.751	0.5923	0.8267	0.8265	0.8313
0.8208	0.9073	0.8275	0.7942	0.7095	0.3373	0.8117	0.7582	0.823
0.4764	0.4764	0.4366	0.0308	0.8995	0.7307	0.9145	0.8711	0.7203
0.7645	0.5775	0.6228	0.7861	0.8262	0.8128	0.8428	0.7302	0.7136
0.9273	0.9612	0.9534	0.9454	0.9349	0.8791	0.9223	0.9	0.8784
0.5241	0.3594	0.3782	0.5449	0.5417	0.4378	0.6231	0.6501	0.6517





Table D2, Second harmonic power of all power in percentage (NDP)

	2310	2320	2330	2340	2350	2360	2370	2380	2390	2400	2410	2420	2430
1	0.2281	0.2773	0.2806	0.0365	0.0576	0.0356	0.0296	0.0361	0.06	0.074	0.1024	0.1928	0.3823
2	0.2158	0.2022	0.1795	0.0181	0.0408	0.0708	0.0991	0.0839	0.1095	0.0983	0.0767	0.064	0.1151
3	0.2006	0.1804	0.1488	0.0167	0.0447	0.0952	0.1292	0.094	0.1138	0.0947	0.0599	0.047	0.0955
4	0.1992	0.0716	0.0425	0.0441	0.1616	0.1811	0.2358	0.0882	0.0785	0.0693	0.093	0.0762	0.0554
5	0.1869	0.1612	0.1407	0.0987	0.0612	0.1586	0.1215	0.0984	0.08	0.0866	0.0888	0.0818	0.0552
6	0.2761	0.1085	0.1127	0.102	0.1036	0.0959	0.164	0.1079	0.0998	0.124	0.0936	0.0885	0.1371
7	0.4185	0.1075	0.124	0.1169	0.1202	0.1147	0.1488	0.1038	0.1015	0.1192	0.1025	0.1303	0.0791
8	0.4775	0.2063	0.187	0.0807	0.1171	0.1865	0.0847	0.1023	0.1123	0.1126	0.1059	0.1263	0.1772
9	0.0189	0.3265	0.2284	0.1502	0.0882	0.1291	0.287	0.1427	0.1649	0.136	0.1599	0.2387	0.3356
10	0.242	0.243	0.2839	0.2272	0.1461	0.174	0.2362	0.1565	0.1785	0.1951	0.1735	0.1716	0.2289
11	0.2981	0.2155	0.2805	0.1892	0.2377	0.2145	0.1625	0.1456	0.1521	0.1686	0.1596	0.2067	0.3678
12	0.1122	0.2069	0.1753	0.2777	0.1721	0.1866	0.2574	0.1695	0.1883	0.1744	0.1385	0.1617	0.287
13	0.1224	0.2027	0.1676	0.2501	0.1723	0.1923	0.3004	0.1693	0.1882	0.177	0.1403	0.1461	0.3198
14	0.7158	0.2296	0.1493	0.1416	0.1433	0.2201	0.2389	0.2243	0.2393	0.1974	0.1737	0.2027	0.2081
15	0.6717	0.3688	0.2494	0.3131	0.4417	0.2813	0.2338	0.1879	0.2192	0.2054	0.1376	0.1677	0.156
16	0.5781	0.4403	0.2922	0.2555	0.347	0.3783	0.2993	0.1968	0.2033	0.2146	0.1382	0.1986	0.3345
17	0.0978	0.4553	0.3764	0.19	0.2303	0.2599	0.5343	0.2352	0.2018	0.1797	0.2297	0.1638	0.2868
18	0.0311	0.4708	0.3483	0.3131	0.0928	0.2407	0.2558	0.2779	0.2675	0.2025	0.161	0.3089	0.4921
19	0.288	0.2079	0.193	0.5206	0.2523	0.3295	0.1282	0.1509	0.2174	0.2318	0.2887	0.1973	0.1051
20	0.282	0.1888	0.1348	0.5181	0.1634	0.3286	0.256	0.155	0.1802	0.2109	0.2535	0.3412	0.4283
21	0.0598	0.2796	0.2538	0.143	0.4465	0.567	0.4209	0.3109	0.2961	0.2115	0.0758	0.0001	0.046
22	0.2157	0.0897	0.1339	0.2662	0.1397	0.1659	0.2047	0.3254	0.4911	0.478	0.2338	0.2035	0.3176
23	0.6678	0.5706	0.4113	0.3942	0.4672	0.5432	0.5001	0.3823	0.3501	0.2372	0.1174	0.0932	0.0652
24	0.0445	0.0239	0.0241	0.0754	0.1762	0.3103	0.5422	0.4753	0.5094	0.5253	0.5231	0.565	0.6938



2440	2450	2460	2470	2480	2490	2500	2510	2520
0.0449	0.5745	0.0628	0.0302	0.0309	0.032	0.0174	0.01	0.0063
0.0362	0.0451	0.0519	0.043	0.0583	0.0835	0.0253	0.0262	0.0102
0.049	0.0576	0.0659	0.0543	0.0596	0.1064	0.0297	0.0305	0.011
0.0436	0.1446	0.0462	0.0301	0.0434	0.1505	0.022	0.0149	0.0078
0.0502	0.2095	0.1002	0.0575	0.0689	0.1202	0.0264	0.0137	0.0109
0.0655	0.3324	0.1335	0.0852	0.0958	0.2781	0.0314	0.0229	0.0111
0.073	0.5525	0.2342	0.0966	0.1207	0.3595	0.0445	0.0192	0.012
0.0764	0.4728	0.178	0.1157	0.1535	0.4398	0.0458	0.0221	0.0129
0.0949	0.3222	0.3149	0.1573	0.1959	0.4707	0.0632	0.0545	0.0335
0.0945	0.2565	0.3106	0.1456	0.1366	0.337	0.0626	0.0411	0.0355
0.0989	0.2592	0.1553	0.135	0.1261	0.386	0.0598	0.0291	0.0312
0.0909	0.2556	0.1412	0.0955	0.1092	0.1322	0.0667	0.0257	0.031
0.0996	0.3147	0.2202	0.1141	0.1175	0.1735	0.0753	0.0309	0.0322
0.1115	0.3761	0.2427	0.1147	0.1192	0.1374	0.0959	0.0417	0.0317
0.127	0.0605	0.1115	0.148	0.1447	0.166	0.1018	0.0444	0.0469
0.1238	0.3253	0.2784	0.1599	0.1798	0.4036	0.1029	0.0376	0.0443
0.153	0.0922	0.2678	0.1755	0.1794	0.1627	0.108	0.0643	0.0611
0.1448	0.2581	0.2996	0.2092	0.1884	0.4413	0.1262	0.0701	0.0542
0.1564	0.5064	0.4711	0.2374	0.2134	0.3599	0.1095	0.0792	0.0607
0.166	0.0726	0.1599	0.1858	0.2646	0.6265	0.1273	0.0993	0.0638
0	0	0.0025	0.0253	0.0833	0.2284	0.1159	0.0599	0.0644
0.2216	0.4162	0.3688	0.1955	0.1493	0.1566	0.0977	0.1124	0.0988
0.0574	0.0168	0.0278	0.0348	0.0404	0.099	0.0249	0.0138	0.0143
0.443	0.6229	0.605	0.4184	0.4158	0.5338	0.2681	0.1587	0.1375



Table D3, Higher harmonic power (3<sup>rd</sup> and higher) of all power in percentage (NDP)

	2310	2320	2330	2340	2350	2360	2370	2380	2390	2400	2410	2420	2430
1	0.0177	0.0696	0.0504	0.0284	0.0172	0.0275	0.0281	0.02	0.0187	0.0124	0.0044	0.0116	0.0199
2	0.01	0.0202	0.0492	0.1419	0.0182	0.0232	0.0216	0.0104	0.0119	0.0107	0.0107	0.015	0.0243
3	0.0564	0.0161	0.0668	0.1714	0.0182	0.0225	0.019	0.0097	0.0127	0.0144	0.0113	0.0145	0.0141
4	0.0137	0.089	0.1517	0.1256	0.0242	0.0197	0.0448	0.0239	0.0222	0.0166	0.0081	0.0066	0.004
5	0.0301	0.0388	0.0749	0.1979	0.0198	0.0323	0.0242	0.0199	0.0195	0.0191	0.0076	0.0113	0.0215
6	0.0593	0.0612	0.1317	0.1345	0.0253	0.0269	0.0344	0.022	0.0213	0.0223	0.0076	0.0108	0.01
7	0.0741	0.0493	0.161	0.0953	0.0254	0.0287	0.0368	0.023	0.021	0.0227	0.0086	0.011	0.0099
8	0.0508	0.1013	0.1105	0.1778	0.0278	0.0361	0.0287	0.0208	0.0213	0.0205	0.009	0.0098	0.0156
9	0.0214	0.1573	0.1818	0.101	0.0283	0.0343	0.0455	0.0265	0.0295	0.0267	0.0099	0.0096	0.0125
10	0.0129	0.0971	0.2173	0.0754	0.0504	0.0574	0.0339	0.0297	0.0263	0.0208	0.0099	0.0091	0.0087
11	0.0197	0.0906	0.2146	0.177	0.0349	0.0516	0.0502	0.0356	0.036	0.0245	0.0091	0.0078	0.0072
12	0.1892	0.0628	0.1009	0.1883	0.0208	0.0307	0.0504	0.0281	0.028	0.0194	0.0069	0.0073	0.0068
13	0.2235	0.0643	0.0987	0.1242	0.023	0.0312	0.0463	0.0294	0.0287	0.0208	0.0096	0.008	0.0046
14	0.0618	0.1357	0.1931	0.3212	0.0337	0.0423	0.0407	0.033	0.0345	0.0247	0.0124	0.0112	0.0058
15	0.0446	0.1042	0.1219	0.0676	0.0443	0.0643	0.0335	0.0312	0.0335	0.0276	0.0094	0.0137	0.0135
16	0.0421	0.1108	0.1973	0.1785	0.0322	0.0568	0.0294	0.0287	0.0324	0.0289	0.0102	0.0131	0.011
17	0.0412	0.193	0.2519	0.1406	0.0171	0.04	0.0363	0.0381	0.0365	0.0279	0.0194	0.0163	0.0081
18	0.0285	0.1214	0.4183	0.2604	0.0194	0.0497	0.088	0.0419	0.0392	0.0301	0.0152	0.0189	0.013
19	0.0169	0.0475	0.3007	0.1654	0.036	0.0307	0.0307	0.0304	0.038	0.0338	0.0234	0.0146	0.0104
20	0.0127	0.0775	0.2472	0.1294	0.0931	0.0574	0.0402	0.0238	0.0232	0.0318	0.0198	0.0174	0.007
21	0.0281	0.0556	0.2071	0.0759	0.0608	0.0702	0.12	0.0539	0.0588	0.0674	0.1273	0.7388	0.9088
22	0.0333	0.157	0.1227	0.173	0.0304	0.0443	0.0519	0.0417	0.0575	0.0652	0.0235	0.0223	0.0113
23	0.1919	0.3896	0.5333	0.4213	0.0424	0.0425	0.0352	0.0176	0.0164	0.0133	0.0093	0.0115	0.0152
24	0.0118	0.0271	0.0463	0.2439	0.054	0.112	0.1268	0.1218	0.128	0.1031	0.0389	0.0373	0.0203



2440	2450	2460	2470	2480	2490	2500	2510	2520
0.0036	0.0207	0.0092	0.0056	0.0143	0.0115	0.0176	0.0276	0.0448
0.0051	0.0046	0.0044	0.0074	0.0138	0.0072	0.021	0.0584	0.0654
0.0061	0.0037	0.0049	0.0068	0.0111	0.0073	0.0182	0.0634	0.0524
0.0046	0.0092	0.0061	0.0065	0.0184	0.0383	0.0232	0.0497	0.0637
0.0054	0.0088	0.0065	0.0086	0.0171	0.0435	0.03	0.0928	0.0794
0.0063	0.0103	0.0141	0.009	0.0167	0.0386	0.0443	0.2081	0.1146
0.0069	0.0148	0.0165	0.0101	0.0187	0.0311	0.0547	0.193	0.1201
0.0068	0.0107	0.0133	0.0113	0.0199	0.0356	0.0524	0.1742	0.153
0.0089	0.0135	0.0121	0.014	0.0193	0.0271	0.0571	0.1696	0.1655
0.0096	0.0093	0.0087	0.0115	0.0167	0.0186	0.0386	0.1113	0.1033
0.0086	0.0088	0.0096	0.0122	0.0168	0.0136	0.0361	0.0704	0.0898
0.0084	0.0081	0.0087	0.0109	0.0144	0.0155	0.0323	0.0591	0.0621
0.0086	0.0095	0.0093	0.0129	0.0164	0.0229	0.0367	0.0626	0.0721
0.0113	0.0148	0.0162	0.0155	0.0171	0.0221	0.0448	0.0976	0.0891
0.0115	0.0101	0.0117	0.0146	0.019	0.0175	0.0458	0.0905	0.1022
0.0109	0.0137	0.0083	0.019	0.0235	0.0235	0.0557	0.0911	0.1007
0.0123	0.0235	0.0168	0.0191	0.0233	0.0219	0.0496	0.0882	0.1429
0.0142	0.0098	0.0077	0.0173	0.0244	0.0326	0.0511	0.0732	0.1022
0.0144	0.006	0.009	0.0236	0.0356	0.0478	0.0638	0.0943	0.108
0.0132	0.0201	0.0126	0.02	0.0259	0.0362	0.061	0.1425	0.1132
0.5236	0.5236	0.5609	0.9439	0.0172	0.0409	-0.0304	0.069	0.2153
0.0139	0.0063	0.0084	0.0184	0.0245	0.0306	0.0595	0.1574	0.1876
0.0153	0.022	0.0188	0.0198	0.0247	0.0219	0.0528	0.0862	0.1073
0.0329	0.0177	0.0168	0.0367	0.0425	0.0284	0.1088	0.1912	0.2108



Table D4, First harmonic power of all power in percentage (Hanoytangen)

	33	34	35	36	37	38	39	40	41	42	43	44	45	46	47
1	0.8039	0.7336	0.8379	0.8768	0.7937	0.9374	0.9438	0.9403	0.9505	0.9672	0.9465	0.9314	0.9384	0.9446	0.9003
2	0.9351	0.9317	0.8646	0.8488	0.4837	0.8419	0.8336	0.8283	0.86	0.8375	0.8212	0.9289	0.9146	0.9212	0.9244
3	0.815	0.6961	0.7906	0.8201	0.6856	0.9084	0.9164	0.9335	0.9321	0.9217	0.9327	0.9042	0.9212	0.9309	0.9114
4	0.86	0.7802	0.823	0.8351	0.8036	0.9096	0.9097	0.8966	0.9366	0.9232	0.9249	0.9226	0.9406	0.9467	0.922
5	0.8943	0.8621	0.8534	0.838	0.8316	0.8866	0.917	0.9059	0.9269	0.906	0.9425	0.9131	0.921	0.932	0.9095
6	0.8554	0.7212	0.8257	0.8408	0.6074	0.9106	0.9233	0.9082	0.9106	0.9119	0.9362	0.906	0.9086	0.9284	0.8898
7	0.8686	0.8307	0.8597	0.8526	0.7167	0.8921	0.9296	0.9303	0.9187	0.8921	0.9325	0.9134	0.9007	0.9175	0.91
8	0.8537	0.7798	0.8454	0.8494	0.8336	0.9124	0.932	0.9103	0.9176	0.8805	0.9093	0.9058	0.8754	0.8971	0.8729
9	0.9202	0.8185	0.8481	0.8106	0.8922	0.8794	0.9402	0.9173	0.8873	0.8943	0.9128	0.9075	0.8865	0.8911	0.8779
10	0.8382	0.7503	0.8478	0.8147	0.8778	0.9049	0.9199	0.9167	0.9007	0.883	0.9089	0.9089	0.9	0.9113	0.8711
11	0.5979	0.7055	0.5315	0.6122	0.4924	0.7112	0.9202	0.8726	0.8528	0.8479	0.8773	0.8032	0.7655	0.8088	0.8298
12	0.9196	0.8179	0.8315	0.8248	0.8183	0.8888	0.9202	0.8914	0.9026	0.9085	0.8868	0.9111	0.8996	0.901	0.8704
13	0.9105	0.8034	0.851	0.8421	0.7192	0.8959	0.926	0.8975	0.8876	0.8955	0.9003	0.8718	0.8941	0.8935	0.8469
14	0.8609	0.8299	0.8544	0.8773	0.6541	0.8683	0.918	0.8928	0.9004	0.8848	0.9037	0.8833	0.8558	0.8631	0.8494
15	0.9057	0.8276	0.8228	0.8612	0.8728	0.9057	0.9265	0.9089	0.9002	0.8548	0.8376	0.8905	0.8781	0.8846	0.8673
16	0.8886	0.8087	0.8408	0.85	0.8484	0.9177	0.9353	0.9173	0.9064	0.8789	0.9166	0.9014	0.905	0.9115	0.8018
17	0.8689	0.7824	0.8942	0.858	0.4922	0.8865	0.9046	0.8916	0.8595	0.878	0.8879	0.8514	0.8752	0.8728	0.8803
18	0.8881	0.7965	0.857	0.862	0.7976	0.922	0.9265	0.8894	0.921	0.8635	0.9252	0.9108	0.8685	0.8806	0.7814
19	0.9149	0.8672	0.8317	0.8236	0.7091	0.9151	0.9044	0.8933	0.8989	0.897	0.877	0.8868	0.9056	0.9038	0.8939
20	0.9079	0.8508	0.8866	0.8284	0.6387	0.8509	0.9435	0.9289	0.8606	0.9135	0.8398	0.8689	0.8542	0.8774	0.7896
21	0.252	0.147	0.4311	0.4373	0.7162	0.7332	0.6777	0.6656	0.7644	0.747	0.829	0.8203	0.799	0.7495	0.7995
22	0.8886	0.8342	0.7086	0.7603	0.7408	0.8713	0.9437	0.9142	0.8611	0.8915	0.8758	0.8162	0.8319	0.841	0.8113
23	0.9312	0.8714	0.9122	0.912	0.8845	0.843	0.7272	0.7322	0.8668	0.7338	0.8887	0.8924	0.8813	0.9014	0.8608
24	0.908	0.7984	0.8795	0.8833	0.8672	0.9001	0.9322	0.9135	0.8814	0.8831	0.8836	0.8883	0.886	0.8802	0.813



49	50	51	52	53	54	55	56	58	59	60	61	62	63
0.9027	0.8632	0.8903	0.8536	0.9055	0.8708	0.922	0.9046	0.9369	0.8712	0.941	0.885	0.9372	0.9063
0.9387	0.8805	0.9512	0.929	0.9543	0.9271	0.9596	0.931	0.9671	0.9067	0.9635	0.9264	0.9643	0.9335
0.9396	0.9052	0.9398	0.9243	0.9574	0.9223	0.9512	0.9442	0.9697	0.9506	0.9739	0.9612	0.9694	0.9551
0.9286	0.9045	0.928	0.889	0.95	0.9168	0.9447	0.9469	0.9655	0.9418	0.9712	0.9606	0.9694	0.9551
0.9343	0.9102	0.9274	0.9099	0.9335	0.9138	0.947	0.9475	0.9573	0.9419	0.9681	0.9538	0.9697	0.9553
0.912	0.8785	0.906	0.8675	0.9242	0.8947	0.9302	0.9141	0.9475	0.9247	0.959	0.9583	0.9632	0.9591
0.8888	0.8624	0.8994	0.857	0.9253	0.8927	0.931	0.9236	0.9436	0.9175	0.9469	0.9531	0.9627	0.957
0.8841	0.8549	0.8995	0.8468	0.9193	0.8579	0.924	0.9053	0.9447	0.9114	0.9441	0.9467	0.9584	0.9594
0.873	0.8532	0.8763	0.8098	0.9	0.8482	0.8954	0.9004	0.9199	0.9129	0.9332	0.9356	0.9495	0.9427
0.8592	0.8454	0.8656	0.8138	0.8926	0.8275	0.895	0.8888	0.9133	0.8995	0.9225	0.9231	0.9393	0.9413
0.7695	0.682	0.8092	0.783	0.8798	0.824	0.8819	0.8487	0.8783	0.881	0.8967	0.9172	0.934	0.9341
0.85	0.8179	0.8571	0.801	0.8822	0.8327	0.8818	0.8821	0.9081	0.8978	0.9186	0.9187	0.9381	0.9353
0.8514	0.8268	0.8625	0.7878	0.8769	0.8189	0.8678	0.8817	0.905	0.8979	0.9166	0.9236	0.9241	0.93
0.8579	0.8306	0.8385	0.7872	0.8848	0.8099	0.8687	0.8779	0.8839	0.8787	0.9105	0.9154	0.9229	0.9295
0.8442	0.8201	0.8306	0.7511	0.8615	0.8281	0.8741	0.8649	0.8879	0.8836	0.8977	0.8967	0.9083	0.9222
0.8406	0.787	0.8309	0.7846	0.8615	0.8024	0.8481	0.8614	0.8994	0.8942	0.905	0.9135	0.9048	0.9141
0.8235	0.7981	0.8432	0.756	0.866	0.8199	0.855	0.8789	0.8765	0.8606	0.859	0.9009	0.889	0.9199
0.8607	0.7846	0.8584	0.8007	0.8566	0.8295	0.834	0.8608	0.8756	0.8609	0.8803	0.8988	0.9029	0.918
0.8058	0.8297	0.7864	0.6929	0.8576	0.7511	0.8702	0.8638	0.8879	0.851	0.8942	0.8945	0.904	0.9043
0.8389	0.7516	0.8101	0.7938	0.828	0.7938	0.841	0.8518	0.8704	0.8725	0.869	0.8688	0.8834	0.9009
0.7506	0.7655	0.7816	0.68	0.8076	0.7863	0.8126	0.8272	0.864	0.8571	0.8388	0.8406	0.8689	0.8415
0.8677	0.802	0.8675	0.8267	0.8872	0.8394	0.8772	0.8575	0.8592	0.7957	0.7868	0.8296	0.8316	0.8365
0.792	0.8086	0.7725	0.6945	0.7558	0.7202	0.7262	0.7514	0.7686	0.7501	0.7365	0.7921	0.7323	0.8084
0.8055	0.7139	0.7558	0.7233	0.784	0.7473	0.8386	0.8534	0.8614	0.8701	0.9242	0.9258	0.9092	0.949



64	65	66
0.9338	0.9535	0.9479
0.9709	0.9797	0.978
0.9667	0.9797	0.9795
0.966	0.9738	0.9732
0.9668	0.9769	0.9747
0.9654	0.9715	0.9679
0.9613	0.9667	0.9642
0.9602	0.9641	0.964
0.9513	0.9574	0.9568
0.9461	0.9467	0.956
0.9338	0.9481	0.9549
0.9453	0.9466	0.9509
0.9401	0.9428	0.9509
0.9262	0.937	0.9454
0.9131	0.9251	0.918
0.9049	0.9142	0.9188
0.9103	0.8962	0.9261
0.9119	0.8962	0.9241
0.8894	0.8902	0.9102
0.8859	0.8788	0.8959
0.8468	0.8264	0.8664
0.8099	0.8515	0.8859
0.7925	0.8798	0.8824
0.9469	0.9446	0.9589



Table D5, Second harmonic power of all power in percentage (Hanoytangen)

	33	34	35	36	37	38	39	40	41	42	43	44	45	46	47
1	0.1578	0.2479	0.143	0.1129	0.1798	0.0372	0.0381	0.0418	0.027	0.0198	0.0426	0.0491	0.0475	0.0458	0.0954
2	0.0505	0.0547	0.1139	0.146	0.4364	0.0989	0.1428	0.1437	0.114	0.1358	0.1693	0.0597	0.0742	0.0693	0.0674
3	0.1502	0.2602	0.13	0.1703	0.2656	0.0722	0.0714	0.0564	0.0488	0.064	0.0616	0.0655	0.0595	0.0573	0.0845
4	0.0928	0.1917	0.1066	0.1519	0.1715	0.0652	0.0765	0.0884	0.0496	0.0669	0.0672	0.0694	0.0535	0.0461	0.0727
5	0.0839	0.1232	0.094	0.1547	0.1267	0.0713	0.0742	0.0845	0.0569	0.0845	0.052	0.0529	0.0576	0.0553	0.0868
6	0.1032	0.2508	0.1108	0.1511	0.3208	0.0746	0.069	0.078	0.0722	0.0763	0.0571	0.0782	0.076	0.0603	0.1043
7	0.1053	0.1487	0.0954	0.1378	0.2558	0.0848	0.0635	0.0613	0.0631	0.0955	0.062	0.0576	0.0758	0.0674	0.0852
8	0.1019	0.1942	0.1137	0.1415	0.1526	0.0611	0.0606	0.082	0.0599	0.1072	0.0827	0.082	0.1097	0.0905	0.121
9	0.0605	0.1525	0.1129	0.1804	0.0535	0.0993	0.0529	0.0719	0.0868	0.092	0.08	0.0675	0.0895	0.0904	0.1161
10	0.0855	0.1693	0.0938	0.1465	0.0755	0.0749	0.0686	0.0756	0.0796	0.1002	0.0819	0.0785	0.0873	0.0775	0.1205
11	0.0877	0.107	0.1082	0.0616	0.0929	0.0513	0.048	0.0604	0.0588	0.0727	0.0632	0.0655	0.0611	0.077	0.123
12	0.0599	0.161	0.1316	0.1619	0.1583	0.0823	0.0722	0.0966	0.0767	0.0776	0.1043	0.0717	0.0853	0.086	0.1221
13	0.0648	0.1563	0.1143	0.1476	0.2268	0.0849	0.0659	0.0965	0.0916	0.0915	0.0927	0.1066	0.0891	0.0905	0.1464
14	0.1211	0.1547	0.1062	0.1156	0.2638	0.1099	0.0718	0.0935	0.0757	0.1022	0.0877	0.082	0.1144	0.113	0.1413
15	0.0816	0.1527	0.1489	0.1319	0.0831	0.075	0.0669	0.0801	0.0742	0.1318	0.1535	0.0786	0.1003	0.0988	0.1227
16	0.0713	0.1444	0.124	0.1297	0.1105	0.0649	0.0565	0.0652	0.0733	0.1046	0.0756	0.0862	0.0799	0.0741	0.1882
17	0.1068	0.1881	0.087	0.1342	0.4538	0.0693	0.087	0.1011	0.1104	0.1074	0.1017	0.1114	0.1016	0.1089	0.113
18	0.0725	0.1735	0.118	0.1277	0.1961	0.0449	0.0652	0.0992	0.0595	0.122	0.0656	0.0607	0.1012	0.0946	0.2108
19	0.0668	0.118	0.1438	0.169	0.2641	0.0751	0.0787	0.0884	0.076	0.0852	0.1149	0.1027	0.0835	0.0852	0.0962
20	0.0744	0.1351	0.096	0.165	0.2785	0.1242	0.0505	0.0653	0.1113	0.0716	0.1483	0.089	0.1105	0.0986	0.2042
21	0.0426	0.0715	0.1067	0.1016	0.0446	0.0936	0.1344	0.1622	0.1254	0.1254	0.0943	0.0809	0.0899	0.099	0.1155
22	0.0952	0.1548	0.2161	0.2215	0.1423	0.1062	0.0493	0.074	0.1018	0.0917	0.1141	0.1663	0.1553	0.1476	0.1773
23	0.0617	0.1217	0.0554	0.0802	0.0705	0.1494	0.259	0.2554	0.1142	0.2452	0.0995	0.065	0.081	0.07	0.1311
24	0.0699	0.18	0.0674	0.1039	0.0789	0.0796	0.064	0.0801	0.1058	0.1096	0.1118	0.1071	0.1096	0.1159	0.1851





48	49	50	51	52	53	54	55	56	58	59	60	61	62	63	64	65	66
0.0661	0.0772	0.1033	0.1066	0.1281	0.0885	0.1057	0.0738	0.0696	0.0603	0.0849	0.0547	0.0601	0.0573	0.0527	0.0615	0.0427	0.0479
0.06	0.0443	0.069	0.0426	0.0411	0.0355	0.0378	0.0328	0.0407	0.0294	0.0534	0.0337	0.0276	0.0314	0.0258	0.0267	0.0183	0.0201
0.0574	0.0484	0.0739	0.0563	0.0579	0.0372	0.0577	0.0408	0.0312	0.0255	0.0277	0.0238	0.0215	0.0268	0.0232	0.0314	0.0187	0.0189
0.0649	0.0588	0.0818	0.0686	0.0982	0.0439	0.0666	0.0479	0.0375	0.0287	0.0401	0.0259	0.0233	0.0269	0.0263	0.0317	0.0247	0.0253
0.0498	0.0512	0.0751	0.0676	0.0772	0.0564	0.0695	0.0443	0.0371	0.0355	0.0429	0.029	0.0303	0.0269	0.0274	0.0315	0.0219	0.0237
0.0672	0.0665	0.1034	0.0875	0.1155	0.063	0.0882	0.0586	0.0662	0.0446	0.0611	0.0373	0.0298	0.0329	0.0313	0.0328	0.0271	0.03
0.0605	0.0935	0.1225	0.0955	0.1275	0.0625	0.0886	0.0578	0.0564	0.0486	0.0647	0.0484	0.0353	0.0337	0.035	0.0372	0.0314	0.0333
0.066	0.0907	0.129	0.0959	0.1369	0.0678	0.12	0.0629	0.0749	0.0464	0.0709	0.0518	0.0411	0.0371	0.0318	0.0381	0.0337	0.034
0.0689	0.0991	0.1327	0.116	0.1722	0.0835	0.1301	0.0888	0.0772	0.0688	0.0688	0.0617	0.0534	0.0462	0.0474	0.0468	0.0406	0.0401
0.0926	0.113	0.1415	0.1245	0.1675	0.0842	0.1508	0.086	0.0942	0.0703	0.0793	0.0727	0.0648	0.0547	0.0495	0.0508	0.0498	0.0409
0.0759	0.098	0.1277	0.1172	0.1826	0.0897	0.1391	0.0962	0.0894	0.0772	0.0861	0.0704	0.0656	0.0528	0.0517	0.0511	0.0461	0.0393
0.0863	0.1223	0.1677	0.1353	0.1813	0.0982	0.1459	0.0991	0.0996	0.0792	0.0862	0.0769	0.0696	0.0571	0.0573	0.0525	0.0507	0.0465
0.0972	0.1183	0.1603	0.1296	0.1947	0.1032	0.1561	0.1105	0.0993	0.0816	0.0832	0.0774	0.0642	0.0696	0.0622	0.057	0.0538	0.0464
0.08	0.1154	0.1551	0.1527	0.1956	0.0952	0.1672	0.1077	0.106	0.101	0.1033	0.0831	0.0732	0.069	0.0637	0.0706	0.0604	0.0517
0.0897	0.1296	0.1689	0.1584	0.2341	0.116	0.1508	0.1043	0.117	0.0959	0.0998	0.0915	0.0869	0.0775	0.0729	0.0826	0.0704	0.0773
0.0883	0.1205	0.1969	0.1588	0.1993	0.1165	0.1761	0.128	0.1207	0.0816	0.0878	0.0811	0.0721	0.0786	0.0811	0.0916	0.0807	0.0763
0.1102	0.1514	0.1893	0.1498	0.2316	0.1144	0.1603	0.1185	0.1032	0.1046	0.1205	0.1214	0.082	0.0902	0.0753	0.0854	0.0993	0.0694
0.0926	0.1025	0.2039	0.1354	0.1874	0.1261	0.1538	0.142	0.1229	0.1057	0.1189	0.1009	0.0828	0.0755	0.0775	0.084	0.0984	0.0713
0.1013	0.1639	0.1591	0.2029	0.2929	0.1191	0.2277	0.1045	0.1216	0.0937	0.1296	0.0871	0.0868	0.0751	0.0925	0.1075	0.1055	0.0859
0.0999	0.1245	0.2382	0.1747	0.1892	0.1422	0.1807	0.1313	0.1326	0.1114	0.1093	0.1103	0.1077	0.0935	0.0945	0.109	0.1175	0.1002
0.0862	0.156	0.174	0.172	0.2678	0.1428	0.1618	0.1365	0.136	0.1022	0.1049	0.1202	0.1109	0.0912	0.1311	0.1342	0.1514	0.1158
0.1174	0.1077	0.1835	0.124	0.1602	0.0952	0.1384	0.1024	0.1319	0.1259	0.1881	0.1838	0.1475	0.1373	0.1583	0.1856	0.1417	0.1076
0.0869	0.1538	0.1828	0.2222	0.2988	0.2334	0.2681	0.2561	0.235	0.2107	0.227	0.234	0.1827	0.2271	0.1848	0.1991	0.1115	0.11
0.109	0.1806	0.2829	0.2357	0.2682	0.1994	0.2402	0.1376	0.1244	0.115	0.1075	0.0555	0.0516	0.0611	0.0428	0.044	0.0473	0.034



Table D6, Higher mode power (3<sup>rd</sup> and higher) of all power in percentage (Hanoytangen)

	33	34	35	36	37	38	39	40	41	42	43	44	45	46	47	48
1	0.0383	0.0185	0.0191	0.0103	0.0265	0.0254	0.0181	0.0179	0.0225	0.013	0.0109	0.0195	0.0141	0.0096	0.0043	0.013
2	0.0144	0.0136	0.0215	0.0052	0.0799	0.0592	0.0236	0.028	0.026	0.0267	0.0095	0.0114	0.0112	0.0095	0.0082	0.0262
3	0.0348	0.0437	0.0794	0.0096	0.0488	0.0194	0.0122	0.0101	0.0191	0.0143	0.0057	0.0303	0.0193	0.0118	0.0041	0.018
4	0.0472	0.0281	0.0704	0.013	0.0249	0.0252	0.0138	0.015	0.0138	0.0099	0.0079	0.008	0.0059	0.0072	0.0053	0.0107
5	0.0218	0.0147	0.0526	0.0073	0.0417	0.0421	0.0088	0.0096	0.0162	0.0095	0.0055	0.034	0.0214	0.0127	0.0037	0.0141
6	0.0414	0.028	0.0635	0.0081	0.0718	0.0148	0.0077	0.0138	0.0172	0.0118	0.0067	0.0158	0.0154	0.0113	0.0059	0.0137
7	0.0261	0.0206	0.0449	0.0096	0.0275	0.0231	0.0069	0.0084	0.0182	0.0124	0.0055	0.029	0.0235	0.0151	0.0048	0.0147
8	0.0444	0.026	0.0409	0.0091	0.0138	0.0265	0.0074	0.0077	0.0225	0.0123	0.008	0.0122	0.0149	0.0124	0.0061	0.0128
9	0.0193	0.029	0.039	0.009	0.0543	0.0213	0.0069	0.0108	0.0259	0.0137	0.0072	0.025	0.024	0.0185	0.006	0.0128
10	0.0763	0.0804	0.0584	0.0388	0.0467	0.0202	0.0115	0.0077	0.0197	0.0168	0.0092	0.0126	0.0127	0.0112	0.0084	0.0148
11	0.3144	0.1875	0.3603	0.3262	0.4147	0.2375	0.0318	0.067	0.0884	0.0794	0.0595	0.1313	0.1734	0.1142	0.0472	0.0938
12	0.0205	0.0211	0.0369	0.0133	0.0234	0.0289	0.0076	0.012	0.0207	0.0139	0.0089	0.0172	0.0151	0.013	0.0075	0.0121
13	0.0247	0.0403	0.0347	0.0103	0.054	0.0192	0.0081	0.006	0.0208	0.013	0.007	0.0216	0.0168	0.016	0.0067	0.0102
14	0.018	0.0154	0.0394	0.0071	0.0821	0.0218	0.0102	0.0137	0.0239	0.013	0.0086	0.0347	0.0298	0.0239	0.0093	0.0093
15	0.0127	0.0197	0.0283	0.0069	0.0441	0.0193	0.0066	0.011	0.0256	0.0134	0.0089	0.0309	0.0216	0.0166	0.01	0.0077
16	0.0401	0.0469	0.0352	0.0203	0.0411	0.0174	0.0082	0.0175	0.0203	0.0165	0.0078	0.0124	0.0151	0.0144	0.01	0.0089
17	0.0243	0.0295	0.0188	0.0078	0.054	0.0442	0.0084	0.0073	0.0301	0.0146	0.0104	0.0372	0.0232	0.0183	0.0067	0.0066
18	0.0394	0.03	0.025	0.0103	0.0063	0.0331	0.0083	0.0114	0.0195	0.0145	0.0092	0.0285	0.0303	0.0248	0.0078	0.0074
19	0.0183	0.0148	0.0245	0.0074	0.0268	0.0098	0.0169	0.0183	0.0251	0.0178	0.0081	0.0105	0.0109	0.011	0.0099	0.0074
20	0.0177	0.0141	0.0174	0.0066	0.0828	0.0249	0.006	0.0058	0.0281	0.0149	0.0119	0.0421	0.0353	0.024	0.0062	0.0063
21	0.7054	0.7815	0.4622	0.4611	0.2392	0.1732	0.1879	0.1722	0.1102	0.1276	0.0767	0.0988	0.1111	0.1515	0.085	0.0757
22	0.0162	0.011	0.0753	0.0182	0.1169	0.0225	0.007	0.0118	0.0371	0.0168	0.0101	0.0175	0.0128	0.0114	0.0114	0.0092
23	0.0071	0.0069	0.0324	0.0078	0.045	0.0076	0.0138	0.0124	0.019	0.021	0.0118	0.0426	0.0377	0.0286	0.0081	0.0043
24	0.0221	0.0216	0.0531	0.0128	0.0539	0.0203	0.0038	0.0064	0.0128	0.0073	0.0046	0.0046	0.0044	0.0039	0.0019	0.0019



49	50	51	52	53	54	55	56	58	59	60	61	62	63	64	65	66
0.0201	0.0335	0.0031	0.0183	0.006	0.0235	0.0042	0.0258	0.0028	0.0439	0.0043	0.0549	0.0055	0.041	0.0047	0.0038	0.0042
0.017	0.0505	0.0062	0.0299	0.0102	0.0351	0.0076	0.0283	0.0035	0.0399	0.0028	0.046	0.0043	0.0407	0.0024	0.002	0.0019
0.012	0.0209	0.0039	0.0178	0.0054	0.02	0.008	0.0246	0.0048	0.0217	0.0023	0.0173	0.0038	0.0217	0.0019	0.0016	0.0016
0.0126	0.0137	0.0034	0.0128	0.0061	0.0166	0.0074	0.0156	0.0058	0.0181	0.0029	0.0161	0.0037	0.0186	0.0023	0.0015	0.0015
0.0145	0.0147	0.005	0.0129	0.0101	0.0167	0.0087	0.0154	0.0072	0.0152	0.0029	0.0159	0.0034	0.0173	0.0017	0.0012	0.0016
0.0215	0.0181	0.0065	0.017	0.0128	0.0171	0.0112	0.0197	0.0079	0.0142	0.0037	0.0119	0.0039	0.0096	0.0018	0.0014	0.0021
0.0177	0.0151	0.0051	0.0155	0.0122	0.0187	0.0112	0.02	0.0078	0.0178	0.0047	0.0116	0.0036	0.008	0.0015	0.0019	0.0025
0.0252	0.0161	0.0046	0.0163	0.0129	0.0221	0.0131	0.0198	0.0089	0.0177	0.0041	0.0122	0.0045	0.0088	0.0017	0.0022	0.002
0.0279	0.0141	0.0077	0.018	0.0165	0.0217	0.0158	0.0224	0.0113	0.0183	0.0051	0.011	0.0043	0.0099	0.0019	0.002	0.0031
0.0278	0.0131	0.0099	0.0187	0.0232	0.0217	0.019	0.017	0.0164	0.0212	0.0048	0.0121	0.006	0.0092	0.0031	0.0035	0.0031
0.1325	0.1903	0.0736	0.0344	0.0305	0.0369	0.0219	0.0619	0.0445	0.0329	0.0329	0.0172	0.0132	0.0142	0.0151	0.0058	0.0058
0.0277	0.0144	0.0076	0.0177	0.0196	0.0214	0.0191	0.0183	0.0127	0.016	0.0045	0.0117	0.0048	0.0074	0.0022	0.0027	0.0026
0.0303	0.0129	0.0079	0.0175	0.0199	0.025	0.0217	0.019	0.0134	0.0189	0.006	0.0122	0.0063	0.0078	0.0029	0.0034	0.0027
0.0267	0.0143	0.0088	0.0172	0.02	0.0229	0.0236	0.0161	0.0151	0.018	0.0064	0.0114	0.0081	0.0068	0.0032	0.0026	0.0029
0.0262	0.011	0.011	0.0148	0.0225	0.0211	0.0216	0.0181	0.0162	0.0166	0.0108	0.0164	0.0142	0.0049	0.0043	0.0045	0.0047
0.0389	0.0161	0.0103	0.0161	0.022	0.0215	0.0239	0.0179	0.019	0.018	0.0139	0.0144	0.0166	0.0048	0.0035	0.0051	0.0049
0.0251	0.0126	0.007	0.0124	0.0196	0.0198	0.0265	0.0179	0.0189	0.0189	0.0196	0.0171	0.0208	0.0048	0.0043	0.0045	0.0045
0.0368	0.0115	0.0062	0.0119	0.0173	0.0167	0.024	0.0163	0.0187	0.0202	0.0188	0.0184	0.0216	0.0045	0.0041	0.0054	0.0046
0.0303	0.0112	0.0107	0.0142	0.0233	0.0212	0.0253	0.0146	0.0184	0.0194	0.0187	0.0187	0.0209	0.0032	0.0031	0.0043	0.0039
0.0366	0.0102	0.0152	0.017	0.0298	0.0255	0.0277	0.0156	0.0182	0.0182	0.0207	0.0235	0.0231	0.0046	0.0051	0.0037	0.0039
0.0934	0.0605	0.0464	0.0522	0.0496	0.0519	0.0509	0.0368	0.0338	0.038	0.041	0.0485	0.0399	0.0274	0.019	0.0222	0.0178
0.0246	0.0145	0.0085	0.0131	0.0176	0.0222	0.0204	0.0106	0.0149	0.0162	0.0294	0.0229	0.0311	0.0052	0.0045	0.0068	0.0065
0.0542	0.0086	0.0053	0.0067	0.0108	0.0117	0.0177	0.0136	0.0207	0.0229	0.0295	0.0252	0.0406	0.0068	0.0084	0.0087	0.0076
0.0139	0.0032	0.0085	0.0085	0.0166	0.0125	0.0238	0.0222	0.0236	0.0224	0.0203	0.0226	0.0297	0.0082	0.0091	0.0081	0.0071

**Chaotic and Stationary Signals**

Table D7, Period of CF oscillation during chaotic period

No.	CF period	No.	CF period
1	0.1225	23	0.124167
2	0.114167	24	0.109167
3	0.093333	25	0.103333
4	0.101667	26	0.1
5	0.111667	27	0.121667
6	0.108333	28	0.134167
7	0.095	29	0.0775
8	0.115	30	0.125
9	0.106667	31	0.130833
10	0.124167	32	0.105833
11	0.126667	33	0.109167
12	0.111667	34	0.118333
13	0.105833	35	0.12
14	0.099167	36	0.121667
15	0.115833	37	0.111667
16	0.100833	38	0.115
17	0.118333	39	0.1075
18	0.104167	40	0.109167
19	0.1125	41	0.1175
20	0.105	42	0.125
21	0.115	43	0.170833
22	0.1225		

Table D8, Period of IL oscillation during chaotic period

No.	IL period	No.	IL period	No.	IL period
1	0.06	31	0.055	61	0.058333
2	0.0575	32	0.046667	62	0.06
3	0.051667	33	0.060833	63	0.058333
4	0.0475	34	0.0575	64	0.06
5	0.059167	35	0.031667	65	0.063333
6	0.056667	36	0.07	66	0.054167
7	0.06	37	0.064167	67	0.051667
8	0.063333	38	0.055	68	0.0575
9	0.060833	39	0.053333	69	0.061667
10	0.061667	40	0.053333	70	0.058333
11	0.0525	41	0.049167	71	0.035833
12	0.051667	42	0.051667	72	0.0575
13	0.058333	43	0.058333	73	0.055833
14	0.059167	44	0.0575	74	0.055833
15	0.041667	45	0.056667	75	0.053333
16	0.0575	46	0.063333	76	0.065
17	0.060833	47	0.043333	77	0.053333
18	0.0575	48	0.046667	78	0.051667
19	0.0325	49	0.050833	79	0.056667
20	0.058333	50	0.049167	80	0.0525
21	0.0625	51	0.066667	81	0.055
22	0.034167	52	0.028333	82	0.059167
23	0.0525	53	0.038333	83	0.064167
24	0.061667	54	0.0575	84	0.066667
25	0.043333	55	0.064167	85	0.060833
26	0.064167	56	0.068333	86	0.061667
27	0.078333	57	0.060833	87	0.054167
28	0.036667	58	0.055833	88	0.055
29	0.065833	59	0.045	89	0.06
30	0.058333	60	0.0525		

Table D9, Period of CF oscillation during stationary period

No.	CF period	No.	CF period
1	0.125	21	0.12
2	0.125	22	0.12
3	0.125833	23	0.125833
4	0.125833	24	0.125833
5	0.1225	25	0.1175
6	0.119167	26	0.120833
7	0.129167	27	0.128333
8	0.125	28	0.12
9	0.1175	29	0.124167
10	0.1225	30	0.126667
11	0.124167	31	0.1225
12	0.1225	32	0.121667
13	0.121667	33	0.124167
14	0.125	34	0.125
15	0.12	35	0.12
16	0.125	36	0.125833
17	0.1275	37	0.125
18	0.124167	38	0.12
19	0.125	39	0.125833
20	0.125833	40	0.128333

Table D10, Period of IL oscillation during stationary period

No.	IL period	No.	IL period
1	0.063333	41	0.059167
2	0.0625	42	0.06
3	0.060833	43	0.060833
4	0.0625	44	0.059167
5	0.0625	45	0.060833
6	0.061667	46	0.0625
7	0.0625	47	0.061667
8	0.0625	48	0.06
9	0.06	49	0.060833
10	0.060833	50	0.06
11	0.061667	51	0.060833
12	0.063333	52	0.063333
13	0.061667	53	0.063333
14	0.060833	54	0.0625
15	0.06	55	0.060833
16	0.060833	56	0.060833
17	0.061667	57	0.061667
18	0.06	58	0.064167
19	0.061667	59	0.0625
20	0.061667	60	0.063333
21	0.061667	61	0.060833
22	0.061667	62	0.060833
23	0.061667	63	0.060833
24	0.06	64	0.0625
25	0.060833	65	0.0625
26	0.064167	66	0.064167
27	0.0625	67	0.060833
28	0.060833	68	0.06
29	0.061667	69	0.06
30	0.0625	70	0.0625
31	0.061667	71	0.0625
32	0.0625	72	0.063333
33	0.061667	73	0.061667
34	0.0625	74	0.060833
35	0.061667	75	0.06
36	0.063333	76	0.061667
37	0.061667	77	0.063333
38	0.064167	78	0.063333
39	0.0625	79	0.063333
40	0.063333	80	0.061667

